The Earth Institute
Columbia University

# The impacts of climate change on coffee: trouble brewing

Jeffrey Sachs, James Rising,
Tim Foreman, John Simmons, Manuel Brahm
The Earth Institute
Columbia University

October 1, 2015

Prepared for the Global Coffee Forum
Milan, Italy

# Contents

# Executive Summary

This report provides new evidence on the present and predicted future impacts of climate change on coffee production and markets.

**Coffee is sensitive to climate.** Arabica coffee is grown at high elevations, in warm regions, with sensitive quality, and multiple positive and negative ecosystem interactions (**??**). All of these can cause high-quality coffee to be threatened by climate change.

**Temperatures are already causing shifts.** Recent temperatures in the coffee belt have been increasing by 0.16°C per decade (1.1), representing an average poleward shift of 46km per decade. In Brazil, low elevation farms are already being impacted (**??**).

**Temperature across the coffee belt is expected to rise by 2.1°C (likely range 1.7 - 2.5°C) by 2050** (1.2). Average future temperatures have high predictability, but uncertain spatial patterns. 60-64% of recent temperatures is explained by a trend, but most of the rest is uncertain year-to-year (1.1.2).

**Precipitation across the coffee belt is expected to increase 1.7% (likely range -0.1 - 3.2%), but dry periods will often be drier** (1.2). Average future precipitation has low predictability. Only 1% of precipitation can be explained by long-term trends, but decadal cycles predictable in the short-term (like El Niño) play a large role.

**We develop a new database of spatial coffee production.** The database combines spatial data from 3 global sources and 8 detailed country sources, and temporal data from 2 global sources and 5 country sources (**??**).

**We present a new technique for coffee suitability analysis.** The technique incorporates properties of soil, climate, and elevation for a statistical model, and combines it with biological conditions from the Global Agro-ecological Zones (GAEZ) project (3.3).

**On average, El Niño years produce 30% hikes in coffee prices and drops in coffee yields.** No corresponding effect is seen globally across La Niña years, except in their interactions with the PDO and AMO signals (**??**).

**Higher temperatures may lead to larger coffee rust outbreaks.** In addition, vigilant farmer action against these outbreaks will decrease small infestations but may increase the probability of large ones (**??**).

**Hot days produce large yield losses.** In Brazil, even an hour over 35°C cause serious losses, and some countries receive losses at temperatures as low as 33°C (**??**). There is evidence that some countries have adapted to high temperatures with lower sensitivity to them.

**Under temperatures in 2050, average yields in existing growing areas are expected to drop 20%.** The variation between countries is large, with some countries losing the majority of their production potential, and others seeing increases (**??**).

**Globally, prices paid to farmers are driven much more by international prices than local competition.** We also find that international prices and consumer demand are more self-determined than driven by changes in production and retail prices, respectively (6).

**Most of the markup associated with producer countries does not go to farmers.** Trade relations suggest that 21% of consumer prices go to production, 44% to distribution, and 35% to the organizations in the consumer's country (**??**).

**Nearly 20 countries could lose all naturally highly suitable coffee land.** Globally, suitable regions will decrease by 56% for Arabica, including 24% of current cultivation, while they increase by 87% for Robusta. (3.7).

**New coffee growing regions will become available further from the equator.** For Arabica coffee, the countries with the most new coffee regions are Brazil, Mexico, and Angola. While many countries will gain new suitable land, globally this is only be 10 - 20% of what may be lost (3.7).

# Introduction

Coffee plays a vital role in many countries, providing livelihoods to 25 million inhabitants of tropical countries and supporting a $81 billion industry (Sharf, 2014), making it one of the most valuable commodities in the world. However, coffee is extremely vulnerable to climate change. Already changes in climate are making disease outbreaks more common and shifting suitable growing regions (Guilford, 2014; Malkin, 2014). The coffee industry consists of a complex web of small-holder farmers, multinational corporations, government policies, and diverse consumers. As coffee demand continues to expand, the international coffee system will respond to pressure from all of these elements.

This research studies the effects of climate change on coffee from a global perspective. As productive coffee regions shift, every aspect of the coffee system will be impacted, from developing country farmers to developed country consumers. By 2050, these long-term shifts will reshape the global coffee market.

The effects of climate on coffee also include shorter timescales. Decadal and interannual climate cycles have long impacted coffee production worldwide. Production in different regions varies in their degree of sensitivity to current climate variability and increasingly extreme temperatures. Understanding these differences is an important input to global planning.

Coffee production has considerable potential for supporting sustainability and economic opportunities for the future, but planning requires a better understanding of the interconnections between production, trade, and the environment. The future of coffee depends on understanding the risks, instituting high-resolution monitoring, and acting in anticipation of future impacts. In this report, we have emphasized new research and reanalyses, rather than reviews of existing knowledge. We build upon the strong foundation laid by recent articles and reports. In particular, a recent report by *coffee&climate* (2015) addresses the challenge that climate poses to coffee farmers and presents an approach to adaptation planning. The International Coffee Organization (ICO) has produced a report detailing the modes of climate impacts on coffee and projects aimed at addressing them (ming). The chapters list many additional references.

Throughout this report, we take a quantitative, empirical approach to questions about the current and future state of the global coffee system. We identify relationships that are closely tied to the physical world, drawing on the strengths of the Earth Institute. Furthermore, the relationships we study are as they are reflected in aggregated data, often at the country-wide level. There are important impacts of climate change on farms and farmers that only appear implicitly in this data and our results.

We emphasize a number of elements underrepresented in the coffee literature. First, we focus on the pervasive uncertainty underlying coffee and climate analyses. This stems from a combination of the inherent variability of climate, the heterogeneity of coffee farming practices, and uncertainty in the statistical results relating them. Without this, the true risk of climate change to coffee can both be misestimated and misattributed. We have incorporated the analysis of uncertainty throughout our work.

Second, and related to this, is the state of coffee production knowledge. Coffee data is often not available at high resolution and not available comprehensively within regions. It is also likely to have considerable bias, since coffee production is highly politicized in many countries. We have developed a new spatial coffee production database to address these problems, and emphasize statistical techniques and tools that account for the erratic data quality.

Third, we have drawn from multiple academic literatures to apply innovative approaches to questions around coffee and climate. These include our Bayesian approach to estimating suitability; our study of interactions between multiple signals to understand variability; and our use of the most robust methods of econometrics to study production.

For future climate and suitability projections, we target the year 2050. Much of the climate change that will occur by 2050 is a result of emissions which have already occurred. These thirty-five years will be instrumental to the future of coffee, as we learn to adapt to rapid climate change.

By 2050, if the international community has not enacted strong, effective carbon controls, the rate of warming will be even greater. 2050 could be the beginning of additional, catastrophic climate impacts on coffee and elsewhere. However, this year provides a useful road mark, far enough into the future to see the impacts but close enough that planning for those impacts can start now. In this report, we distinguish between the effects of climate on coffee across different "time scales". The nature of climate impacts, and the appropriate methods for analysis, differ for different scales. To understand these differences, it is important to understand the difference between weather and climate.

"Weather" describes the actual temperature, rainfall, and other atmospheric features that we observe. Weather is constantly changing, even when climate is not changing. "Climate" is traditionally defined as the 30-year average of weather (**?**). When coffee plants wilt because of low rainfall, they are responding to weather, and we can study those responses irrespective of changes in climate. When coffee can no longer be productively grown in an area because droughts are too frequent, this is a response to climate (even though it is mediated by individual weather events).

A third time scale for understanding climate impacts lies between daily weather and 30-year averaged climate. The climate goes through natural cycles that can last many years. For example, the El Niño / La Niña cycle lasts 2 to 7 years, and has a large impact on seasonal weather. Other climate cycles are called "decadal" or "multidecadal", because they can persist in one state for over 10 years, such as the currently high temperatures in the northern Atlantic ocean.

To understand the effects of weather, we study how year-to-year changes in yield are driven by the patterns daily weather observed during each year (see chapter **??**). Most year-to-year changes in yields are the result of variability in weather. We can look at historical weather and historical changes in yields as a way to predict how coffee will respond in the future under hotter temperatures.

We study multi-year climate cycles, including both El Niño and multidecadal cycles, in a second analysis (see chapter **??**). As with other aspects of climate, the impacts of these cycles occur through their effects on local weather, but they reveal their secrets better when studied globally and over many years.

Finally, to understand the effects of climate, we perform a suitability analysis (see chapter **??**). Long-term trends will shift the suitable regions for coffee, and we study these impacts distinctly from those that determine yields. Our model of coffee suitability is based on the pattern of current coffee cultivation, rather than yields as with the previous two analyses. We then apply this model of suitability to future climate to determine where coffee will be able to be productively grown.

This report is organized into multiple chapters, exploring different aspects of the climate-coffee connection.

- **Chapter 1** discusses the state of knowledge and uncertainty about climate change in the coffee

belt.

- **Chapter 2** presents the new database of coffee production for studying climate impacts.
- **Chapter 3** presents a new approach to suitability and the changes we predict under the future climate.
- **Chapter 4** studies the El Niño / La Niña cycle and other climate signals of internal variability.
- **Chapter 5** builds a robust and multi-level model of coffee production based on weather variation.
- **Chapter 6** discusses our results for the global coffee market and the effect of production on prices.
- **Chapter 7** provides some thoughts on the future of coffee and coffee research.

A number of additional analyses are reported in Appendix A, many of which offer avenues for future research. Appendix B describes the coffee production database we generated and the principles behind it. Appendix C provides documentation for decision-support tools that we have generated in the course of our research.

# Chapter 1

# Climate change in the coffee belt

## 1.1 Recent climate change and uncertainties

The coffee belt is the band of coffee suitable regions between the tropics of Cancer and Capricorn, from around 23°S to 23°N. This area has experienced a sharp increase in temperatures since the 1960s, and this trend is expected to increase. Figure 1.1 displays the yearly average temperature in this belt over the instrumental record. The average increase in recent decades has been 0.16°C per decade. The equator is generally expected to warm more slowly than the poles. This correspondingly represents an intermediate rate of warming, greater than the rate of ocean warming at 0.11°C per decade and less than the global average for land at 0.28°C per decade (GISTEMP Team, 2015; Hansen et al., 2010).

As temperatures increase, coffee production will be forced toward the poles and to higher elevations. If warming continues at its current rate, with an average increase of 0.16°C degrees per decade, coffee production will need to shift an average of 46km per decade toward the poles or 29m higher per decade.[1]

### 1.1.1 Counterbalancing effects

Not all of the effects of climate change are necessarily detrimental to coffee production. One of the major threats to coffee farms is frost (Varangis et al., 2003), and where minimum temperatures shift away from 0°C without otherwise affecting conditions, coffee production will benefit. Elsewhere, the variability of temperature will become greater, increasing the risk of cold snaps and frost damage even as average temperatures warm.

Carbon fertilization will also have uncertain effects. Many crops see yield benefits from carbon fertilization (McGrath and Lobell, 2013), as plant produce more carbohydrates (Körner et al., 2007). However, a wider carbon-to-nitrogen ratio generally produces a loss of quality for agricultural products. Quality coffee production may need to move to higher elevations to offset this increase in carbohydrate productivity. At higher elevations, bean development slows and flavors have more time to accumulate, but this also places coffee back into zones of high frost risk.

[1] Average change in temperature with latitude and elevation from `http://landterms.com/Articles_and_FAQ_s/Conservation_and_Ecology_Articles_and_FAQ_s/Latitude__Elevation_and_Temperature/`, reported as 3°F / 300 miles latitude and 3°F / 1000 ft elevation. This equates to 290 km / °C and 183 m / °C.

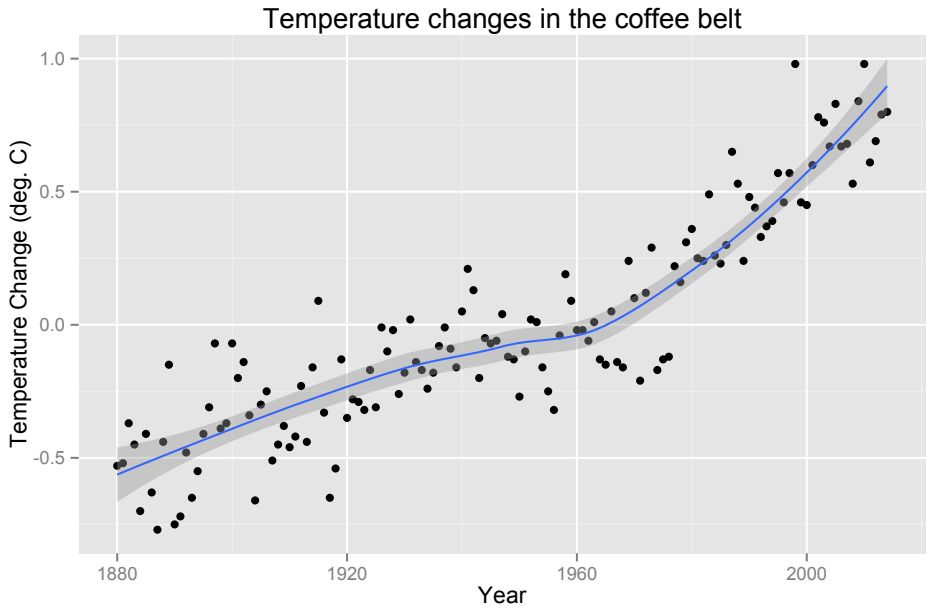


Figure 1.1: Yearly average temperatures in the coffee belt (dots), including temperatures over land and oceans, and a smooth running average with 95% confidence intervals.

As temperatures rise, coffee will be forced generally up slopes and away from the equator. Under 2-2.5°C of warming, the minimum altitude suitable for coffee production in Central America and Kenya is expected to increase by around 400m (IPCC, 2014). However, this will open up new areas to coffee production, even as it eliminates traditional areas, for example in high-elevation regions of Guatemala.

### 1.1.2 Climate predictability

The primary drivers of yields, suitability, and other responses of coffee to climate are temperature and precipitation. Although we have extensive predictions of future temperature and precipitation patterns through the end of the century, these need to be treated with some circumspection. Our understanding of the future impacts of climate on coffee is limited by the fundamental predictability of the climate system.

Climate change and the long-term increase in global average temperatures are a virtual certainty. However, predictions for the equilibrium change in global temperature resulting from a doubling of $CO_2$ range from 1°C to 6°C (Stocker et al., 2014, Box 12.2). Many feedback loops in the climate are poorly understood, and predictions that agree on eventual changes in the climate can disagree on the timing. Furthermore, the patterns of how temperature, precipitation and other aspects of weather will change locally are more uncertain than the global average. Finally, the uncertainty around how society will respond to climate change is even greater than the uncertainty in climate.

One way to understand the amount of uncertainty in annual average temperatures and precipitation in coffee-growing regions that results from the natural climate system is to identify the sources of variability in historical temperature and precipitation. We can separate the series of average temperature and

precipitation totals per year into components that are driven by (1) long-term trends, (2) decadal cycles, and (3) interannual variation.

Long-term trends can be predicted many years in advance. Decadal cycles are more difficult to predict, but forecasts are often available months or years ahead. The remaining unpredicted changes in temperature and precipitation are idiosyncratic to a particular year and typically unpredictable before that year.

The table below shows the portion of variability over the past hundred years that falls into each of these three components for land areas between 30°N and 30°S.

Temperature and precipitation show very different patterns of uncertainty. A large part of the region's temperature is described by the long-term trend (60-64%), reflecting the relative certainty of long-term temperature increases. Most of the remaining uncertainty for temperature is represented by inter-annual variation, and this portion of each year's temperature is very difficult to predict.

In contrast, there is very little long-term trend in precipitation. While climate change is expected to increase the rate of precipitation on average, observed changes are very small. However, in the case of precipitation, decadal cycles explain some amount of the variation (17-25%), with changes in ocean temperatures driving decade-long increases and decreases in precipitation. There remains still a large fraction of each year's precipitation which is unaccounted for.

| Temperature | Component | Annual Average | Sep. - Nov. |
|---|---|---|---|
| | Long-term Trend | 64% | 60% |
| | Decadal Cycles | 6% | 11% |
| | Inter-Annual Variation | 29% | 26% |
| Precipitation | Long-term Trend | 1% | 1% |
| | Decadal Cycles | 17% | 25% |
| | Inter-Annual Variation | 81% | 69% |

Table 1.1: From `http://iridl.ldeo.columbia.edu/maproom/Global/Time_Scales/temperature.html` and `http://iridl.ldeo.columbia.edu/maproom/Global/Time_Scales/precipitation.html`. Blossoming has been found to be the most sensitive time for coffee plants[2], and Sep. - Nov. is this period in Brazil, the largest coffee producer.

As the relative importance of each of these components varies widely by location, it is useful to look at regional maps of these patterns. The Time Scales Maproom from the International Research Institute for Climate and Society (IRI) provides a way of decomposing variability in temperature and precipitation over space. This decomposition represents how much of the "story" of year-to-year temperatures and precipitation amounts is explained by either a long-term trend, a 10-year long running average, or by neither of these. Decompositions for temperature and precipitation, against the long-term trend and decadal cycles drivers, are shown in figures 1.2 and 1.3.

The temperature maps show that little of the year-to-year variation is explained by a long-term trend in many coffee-growing regions. In particular, this historical analysis shows almost no explanatory capacity for Colombia and much of Indonesia. However, coffee growing regions of Brazil and India are strongly explained by the long-term trend, suggesting that future climate predictions for these areas will be most reliable. As above, almost none of the the year-to-year variation in precipitation is explained by the long-term trend, but moderate amounts driven by decadal cycles, particularly in Colombia and India.

[2] E.g., for Nicaragua: `http://www.academia.edu/2243528/Coffee_yield_variations_and_their_relations_to_rainfall_events_in_Nicaragua`.

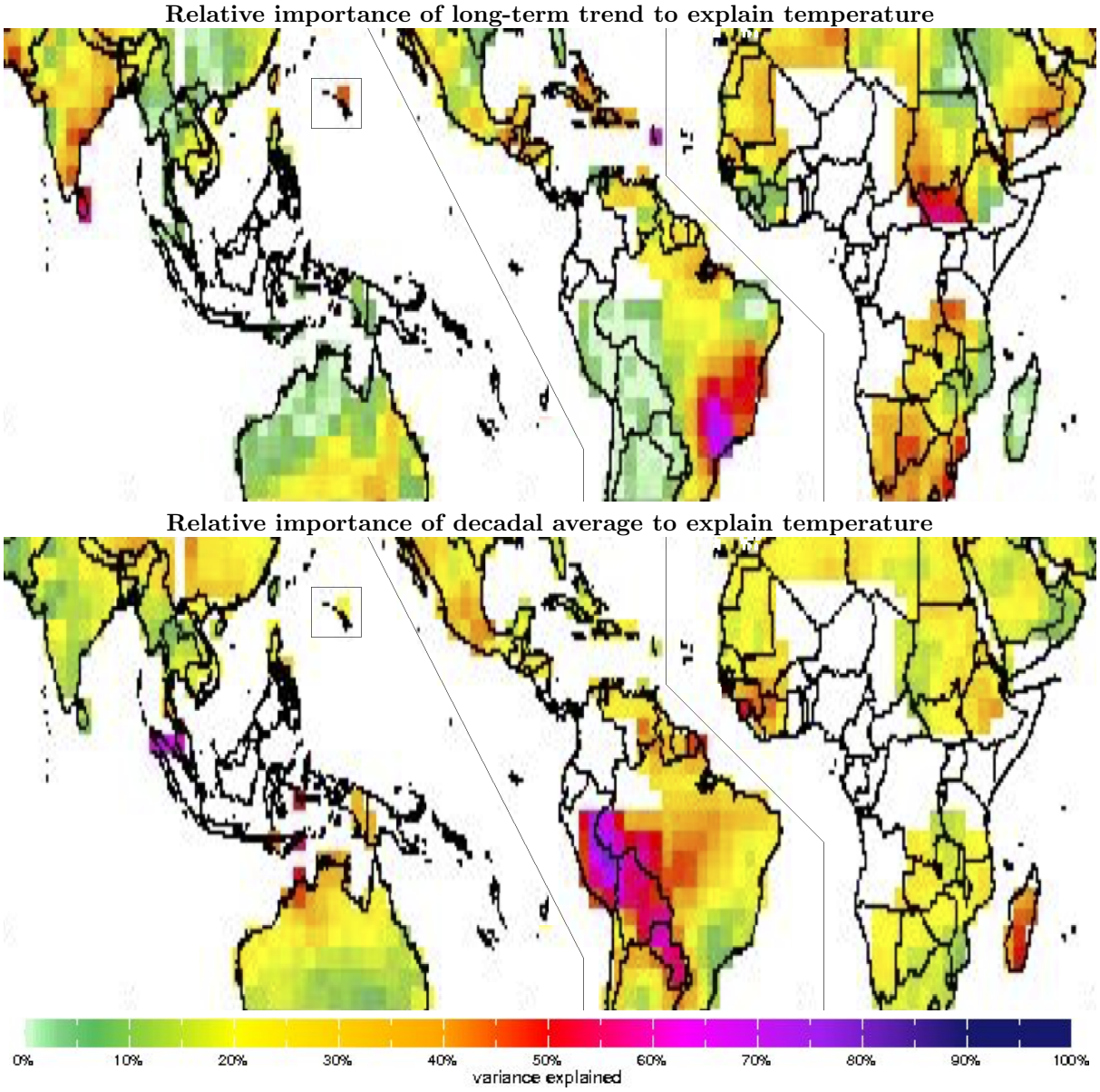


Figure 1.2: The role of long-term and decadal variation in temperature for explaining total temperature variation, from `http://iridl.ldeo.columbia.edu/maproom/Global/Time_Scales/temperature.html`. The colors show the percentage of variance in year-by-year annual temperatures explained by a trend (top) or decadal average (bottom).

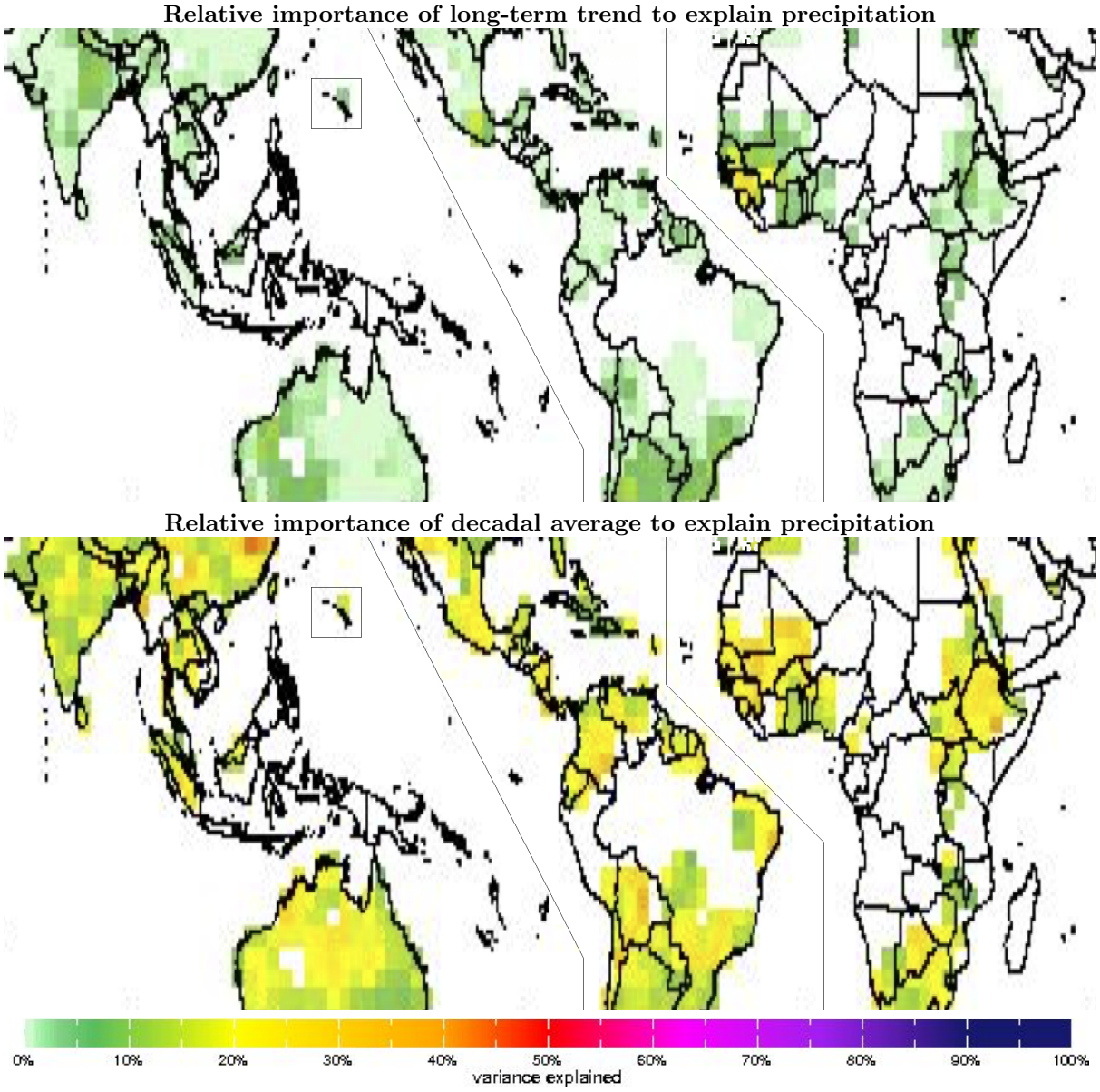


Figure 1.3: The role of long-term and decadal variation in precipitation for explaining total precipitation variation, from `http://iridl.ldeo.columbia.edu/maproom/Global/Time_Scales/precipitation.html`. The colors show the percentage of variance in year-by-year annual precipitation totals explained by a trend (top) or decadal average (bottom).

## 1.2 Future climate projections

Climate projections are produced by sophisticated physical models called Global Climate Models (GCMs). They apply scientific knowledge about the radiative heating of the atmosphere, its interaction with the ocean, and the movement of heat and water in response to human and natural drivers. The most recent report from the IPCC (Stocker et al., 2014) was produced in conjunction with a project to collect and harmonize results from all available GCMs. We use these 'CMIP5' models to study the changes in future climate and uncertainty surrounding them.

GCMs are calculated at a lower spatial resolution than we require to study coffee. A further process of downscaling expands the changes predicted by GCMs to produce high resolution projections. This process comes with additional uncertainty, since the feedbacks embodied in the GCM are not used when the resolution is improved. The downscaling dataset we use is WorldClim (Hijmans et al., 2005), available at a resolution of 5 arc-minutes (about 9km at the equator), the same resolution as the coffee database. WorldClim contains downscaled results for 17 GCMs under the "business-as-usual" emissions scenario, IPCC RCP 8.5. We study not only the impact of the expected change in climate, but also the range of impacts across the available models of future climate. Table 1.2 and figure 1.4 describe shifts in average climate metrics. The baseline climate is representative of 1950 - 2000. Changes in climate are shown as a distribution over estimates of the change in 2050, according to each GCM. The range of uncertainty in these models is a proxy, but almost certainly an underestimate, for the total uncertainty in future climate.

| Quantity | Baseline (1950-2000) | Change (to 2050) | 50% range |
|---|---|---|---|
| Annual mean temperature | 23.6°C | 2.1°C | [ 1.7 - 2.5 ] |
| Mean diurnal range | 12.6°C | -0.5°C | [ -0.6 - -0.5 ] |
| Temperature seasonality | 3055.0 | 3.9 % | [ 1.9 - 4.4 ] |
| Max temperature of warmest month | 34.2°C | 2.5°C | [ 1.9 - 2.7 ] |
| Min temperature of coldest month | 12.3°C | 1.9°C | [ 1.7 - 2.4 ] |
| Annual precipitation | 1068.0 mm | 1.7% | [ -0.1 - 3.2 ] |
| Precipitation of wettest month | 191.0 mm | 8.0% | [ 5.5 - 11.3 ] |
| Precipitation of driest month | 22.0 mm | -6.8% | [ -12.3 - -2.0 ] |

Table 1.2: Mean changes over the coffee belt and the 25% to 75% quantiles.

As an example, figure 1.5 shows the range of changes in one coffee growing region of Colombia across these 17 GCMs. For some of the aspects of climate listed in table 1.2, all 17 GCMs agree on the direction of the change in this region. The annual mean temperature, and maximum and minimum temperatures are all expected to increase about 2°C over a baseline period from 1950 - 2000. This represents a future average increase of 0.28°C per decade, 75% greater than the current rate. The temperature seasonality, defined as the standard deviation of temperature, is also expected to increase. The other values are less certain, with some models predicting increases and others decreases.

### 1.2.1 Spatial patterns of change and uncertainty

The median changes in climate across 17 GCMs are displayed in figures 1.6 and 1.8 as they vary across the coffee belt in 2050, under a business-as-usual scenario. We report impacts consistent with RCP 8.5, the highest IPCC emissions pathway, throughout this report because current emissions appear to be following this path. Strong climate change action can mitigate these impacts, but the largest benefits of such mitigation will occur after 2050.

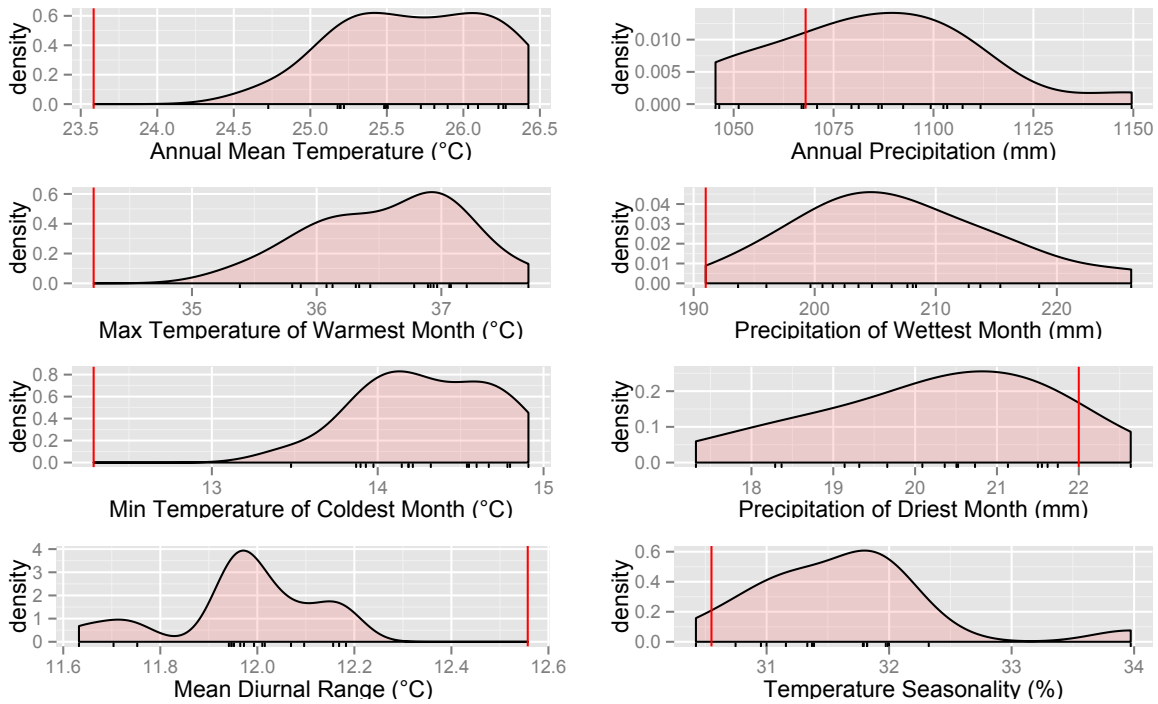


Figure 1.4: The average baseline climatology (red lines) and distribution of possible future climate values in 2050 under RCP 8.5, averaged over all tropic belt land. Small dashes at the bottom show the estimates of each individual GCM model, with the area above it representing this distribution as a curve.

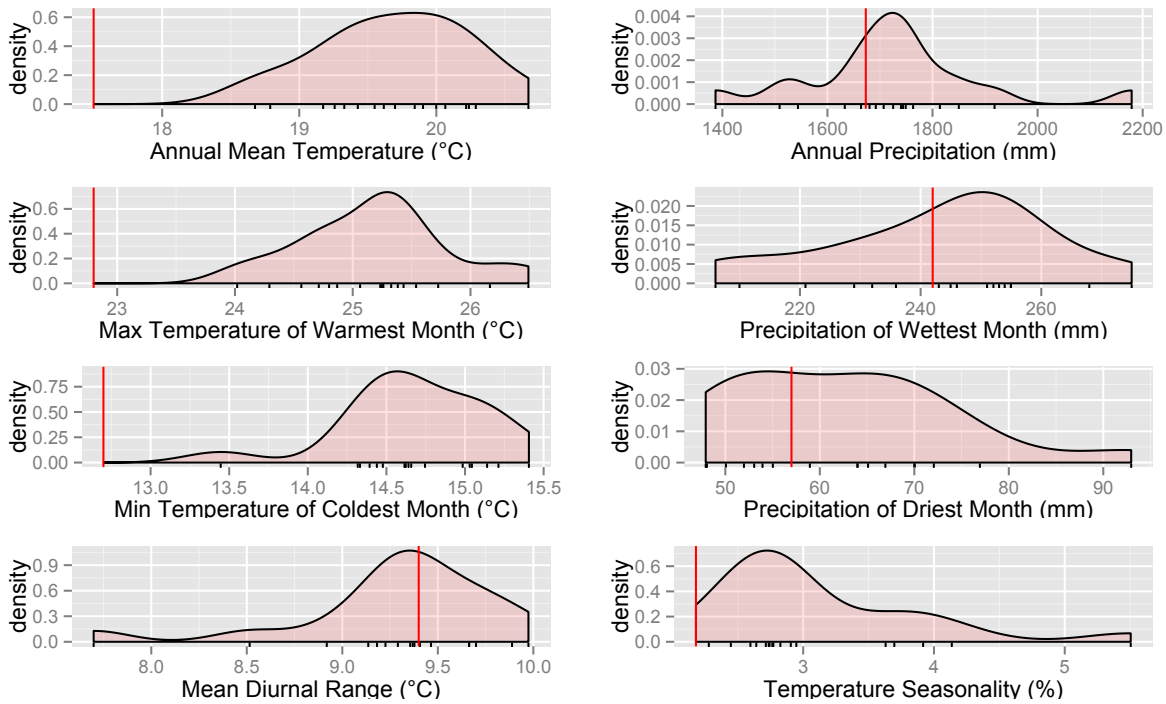


Figure 1.5: The baseline climatology (red lines) and distribution of possible future climate values in 2050 under RCP 8.5, for a location in Colombia at 4°N 76°W. Small dashes at the bottom show the estimates of each individual GCM model, with the area above it representing this distribution as a curve.

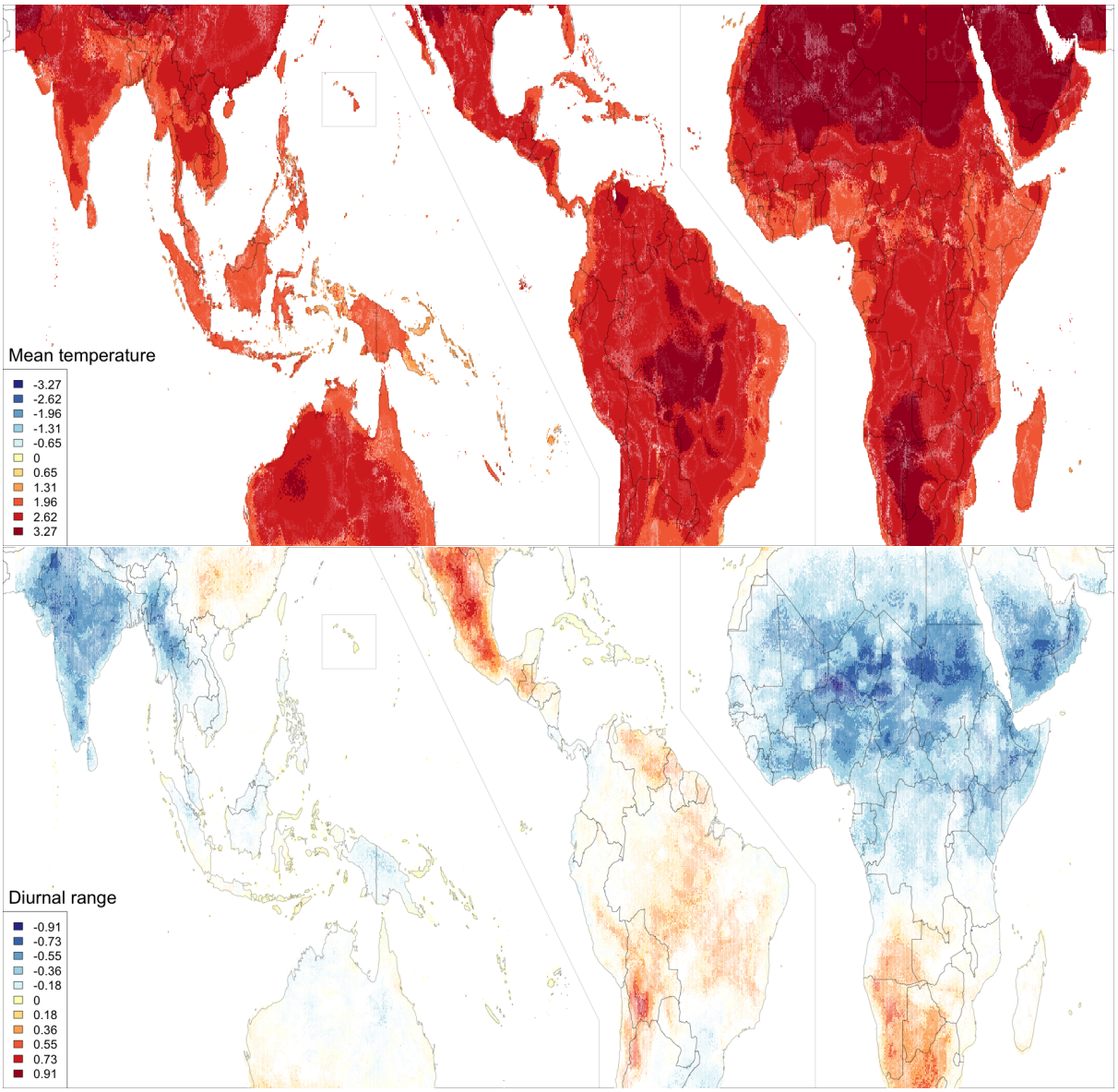


Figure 1.6: Global patterns of level changes in mean annual temperature and diurnal temperature range for 2050 from Hijmans et al. (2005). Areas are faded in proportion to the number of GCMs that do not agree with the sign of the median GCM.

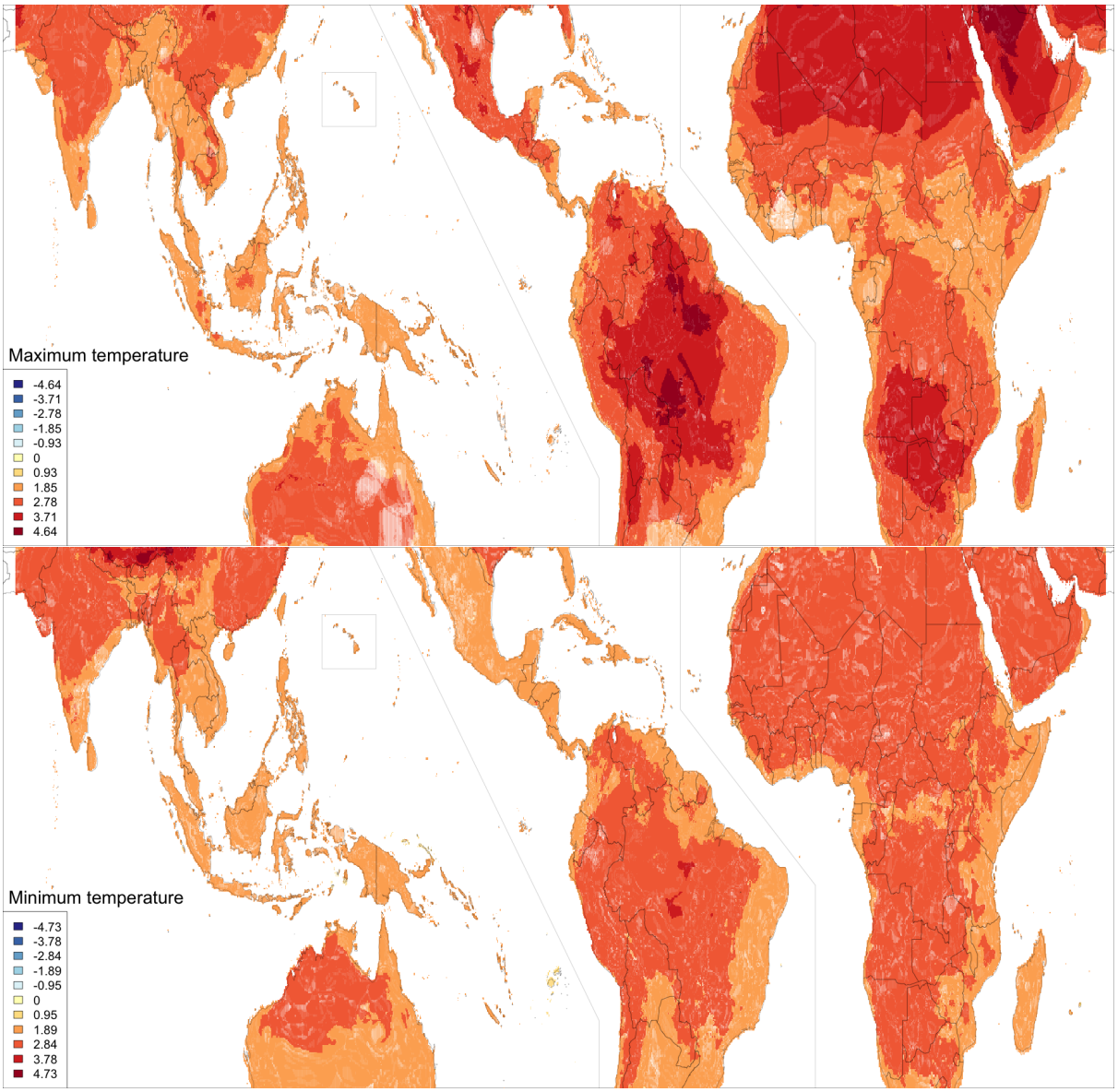


Figure 1.7: Global patterns of level changes in maximum yearly temperature and minimum yearly temperature for 2050 from Hijmans et al. (2005). Areas are faded in proportion to the number of GCMs that do not agree with the sign of the median GCM.

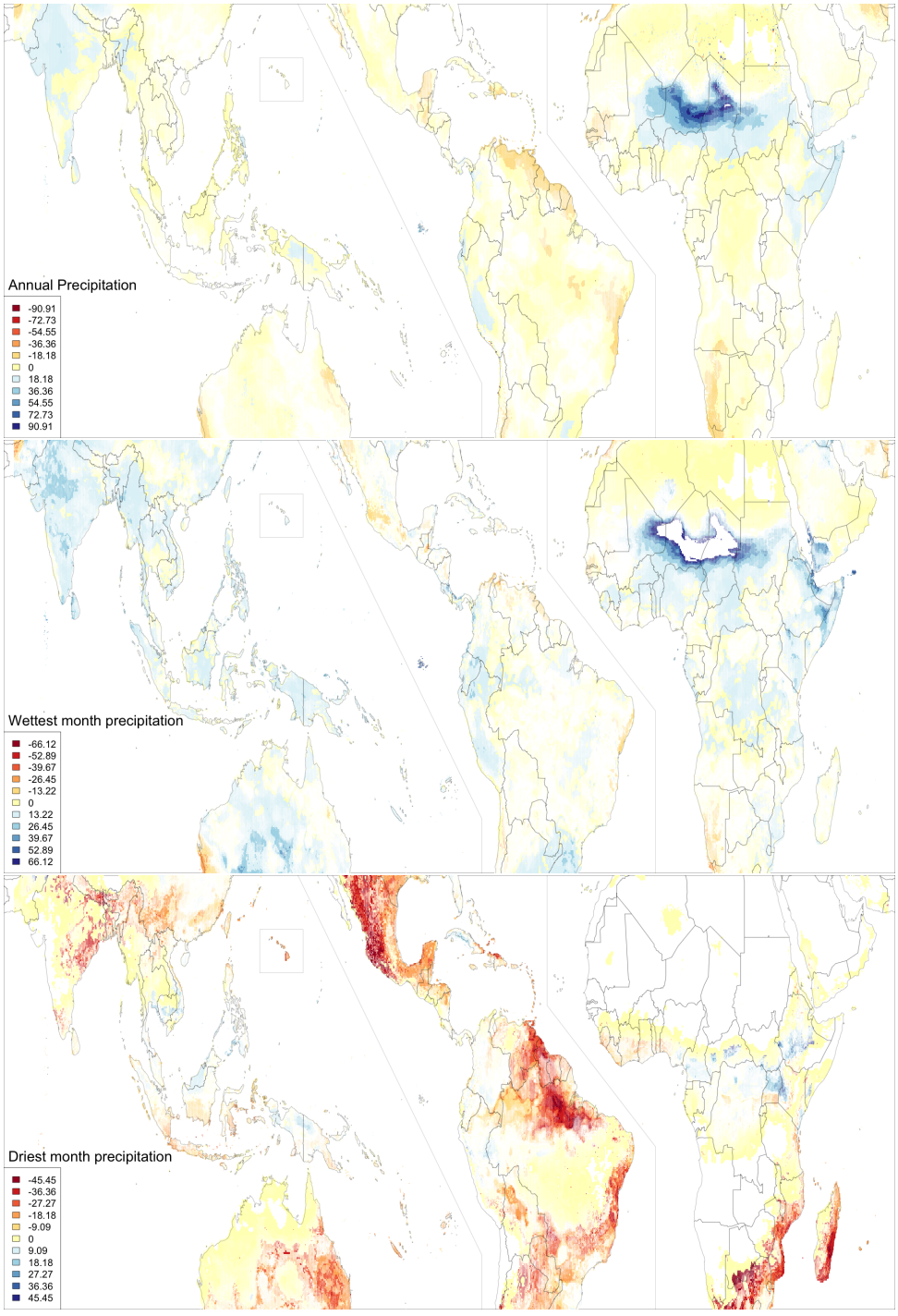


Figure 1.8: Global patterns of percent changes in annual total precipitation, precipitation in the wettest month, and precipitation in the driest month, for 2050 from Hijmans et al. (2005). Areas are faded in proportion to the number of GCMs that do not agree with the sign of the median GCM.

Temperatures increase across the entire region with high confidence, within the explanatory power of these GCMs. The size of these temperature changes generally increases away from the equator, with most coffee growing regions seeing an increase of 1 - 2°C by 2050. The pattern for the diurnal (day-night) temperature range is more complicated, with increases in the Americas and decreases across northern Africa and South Asia. Precipitation changes are less certain, with decreases on the coasts of Brazil, and increases in northern Africa and India.

# Chapter 2

# A new coffee production database

In this report, we identify the relationships between climate and coffee through careful, empirically-grounded methods. Identifying the locations of coffee production is essential for understanding how coffee is already interacting with the climate and how it will respond to climate change. High resolution weather station and gridded weather data are readily available, to identify regions subjected to high temperatures, frosts, precipitation, and humidity, but their impacts is most clear when the weather and coffee data are closely aligned in space. Similarly, climate change suitability maps are more useful when compared to high-resolution information about the current location of coffee growing areas.

Applying robust spatial methods requires a new global database of coffee production. We develop an initial version of this database, combining existing records of coffee production with geospatial maps of coffee producing areas. However, much work remains to be done. Over 50 countries produce coffee, but information stored in the database for most of these countries is sparse.

Many groups can contribute to the database as we have created it. As part of the database, we have developed standardized formats and a clear flow for combining multiple kinds of spatial and temporal data. Organizations involved in collecting and organizing coffee production data can contribute to a collaborative process, which together will provided better data for a large range of research activities.

Previous global datasets only provide coarse information on coffee production. The most reliable global information on coffee production, at the ICO, the FAO, and the USDA Foreign Agricultural Service, is only available on a per-country basis. CIAT has constructed a database of information on coffee farms (see figure 2.1), but our analysis requires production information as it changes over time. To our knowledge, there is no previously existing global dataset of coffee producing regions at the subnational level.

Monfreda et al. (2008) provide an approximate geographic distribution for coffee, by first identifying global cropland at high resolution (5'), and then using country-specific databases of coffee production, where available, to refine the areas. The quality of the resulting production areas varies widely by country, as shown in figure 2.2. For most countries, only country-level production is available. Four countries have county-level data on coffee production, and 13 others have state-level production information.

We have combined the information from the FAO, the UDDA, the CIAT farm map, and Monfreda et al. with detailed maps of coffee production regions for 8 major coffee producing countries. These countries produce roughly 85% of the world's coffee. These high-resolution country-specific maps allow us to assess the characteristics of coffee production at much greater detail, both in terms of climate variables such as temperature and precipitation, and, in chapter **??**, geographical variables, such as latitude and elevation. Combining these factors with data on yields in these areas allows us to estimate the effects

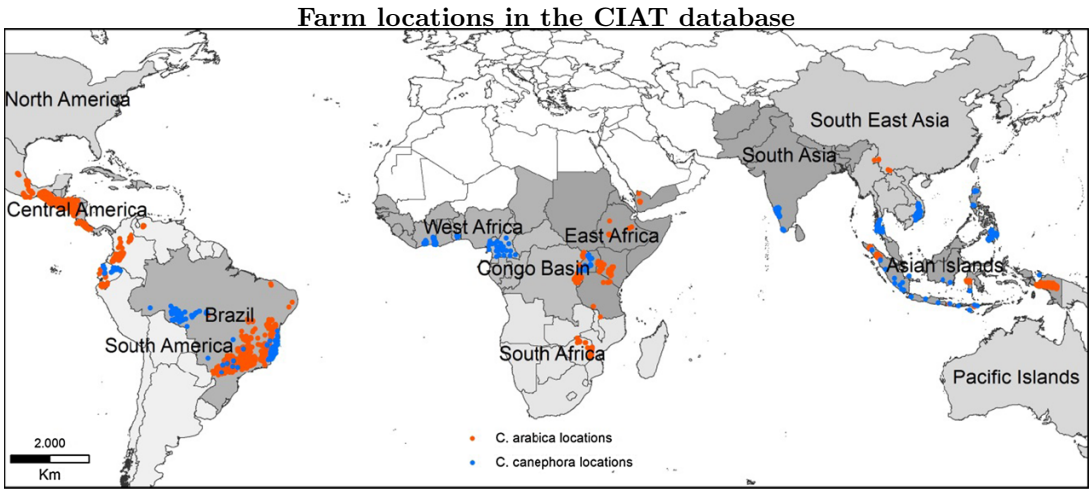


Figure 2.1: Arabica and Robusta coffee producing farms in the CIAT database.

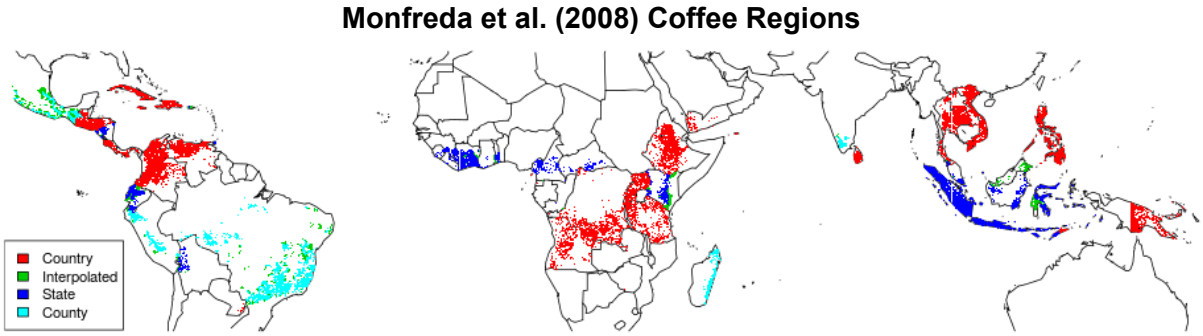


Figure 2.2: Quality of geospatial production data for coffee, from Monfreda et al. (2008). Global agricultural areas are intersected with country-specific datasets to create a global map of coffee production areas.

of weather patterns on coffee growing, as well as study the range of climates where coffee can be grown successfully.

A summary of this information is provided in table 2.1 and some production area maps are included in appendix B, along with a description of the process for combining these maps.

| Country | Production | Coverage | Resolution | Source |
|---|---|---|---|---|
| Brazil | 2,720 kt | country-wide | municipality (5503) | IBGE |
| Vietnam | 1,650 kt | country-wide | raster image | Cafecontrol |
| Colombia | 696 kt | country-wide | raster image | Oficina de E. y P. Básicos Cafeteros |
| Indonesia | 411 kt | 6 regions | raster image | Schroth (2014) |
| Ethiopia | 390 kt | country-wide | raster image | GAIN (2013) |
| India | 300 kt | country-wide | state (13) | Coffee Board (India Gov.) |
| Mexico | 270 kt | country-wide | raster image | **?** |
| Guatemala | 240 kt | country-wide | vector layers | MFEWS |
| El Salvador | 82 kt | country-wide | raster image | Poyecto Programa Ambiental |
| Nicaragua | 78 kt | country-wide | raster image | MFEWS |
| Tanzania | 50 kt | country-wide | raster image | Caparo et al. (2015) |
| Haiti | 21 kt | country-wide | vector image | Coffee Supply Chain Risk Ass. Miss. |
| Rwanda | 21 kt | country-wide | points | Nzeyimana (2014) |
| Yemen | 14 kt | country-wide | raster image | **?** |
| Total | 7,766 kt | global | country | ICO, FAO, USDA FAS |
| | | global | inferred raster | Monfreda et al. (2008) |
| | | global | points | Bunn et al. (2015), CIAT |

Table 2.1: Sources of spatial coffee production, from academic literature, government agencies, and NGO reports. Average production values are taken over the past decade. The resolution is listed as either a reporting level (municipality, state, country), as a graphical map (raster image, vector layers), a gridded analysis (inferred raster), or individual points (points).

Similarly, yield data for coffee at a finer resolution than the country level helps identify more closely the impact of existing climate dynamics on yield. Table 2.2 summarizes the data collected on yields, production, area planted and harvested, and fertilizer use. Yields are typically reported as the quantity of coffee produced in an area (which we standardize to metric tonnes), divided by the area undergoing harvest which we report in hectares). A better measure of yield would divide the number of hectares that was planted, as measured two to three years before the harvest to capture the potential loss of plants before and after maturity.

| Country | Variables | Time | Space | Organization |
|---|---|---|---|---|
| India | Planted, Produced, Yield | 32 years (1951 - 2013) | 15 growing regions | Knoema |
| Brazil | Harvested, Produced | yearly (1990 - 2012) | 5624 municipalities | IBGE |
| Indonesia | Area, Produced, Yield | 2011 | 20 districts (Kecamatan) | Dinas Pertanian |
| Rwanda | Area, Agroforested, Yield | 2005 | 10 growing regions | NAEB |
| Vietnam | Area | 2012, 2013 | 11 provinces + other | GAIN |
| Brazil | Fertilizer use | 2002 | 5 regions | FAO |
| global | Harvested, Produced, Yield | 1961 - 2012 | 86 countries | FAO |
| global | Produced (by variety), Stocks, Export, Consumption | 1960 - 2013 | 79 countries | USDA FAS |
| global | Fertilizer use | 1995 - 2002 | 24 countries | FertiStats |

Table 2.2: Sources of global and sub-country data on coffee yields, total production, and planted and harvested area.

### 2.0.1 Confidence maps

The first result of the database is its own measure of confidence in the geographic data across the globe. The confidence maps reflect the combined amount of information available, across the multiple map inputs. Each contributing map is assigned its own confidence, with maps of global harvest having low or medium confidence and maps detailing a given country with high confidence. Where multiple input maps corroborate each other, the confidence increases (see appendix B.2.1). In figure 2.3, dark green represents low confidence, and yellow and tan colors represent high confidence. The band of lighter green in the middle shows the overlap between maps from Thurston et al. (2013), Monfreda et al. (2008), and Bunn et al. (2015).

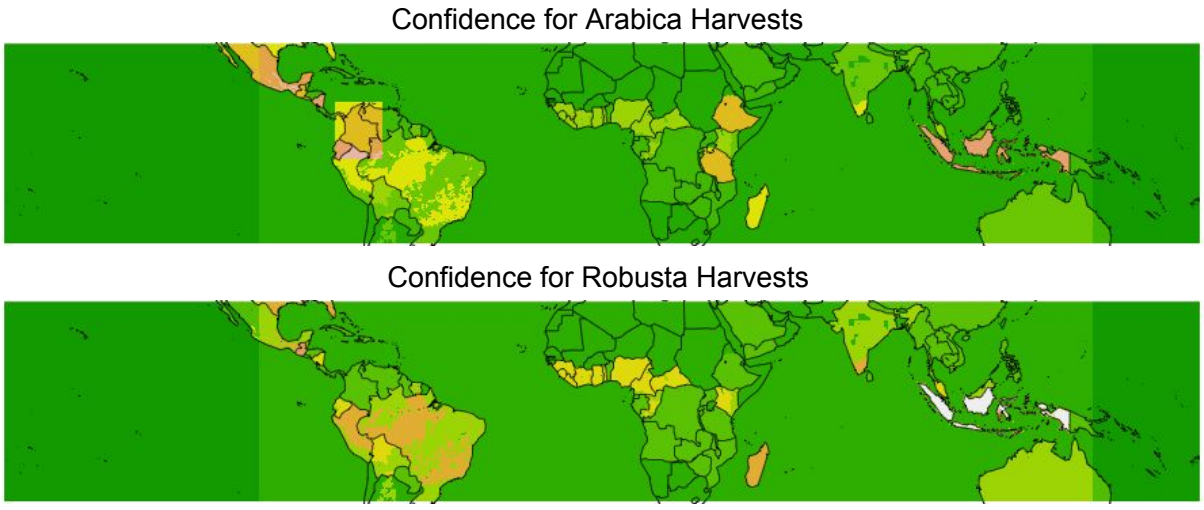


Figure 2.3: Database geospatial harvest confidence, based on the amount and scale of data available.

### 2.0.2 Harvest maps

The harvest maps are the main output of the spatial portion of coffee database. For each month, these combine country-specific information (some of which specifies harvest months as they differ across the country), with global harvesting regions applied to a calendar of harvest months from Sweet Maria (2015). Some country calendars are unavailable, so these harvested regions show throughout the year. The added weight of these multiple instances will be handled next.

A visual representation of the coffee database is shown in figure 2.6. We use average country-wide total harvest areas from FAO to translate harvest patterns into a description of the portion land area that is harvested. In areas where only country-level data is available, such as China, the entire country is shown as having a uniform low harvest. Where detailed coffee production data is available, such as in Brazil, the intensely cultivated areas are distinguished from those where coffee is absent. The values shown in the figure are used to combine weather information when estimating the effects of weather revealed in country-wide production records.

A visual representation of the coffee database is shown in figure 2.6. We use average country-wide total harvest areas from FAO to translate harvest patterns into a description of the portion land area that is harvested. In areas where only country-level data is available, such as China, the entire country is shown as having a uniform low harvest. Where detailed coffee production data is available, such as in Brazil,

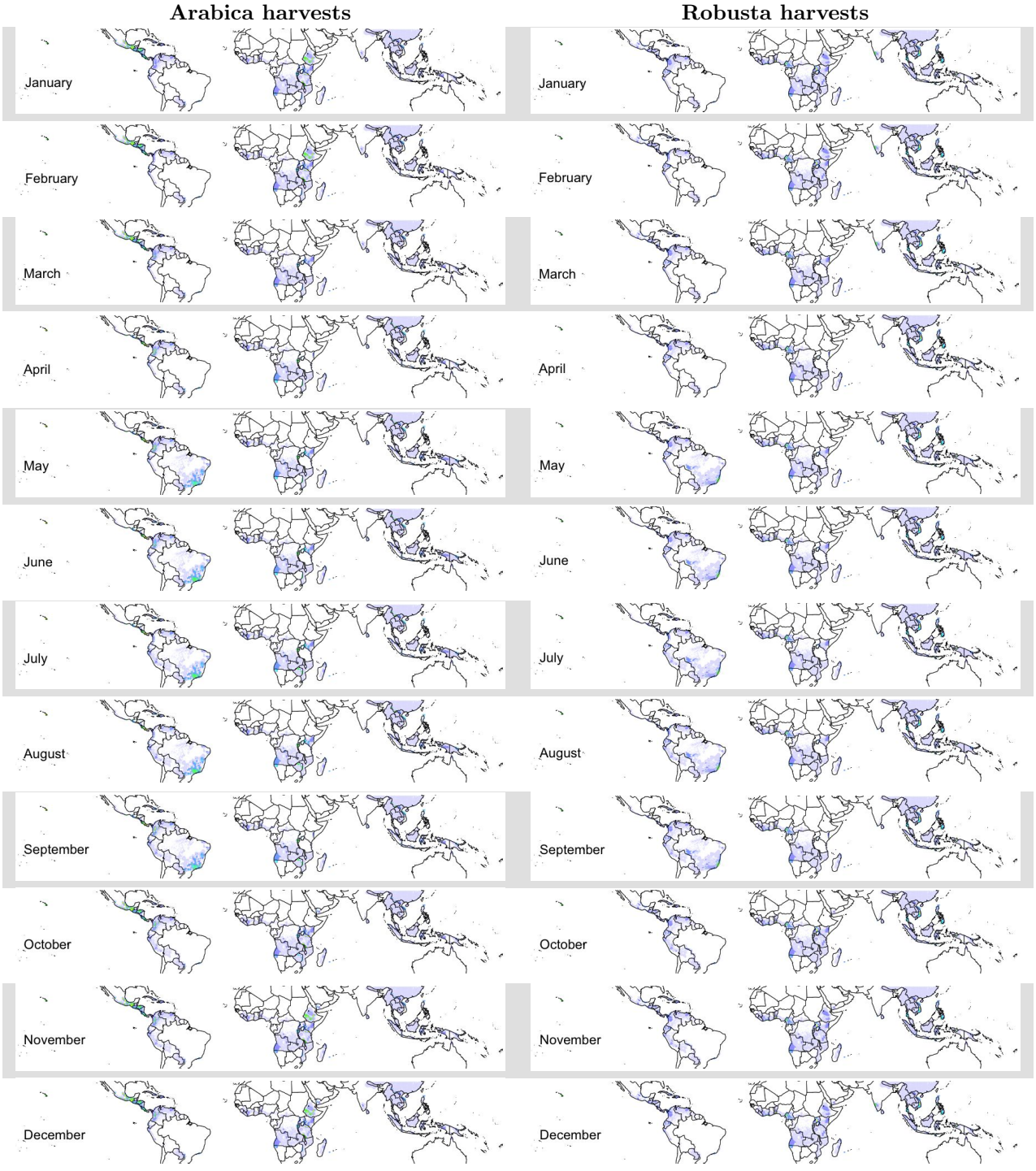


Figure 2.4: Harvest maps for Arabica and Robusta varieties, during each month. Darker colors represent higher levels of evidence that these regions are undergoing harvest in the given month.

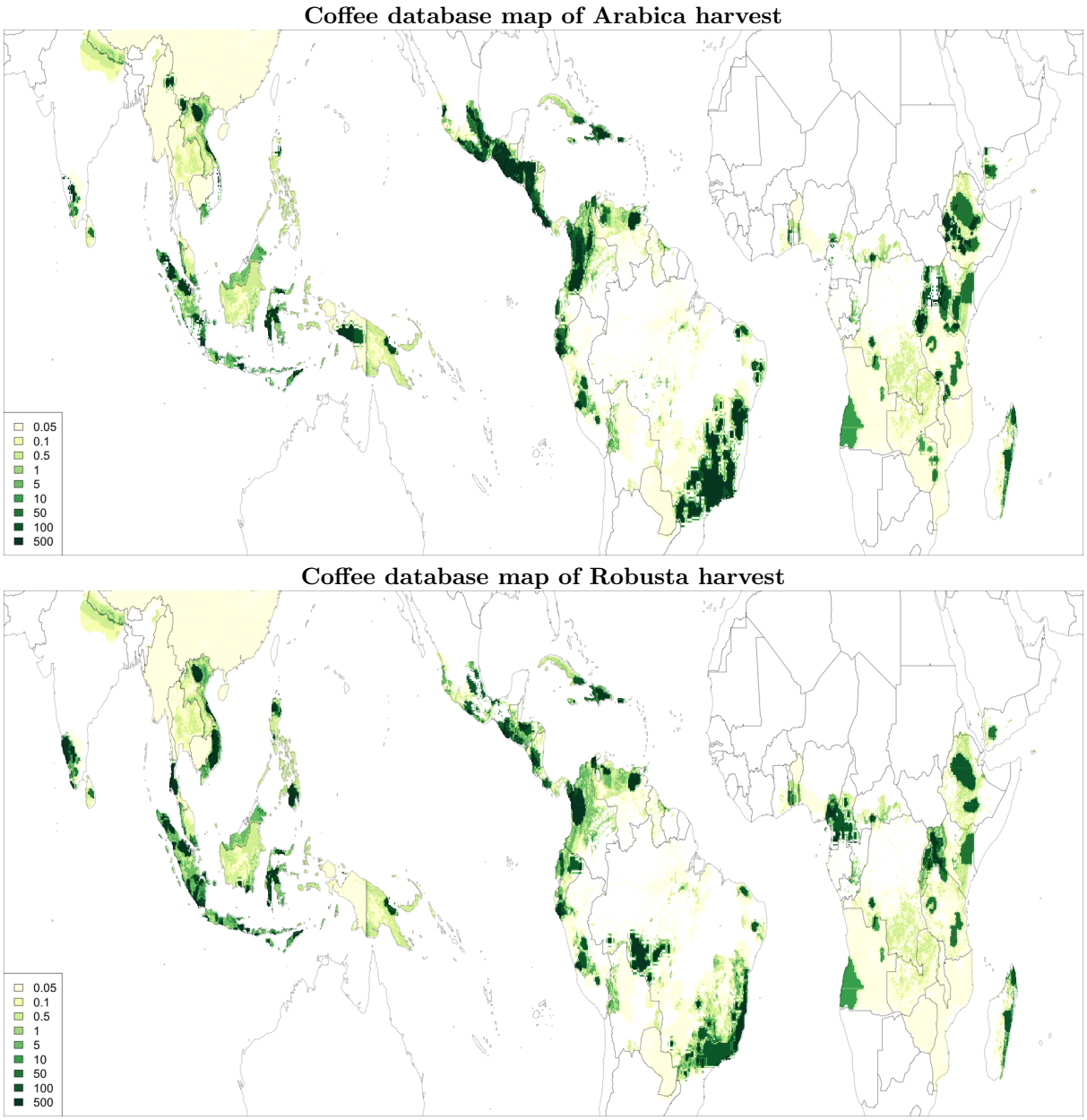


Figure 2.5: The spatial distribution of Arabica and Robusta harvests, as represented by spatial harvest maps. Harvest maps are combined across all months, and re-weighted so that the sum of grid cell values within a country is equal to the average harvested area in the most recent years of harvest.

the intensely cultivated areas are distinguished from those where coffee is absent. The values shown in the figure are used to combine weather information when estimating the effects of weather revealed in country-wide production records.

### 2.0.3 Time series data

Both FAO and the USDA Foreign Agricultural Service report production information for coffee, but the information they provide is quite different. FAO reports total production and harvested area, for all varieties of coffee combined, with a total of 4242 observations. The USDA reports only production information, but divides it out by Arabica and Robusta production, with 3211 observations per variety. The number of countries included also varies by year (see figure 2.7).

A second complication arises from the definition of the reported year. FAO reports production for calendar years, while USDA reports it for market years which vary by country. This can be an opportunity, allowing us to determine more precisely when production occurs. For example, in Brazil, coffee is harvested mainly between May and September. However, the USDA market year for Brazil is from July to June. So, discrepancies between the FAO and USDA production totals allow us to distinguish, approximately, between the share of production before and after July, the start of the market year cycle.

**Calculating intra-year production**

The diagram below shows how the USDA and FAO calendars align. The actual division is different for each country, depending on the start of the USDA market year.

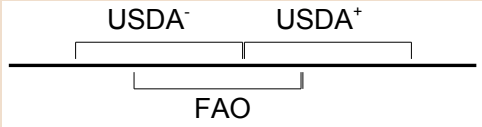


We divide each USDA value into "left" and "right" parts, with $USDA^L = \alpha USDA$ and $USDA^R = (1-\alpha)USDA$, where the coefficient $\alpha$ is unknown. Further, we know from the diagram that $USDA^R_- + USDA^L_+ = FAO$; that is, the FAO year consists of the 'right' (latter) portion of one market year and the 'left' (early) portion of the next one. Finally, we can use the difference to estimate $\alpha$ from

$$FAO_t - USDA_{t+} = \alpha(USDA_{t-} - USDA_{t+}) + \epsilon_t$$

We estimate this division for each country. In the case of Brazil, we find that 12% of production occurs between May and June, and 88% between July and September. A full table of these portions is shown in table 2.3. Where there are blanks, the two datasets could not be consistently combined.

Using these values, we can construct a monthly timeseries of production, as shown in figure 2.8.

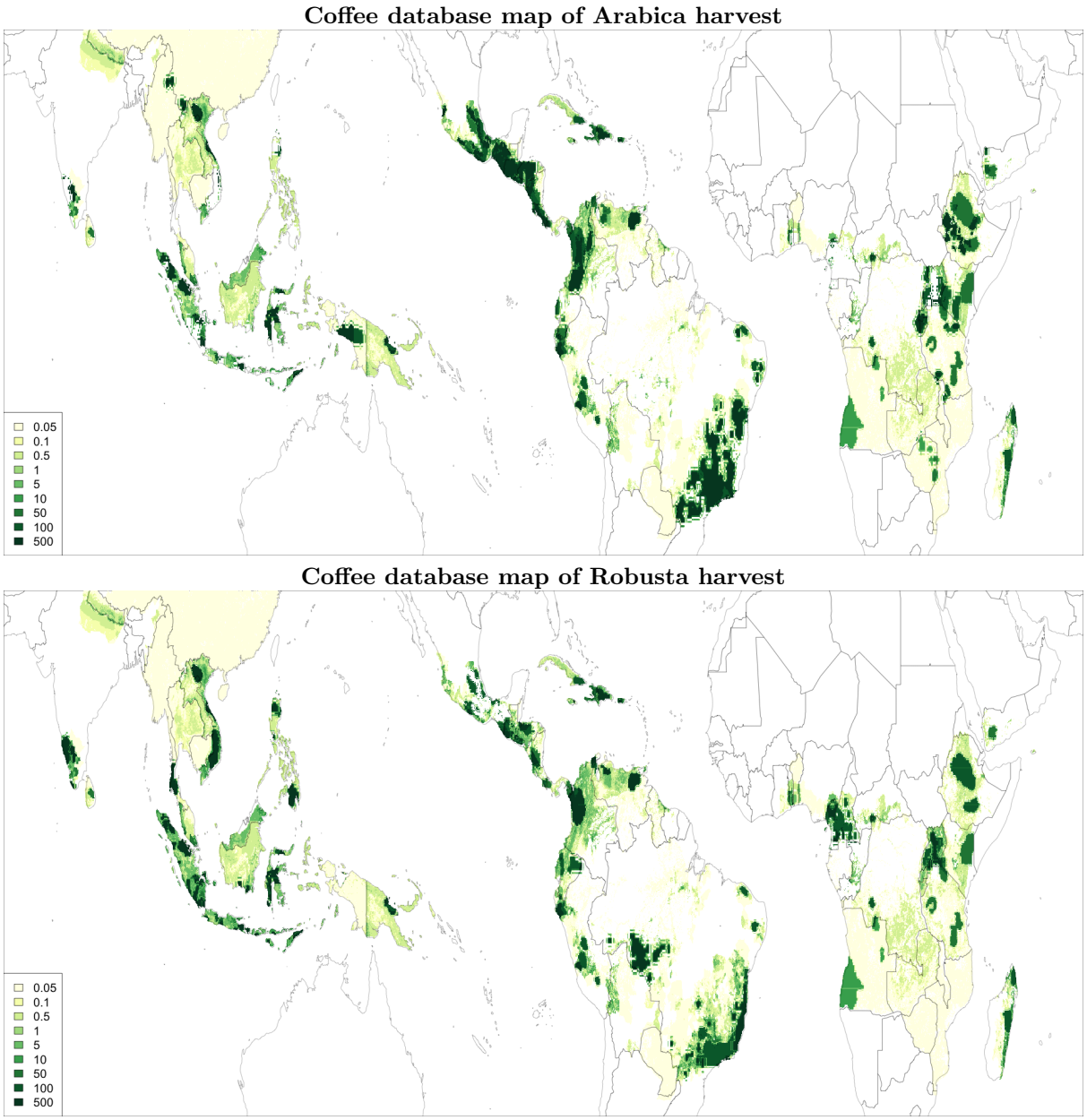


Figure 2.6: The spatial distribution of Arabica and Robusta harvests, as represented by spatial harvest maps. Harvest maps are combined across all months, and re-weighted so that the sum of grid cell values within a country is equal to the average harvested area in the most recent years of harvest.

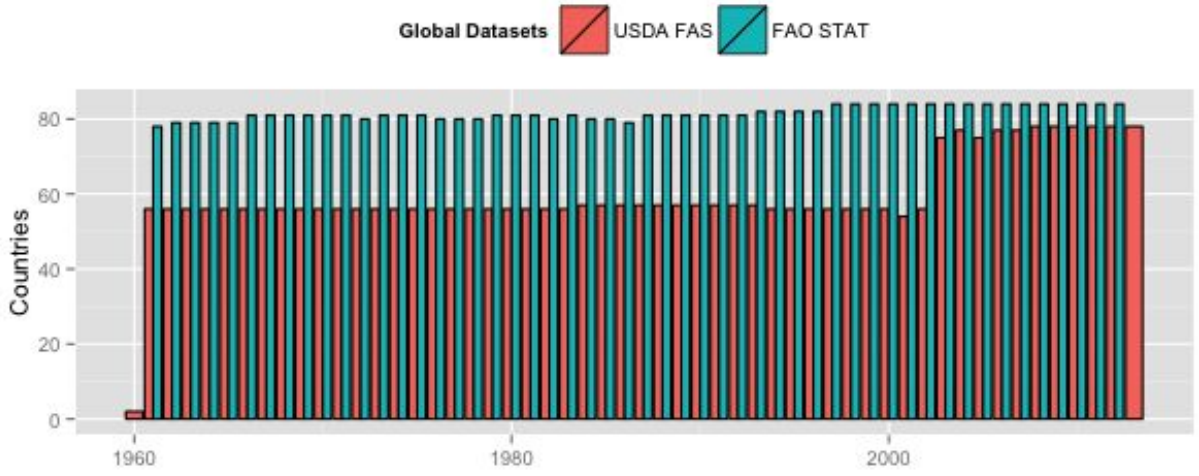


Figure 2.7: The number of countries with coffee production data available by year.

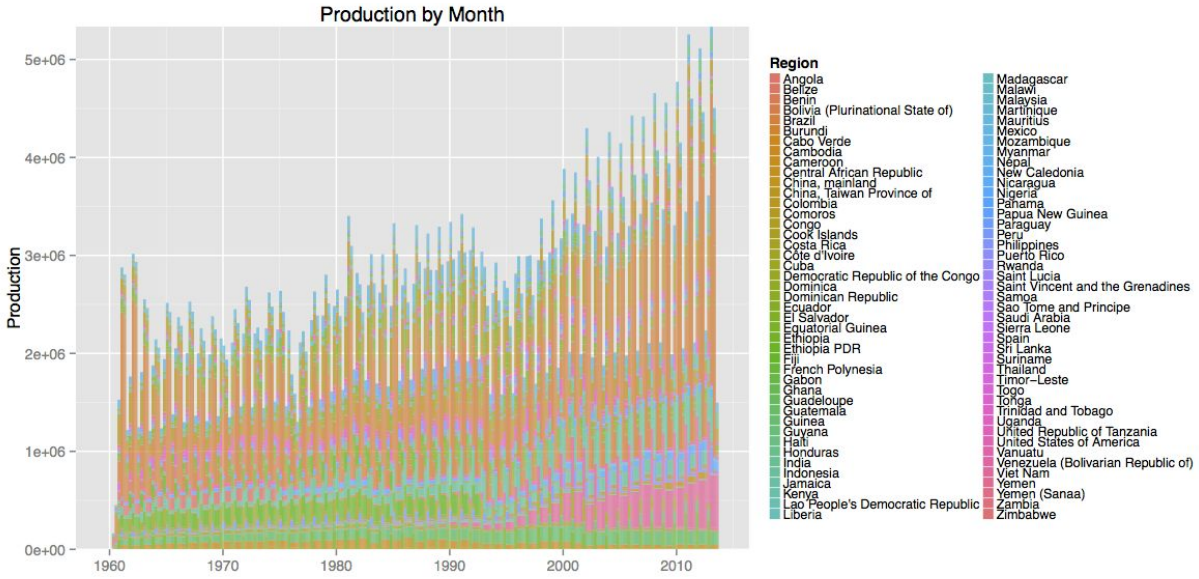


Figure 2.8: Production by month and country, inferred by the discrepancies between USDA FAS and FAO accounting systems.

| | Market Year | Previous Year | Following Year | Std. Err. |
|---|---|---|---|---|
| Brazil | Jul - Jun | 0.12 | 0.88 | 0.05 |
| Madagascar | Apr - Mar | 0.50 | 0.50 | 0.25 |
| Kenya | Oct - Sep | 0.91 | 0.09 | 0.04 |
| Guinea | Oct - Sep | 0.37 | 0.63 | 0.33 |
| Panama | Oct - Sep | 0.68 | 0.32 | 0.28 |
| Costa Rica | Oct - Sep | 0.50 | 0.50 | 0.06 |
| Ethiopia | Oct - Sep | | | |
| Rwanda | Apr - Mar | 0.17 | 0.83 | 0.08 |
| United Republic of Tanzania | Jul - Jun | 0.67 | 0.33 | 0.11 |
| Sri Lanka | Oct - Sep | | | |
| Peru | Apr - Mar | 0.07 | 0.93 | 0.10 |
| Lao People's Democratic Republic | Oct - Sep | | | |
| Bolivia (Plurinational State of) | Apr - Mar | | | |
| Cameroon | Oct - Sep | 0.09 | 0.91 | 0.11 |
| Côte d'Ivoire | Oct - Sep | 0.89 | 0.11 | 0.07 |
| Ecuador | Apr - Mar | 0.41 | 0.59 | 0.25 |
| Benin | Oct - Sep | 0.60 | 0.40 | 0.20 |
| Ghana | Oct - Sep | 0.80 | 0.20 | 0.16 |
| Cuba | Jul - Jun | 0.46 | 0.54 | 0.16 |
| El Salvador | Oct - Sep | 0.40 | 0.60 | 0.05 |
| Venezuela (Bolivarian Republic of) | Oct - Sep | 0.57 | 0.43 | 0.15 |
| Papua New Guinea | Apr - Mar | 0.26 | 0.74 | 0.07 |
| Malawi | Oct - Sep | 0.10 | 0.90 | 0.16 |
| Togo | Oct - Sep | 0.44 | 0.56 | 0.16 |
| Guatemala | Oct - Sep | 0.42 | 0.58 | 0.17 |
| Zimbabwe | Oct - Sep | 0.19 | 0.81 | 0.10 |
| Viet Nam | Oct - Sep | 0.63 | 0.37 | 0.07 |
| Dominican Republic | Jul - Jun | 0.55 | 0.45 | 0.15 |
| Nigeria | Oct - Sep | 0.68 | 0.32 | 0.19 |
| Liberia | Oct - Sep | 0.56 | 0.44 | 0.14 |
| Democratic Republic of the Congo | Oct - Sep | 0.61 | 0.39 | 0.14 |
| Paraguay | Oct - Sep | 0.60 | 0.40 | 0.34 |
| Trinidad and Tobago | Oct - Sep | 0.77 | 0.23 | 0.10 |
| Philippines | Jul - Jun | | | |
| Indonesia | Apr - Mar | 0.23 | 0.77 | 0.29 |
| Central African Republic | Oct - Sep | 0.22 | 0.78 | 0.14 |
| New Caledonia | Oct - Sep | | | |
| United States of America | Oct - Sep | 0.19 | 0.81 | 0.65 |
| Guyana | Oct - Sep | | | |
| Honduras | Oct - Sep | 0.56 | 0.44 | 0.08 |
| Yemen | Oct - Sep | 0.36 | 0.64 | 0.86 |
| Haiti | Jul - Jun | 0.36 | 0.64 | 0.19 |
| Thailand | Oct - Sep | 0.77 | 0.23 | 0.07 |
| Jamaica | Oct - Sep | 0.69 | 0.31 | 0.98 |
| Angola | Apr - Mar | 0.62 | 0.38 | 0.11 |
| Equatorial Guinea | Oct - Sep | | | |
| Mexico | Oct - Sep | 0.62 | 0.38 | 0.22 |
| India | Oct - Sep | 0.98 | 0.02 | 0.02 |
| Sierra Leone | Oct - Sep | 0.98 | 0.02 | 0.60 |
| Malaysia | Oct - Sep | 0.58 | 0.42 | 0.33 |
| Congo | Oct - Sep | 0.28 | 0.72 | 0.26 |
| Colombia | Oct - Sep | 0.72 | 0.28 | 0.06 |
| Burundi | Apr - Mar | 0.06 | 0.94 | 0.09 |
| Gabon | Oct - Sep | 0.23 | 0.77 | 0.17 |
| Uganda | Oct - Sep | 0.83 | 0.17 | 0.09 |
| Nicaragua | Oct - Sep | 0.13 | 0.87 | 0.08 |
| Zambia | Oct - Sep | 0.93 | 0.07 | 0.35 |

Table 2.3: Portion of the production for each market year attributed to the previous calendar year and to the next one.

# Chapter 3

# Climate suitability

Land areas that are suitable to coffee production will shift drastically over the next 35 years. In this chapter, we develop a new approach to estimating suitability, drawing upon surveys, records, model data, and biological knowledge.

Historically, the coffee plant has already managed vast climatic transitions, spreading from Ethiopia and Yemen to over 70 countries. These may be an indication of further adaptive potential. However, when coffee is cultivated in marginal areas, bean quality drops and the plant becomes more susceptible to disease. Estimates of suitability are always uncertain, since we have never experienced a climate like that 2050. In light of this, it is important to develop an approach to suitability that represents the uncertainty of its estimates and is conservative in light of the lack of knowledge.

## 3.1 Observed suitability changes

Coffee yields have shifted over the past decade, as a result of many factors including climate change. Some areas have seen increases in per-hectare yields from improved agricultural practices and varieties, while others have been hit by expanded diseases. In some cases, these diseases are also driven by changes in climate: for example, the coffee berry borer and coffee white stem borer have benefited from increases in temperatures in Africa (Jaramillo et al., 2011; Kutywayo et al., 2013), and coffee rust responds to changes in humidity (Alves et al., 2011). Trends in yields reflect a combination of all of these factors.

As shown in figure 3.1, yields have shifted for each country since 2000. Many equatorial regions have been hit hardest, particularly central and west Africa. The greatest decrease in yields has been experienced by Zimbabwe, with an average of an almost 8% decrease in yields per year, from 14,000 Hg/Ha in 2000-2003 to 4,500 Hg/Ha in 2009-2012. The greatest increase is nearby, in Angola, from 1,100 Hg/Ha in 2000-2003 to 13,000 Hg/Ha in 2009-2012.

We can explore the climate connection more closely in Brazil, where coffee yields are reported at the high-resolution municipality level. Trends across Brazil vary from positive to negative, as shown figure 3.2. Many of these trends are not the result of climate or weather. New management practices, seed varieties, and changes in the quality of land used to grow coffee can be important drivers.

However, in addition to these socioeconomic and biological drivers, yield changes over the past decade in Brazil are partly predicted be predicted by elevation, suggesting a climate-related driver. With the exception of large and relatively unproductive regions in the north, the regions with the largest negative trends tend to be on the edges of the broad coffee producing region, suggesting that shifts in suitability

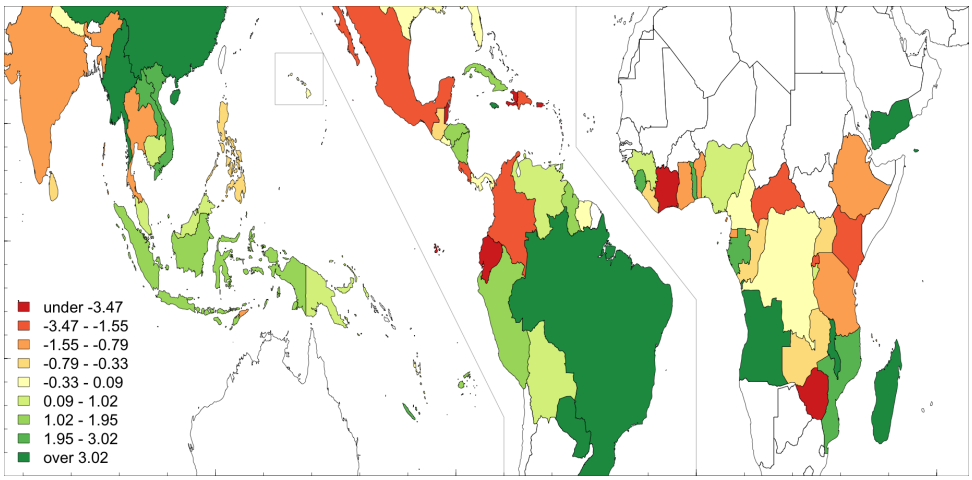


Figure 3.1: Trends in coffee yields since 2000 by country. Values represent the rate of yield change per year, since 2000 and relative to yields in 2000: Countries colored green have shown significant increases in per hectare yield, while those in red and orange have shown decreases.

are squeezing these border regions out. Many of the areas with positive trends are in higher hills than those with negative trends.

If temperatures are forcing coffee to higher elevations, it will be reflected in a fall in yields in municipalities at low elevations and increases at higher elevations. Figure 3.3 shows such a pattern from the municipality data. On average, counties of every elevation have increasing yields, reflecting the broader trend in Brazil. However, counties with high elevations (greater than 700 m) have on average higher increases yields than those with lower elevations (below 500 m). These lower averages at low elevations also reflect a greater number of municipalities with negative trends.

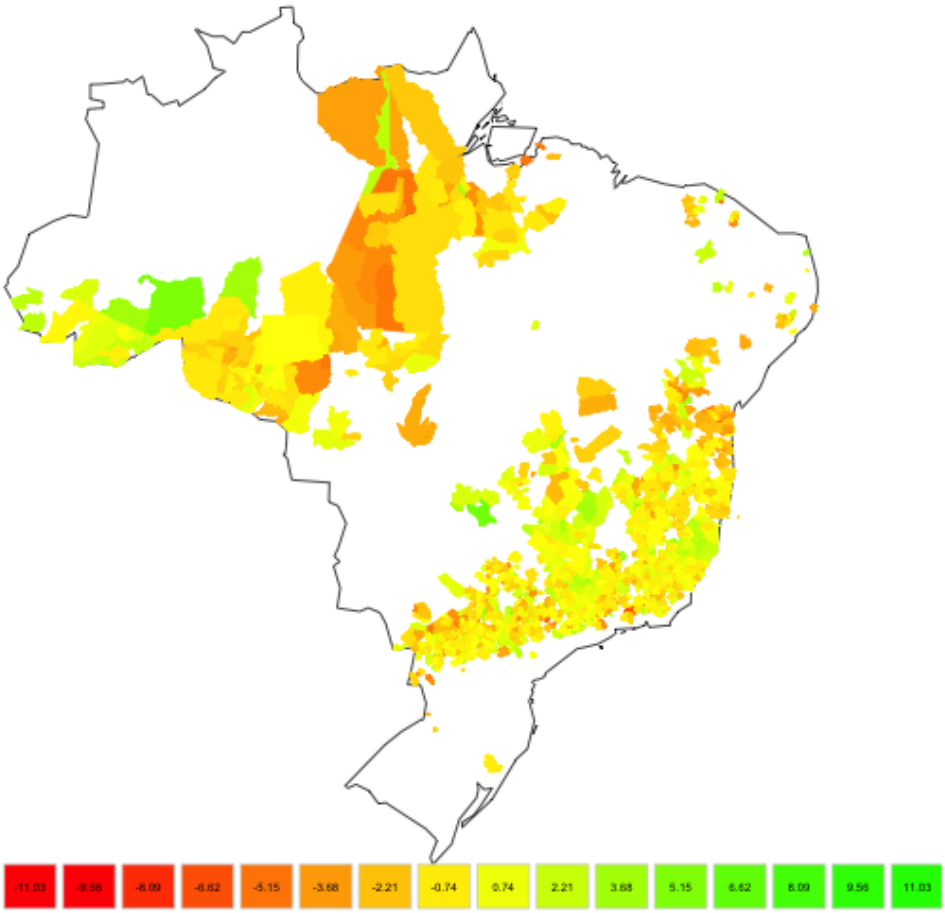


Figure 3.2: Trends in coffee yields since 2000 for Brazilian municipalities. Values represent the yearly decrease in percent terms: Countries colored green have shown significant increases in per hectare yield, while those in red and orange have shown decreases.

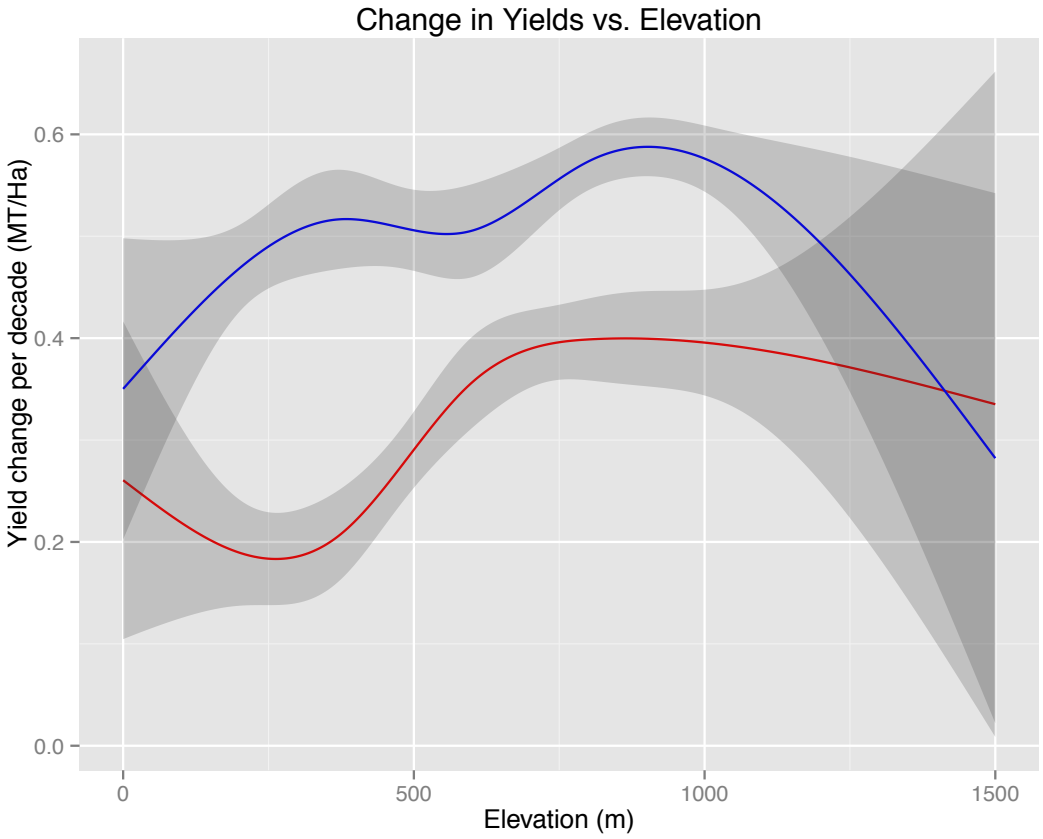


Figure 3.3: Changes in yields as a function of elevation. The red line shows municipality-level yields against elevation, showing a sharp increase in yields above 500 m. Blue shows the same relationship, but weighted by municipality harvests, and a more minor division around 700 m.

## 3.2 Previous coffee suitability literature

Suitable lands for coffee are expected to shift poleward and to higher elevations as temperatures rise. A number of regional estimates of these effects have been made, mostly using the Maximum Entropy (MaxEnt) methodology (see table 3.1). MaxEnt is a powerful technique in its ability to extrapolate suitability conditions from very sparse data, however robustness is difficult to assess with this techique. In this chapter we introduce a different approach we believe is more appropriate to the coffee context. We develop a Bayesian odds technique, which applies the data in our spatial coffee database.

| Regions | Approach | Reference |
|---|---|---|
| Nicaragua, Mexico | MaxEnt | Laderach et al. (2009) |
| Kenya | MaxEnt | CIAT (2010) |
| Ethiopia | MaxEnt | Davis et al. (2012) |
| Haiti | MaxEnt | Eitzinger et al. (2013) |
| Uganda (data from Uganda, Tanzania, Kenya) | MaxEnt | Jassogne et al. (2013) |
| Rwanda | Qualitative criteria | Nzeyimana et al. (2014) |
| | | |
| Indonesia | MaxEnt | Schroth et al. (2014) |
| Global | MaxEnt, SVM, Random Forest | Bunn et al. (2015) |
| Global | MaxEnt | Ovalle-Rivera et al. (2015) |

Table 3.1: Recent analyses of current and future coffee suitability.

The most comprehensive previous estimates of changes in suitability are from the Global Agro-Ecological Zones (GAEZ) version 3.0 (2012), and from Bunn et al. (2015). GAEZ uses a potential yield model with soil physics and parameters derived from field experiments. Bunn et al. use a variety of data-mining methods, relating current occurrence to climate characteristics. The two approaches provide a useful comparison.

Figure 3.4 shows the GAEZ potential yield maps for the baseline period (1961 - 1990) and in 2050 under a business-as-usual trajectory (IPCC A2).

These maps account for the additional benefit of CO2 fertilization and an intermediate level of fertilizer inputs.

A few results are visible in these figures. First, the current range of suitable climate is predicted to be large in many areas, particularly South America and central Africa. Actual coffee production areas are much more limited. The extent and quality of coffee producing areas in 2050 is predicted to be much smaller than the suitable areas in the baseline period, but also tends to more closely match existing areas of cultivation. Some countries are predicted to no longer have any land suitable for growing coffee (e.g., Ghana and Nigeria) while other regions have new potential (e.g., Florida and South Africa).

These shifts in coffee production can be seen more clearly in the difference between current coffee production potential to future coffee production, as shown in figure 3.5.

Most areas show large decreases in coffee production potential, except for Florida, southern Brazil, South Africa, Ethiopia, northern India, Myanmar, and China. The dashed lines show the tropics of Cancer and Capricorn, the traditional bounds of the coffee belt. Almost the entire region within these bounds decreases in suitability, while increases are generated in the region beyond it. A table of the country-by-country changes in amount of suitable area from GAEZ is included in Appendix A.1.1.

Bunn et al. (2015) provide a more nuanced picture (see figure 3.6). While Bunn et al. still estimate

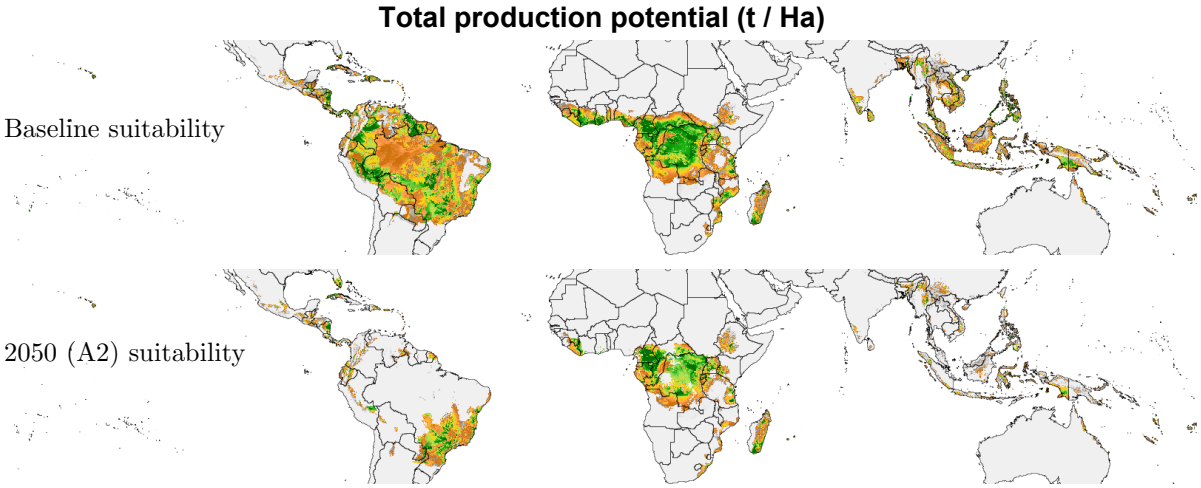


Figure 3.4: Coffee suitability maps for 1961-1990 (above) and for 2050 (below) under IPCC's A2 scenario (Hadley GCM). Color represent total production capacity, from 0 (grey) to .98 t/ha (green). Source: GAEZ

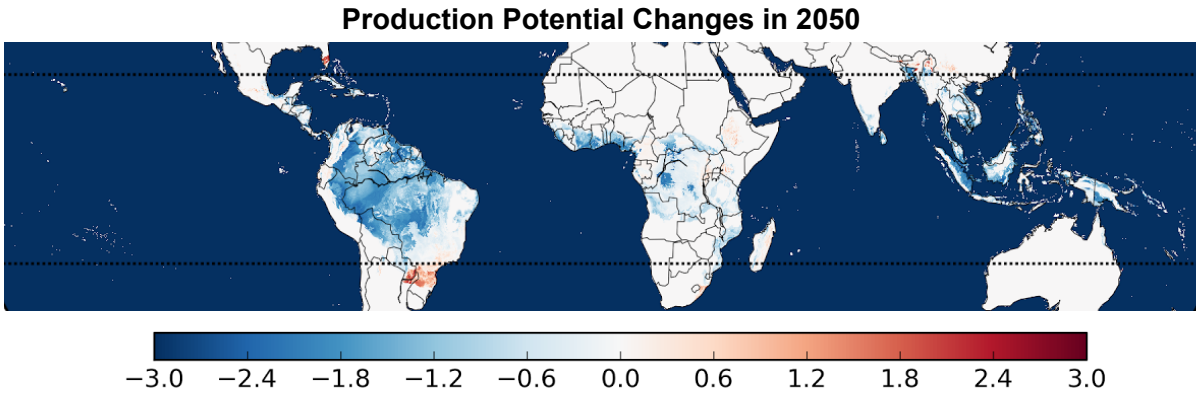


Figure 3.5: Changes in coffee suitability, in terms of production potential in t/ha, between 1961-1990 and 2050 under IPCC's A2 scenario, under a high-input farming system. Adapted from GAEZ.

decreases in climatic suitability between now and 2050 across much of the current coffee producing area, they also find neighboring areas in many cases that show increases in suitability. For example, regions in Colombia, Central America, and Indonesia can shift to higher elevations, and Brazil production can shift south. The coffee production potential in much of Uganda and Tanzania shifts into Kenya and the Democratic Republic of the Congo.

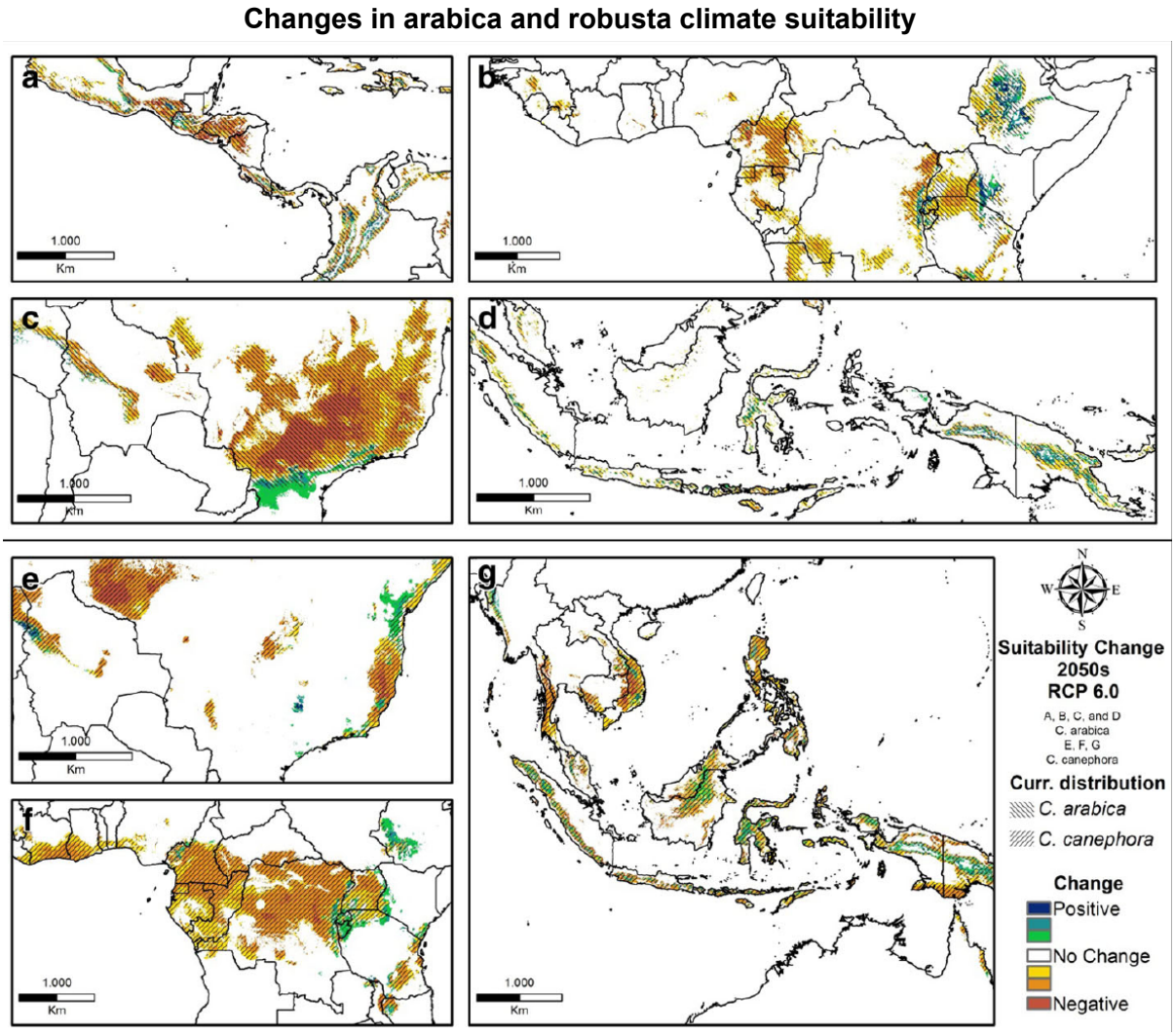


Figure 3.6: Suitability changes between present climate and 2050. Figures a - d show Arabica production and figures e - g show Robusta. Reproduced from Bunn et al. (2015).

### 3.2.1 The role of management

Fertilizer and irrigation use can open up new areas to coffee production. Figure 3.7 compares suitability according to GAEZ for low-input and high-input management. High-input management can produce yields 5 times that of low-input management.

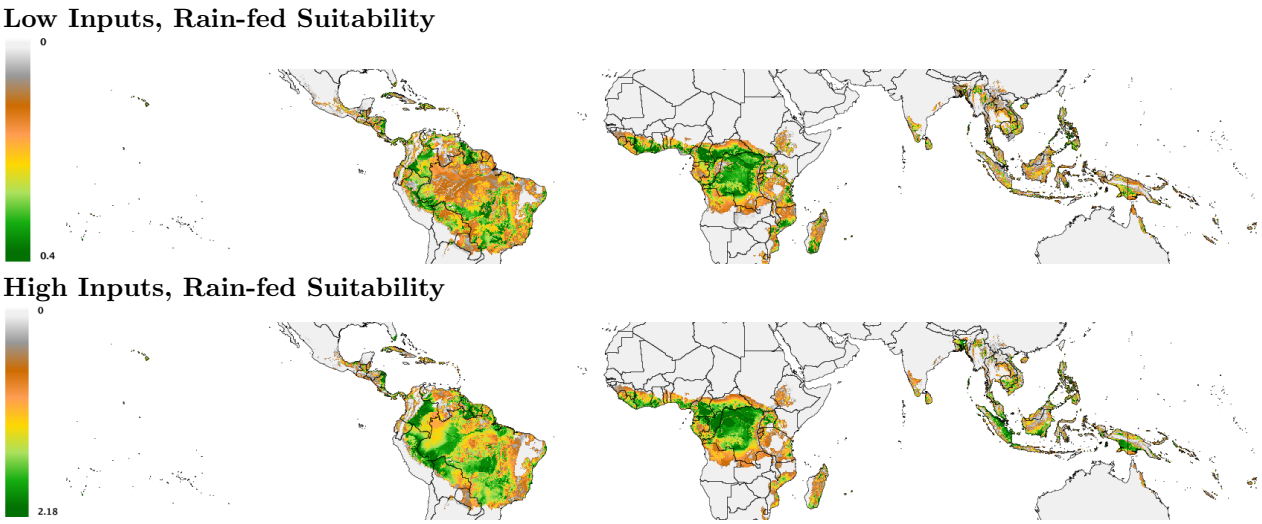


Figure 3.7: Both maps are copyright of IIASA and FAO.

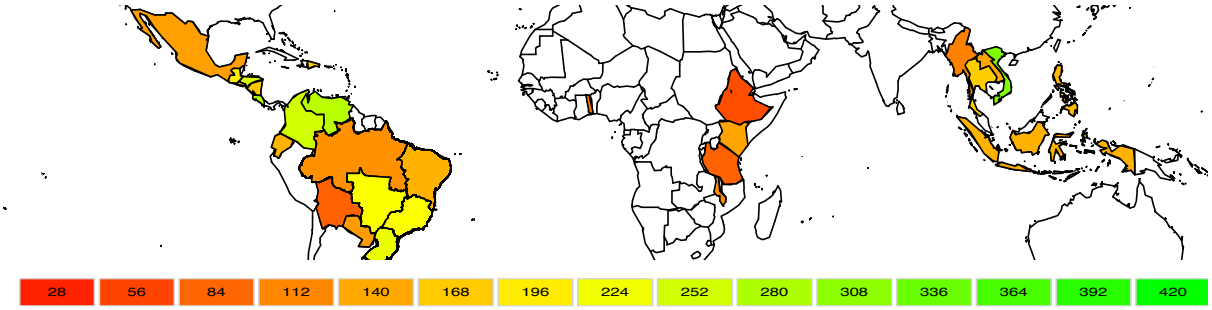


Figure 3.8: Average fertilizer use for coffee, from FertiStats (FAO), and including Brazil regional breakdown from `ftp://ftp.fao.org/agl/agll/docs/fertusebrazil.pdf` (FAO). The greatest amounts of fertilizer are used by Vietnam, Venezuela, and Costa Rica, and the least by Ethiopia and Tanzania.

Figure 3.8 shows the amount of fertilizer used by countries and distinguished for regions with Brazil, using FAO data (FertiStats). A wide range of fertilizer amounts are used, with the greatest amounts of fertilizer used by Vietnam, Venezuela, and Costa Rica, and the least by Ethiopia and Tanzania. This material is to be added to the production model.

## 3.3 A Bayesian suitability approach

Our approach to estimating suitability is diagrammed in figure 3.9. Using existing environmental characteristics, we compute a statistical model, which we apply to future environmental characteristics and compare the result to previous estimates. This section describes the basic principles used to construct that model.

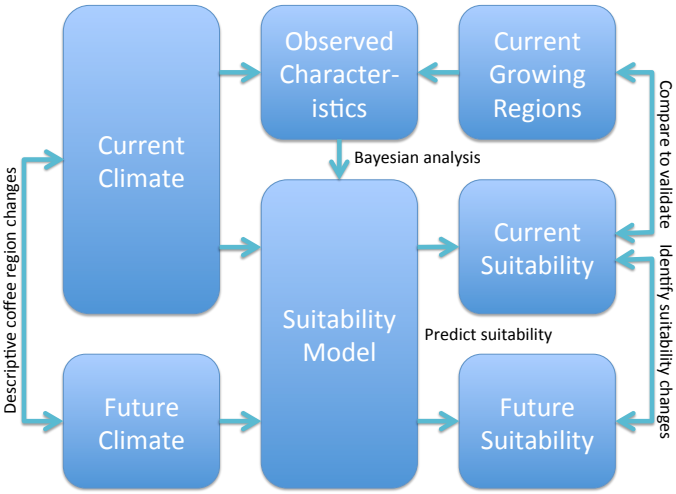


Figure 3.9: Diagram of the process for determining future climate suitability for coffee. On the left is global weather data, fed into both the model creation process and the model itself in the center. These then are used to produce current and future suitability maps.

**Derivation of the Bayesian odds measure**

Given any environmental condition, we can use Bayes rule to provide a empirical estimate of suitability. We write Bayes rule as an odds ratio:

$$\frac{p(\text{coffee} = 1|\vec{x})}{p(\text{coffee} = 1)} = \frac{p(\vec{x}|\text{coffee} = 1)}{p(\vec{x})}$$

The left-hand-side describes the ratio of the probability of coffee in a region given the observed conditions, to the probability of coffee generally. If this is greater than 1, the area is more suitable than the average location.

To calculate the coffee probability, the right-hand-side describes a ratio between the distribution of a property across harvested areas, and the distribution of that property across the entire region. As conditioning data, we use soil properties, climatic properties, elevation, and latitude.

Climatic and soil properties are not mutually independent, complicating our ability to calculate this ratio given the large number of properties we have available. We use the statistical "copulas" technique to disentangle the marginal distributions of each property from their dependence structure (Nelsen, 2013). We use a Gaussian copula, which captures the correlation between the various properties.

To incorporate a new property, we determine its unweighted distribution across the entire region from 30°N to 30°S. Then we create a weighted distribution, with properties from the region weighted by harvested area. Finally, we calculate Spearman's rho, between the new property and all existing properties, to represent the dependence structure.[1]

Then, to determine $p(\vec{x})$ and $p(\vec{x}|\text{coffee} = 1)$ for a given location, we reverse the normal copula process. In this case, we determine the span in $\vec{u}$-space (rank space) that a small region of $\vec{x}$-space represents $(\vec{x} \pm \vec{\Delta x})$, using each marginal distribution and the probability integral transform. If there is very little mass in the marginal distribution in the region of $x_i$, the corresponding $\Delta u_i$ will be small. Then we evaluate

$$\int_{\vec{\Delta u}} c_R^{\text{Gauss}}$$

Above, $c_R^{\text{Gauss}}$ is the Gaussian copula, which can be written as,

$$c_R^{\text{Gauss}}(u) = \frac{1}{\sqrt{\det R}} \exp\left( -\frac{1}{2} \begin{pmatrix} \Phi^{-1}(u_1) \\ \vdots \\ \Phi^{-1}(u_d) \end{pmatrix}^T \cdot \left(R^{-1} - \mathbf{I}\right) \cdot \begin{pmatrix} \Phi^{-1}(u_1) \\ \vdots \\ \Phi^{-1}(u_d) \end{pmatrix} \right)$$

where $\Phi^{-1}$ is the inverse cumulative distribution function of a standard normal (Arbenz, 2013), and $R$ is the matrix of correlations, equal to $2 \sin \rho_{ij} \frac{\pi}{6}$ for each Spearman's rho, $\rho_{ij}$, between property $i$ and property $j$.[2]

### 3.3.1 Comparing MaxEnt and Bayesian odds techniques

Both the MaxEnt and Bayesian techniques are sophisticated and represent the uncertainty of their result with high integrity. Table 3.2 provides a comparison of the main strengths and weaknesses of the two techniques.

MaxEnt has been used to study species suitability for a long time, and is designed for situations where a species is observed only at particular locations. The spatial coffee database gives us a much clearer picture of where coffee currently is grown and is not.

MaxEnt is most appropriate when there are underlying motivations for the constraints that are used as a central part of the method: for example, a common constraint is to require that that the mean and variance of temperatures for observed coffee match the mean and variance for future coffee. Unfortunately, MaxEnt constraints are often chosen arbitrarily and without a physical foundation. The Bayesian odds approach incorporates the entire distribution of environmental indicator values where coffee is grown, rather than a small collection of moments.

| | MaxEnt | Bayesian Odds |
|---|---|---|
| Form of observation data | A set of point locations, for where the species was observed | A weighted grid of presence across all space |
| Use of environmental data | Mean and other moments of the environmental data are used, based on the constraints chosen | The full distribution of values for any environmental indicators are included |
| Use of constraints | Constraints are central to the technique | Constraints are not used |
| Result uncertainty | Fully maintained | Fully maintained |
| Key simplification | Only chosen constraints describe the distribution of environmental indicators | Dependence between indicators is assumed to be captured by a rank correlation. |

Table 3.2: Comparison between the features of MaxEnt and Bayesian odds methods.

### 3.3.2 Suitability data

We calculate suitability using the following environmental variables, all available at 5 arc-minute resolution. These are shown in figure 3.10.

- Soil texture data from the Harmonized World Soil Database (FAO/IIASA/ISRIC/ISSCAS/JRC, 2012). This consists of three macro-soil components (sand, silt, and clay), and three trace components (organic carbon, calcium carbonate, and gypsum). These six properties are available at high resolution (a 0.5' or about 1km grid) for the topsoil (0 cm to 30 cm) and again for the subsoil (30 cm to 100 cm).
- Land elevation from the SRTM elevation database (Jarvis et al., 2008).
- Gridded bioclimatic data from the WorldClim dataset (Hijmans et al., 2005). This database includes 19 variables, including annual mean temperature, diurnal range, maximum and minimum temperatures, annual precipitation, maximum and minimum precipitations, temperatures in wet and dry months, and precipitation in hot and cold months.
- Urban areas from Natural Earth and derived from 2002-2003 MODIS satellite data (Schneider et al., 2003).
- Protected regions from the World database on protected areas (WDPA Consortium, 2004). Protected areas and urban areas are important both as constraints on current coffee producing regions and on future ones.

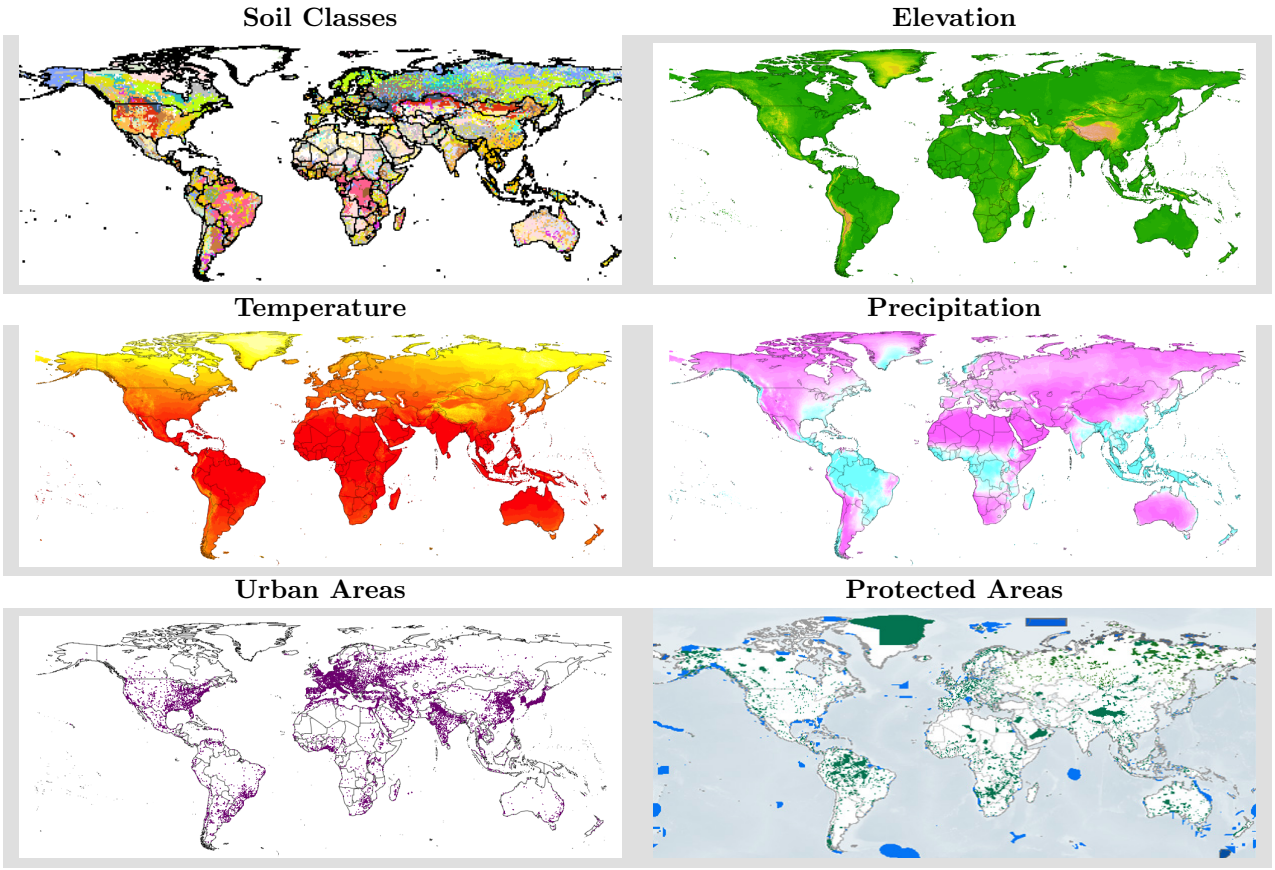


Figure 3.10: Inputs to the suitability analysis. See the text for details.

## 3.4 Baseline Bayesian odds map

The result of the Bayesian odds procedure for current coffee suitability is shown in figure 3.11. Dark green regions (high suitability) are rare, unlike the analyses by GAEZ and Bunn et al.. While they typically match areas of actual coffee growth (in Brazil, Colombia, and Central America), there are several places where there are large mismatches (in North Africa and Western India). While this provides a high resolution and data-driven map, it cannot stand alone.

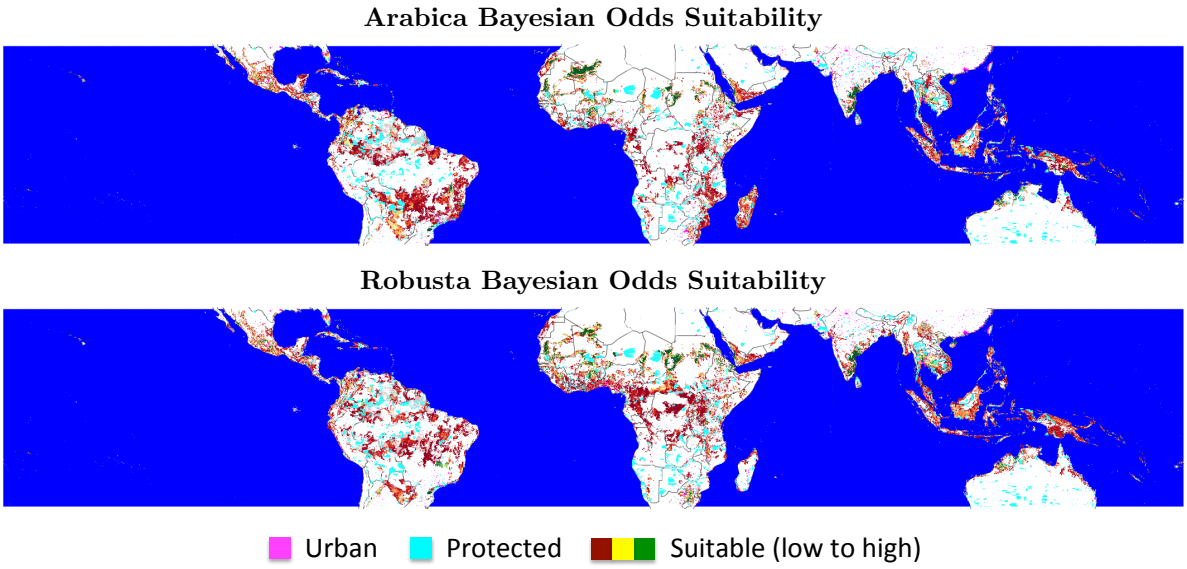


Figure 3.11: Suitability for Arabica coffee (top) and Robusta coffee (bottom). Colors range from red (slight suitability odds) to yellow to green (very strong suitability odds). The map also shows protected areas (cyan), urban areas (purple), and managed areas (faded).

## 3.5 Incorporating biological process

The Global Agro-ecological Zones (GAEZ) project uses biologically-motivated calculations to estimate suitability. GAEZ suitability indexes are normalized to be between 0 and 100, so a comparison between the Bayesian results and GAEZ requires constructing a common scale. We do this by comparing the results in ranks, rather than levels. In other words, we look for differences in the percentile quality of land (see figure 3.12).

Some areas match closely (southern Brazil, Colombia, and parts of Indonesia), while GAEZ attributes suitability to large regions not supported by the Bayesian methods, such as Amazonian and Congo rainforest. This indicates a complementarity between GAEZ and the Bayesian odds approach, where GAEZ provides physical constraints while the Bayesian approach forces the results to match observed data.

**Computing a combined metric**

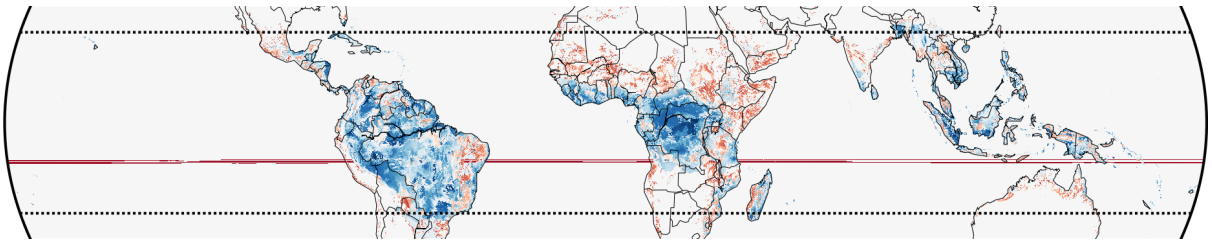

Figure 3.12: Comparison between GAEZ and the Bayesian odds technique for Arabica. Blue regions have greater quantile suitability in GAEZ than for the Bayesian odds approach; red regions show lower suitability in GAEZ, and white regions agree.

We combine the two approaches by mapping the following:

$$s(x,y) = p(x,y)\frac{b(x,y)}{1+b(x,y)}$$

This attributes zero suitability where either approach specifies it, and otherwise allows them to reinforce each other. The results are shown in figure 3.13. It also normalizes the result to match GAEZ 0 - 100 scale.

The combined result shows high suitability in many fewer places, scattered based on where both techniques support their suitability. This provides a stronger basis for identifying the shifts in suitability, conservatively matched to only the highly suitable regions.

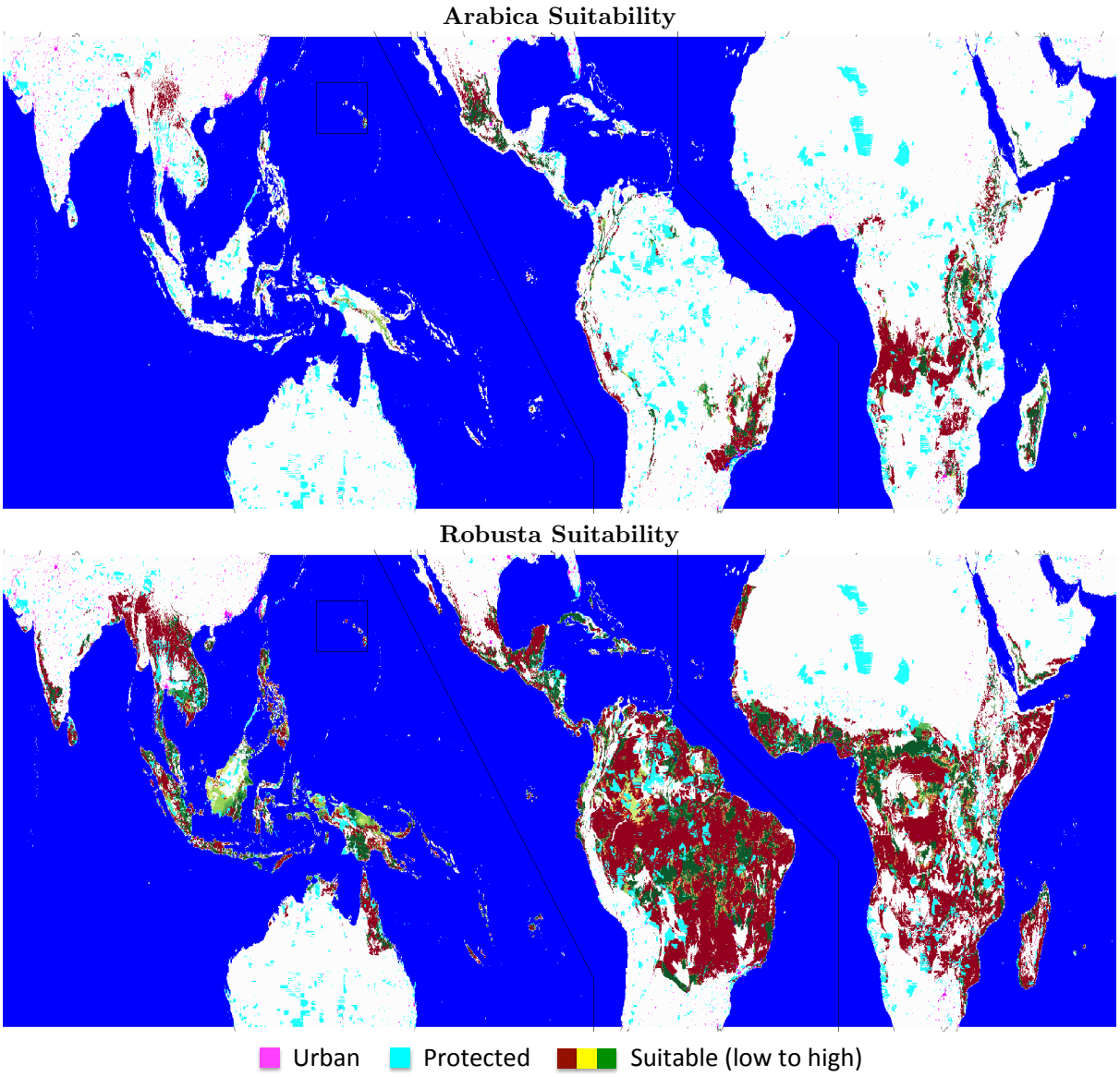


Figure 3.13: Combined Bayesian and GAEZ results for Arabica and Robusta.

## 3.6 Suitability comparison with Bunn et al.

A recent paper by Bunn et al. (2015) uses data mining methods, such as MaxEnt, on coffee-growing presence at 42 000 individual farms to estimate suitability. Above, we build upon this work by incorporating the coffee presence map from their paper into our database. We also use the same collection of 19 bioclimactic variables, on top of which we add soil variables, and we extend the study of future uncertainty by using 12 additional global climate model results. While we believe that our approach, based on Bayesian updating of presence and absence information, is better grounded theoretically and less arbitrary than their MaxEnt and other data-mining techniques, Bunn et al. provides an important comparison for our results.

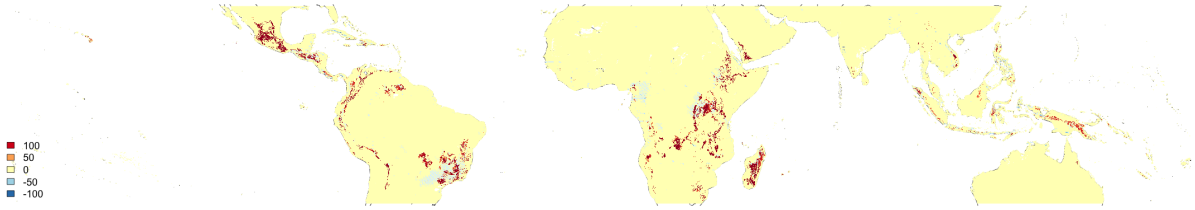


Figure 3.14: Comparison between Bunn et al. (2015) and the combined Bayesian-GAEZ approach. Blue areas have higher suitability in the baseline map produce by Bunn et al., while red is higher using our approach.

Figure 3.14 displays a comparison of current suitability between the two methods. Most of the world in this figure is colored yellow, where both techniques specify very little suitability. Some areas, such as Brazil and Kenya, show differing patterns between the two approaches. In these cases, our approach produces a result that more closely matches the patterns in the coffee database.

## 3.7 Future suitability

Estimating future suitability requires taking careful account of the uncertainties involved in future predictions. We estimate suitability for each of 17 GCMs for Bioclim and 4 GCMs for GAEZ. We display three maps for each of Arabica and Robusta suitability. The first is just the measure of median changes in suitability, without protected and urban areas. The second shows the level of confidence that the direction of the suitability change is as shown. The third shows the full map, where areas are also faded in proportion to their level of uncertainty.

The maps show that many traditional coffee growing areas are going to experience large losses in suitability by 2050. This includes parts of Brazil, southern Mexico, Kenya, and Madagascar. Few places show increases, but these include other parts of Brazil and Angola.

Appendix A.1.3 shows the total area by country expected to increase and decrease, both by suitability and within harvested regions. These are summarized at the global level in table 3.3.

In absolute suitability changes, Brazil has the most lost of suitability in regions that are currently suitable, and the most gain in new regions becoming suitable. As a fraction of the current suitable area, a number of countries are tied in losing all of their suitable land: Belize, the Central African Republic, Côte d'Ivoire, Republic of Congo, Fiji, Gabon, Guinea, Equatorial Guinea, Cambodia, Paraguay, Sierra Leone, and Thailand. Although Taiwan also losses its entire allotment of suitable areas (of which it is

**Suitability changes for Arabica**

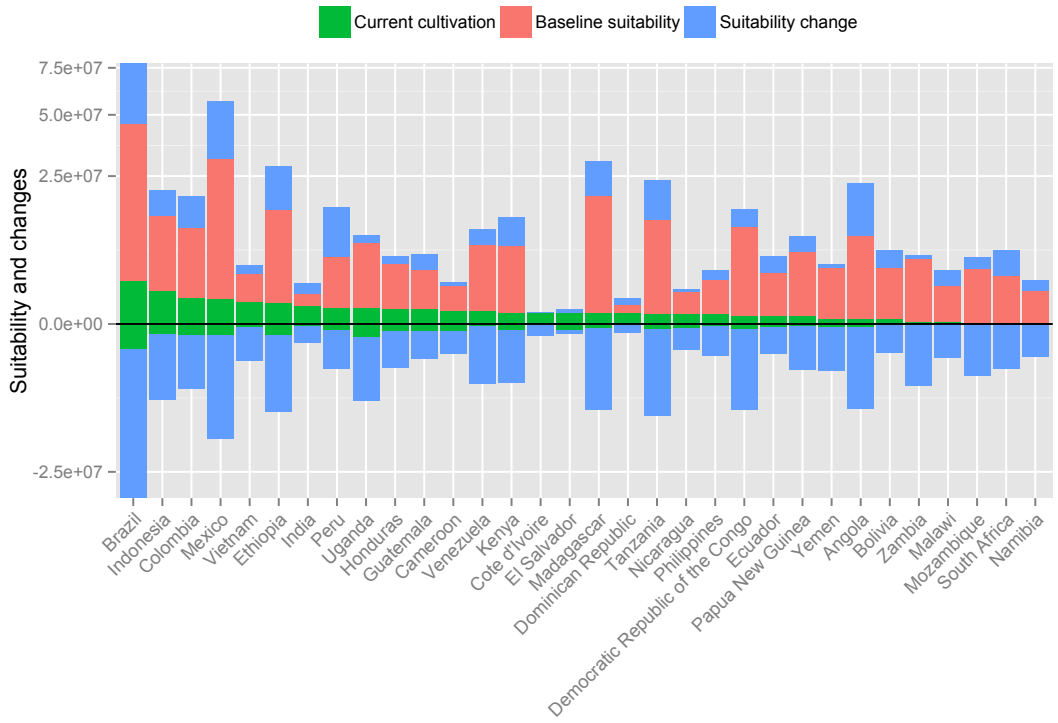


**Suitability changes for Robusta**

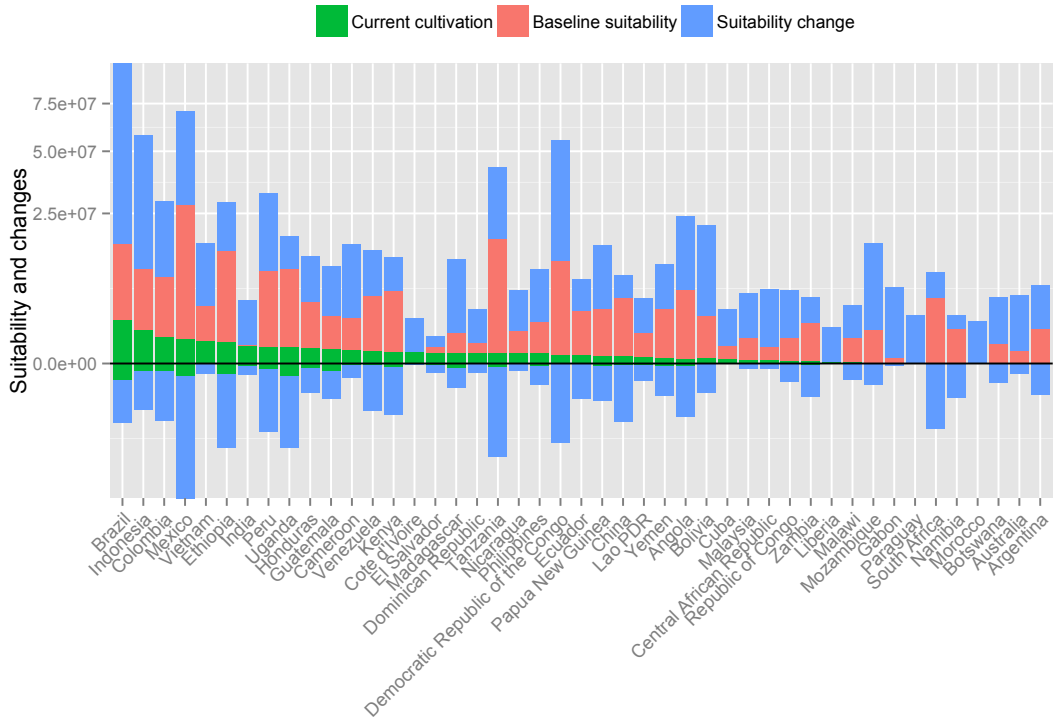


Figure 3.15: Increases and decreases in suitability and current cultivation by 2050. Green bars above the line describe current harvested areas, and below the line is the median predicted loss by 2050. Red above the line is the total baseline suitability. Blue above the line is new areas of suitability by 2050, and blue below the line lost areas.

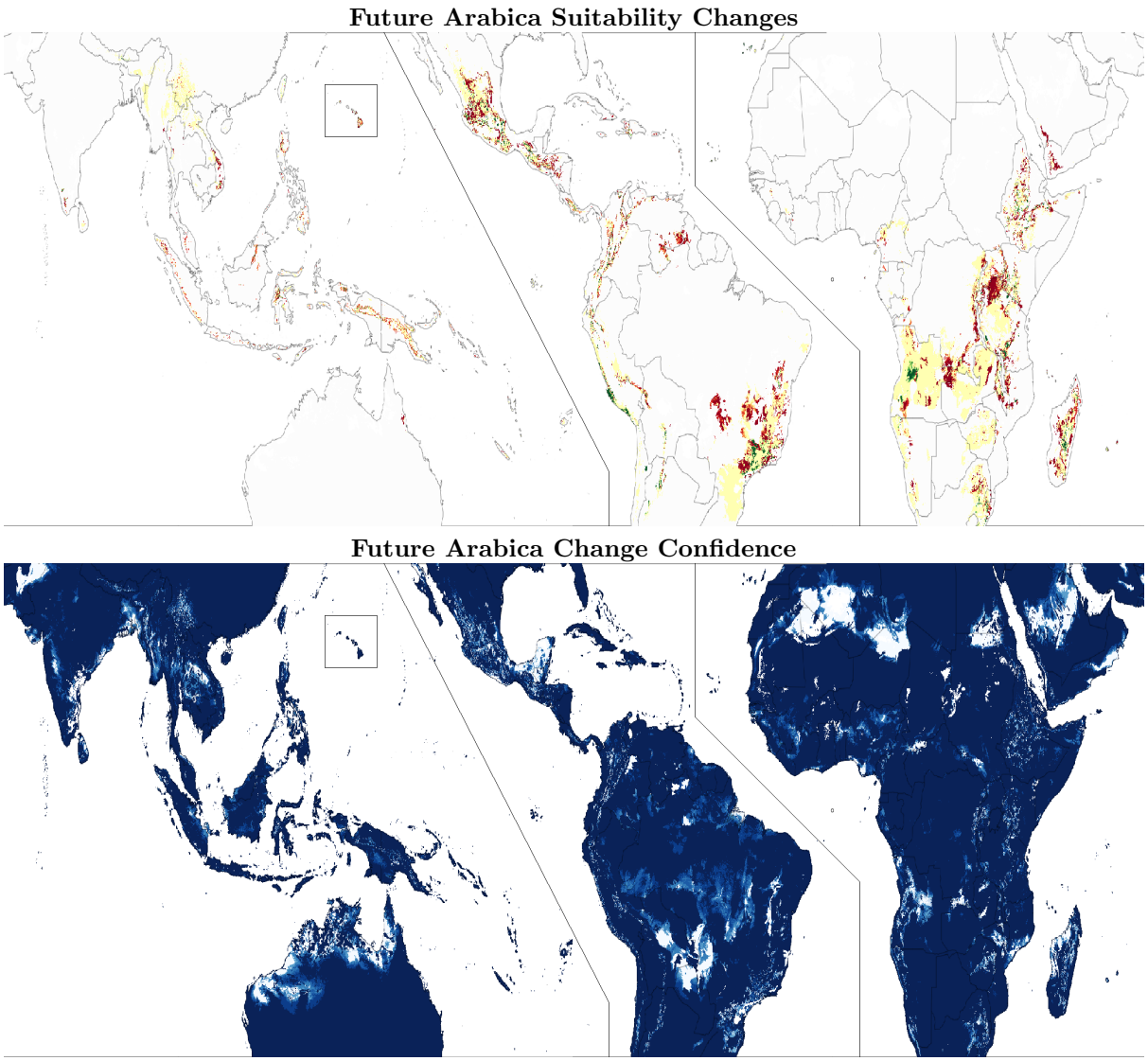


Figure 3.16: Maps of future Arabica suitability changes, showing the median suitability change (top) and the confidence level behind the direction of that change (bottom).

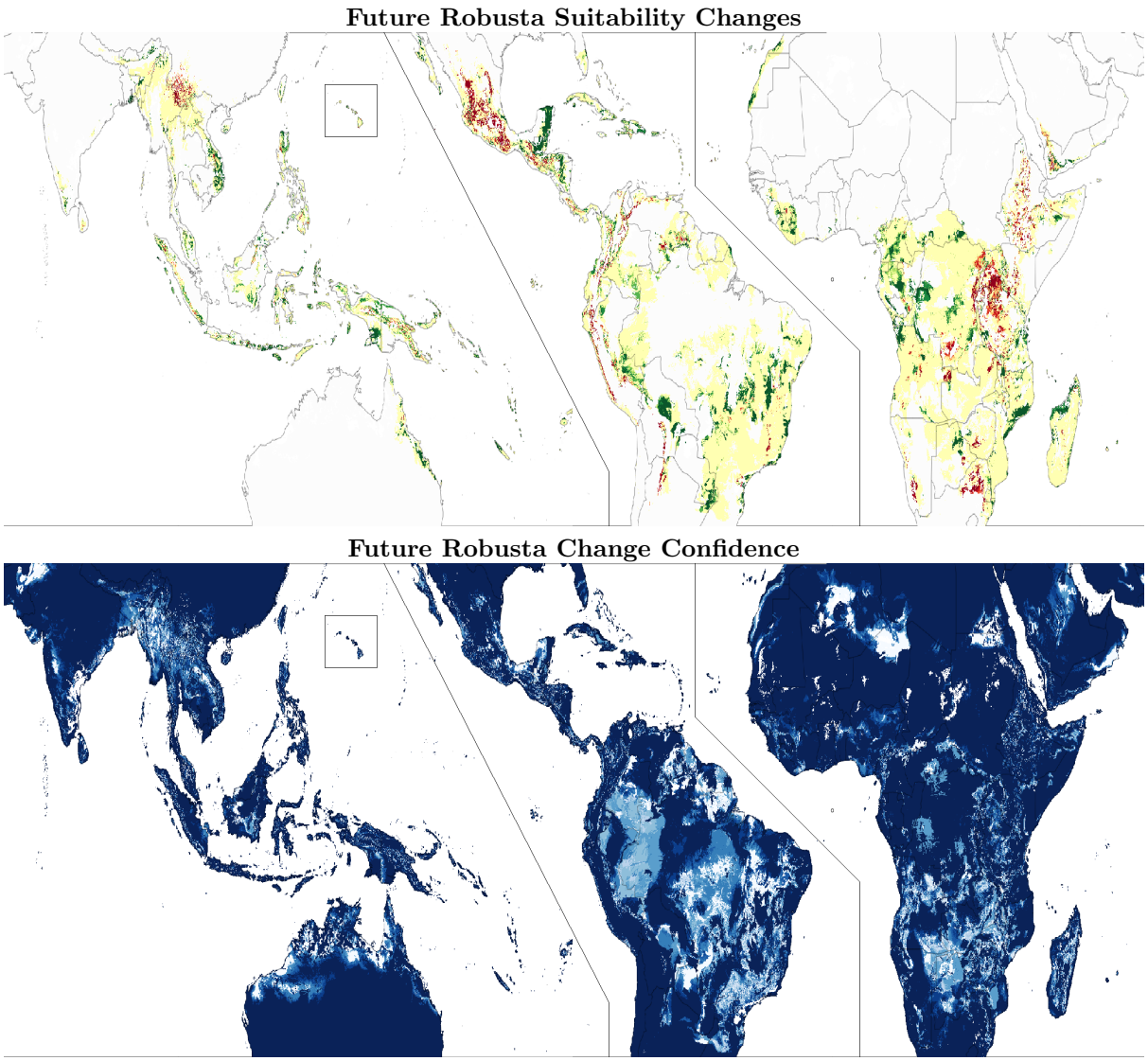


Figure 3.17: Maps of future Robusta suitability changes, showing the median suitability change (top) and the confidence level behind the direction of that change (bottom).

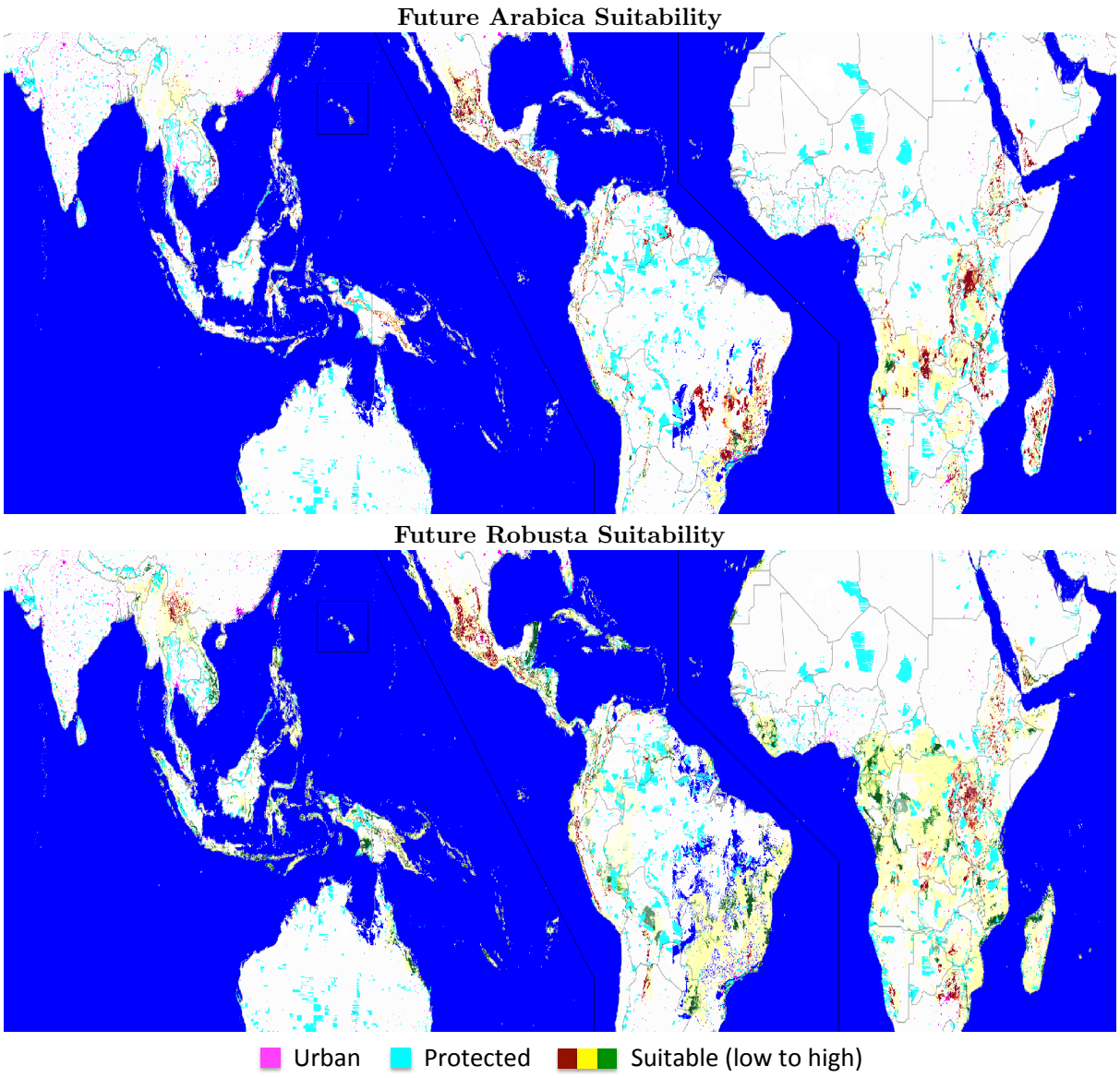


Figure 3.18: Maps of future Arabica and Robusta suitability as combined land use maps with suitability changes faded according to confidence.

| | Arabica | Robusta |
|---|---|---|
| Baseline suitable area (Ha) | 187626000 | 14663700 |
| New suitable area (Ha) | 27247000 | 21598800 |
| Existing suitability loss (Ha) | -132070000 | -88827000 |
| Loss from baseline (%) | -70.4 | -60.6 |
| Change from baseline (%) | -55.9 | 86.7 |
| Current harvest (Ha) | 10034618 | 10069911 |
| Loss from harvested areas (%) | -24.3 | -12.1 |

Table 3.3: Global changes in suitability for Arabica and Robusta varieties. Robusta is expected to see large increases in general, while Arabica will experience decreased suitability.

currently using none), it also shows the largest percentage increase in suitable regions, gaining 50% more than it loses.

This result is more extreme than most suitability results in the literature, which typically do not predict losses in suitability beyond 95% in any country (Jaramillo, 2013). It is a consequence of our estimation approach, which relies on both biological and statistical factors. There are currently regions within these countries that satisfy both criteria, suggesting that they are likely to be highly productive. It may be that these areas will continue to be capable of producing quality coffee, but we predict that they will experience significant losses in their capacity.

Across the globe and under the median change, 130 million hectares of currently suitable land will be lost, and only 30 million hectares will be gained. Coffee is currently harvested on 10 million hectares.

These changes apply to suitable land, whether or not it coincides with our data on changes within areas of current cultivation. However, the story for current cultivation is similar: the countries that lose all of their harvested land are exactly the same as those that lose all of their suitable land. In total, 19 countries lose more than half of their currently harvested land to losses in suitability by 2050.

# Chapter 4

# Internal variability

While long-term climate change is going to alter the landscape of coffee, many climate impacts are already occurring and represent shifts on shorter time-scales. While the most commonly known cycle in the coffee industry is the biennial production cycle, the climate has internal cycles that affect coffee production. These are produced by climate decadal variability, and are some of the most important climate dynamics for the coffee industry.

We find that the most important of these cycles is the El Niño/La Niña cycle, known as ENSO. The ENSO cycle produces vast shifts in weather climate patterns over much of the tropics. While each El Niño event is unique, they produce somewhat predictable patterns of increases and decreases in precipitation (see 4.1). ENSO is of particular concern today, as we enter what may be the largest El Niño event in a generation. During the last large El Niño in 1997-98, the tropics were hit by both droughts and floods, as shown in figure 4.2.

It also coincided with infectious outbreaks in Africa (Epstein, 1999), megafires in Indonesia (Page et al., 2002), and crop failures across the tropics (Hsiang and Meng, 2015). El Niño and La Niña events can often be predicted before their impacts are felt, and knowing what to expect can make a big difference in the outcomes. In fact, it can be argued there should be fewer disasters during El Niño and La Niña because the increased predicatibilty of the seasonal climate during these events can be used to increase our preparedness for adverse climate impacts (**?**).

The ENSO cycle is not the only multi-year climate cycle. We study the effects of five climate cycles and their effects on coffee production. The results are important beyond the direct quality of our predictions, for a pragmatic reason and a theoretical reason. Pragmatically, predictions that are based on globally available climate metrics can help farmers living in areas that do not have readily available or reliable weather forecasts. For these farmers, the information that a season will be wetter or drier than normal could be more important than the particular pattern of rainfall events. Determining the predicted impacts of climate indices, using our model, relies only on globally available metrics.

This dependence on global metrics also has a theoretical benefit. Complicated feedback systems can exist between agriculture in an area and the weather that area experiences; for example, deforestation can lead to decreases in precipitation. These feedbacks make it difficult to distinguish the effect of climate from the effect of farmers responding to, anticipating, or influencing climate. This problem is eliminated for models that use distant indices, as is the case with all of the multi-year climate cycles.

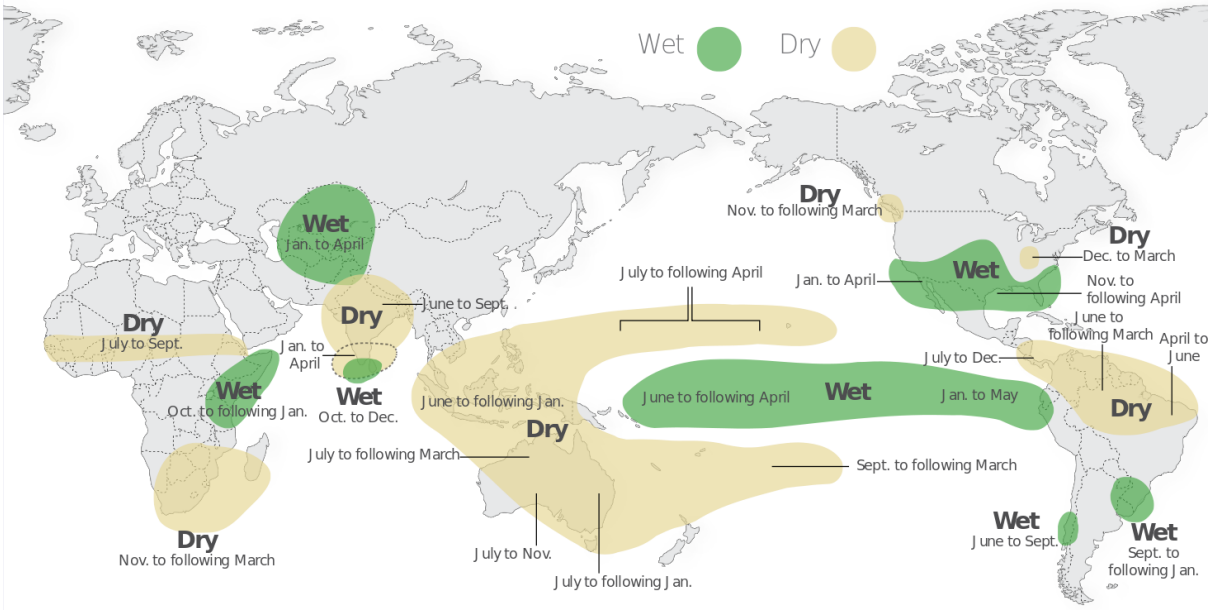


Figure 4.1: The typical precipitation impacts of an El Niño event, from **?** and **?** as modified by **?**.

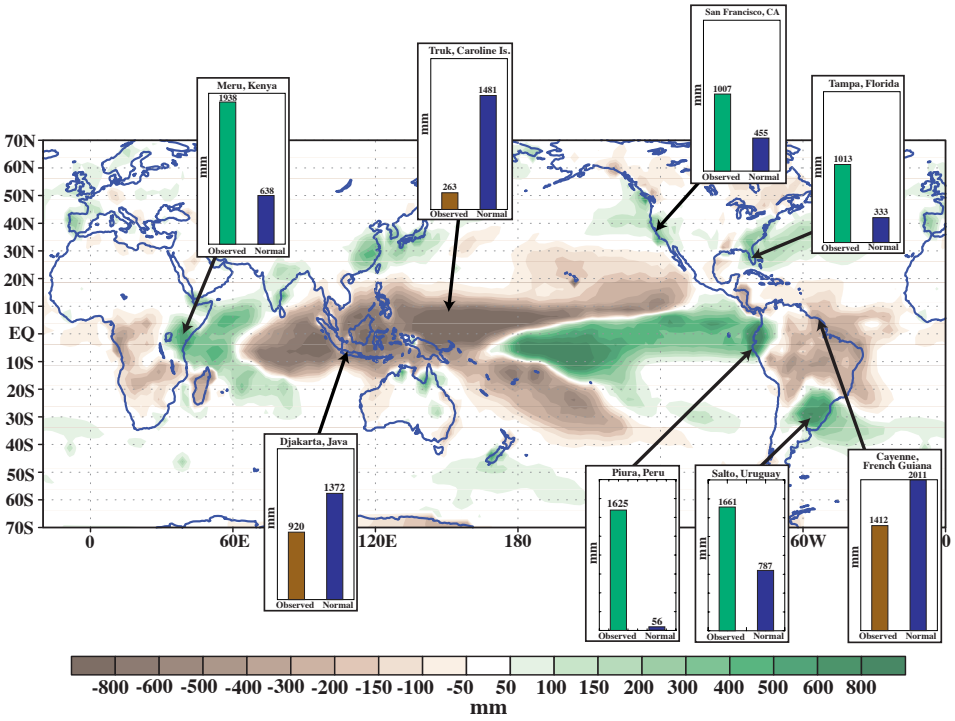


Figure 4.2: Rainfall anomalies from November 1997 to April 1998. Reproduced from Bell et al. (1999).

## 4.1 Impacts of El Niño

The ENSO cycle is both a concern and an opportunity for coffee production. Many coffee-producing countries are significantly impacted by these events, with changes in temperature, precipitation, and blossoming conditions. Furthermore, since El Niño and La Niña are global, they can produce large impacts on the coffee market. Like all climate events, El Niño affects both coffee plants and their associated farming communities in a way that is difficult to disentangle.

The scientific understanding of the ENSO cycle continues to evolve. Here we do a quantitative analysis of ENSO on recorded coffee prices and yields, although this is only a part of the picture. El Niño events can cause severe storms that increase erosion, producing a long-term effect that is only reflected tangentially in our data. El Niños can also affect a coffee farming operation by affecting the welfare of its farmers.

Our first analysis uses a consensus categorization of years into El Niño, La Niña, and ENSO-neutral years, as an indicator for studying impacts. These years and the shape of the NINO 3.4 indicator that corresponds to them is shown in figure 4.3.

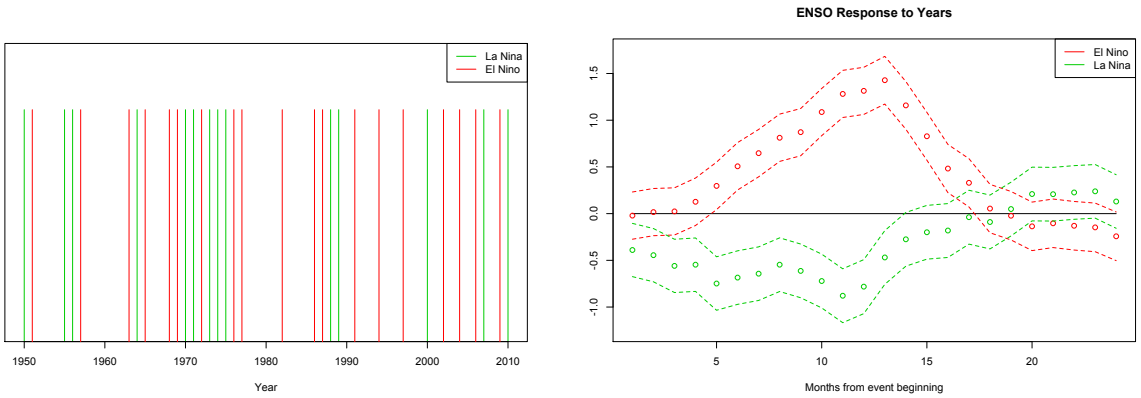


Figure 4.3: **Left:** The years categorized as La Niña years and El Niño years. **Right:** The estimated 24-month impulse response of the NINO 3.4 indicator to each of the three ENSO year types.

We see these impacts in the prices of Arabica and Robusta beans in El Niño years, relative to ENSO-neutral years, as shown in figure 4.4. In expectation, from the beginning of an El Niño year, prices climb for about 15 months, before beginning to decline. At their peak, prices are over 30% higher than they are predicted to have been in the absence of the El Niño event. We do not see a similar effect for La Niña events. These effects are similar in duration and form to those found by Ubilava (2012).

**Computing ENSO impacts**

We estimate the impacts of El Niño and La Niña by estimating an "impulse response", which accounts for the multiple overlapping effects of different ENSO years and the monthly climatology of the NINO 3.4 signal.

$$y_t = \alpha + \sum_{Y=Year(t)-N/12+1}^{Year(t)} \sum_{M=1}^{N} \beta_{12(Year(t)-Y)+M}^{Class(Y)} + \gamma \sum_{s=1}^{24} \frac{y_{t-s}}{24} + \mu_{Month(t)}$$

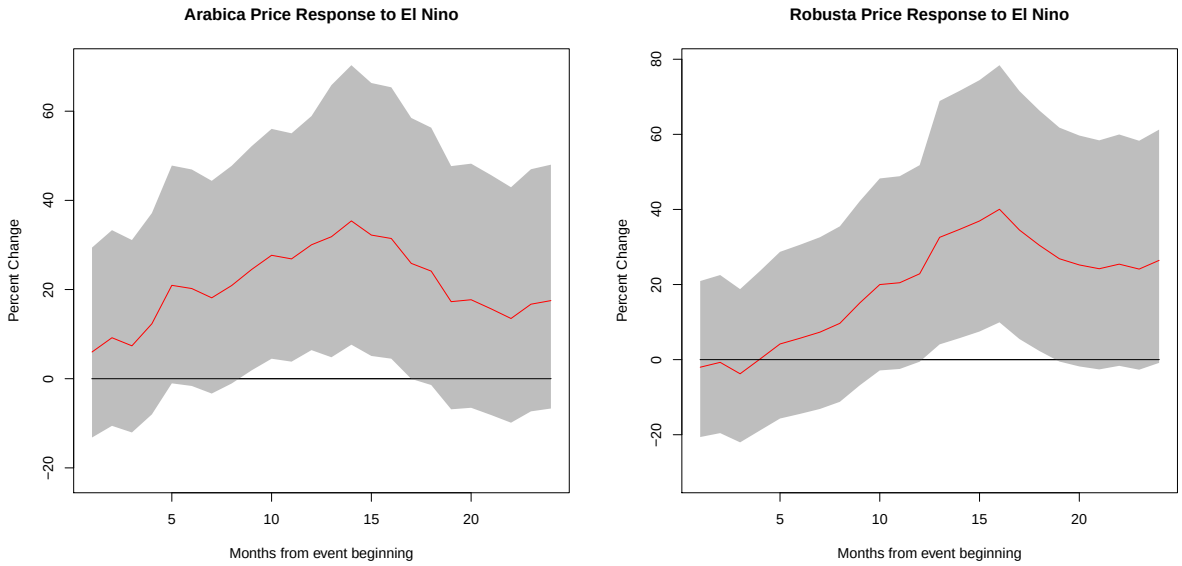


Figure 4.4: The graphs above show how international coffee prices respond to an El Niño event. Both Arabica and Robusta prices show increase of 20-40% over the course of the event, with potentially long-lasting impacts.

$Year(t)$ is the year for time $t$ and $Month(t)$ is the month for time $t$; $Class(Y)$ is the class of ENSO event that happened in year $Y$ (El Niño and La Niña). $N$ is the number of months to include in the impulse responses.

Here, the $\beta_m^k$ variables describe impulse responses of length $N$ for each class of ENSO event.

Little research has been done on the effects of the El Niño/La Niña cycle on coffee yields. Villegas et al. (2012) find that in Colombia the location of the Inter-Tropical Convergence Zone is a more important factor affecting yields, but global estimates of these effects do not appear to be available. We consider the impacts of El Niño and La Niña years globally and for each country.

An impact analogous to the price change is evident in the yields across countries. In El Niño years, yields decrease on average by 100 Hg/Ha, against an average of 6800 Hg/Ha in recent years, after accounting for long-term trajectories in yields. While this is only a drop of 1.5%, the average hides larger effects in specific regions and variability between El Niño years. No effect is seen globally in La Niña years.

Looking at individual regions, using country-level data, only a few countries appear to have large impacts from El Niño, after accounting for each country's long-term evolution in yield and production. The French Polynesia, Gabon, Polynesia, and Thailand all show significant impacts in yields, although the directions of the impacts differ. Mauritius, Papua New Guinea, and Sri Lanka have significant impacts in total production, with large decreases for Papua New Guinea and Sri Lanka. Because of the lack of information on coffee planting areas, yields are calculated with respect to harvested areas. As a result, the countries that show impacts on production but not on yield probably reflect El Niño impacts that are hidden by selective harvesting decisions.

**Regions with observed El Niño / La Niña impacts**

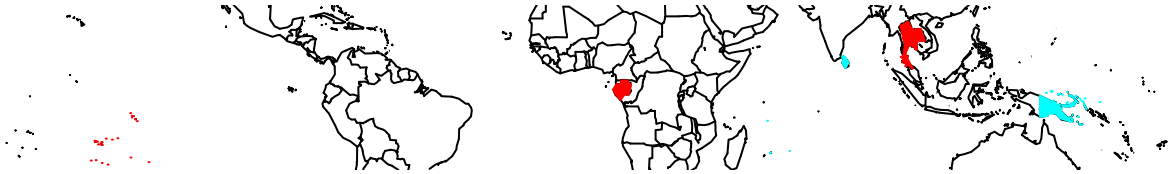

| Yields | El Niño | El Niño + 1 | La Niña | La Niña + 1 |
|---|---|---|---|---|
| **French Polynesia** | -650 Hg/Ha | N.S. | N.S. | N.S. |
| **Gabon** | +940 Hg/Ha | N.S. | N.S. | N.S. |
| **Polynesia** | -650 Hg/Ha | N.S. | N.S. | -600 Hg/Ha |
| **Thailand** | N.S. | N.S. | N.S. | +1400 Hg/Ha |
| **Productions** | **El Niño** | **El Niño + 1** | **La Niña** | **La Niña + 1** |
| **Mauritius** | +17 MT | +13 MT | +18 MT | +17 MT |
| **Papua New Guinea** | -7,600 MT | N.S. | N.S. | N.S. |
| **Sri Lanka** | N.S. | N.S. | -2,000 MT | N.S. |

Figure 4.5: Regions where country-level yield and production are teleconnected with El Niño and La Niña events. The location of the regions is shown at top, with yields affected by ENSO in blue and production affected by ENSO in red. In the table, values are the predicted change in yields or production in El Niño years, the year after an El Niño year, and the same for La Niña years. Entries with "N.S." show no statistically significant change at a 10% level.

## 4.2 Coherent movements

The relatively weak statistical relationship found between El Niño and country-specific yields is not uncommon among agricultural crops, but it drove an interest in our group into dissecting more clearly the relationship between global climate signals and country production. We collected five oceanic signals to explore this further, as shown in figure 4.6.[1]

A principal component analysis identifies regions of coherent marginal changes, across multiple time-series. This technique can be used to better understand patterns in large datasets, like the one describing country coffee production.

For each year, monthly values of the climate signals (delayed 6 months, to capture their impacts on coffee flowering) and country yields (detrended with locfit and normalized) are included. The first principal component represents the largest coherent movement of change, followed by the second component, and so on. Between the first three components, over 50% of the variation in yields can be described. The share of each of these components by year is shown in Appendix A.2.2. Each of the components and what it suggests about the relationship between climate and yields is described below.

The first principal component describes how yields have shifted on average over the past 50 years. Brazil, Mexico, and China have seen some the largest increases in yield, while Thailand, Myanmar and many countries in Africa have experienced the largest decreases. Most climate signals have not shown any trend, except for the Atlantic multidecadal oscillation (AMO) which is currently much higher than it was in the 1960s. As a result, all of the climate signals in the lower graph are near zero, except for AMO.

The second and third principal components are dominated by ENSO (the El Niño/La Niña cycle),

[1]NINO 3.4, NAO, SOI, PDO from NOAA Climate Prediction Center (CPC) (2015), unsmoothed AMO from Enfield et al. (2001).

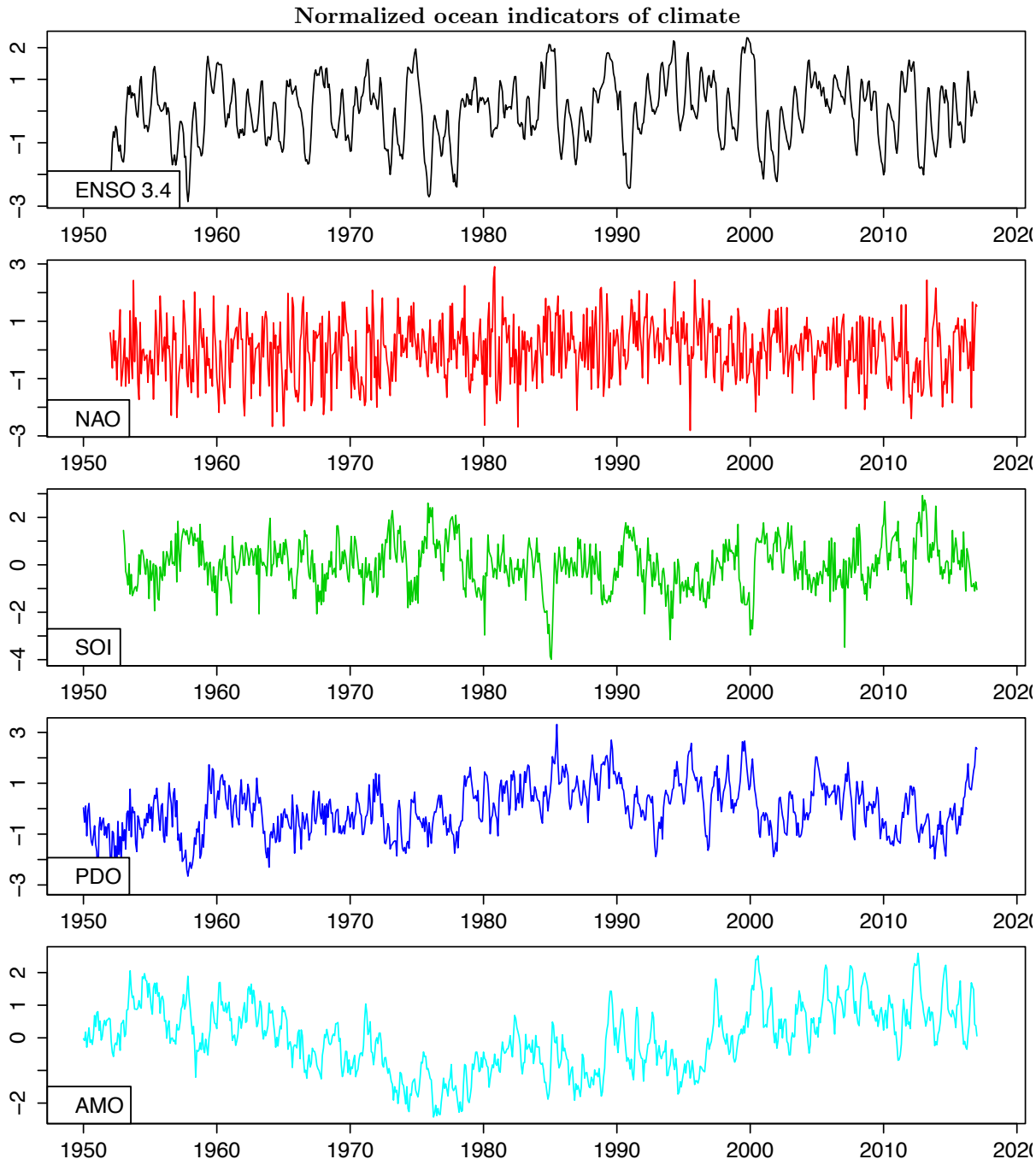


Figure 4.6: Normalized indicators used to study global and regional climate, sampled monthly. Each of these shows wide variability, but different periodicities. The interactions between these different signals can explain impacts in ways that individual signals cannot.

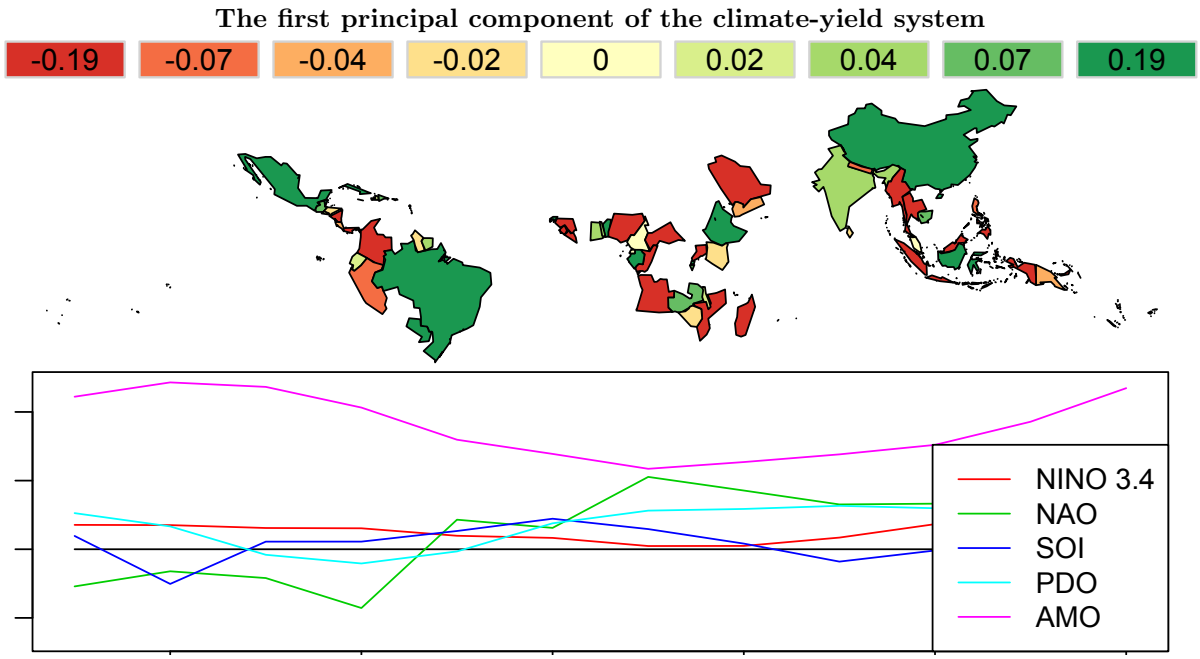


Figure 4.7: Spatial and temporal representation of the first principal component of the climate-yield system. Colors in the map represent increases (green) and decreases (red), and the plot below shows the climate signals across the year (delayed 6 months, so month 1 is July and month 12 is June). Explanation in the text.

represented by the NINO 3.4 index and the Southern oscillation index, which is known to be strongly correlated with ENSO but with an opposite sign. PC 2 is represented in the data when NINO 3.4 is high (El Niño) and the Pacific decadal oscillation (PDO) is also high, and its effects are reversed when these signals are both opposite in the direction of their anomalies. The largest effect of this combination, as shown in the map, is that Brazil, Paraguay, and Papua New Guinea have decreases in yields while India sees increases. This suggests that yields in these regions will often move in opposite directions, during many El Niño and La Niña years.

Observations with low values of PC 2 occur before 1975 and after 2000, while those with high values of PC 2 occur mostly in the 1980s and early 1990s. This may be driven by the slow oscillation of PDO. Since only one such cycle has occurred, it is difficult to distinguish the effects of the climate signals from socioeconomic effects, although most of this was be removed by the flexible trend used in the preprocessing step.

The third principal component also occurs when ENSO is in its El Niño state, and AMO is high or increasing. In this case, India, Peru, and southern areas in Africa show decreases, while other areas are not heavily affected. Both PC 2 and PC 3 can equally be understood in their La Niña form (and associated low values of PDO for PC 2 and low values of AMO for PC 3), which produce changes in yields in the opposite direction.

Between PCs 2 and 3, the effects of El Niño and La Niña appear across much of the globe. Because the impacts on most countries result from an interaction between the ENSO cycle and AMO or PDO, the results did not appear in the initial analysis.

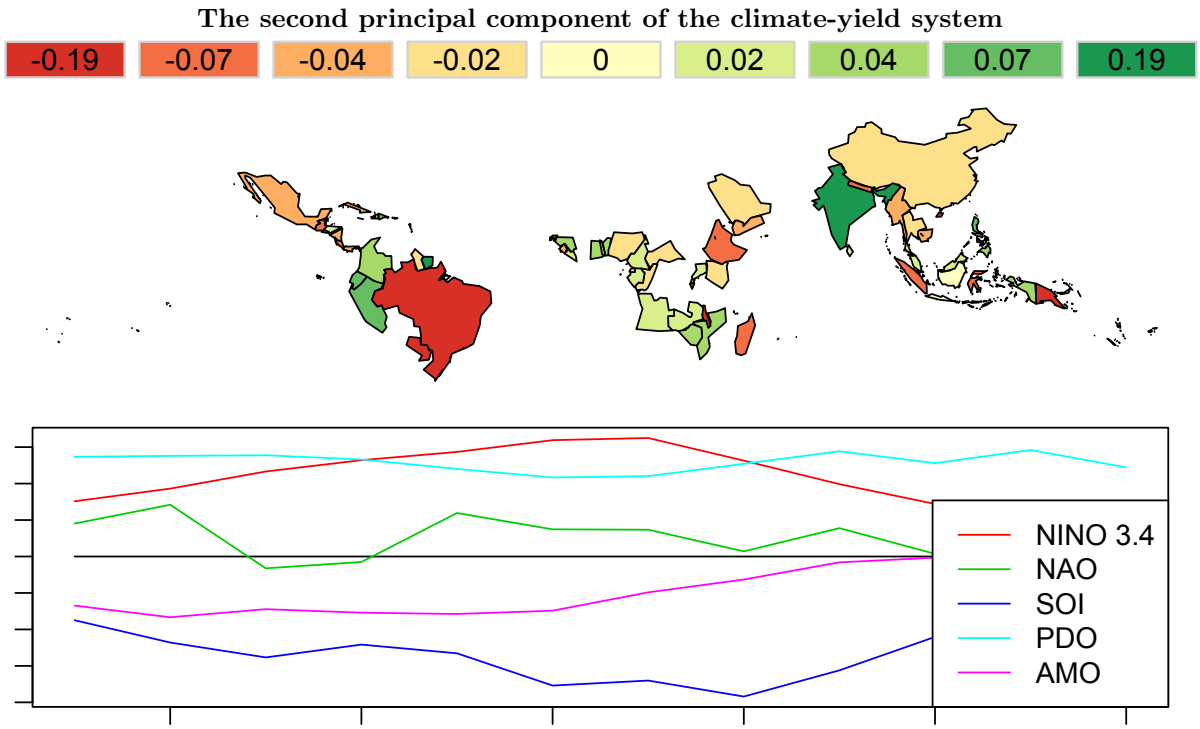


Figure 4.8: Spatial and temporal representation of the second principal component of the climate-yield system. Colors in the map represent increases (green) and decreases (red), and the plot below shows the climate signals across the year (delayed 6 months). Explanation in the text.

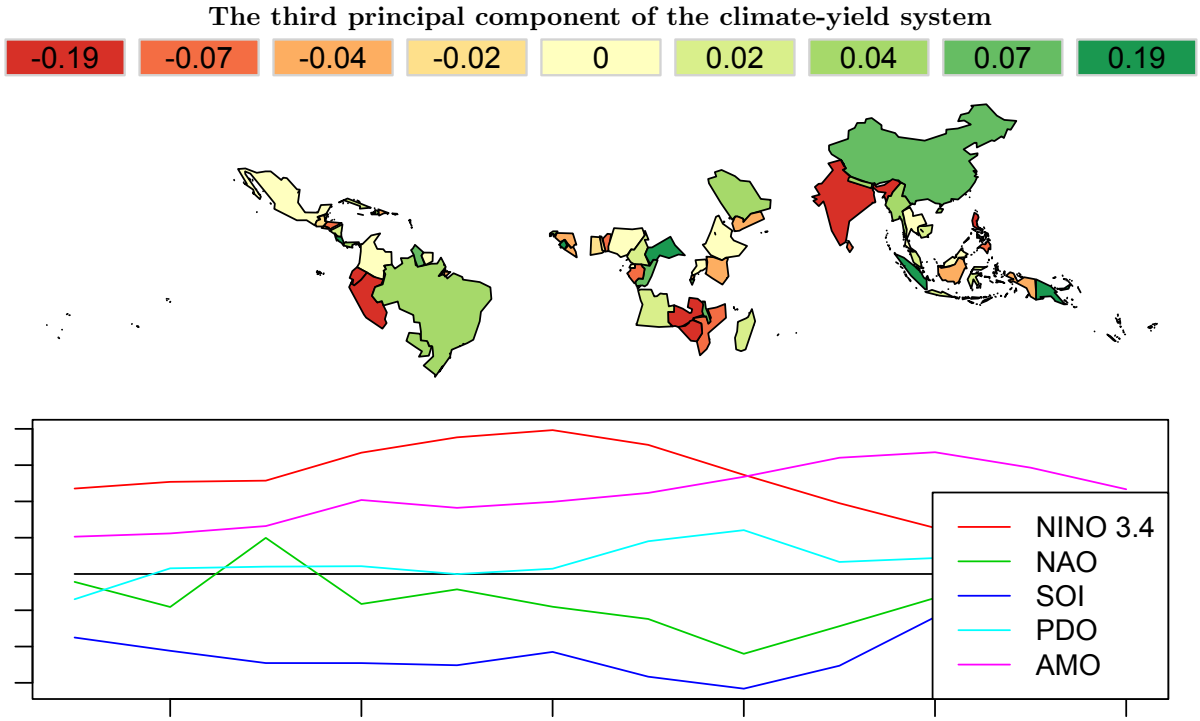


Figure 4.9: Spatial and temporal representation of the third principal component of the climate-yield system. Colors in the map represent increases (green) and decreases (red), and the plot below shows the climate signals across the year (delayed 6 months). Explanation in the text.

## 4.3 Projection for 2015-2016

The El Niño predicted of 2015-16 is expected to have a similar magnitude to the event in 1997-98. However, there is considerable unresolved uncertainty in our analysis as to the most likely outcomes of this event.

The El Niño of 1997-98 produced catastrophic impacts in many areas, but its effect on coffee was fairly minor, coinciding with in a 9.6% drop in production. A large fraction of this global effect was due to Brazil, which had a 32% drop in yields, largely as a consequence of its biennial cycle. Excluding Brazil, the rest of global production only decreased 1.3%. The regional picture is more nuanced, with large decreases also in Oceania. The top part of figure 4.10 shows these results

From the analysis above, the most damaging El Niños coincide with consistently high values in PDO, such as we see today. By decomposing the existing constellation of climate signals into the three coherent groupings shown above, we project the estimates shown in figure 4.10. As described above, there may be large decreases in yields in Brazil and Central America. Our projection also identifies losses in India, and Southern Africa. This is at odds with the recorded values from 1997-98, which saw the most widespread losses across Indonesia and Papua New Guinea.

**Inputs to the El Niño projection**

Our projection is based on the most recent consensus projection of the NINO 3.4 index of ENSO, from International Research Institute for Climate and Society (2015). We try to apply reasonable values to the other indices, using the negative of NINO 3.4 for SOI, given its $-0.6$ correlation with NINO 3.4; a zero value for NAO, given its rapid shifts; and constant extrapolations for PDO and AMO at their most recent value, given the slow shifts in these signals.

Projecting these signals onto the principal component axes gives loadings of 1.3, 3.3, and 1.9, for the three components respectively.

To account for any spurious effect of our decision-making process, we estimate the values for 2014-15 as well, and report the difference.

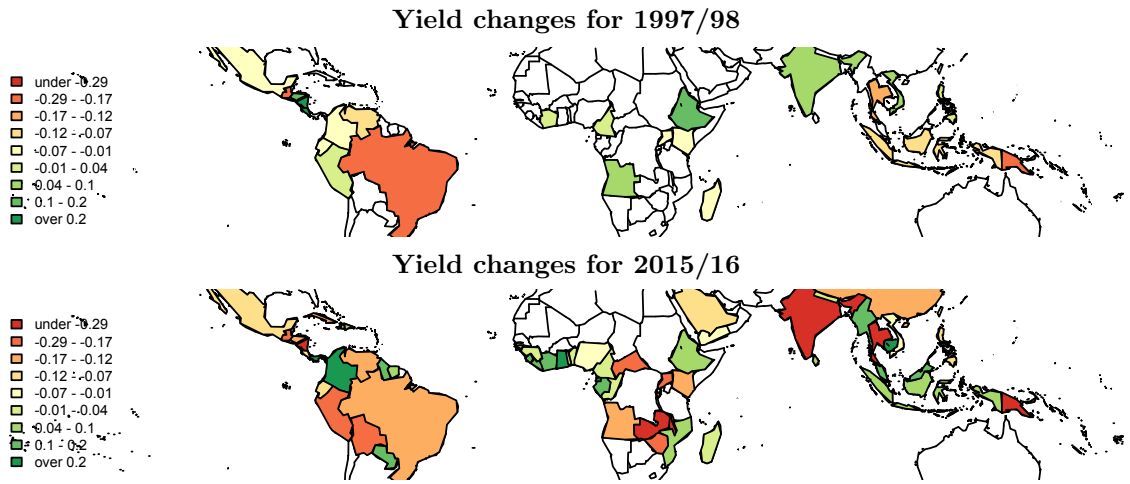


Figure 4.10: **Above:** Yield changes coinciding with the 1997/98 El Niño, relative to 1996/97, from International Coffee Council (1998). **Below:** Yield changes predicted for the 2015/16 El Niño, relative to 2014/15.

## 4.4 Pest growth and control

An associated project for this report explored the effects of temperature in agricultural pest outbreaks. The project focuses coffee rust fungus, La Roya, in Guatemala, an area of high coffee production and recent extreme rust outbreaks (Georgiou et al., 2014). It examined how changes in monthly temperature, the associated 'incubation period' for the fungus (*Hemileia vastatrix*), and the inclusion of a vigilant farmer can affect the outbreak size distribution over time.

Hotter conditions have supported the increase of fungus spread that is killing coffee trees in altitudes that were once free of fungus. This has even caused farmers to switch to more resistant, but lower quality strains of coffee such as Coffea Robusta. This problem impacts the export earnings of coffee-producing countries but more importantly it directly impacts the employment of hundred of thousands of coffee workers who depend on the harvesting earnings to feed their families, with little income to cover a lost season (Magrath, 2014). Additionally, as coffee is a globally traded commodity and Central America is one of the top exporters, the proliferation of coffee rust fungus also has implications for other countries around the world.

Many attempts have been made to find simple and mechanistic solutions to both understand and predict the outbreaks dynamics, but as shown by Lockwood and Lockwood (2008), it has often proven fruitless to capture the effects of weather through linear models. Though many techniques have been utilized to capture the non-linear behavior for different spatial and temporal domains, this project follows their strategy of using a spatial, agent-based model to understand the interactions of space and time.

### 4.4.1 A rust model

We make a number of simplifications to study the fungus outbreaks. First, we will only consider the fungus's interaction with the host plant, even though it has been found to utilize other plants for different stages of its growth cycle. Secondly, we assume that the only factors influencing it spread are temperature and the health of the host plant, thereby ignoring wind and rain impacts that are also known to be important (Ferreira and Boley, 1991). Similarly ignored are higher order effects from the application

of fungicide, where fungicide can also impact some flora and fauna that regulate the fungus, leading to potentially unpredictable disruptions in the natural system.

The model is initialized as a two-dimensional grid of farm space, each grid cell having a certain probability of an appearance of a fungal outbreak. For each time-step, chosen to be one month after examining the reproductive cycle of coffee rust, the outbreak will begin to increase in size as a function of both its current size, the temperature, the amount of host plants available and spread to neighboring grid-cells. The temperature used in the model was obtained from surface temperature Reanalysis Data from the National Center of Atmospheric Research, spatially averaged over the area of Guatemala (without ocean cells) and temporally averaged to each month (NCAR, 2015). A time series of these average temperatures is shown in Figure 4.11, left. Here, one can note a relatively consistent seasonal amplitude of ˜2.5°C around a mean of ˜22°C, with a slight upwards skew.

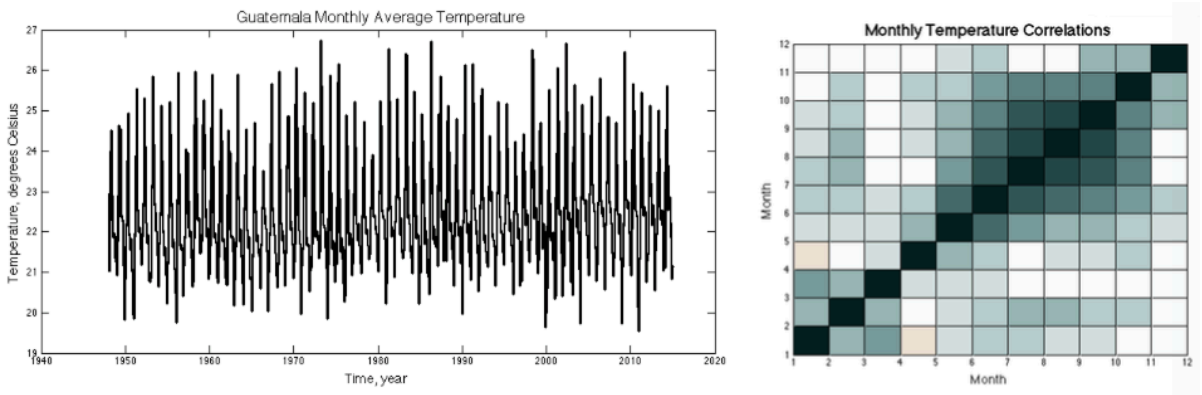


Figure 4.11: **Left:** Timeseries of temperatures. **Right:** Autocorrelation of monthly temperature.

The high level of correlation between months requires that the temperature selected in each monthly time step depend on the temperature in the previous month (see figure 4.11, right). In particular, the summer months are highly correlated, reaching correlations of 0.8 with the previous month in some cases. To account for this, the model is set up to draw a random season from the 67-year time series, employing a three month time series corresponding to an instance of summer, fall, winter or spring, depending on which is needed.

Our basic growth equation can be described by the following equation, with the basic assumption being that higher temperatures increase the growth rate of the fungus (at least at the temperatures seen in Guatemala).

$$N_{t+1} = N_t e^{r_i T_t / T_c}$$

where $N$ is the population of a particular grid cell, $r_i$ is the initial growth rate, $T_t$ is the temperature at that specific time, $T_c$ is the average temperature (over all months). Normally, the quantification of the growth rate is usually conducted with a consideration of both the daily maximum and daily minimum temperature (Magrath, 2014). However this was simplified for inclusion in our model.

When an additional population of fungus is created in subsequent time steps, it is distributed among the original and nearby grid-cells proportional to the health of the host plant in the new grid cell, the population of the source grid-cell and a multiplicative term similar to the prior growth equation. The maximum fungus population for each grid cell is 1, representing 100% infection of the host plant.

The disturbance of each grid-cell is also be subject to density-dependent pressure from predators, in this case the farmer spraying fungicide. Once a particular grid cell reaches a certain percentage of infection

it is detected by the farmer. Detected, the population is decreased by a certain fraction, through the application of the fungicide. In addition, the fungus population will also decrease at a rate proportional to its current population and the relative health of the host species, independent of temperature.

$$N_{t+1} = N_t - N_t(F - 1)$$

where F is the percentage of available host plants for the fungus to grow on.

### 4.4.2 Experiments and results

To evaluate how temperature affects the spread of pests, experiments with three temperature scenarios were run. The first one uses each time step temperature (month) from the historical seasonal data for the region. The other two temperature scenarios considered global warming, one where the mean temperature was increased by 2°C and the other by 4°C. Those three temperature scenarios were run under two pest control conditions, the first one without any kind of pest control and the second one with a farmer's control by using fungicide that eliminated a fraction of the fungus when detected.

### 4.4.3 Historical temperature data without pest control

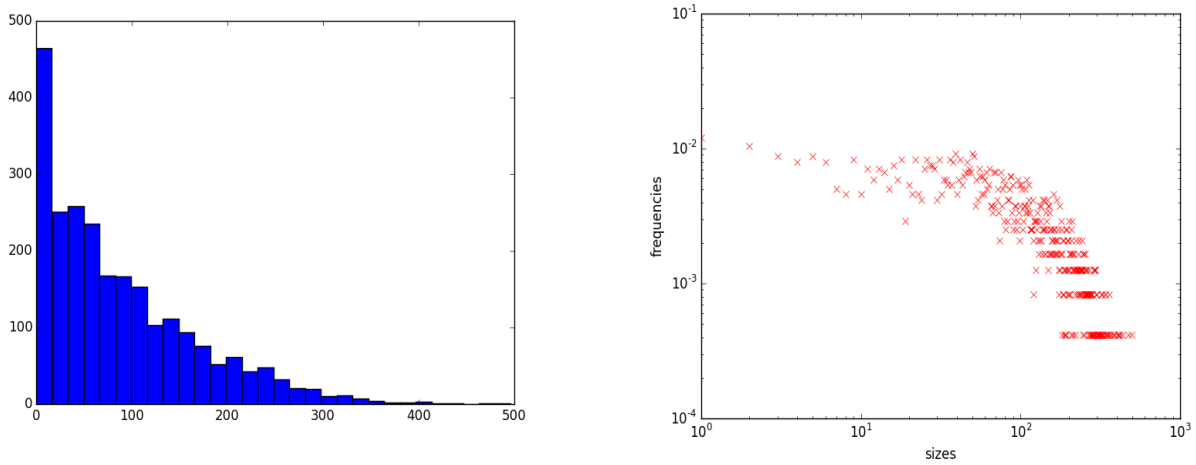


Figure 4.12: Historical temperature data without pest control. **Left:** Histogram of outbreak sizes. **Right:** Log-Log Plot of outbreak sizes.

We set the 'infected threshold' to about 0.3, from the simple fact that we found several instances in which leaves about 1/3 covered in coffee rust where considered 'heavily infected'. In figure 4.12 we have plotted the distribution of outbreak sizes, counting each heavily infected grid-cell at each time step. Please note that as we utilized a 30 by 30 grid cell, complete infection can be represented by a score of 900. Therefore, 490, the largest event, signifies that 54% of the crop is heavily infected.

The Log-Log result, though resembling a power law from 100 on, demonstrates some inconsistent behavior in smaller events. Indeed, in the histogram shelves can be observed where lower values have relatively the same probability. With no warming, the most common event is between 0 – 17, or between 0 and 2% of the crop (though this refers to a single month, not a harvest cycle). The largest event, at 54% of the crop is actually lower than the actual 70% loss in Guatemala in 2012, though there was not an

indication of how this figure was calculated. Nevertheless, the model predicts scenarios where the fungus infects over 30% (300 sites) of the field.

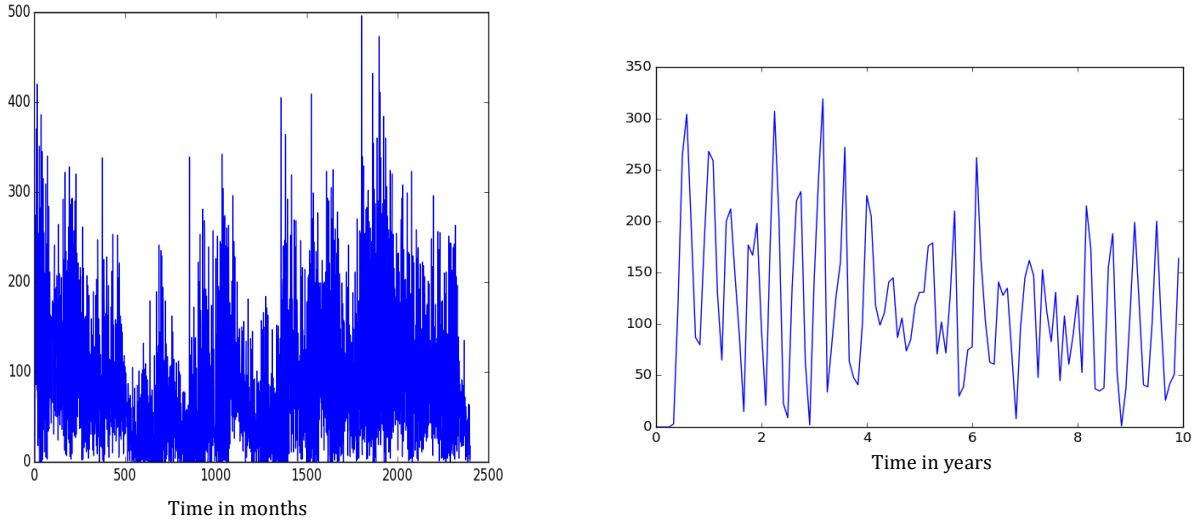


Figure 4.13: **Left:** Time series of outbreak sizes by month. **Right:** Time series of outbreak sizes by year.

Figure 4.13 shows the time series of the previous figure in months. It is clear that the system can be entrenched within certain domain (i.e., large or small events) for many years. As the behavior between 1750 and 2000, a 21-year period, consistently shows some of the highest outbreaks, while still containing intervening low events. This is possibly because the growth of fungus and plant, which are both tied to temperature, sometimes became more synchronous. However, this cannot be determined outright, and thus for future study we might want to run for more time steps, to understand more fully the nature of this large- scale periodicity.

On smaller scales, it can also be noted that many of the largest events come directly after a period of relative calm, as the host plant has had a chance to regain health and provide much more nourishment to the attacking fungus. This small scale rebound, can be seen with more detail. Though the rapid up and down movement can be shown on a scale of a few months, there always seems to be a larger periodicity on the scale of a few years; however, the randomness in the system makes it difficult to conclude anything concrete.

### 4.4.4 Historical temperature data with pest control

Next, we implemented the farmer control, where obvious pest presence would immediately be sprayed with a fungicide and reduced to a fraction of its value in the next month. This fungicide and the necessary training to use it correctly may currently be absent within the poorer farms in the area. Thus, this allows us to see how implementation might change the situation in the future. In Figure 4.14, the distribution has a much smaller mean and median than the without the pest control measures. We note a stronger power law relationship, though like the last iteration, it is slightly concave down. This suggests that moderate events are marginally more likely than they would have been. However, the histogram might be slightly skewed by a larger prevalence of zero events. Additionally, one can note a larger spread than the previous model run for lower probability events.

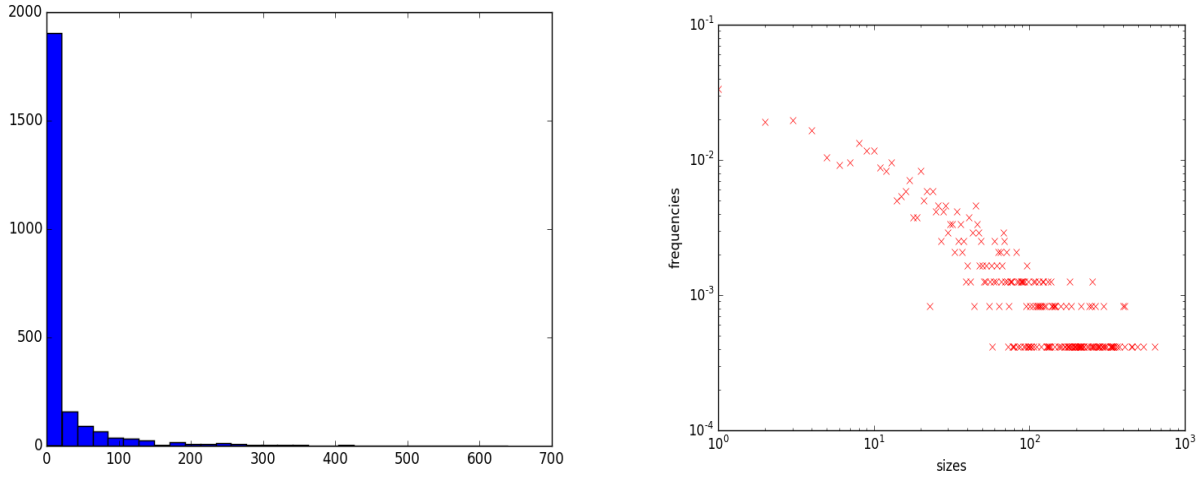


Figure 4.14: Historical temperature data with pest control. **Left:** Histogram of outbreak sizes. **Right:** Log-Log Plot of outbreak sizes.

Unexpectedly, the largest event, 643, signifying about 77% of the crop, is much higher than the previous iteration. This suggests that though fungicide keeps the fungus levels low for the average month, the healthy status of the host plant will make it so the correct temperature conditions or perturbation can cause a huge event, even before the farmer can react (here at a 1 month lag). This is very reminiscent of real world pest control experiences, where application can have unforeseen consequences, such as diminishing the population of a pest predator, and thus upsetting the natural structure of the system and allowing a pest to flourish later (Modern Farmer, 2014). However, catastrophic losses at a few points do not offset the considerable gains shown across the histogram.

Nevertheless, this line of thinking is further corroborated by figure 4.15, where decent periods of little activity are punctuated by huge events, a common feature in nonlinear spatial systems. However, when zoomed in to a period of 10 years, one can note the similarity between the control and non- control scenarios, where the lower bound in the control situation (within inter-month cycles) is replaced with 0.

### 4.4.5 2°C global warming temperature data without pest control

For the next run, we linearly increased the temperature of each month by 2 degrees, in order to represent possible regional warming over the next century. Increasing the temperatures to above normal, and thus often increasing the ability of the fungus to reproduce, causes the histogram of outbreak sizes to shift rightward. The log-log plot, while showing linear behavior for the right tail of the distribution, mimics this change. In an average month 10% of the crop is considered heavily infected, with the tail hitting about 75% of the crop as a maximum value. The time series (Figure 4.17) shows very few events with absolutely no fungus though the behavior in terms of both large-scale and small-scale periodicities does not seem to be drastically different.

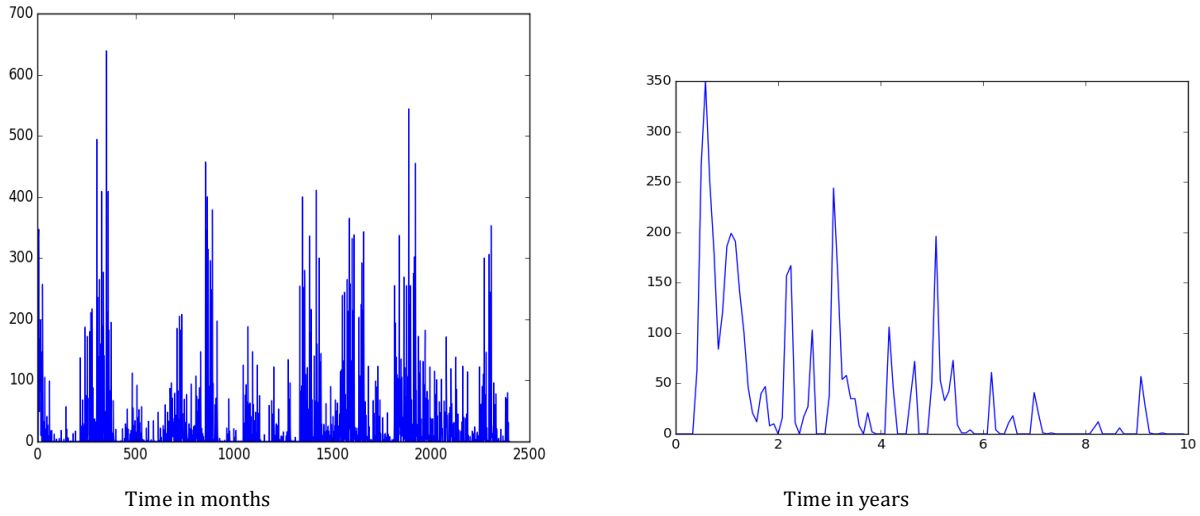


Figure 4.15: **Left:** Time series of outbreak sizes by month. **Right:** Time series of outbreak sizes by year.

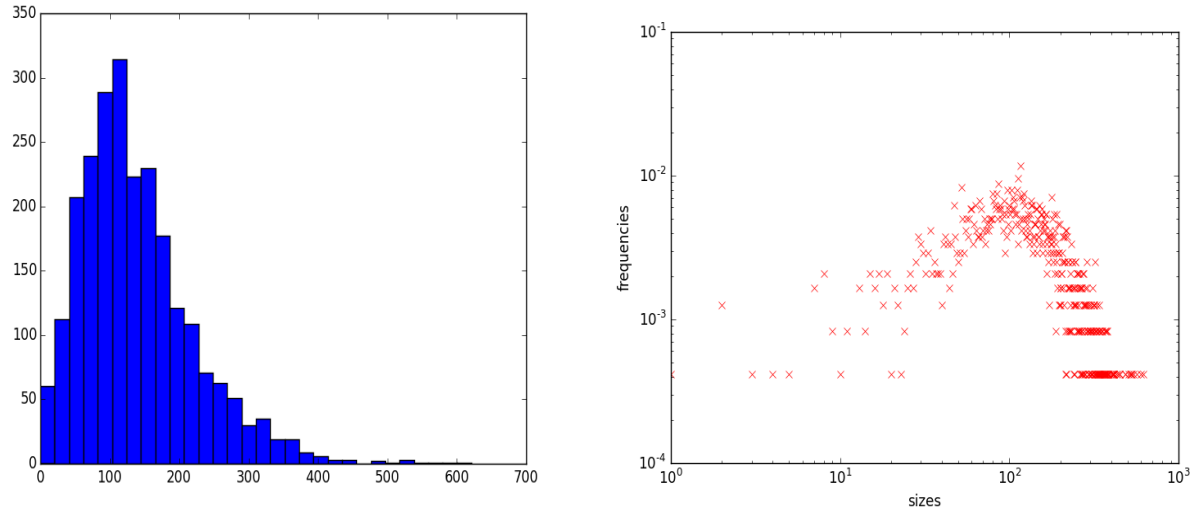


Figure 4.16: 2°C global warming temperature data without pest control. **Left:** Histogram of outbreak sizes. **Right:** Log-Log Plot of outbreak sizes.

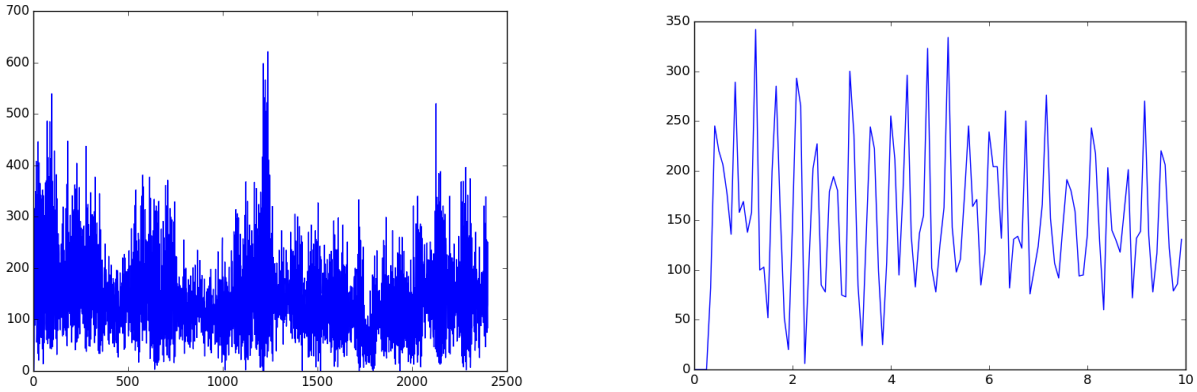


Figure 4.17: **Left:** Time series of outbreak sizes by month. **Right:** Time series of outbreak sizes by year.

### 4.4.6 2°C global warming temperature data with pest control

The addition of pest controls to the warmed scenario has a similar effect as we have noted in the previous iteration. The distribution begins to resemble a power law, however here with a slightly thinner tail. Nevertheless, even in the warmed environment the measures do a reasonable job of controlling the pests, with levels far below the untreated, cooler scenario. The Log-log plot, is however slightly more concave than the previous scenario with pest control.

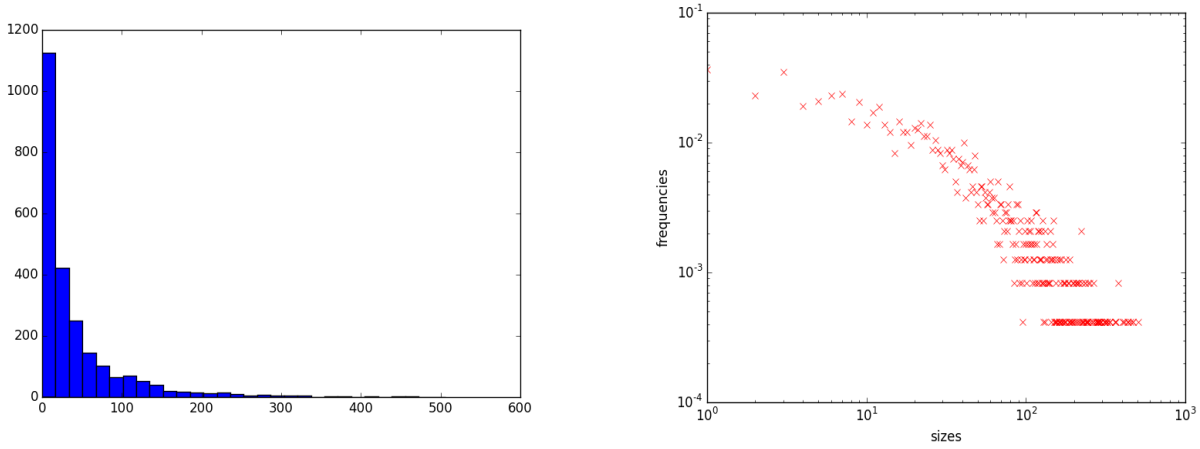


Figure 4.18: 2°C global warming temperature data with pest control. **Left:** Histogram of outbreak sizes. **Right:** Log-Log Plot of outbreak sizes.

Results for a warming of 4°C are included in Appendix A.2.4. Under these conditions and without pesticide, the health of the crop is so poor that it cannot maintain a full outbreak. Even with pesticide, it is impossible to full contain the disease.

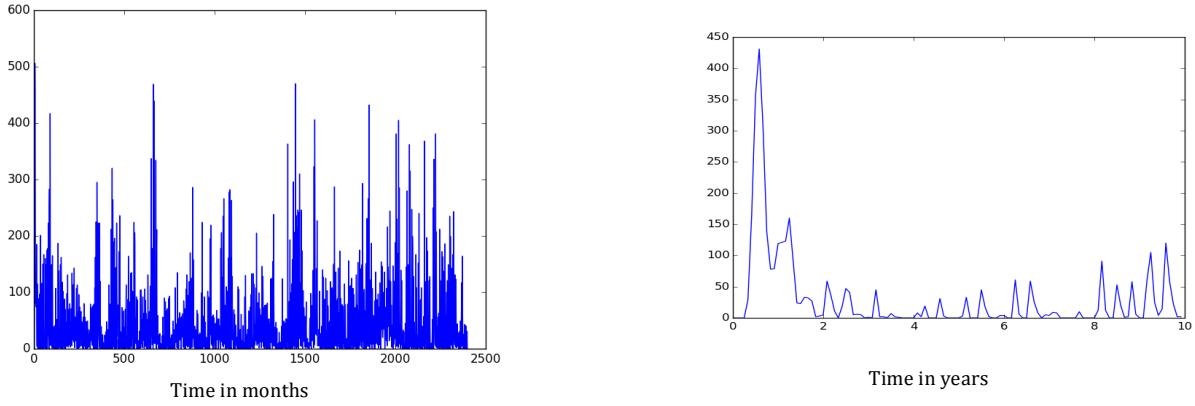


Figure 4.19: **Left:** Time series of outbreak sizes by month. **Right:** Time series of outbreak sizes by year.

### 4.4.7 Discussion

Throughout the drafting and modeling process, we made many other simplifications. We ignored rain and wind as possible spreading agents, instead opting for a random approach. We chose significant parameters such as our time step through very simplified observations of the fungus. We ignored the vegetation cycle (as Guatemala has a very defined wet and dry season which must affect plant growth), though this might be somewhat mitigated by the fact that we tied temperature to the growth of the host plant. We also made considerable simplifying assumptions about the qualities of fungicide application and fungus growth and spread.

Nevertheless, we believe that our results in the change of distribution are representative of what might occur in the real world, given a particular coffee field. We have noted that warming induces a rightward shift in event distribution. The subsequent health decline of the plants may inhibit huge shocks to the system, as the conditions are not ideal for a full fungus takeover. Pest control, while curtailing the infection of an average month can lead to thicker tails and larger rare events. This is possibly because plants are kept at a healthier level, an ideal condition for a quick fungus take over and a drawback of an artificially controlled environment. Additionally, pest control appears to be efficient at compensating for the increased fungus growth rates caused by warming, as even in the 4°C warmer environment, it is able to bring the distribution back to the less disastrous approximate power law, albeit with a mode higher than zero. In the future, under the extreme scenario, it is very possible that some sort of artificial control will be necessary to continue to grow coffee in this region. This will possibly bring more complications and unpredictable dynamics that we cannot comment on with such a simple model.

# Chapter 5

# Empirics of production

In this chapter, we develop a globally applicable coffee production model, which describes the predictability of yields under current and future weather.

## 5.1 Crop modeling approaches

One broad approach to predicting crop development and providing decision-support tools to farmers is through biological process models. These models capture the process of plant development (phenology) at the individual plant level, and are available for many crops as models for widely-used crop modeling systems such as DSSAT and APSIM[1]

Biological process models of coffee production appear to be in their early stages. The most advanced may be the one developed by Rodríguez et al. (2011), with a "tri-trophic, physiologically-based system perspective", capable of studying water and light needs and pest impacts. The next generation of biological models, represented by Dauzat et al. (2014) and Maro et al. (2014) are still under development. This state of the literature motivated our focus on statistical models.

A statistical production model relates high-resolution weather data (such as temperature and precipitation) with observed yields (Schlenker and Roberts, 2009). The most advanced of these estimate the effect of growing degree-days (GDDs) and "killing degree-days"(KDDs) in a non-linear fashion, and account for varying unobserved characteristics that are idiosyncratic to each region, such as management, elevation, and soil properties. Statistical approaches have been used to study individual regions (e.g., Gay et al., 2006; Guzmán Martínez et al., 1999). We use our global coffee production database and to generate a global model which with elements that vary from one country to another.

The statistical techniques we use fall under the heading of econometrics. Econometric techniques allow for the inclusion of many different parameters and a treatment of differences between regions which are not directly captured in our data. They also allow for the careful identification of "causal" relationships, rather than simple correlation. We then extend this statistical model with a new technique developed here, which we call hierarchical modeling. The hierarchical model consists of three levels of hierarchy: sub-national models, national models, and a global model. At each level, different regions are allowed to have different responses of yields to weather, but are also informed by the effect estimated across all regions (e.g., all national models are informed by the global combined model).

[1]DSSAT is the Decision Support System for Agrotechnology Transfer(**?**) and APSIM is the Agricultural Production Systems Simulator(**?**).

These statistical models are estimated using natural experiments, by comparing observed yields in years with different distributions of weather to estimate the effect of weather in general. These experiments completely inform our models of production. The models below include daily minimum and maximum temperatures, precipitation, and humidity. We do not include soil properties in this chapter because it is impossible to do statistical experiments where soil characteristics vary over time, to see its effects. As a result, the statistical model cannot determine the effects of soil.

This approach puts a "black box" around the complicated system surrounding production, and makes no attempt to disentangle the effects of farmers responding to weather, the effects of that weather on the crops themselves, and the effects that these have on the plant's susceptibility to disease. This black box is both a strength and a limitation. It captures realistic relationships between weather and yields, rather than theoretical responses of the crops in an experimental setting. It can capture the environmental determinants of coffee disease spread, and their impacts implicitly. It can also be used to predict yields under climate change and weather events. However, because it cannot distinguish the social and natural causes, it makes an implicit assumption that yields will continue to respond the same way to increasing temperatures over time.

The production model can also be used to predict yields months before a harvest. By combining climatological signals, like ENSO, for which there is some predictive skill, with yearly averages (climatologies), it is possible to generate plausible weather patterns to apply to the model. However, these results could only be taken as suggestive: the statistical models we produce only account for about 32 - 38% of the variation in yields across time and space. The biennial cycle of coffee, for example, is not explicitly captured in our model, which considers only effects driven by weather (Bernardes et al., 2012).

In addition to the biennial cycle, there are a large number of factors which drive coffee yields that are not explicitly included in this model: market drivers, evolving technology, changing varieties, and the governance and politics which frequently affect the coffee sector. These are all important. By limiting our analysis to the student of weather and climate change, we can better understand those elements.

## 5.2 Weather and climate data

The current climate is represented by weather records from recent history. We use weather data since 1979 from the Climate Forecast System Reanalysis (CFSR). This data product combines station and satellite measurements using weather models to produce reliable weather estimates at a high spatial and temporal resolution. The spatial resolution is .32°x.32°, a grid with boxes that are about 35 km on a side at the equator. The temporal resolution is hourly, which we use to generate growing degree-days at a daily scale.

Yields and production data are not available in a high-resolution, gridded form. Instead, yields, in the form of production quantities and harvested areas, are reported for political units. High resolution information about coffee producing regions needs to be combined with these low resolution recorded yield data. For example, coffee is grown exclusively in the southwest of Guatemala, in regions that cover 8.7% of the land area, but production data is reported for the entire country. Since we know that the country-wide production is coming only from these regions, we can limit the weather and other data used to infer coffee production relationships. To match the gridded weather data with growing regions, we use our coffee production database to spatially aggregate the weather data.

**Climate Forecast System Reanalysis**

The Climate Forecast System Reanalysis is a global weather product constructed by NOAA (Saha

et al., 2010). CFSR merges the overlapping ranges of satellite products, as they are available across years:

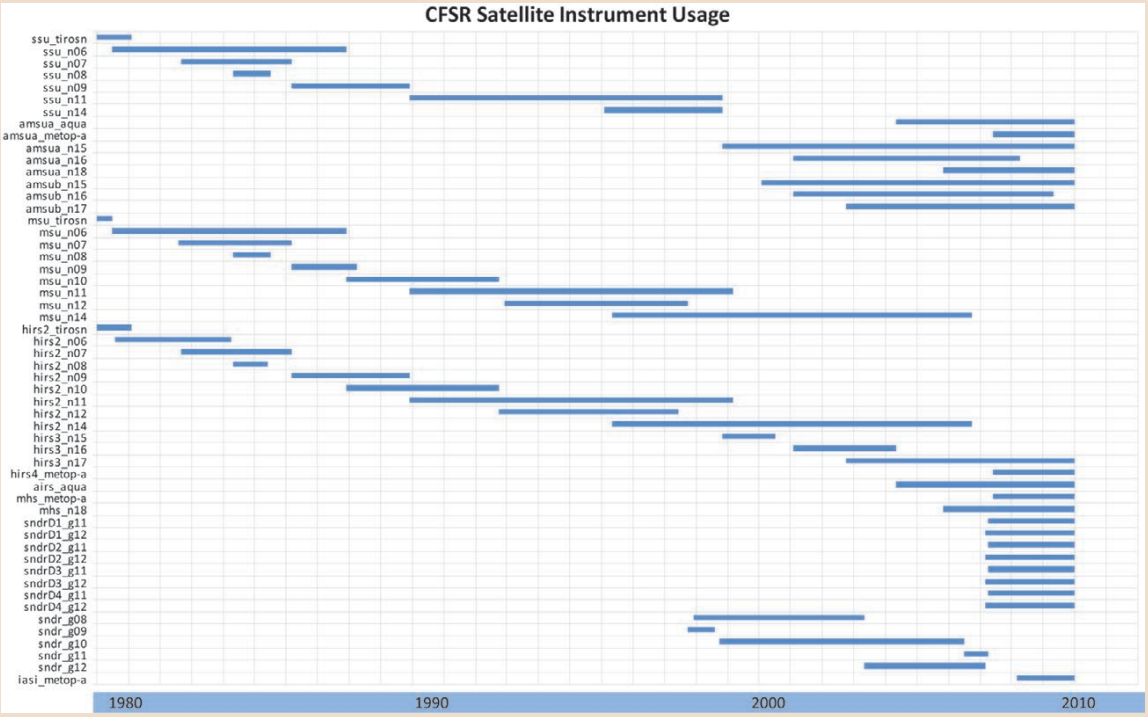


CFSR combines both conventional and satellite data from the following sources:

**Conventional:** Radiosondes and Pibals, AMMA special observations, Aircraft and ACARS data, Surface observations, PAOBS, SATOB observations, SSM/I ocean surface wind speed, Scatterometer winds

**Satellite-radiance:** TOVS radiances, Recalibrated MSU radiances, ATOVS radiances, GEOS radiances, Aqua AIRS, AMSU-A, and AMSR-E data, MetOp IASI, AMSU-A, and MHS data, CHAMP/COSMIC GPS radio occultation data.

**Spatially-weighting weather**

To generate weather observations at the same spatial aggregation as yields, we perform the following procedure. For each political unit,

1. Translate CFSR grid cells into a lattice of points.
2. Find all grid lattice points within a given country.
3. Identify the measure of harvested area in the coffee database nearest to each lattice point.
4. Take the weighted average of weather observations, weighted by coffee harvested area.

An example is shown below for grid cells that fall within Colombia.

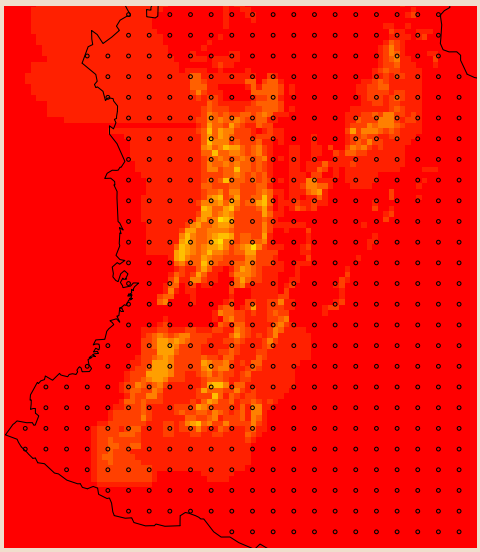

Circles show the location of CFSR grid lattice points. Colors show the coffee weights.

## 5.3 Brazil case study

The Brazilian Institute of Geography and Statistics (IBGE) provides municipality-level production for coffee in Brazil since 1990. Nearly 2,700 municipalities with coffee production histories are included, and representing an average resolution of less than 40 km. This dataset allows for a broad case study of the impacts of climate change at a high spatial resolution. We refine the structure of our production model for Brazil before applying it globally.

### 5.3.1 An empirical model of production

Using the IBGE Brazilian coffee production estimates, combined with high resolution weather from the CFSR reanalysis product, we estimate a physically-based statistical model of coffee production. The model predicts yields using a nonlinear relationship with temperature and precipitation. We base our model on Schlenker and Roberts (2009), and divide GDDs into three groups: beneficial growing degree-days between 0°C and 33°C, killing degree-days above 33°C, and frost degree days below 0°C. We also use the average minimum temperature, which appears to be more significant than frost degrees. This kind of statistical relationship is based on the biological response of coffee to temperature, but puts a "black box" around farmer responses and ecosystem and pest dynamics. If farmers are providing sufficient irrigation and shade to coffee plants, the effect of high temperatures will be mitigated beyond what biological models suggest on their own.

**Calculating growing degree-days**

Growing degree-days (GDDs) are calculated using a continuous sinusoidal fit to minimum and maximum daily temperatures, as shown below:

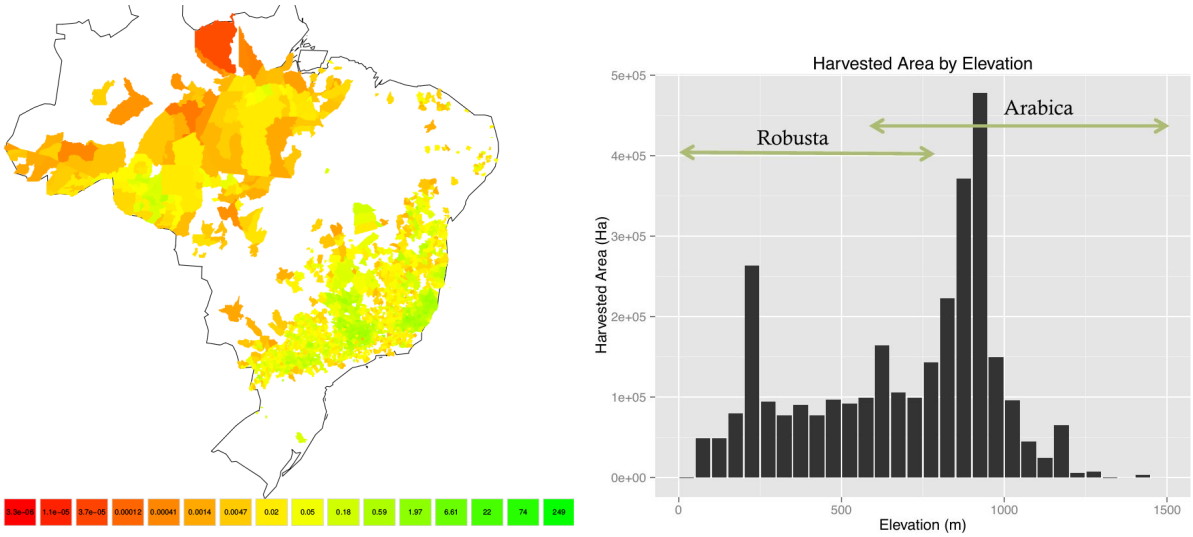


Figure 5.1: Brazil dataset across space and elevation. **Left:** Density of coffee production, as the average production divided by municipality area. Regions in green account for the majority of production. Most production occurs in the south, however there are coffee producing regions also in the southern Amazon. **Right:** Distribution of coffee producing area, displayed across the average elevation of each municipality. The greatest extent of coffee production occurs in municipalities with around 900 m of elevation, but coffee is also produced in municipalities with a much lower elevation, including a peak around 200 m. The range of typical elevations for growing Arabica and Robusta are shown above the histogram.

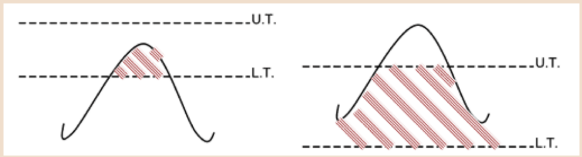


Calculations for growing degree-days and killing degree-days. Any temperatures above a given lower threshold (L.T.) are included, up to a maximum of an upper threshold (U.T.). As temperatures shift over the course of a day, fractional growing degree-days are accumulated.

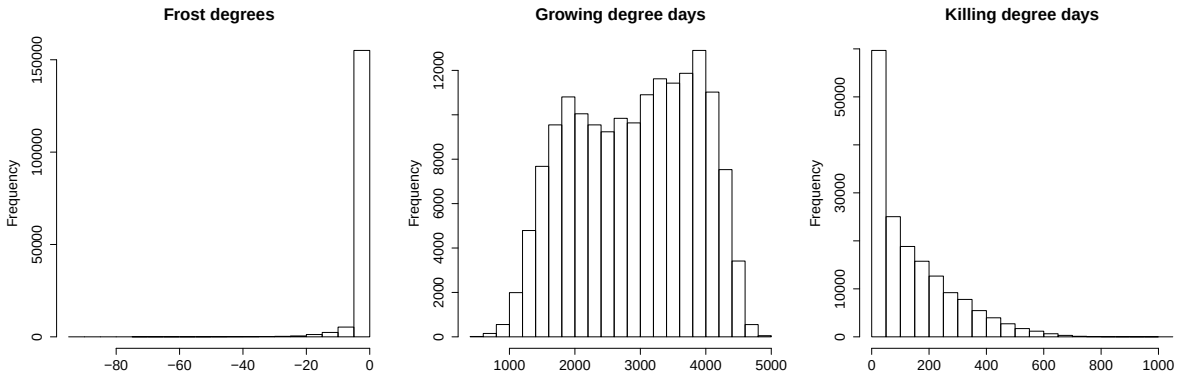


Figure 5.2: Histograms displaying the number of growing seasons with a given number of frost degree-days, growing degree-days, and killing degree-days. The exponential decays in frost and killing degree days are useful for capturing the impact of extreme events. The broad range of growing degree-days represented in the center histogram allows for accurate estimates of the coffee growth response.

We also include precipitation, as the total accumulated precipitation over the six months before harvest. Precipitation is included as a quadratic, to capture the expectation that both too little precipitation and too much precipitation are harmfully impact yields.

### 5.3.2 Optimal temperature range

Guzmán Martínez et al. (1999) suggest that 10°C is the appropriate base temperature for calculating GDDs for coffee. We explore a large range of minimum and maximum temperatures for GDDs, seeking the limits that provide the greatest predictive capacity. See Appendix A.3.1 for predictive capacity of a range of possible limits. We find that a minimum temperature of 0°C and a maximum temperature of 33°C for beneficial GDDs is optimal. This means not only that all days over 0°C are estimated as beneficial, but that higher temperatures up to 33°C are progressively more beneficial. A day above 33°C is not immediately detrimental, but it has a progressively smaller benefit until it becomes negative, and we find that temperatures over about 35°C are detrimental in Brazil.

### 5.3.3 Predictive periods

Coffee production is very sensitive to weather during flowering, and the period during which we correlate weather with yields is important. To determine the optimal span of weather for predicting yields, we try out many combinations of starting and ending months. The harvesting period in Brazil ends in September, so we consider months starting with October to predict the yield in the next year. The coefficients of models for each of these periods are shown in figure 5.3.

A few features are important in these results. In the top graph displaying coefficient values, areas in the upper-left are gray, denoting that models that use only the months shortly preceding harvest do not produce significant results. Second, we expect the effect of GDDs to be positive, KDDs negative, the linear component of precipitation (`precip`) to be positive, and the quadratic component of it (`precip2`) to be negative. This is confirmed for most date ranges, and we want to avoid regions that misestimate these values due to noisy or minor effects. Finally, the t-values figures show the confidence in these values, and are a measure of the statistical significance of the model as a whole. These values generally decrease as the starting month becomes later.

Figure 5.4 shows the combined t-values for the GDD and KDD coefficients. The highest t-value is for GDD and KDD values calculated just for January and February. The probably reflects a highly sensitive period for the berry production. Nearly as high, and covering a six-month span, is December through May. We will use this as our span for calculating weather impacts.

### 5.3.4 Econometric model

The form of the statistical model is,

$$\log y_{it} = \alpha_i + \gamma g_{it} + \kappa k_{it} + \mu m_{it} + \pi p_{it} + \psi p_{it}^2 + P_{3,s(i)}(t) + \epsilon_{it}$$

Above and in the other models below, the observation variables and their corresponding effect estimating coefficients are:

| | Var. | Coeff. |
|---|---|---|
| Growing degree-days | $g_{it}$ | $\gamma$ |
| Killing degree-days | $k_{it}$ | $\kappa$ |
| Average minimum temperature | $m_{it}$ | $\mu$ |
| Total precipitation (linear) | $p_{it}$ | $\pi$ |
| Total precipitation (quadratic) | $p_{it}^2$ | $\psi$ |

where $i$ indexes municipalities, $t$ the years, and $P_{3,s(i)}(t)$ is a state-specific cubic trend to capture shifting productive capacity. We aggregate weather from December to May, and use 0°C to 33°C as the limits for computing growing degree-days.

**Interpreting regression tables**

Many of the results in this chapter are in the form of multiple regression tables. Each regression is of the form,

$$y_i = \alpha + \beta_1 x_{1,i} + \cdots + \beta_k x_{k,i} + \epsilon_i$$

which describes the relationship between a dependent variable, $y_i$, taking different values for each $i$th observation, and a linear combination of independent variables, $x_{1,i}, \ldots, x_{k_i}$. The $\epsilon_i$ term represents the remaining error that cannot be explained by the model. In addition, these models use "fixed-effects", which are parameters unique to each region, so that the model is effectively estimated by

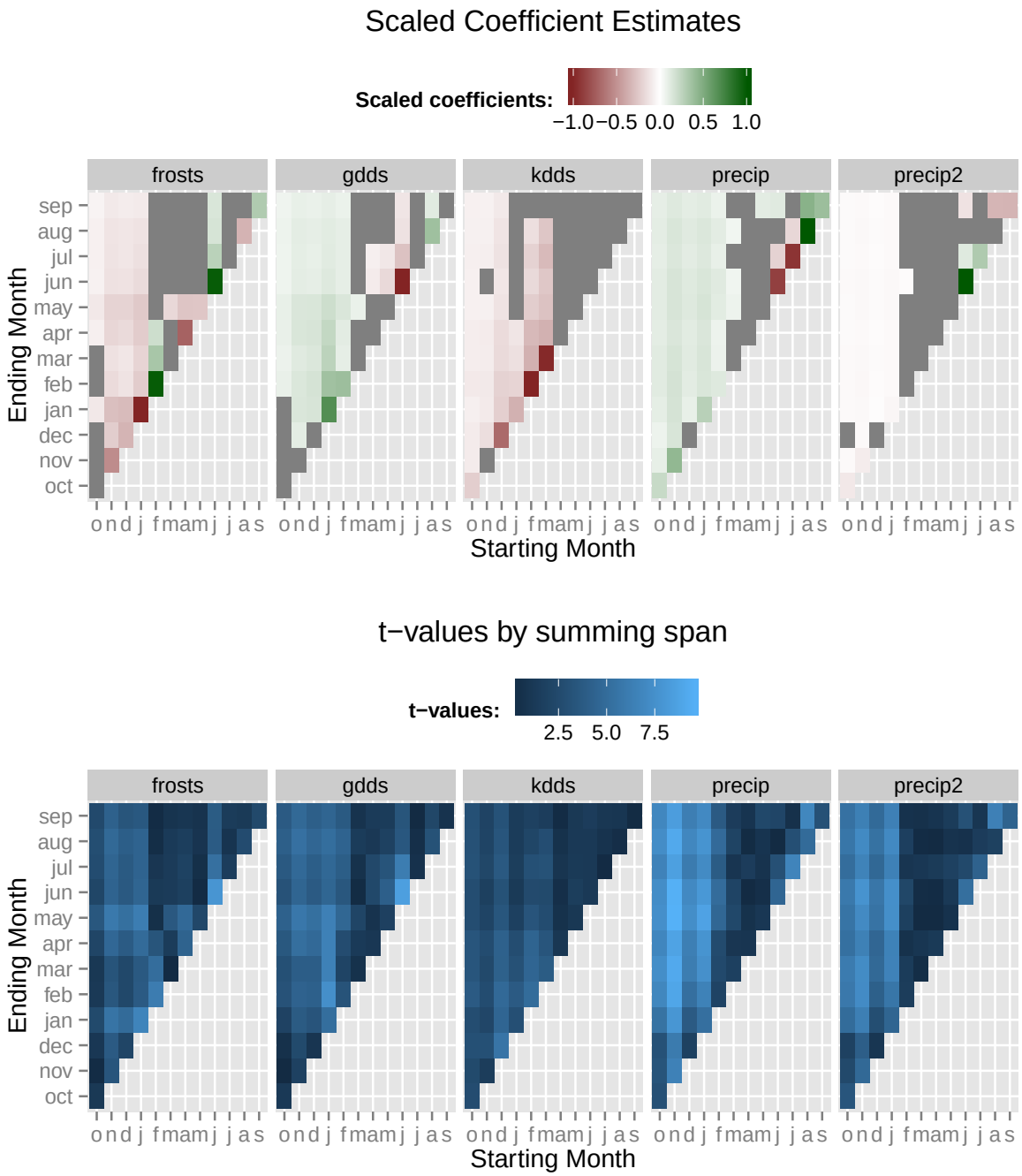


Figure 5.3: Coefficients from estimating models with different month spans, and the t-values intervals associated with each coefficient. The top 118 municipalities in harvest density were used.

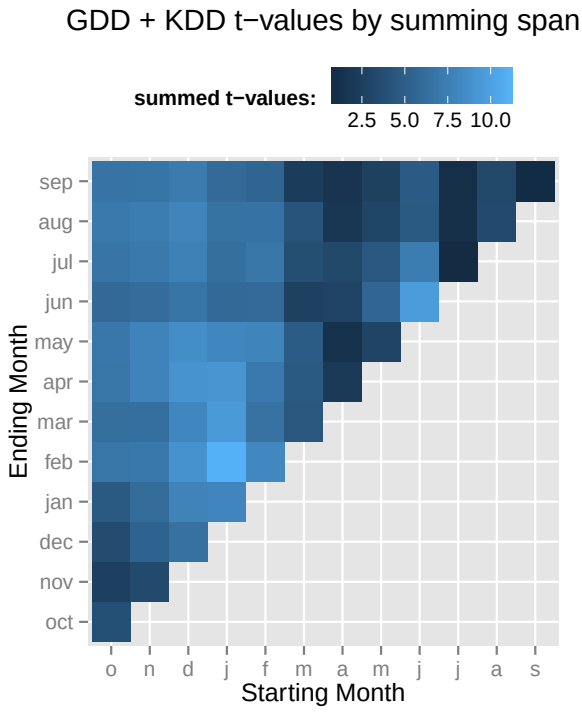


Figure 5.4: The sum of t-values across the GDD and KDD coefficients, for identifying the most effective range.

considering the effects of changes in the independent variables, rather underlying static differences between them.

The regression tables are mean to be read in columns. The first column specifies the variable for which an effect is reported, and the model columns specify the size of that effect. If a coefficient estimated is 10, that means that the dependent variable increases by 10 for every unit the independent variable increases.

The numbers directly below each effect and reported in parentheses are the values 'standard errors', a measure of the uncertainty of that value. If the standard error is less than half of the value, then there is 95% confidence that the sign of the coefficient in question is correct. This corresponds to the statistical significance of the estimate, and is denoted by asterisks (***).

The results are shown below as a table of statistical coefficients. Table 5.1 displays the results across all municipalities, and 5.2 is for the 118 municipalities with the greatest density of coffee harvesting.

| | | *Dependent variable:* | |
|---|---|---|---|
| | Means | Log Yields | Harvested Hectares |
| | | (1) | (2) |
| GDDs / 1000 | 2.946 | 0.152*** | 72.869 |
| | (0.931) | (0.050) | (124.246) |
| KDDs / 1000 | 0.149 | −2.806*** | −2,197.369*** |
| | (0.146) | (0.342) | (555.055) |
| Avg. Min. | 0.944 | −0.091*** | −25.0 |
| | (3.499) | (0.018) | (34.0) |
| Precip. (m) | 1.421 | 0.347*** | −9.587 |
| | (0.719) | (0.028) | (64.092) |
| Precip.$^2$ (m) | 2.538 | −0.366*** | −8.520 |
| | (2.439) | (0.036) | (84.618) |
| State cubic trends | | Yes | Yes |
| Observations | | 43,165 | 43,185 |
| $R^2$ | | 0.383 | 0.655 |
| Adjusted $R^2$ | | 0.343 | 0.633 |
| Residual Std. Error | | 0.535 (df = 40542) | 4,300.446 (df = 40561) |
| *Note:* | | *p<0.1; **p<0.05; ***p<0.01 | |

Table 5.1: Estimates for statistical models relating growing degree-days, killing degree-days, average minimum temperature, and precipitation to the logarithm of yields, and to harvested area, for all municipalities. Stars (***) represent statistical significance levels, showing that most coefficients appear to have a relationship with production outputs.

We find that increases in temperature below a daily maximum temperature of 33°C limit are beneficial, resulting in higher yields and higher total production (see Appendix A.3.1). Based on this, we compute "growing degree days" (GDDs) as the degree days[2] between 0°C and 33°C. All temperatures above 33°C

[2]An explanation of degree days is at `https://en.wikipedia.org/wiki/Degree_day` and Appendix 5.3.1 for our method of calculating them.

| | *Dependent variable:* | |
|---|---|---|
| | Log Yields | Harvested Hectares |
| | (1) | (2) |
| GDDs / 1000 | 0.475*** | 1,700.306* |
| | (0.109) | (976.997) |
| KDDs / 1000 | −2.989** | −23,179.330*** |
| | (1.423) | (8,681.404) |
| Avg. Min. | −0.183*** | −290.009 |
| | (0.0183) | (335.665) |
| Precip. (m) | 0.441*** | −1,168.520* |
| | (0.076) | (677.845) |
| Precip.$^2$ (m) | −0.494*** | 1,978.722** |
| | (0.099) | (854.580) |
| Observations | 3,181 | 3,181 |
| $R^2$ | 0.320 | 0.485 |
| Adjusted $R^2$ | 0.290 | 0.462 |
| Residual Std. Error (df = 3043) | 0.364 | 14,412.800 |
| *Note:* | *p<0.1; **p<0.05; ***p<0.01 | |

Table 5.2: Estimates for statistical models relating growing degree-days, killing degree-days, average minimum temperature, and precipitation to the logarithm of yields, and to harvested area, for the top 118 municipalities by production density. Stars (***) represent statistical significance levels, showing that most coefficients appear to have a relationship with production outputs.

are combined into the measure of "killing degree days" (KDDs).

Any days in which the maximum temperature exceeds 35°C have a sharply harmful effect. As a result, even small increases in temperatures under climate change can produce large decreases in yields, particularly in regions where temperatures are currently nearly optimal. This is consistent with other work on the nonlinear effects of high temperatures (Schlenker and Roberts, 2009).

Every additional 1000 GDDs (of which there are about 3000 on average in coffee-growing municipalities in Brazil) increases yields by about 16%. Every additional 100 KDDs (an average year will have only 150 KDDs) decreases yields by 76%. These values are estimated using marginal changes, so the average year is the baseline from which these percent changes are applied.

Figure 5.5 shows a graphical representation of the growing degree-day production model, with 95% confidence intervals. The assumptions are as described before: growing degree-days and precipitation are calculated using hourly reanalysis data; state cubic trends capture the evolution of coffee production.

There is also a large and statistically significant negative effect on harvested acres. This suggests that in hot years where the crop is damaged, the plants are simply not harvested. As a result, the actual damaging effects of high temperatures on yields are likely to be greater than reported. The yield numbers hide the fact that unproductive plots in poor years can be left unharvested, causing both total production and harvested acres to decrease without as large of decreases in yield.

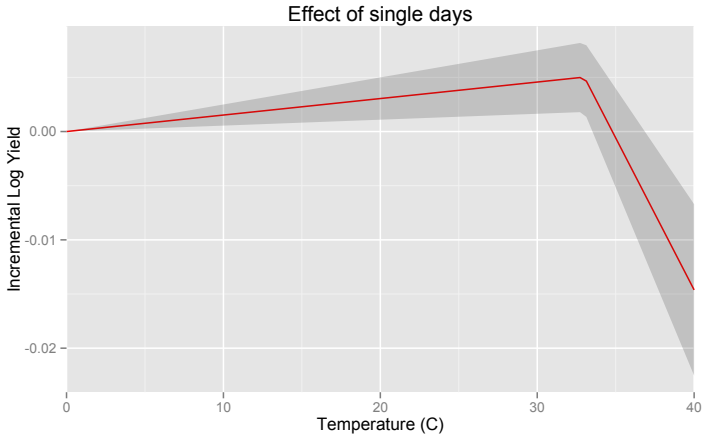


Figure 5.5: Marginal impact on log yields for an additional day at a given temperature. Up to 33°C, additional temperature results in greater yields. Above 33°C, this effect is sharply diminished and hot days above 35°C result in large decreases in yield. The grey band shows the 95% confidence intervals around the estimated effect for a single day at a given temperature.

### 5.3.5 Multilevel Brazil model

Next we extend the model to include "multilevel" effects. The multilevel model studies how the estimated coefficients vary across other characteristics of the municipalities. In this case, we consider how the effect of GDDs, KDDs, and average minimum temperature vary with elevation. Elevation is both an important determinant of coffee quality, and is a proxy for the variety of coffee grown: Brazil grows both Arabica and Robusta coffees, but does not report their production separately (until recent years).

The multilevel relationship is that:

$$\begin{aligned}
\log y_{it} &= \alpha_i + \gamma_i g_{it} + \kappa_i k_{it} + \mu_i m_{it} + \pi_i p_{it} + \psi_i p_{it}^2 + \epsilon_{it} \\
\gamma_i &= \gamma_0 + \beta_\gamma Elevation_i + \eta_{\gamma,i} \\
\kappa_i &= \kappa_0 + \beta_\kappa Elevation_i + \eta_{\kappa,i} \\
\mu_i &= \mu_0 + \beta_\mu Elevation_i + \eta_{\mu,i} \\
\pi_i &= \pi_0 + \beta_\pi Elevation_i + \eta_{\pi,i} \\
\psi_i &= \psi_0 + \beta_\psi Elevation_i + \eta_{\psi,i}
\end{aligned}$$

where the top line is the normal regression relationship, but with separate coefficients for each municipality $i$. The remaining lines relates all municipality coefficients together according to their varying elevations. The results are shown in table 5.3 and in a graphical form in figure 5.6.

Next we consider how the sensitivity to temperature varies with elevation. The parameters that mediate this sensitivity– the positive effect of GDDs and the negative affect of KDDs– are shown in figure 5.6. We find that temperatures above 33°C at 1000m above sea level are five times as damaging as they are at 250m. These results support the common wisdom: Arabica, grown at higher elevations, is much more sensitive to weather than Robusta. We find that as elevation increases, the potential increased yield from higher temperatures as well as the potential damage due to extreme temperatures increase.

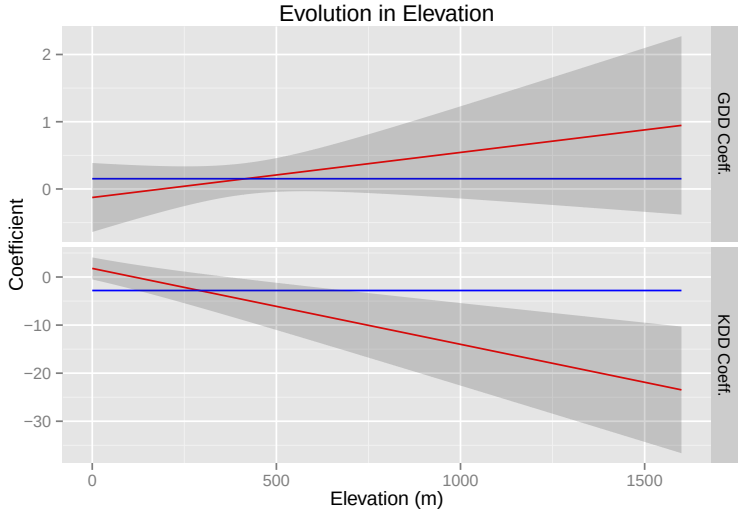


Figure 5.6: The effect of an additional GDD and KDD as these vary by elevation. As elevation increases, plants become more sensitive to temperatures. The effect of GDDs increases, though very slightly. The harmful effects of KDDs increase quickly.

### 5.3.6 Yield estimates under a warmer climate

We can apply the production model to weather produced from climate change. As a proxy for climate change, we estimate yields using historical weather data increased by 2°C. Precipitation values are left

| | *Dependent variable:* | |
|---|---|---|
| | Log Yields | Harvested Hectares |
| | (1) | (2) |
| GDDs / 1000 | 0.208*** | 40.303 |
| | (0.051) | (130.508) |
| Elev. GDDs / 1000 | 0.001*** | 2.110*** |
| | (0.0002) | (0.657) |
| KDDs / 1000 | −6.106*** | −4,600.562*** |
| | (0.516) | (725.931) |
| Elev. KDDs / 1000 | −0.016*** | −17.054*** |
| | (0.002) | (3.653) |
| Avg. Min. | −0.183*** | −25.750 |
| | (0.018) | (34.334) |
| Elev. Avg. Min. | −0.00000** | −0.183 |
| | (0.00000) | (0.183) |
| Precip. (m) | 0.358*** | −32.650 |
| | (0.030) | (76.846) |
| Elev. Precip. (m) | 0.0001 | −0.164 |
| | (0.0001) | (0.285) |
| Precip.$^2$ (m) | −0.391*** | −10.825 |
| | (0.039) | (98.941) |
| Elev. Precip.$^2$ (m) | 0.0001 | 0.648* |
| | (0.0001) | (0.390) |
| Observations | 42,141 | 42,161 |
| $R^2$ | 0.378 | 0.651 |
| Adjusted $R^2$ | 0.338 | 0.628 |
| Residual Std. Error | 0.538 (df = 39582) | 4,282.486 (df = 39601) |
| *Note:* | | *p<0.1; **p<0.05; ***p<0.01 |

Table 5.3: The effects of GDDs, KDDs, and average minimum, as each varies by elevation. While the estimates are not significant, they suggest increasing sensitivity to temperature in the form of both GDDs and KDDs as elevation increases. All municipalities in Brazil used.

unchanged, since they show an unclear trend. This change produces several effects: it increases the number of GDDs benefiting yields, increases the number of KDDs harming yields, and increases average minimum temperature. The resulting balance between these three impacts is not evident *a priori*. The figure below shows the distribution for municipality yields across Brazil, from observed data, and under climate changed weather predictions.

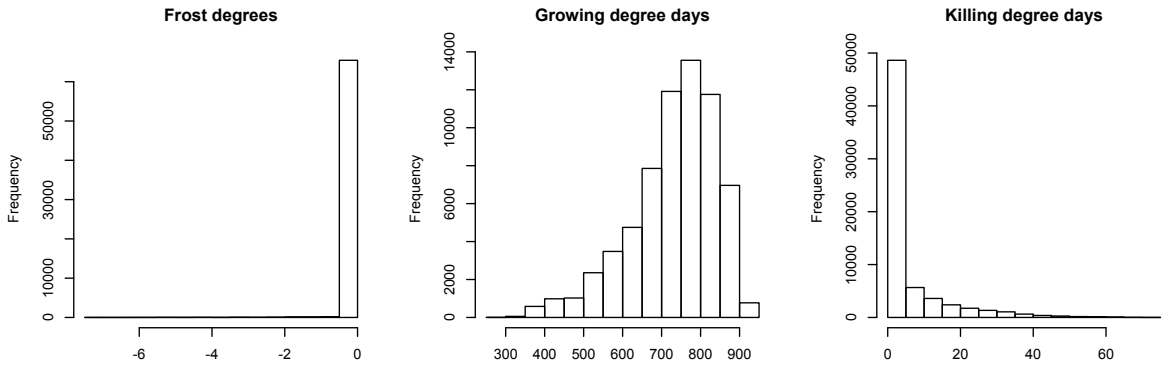


Figure 5.7: Growing degree day histograms, after an increase of 2°C.

As shown in figure 5.8, the observed yields show wide variation. The blue distribution is shifted to the left, eliminating some of the most spectacular yields and lowering the average yield. The average yield in the warmer experiment is about 80% of the original yields (see figure 5.9).

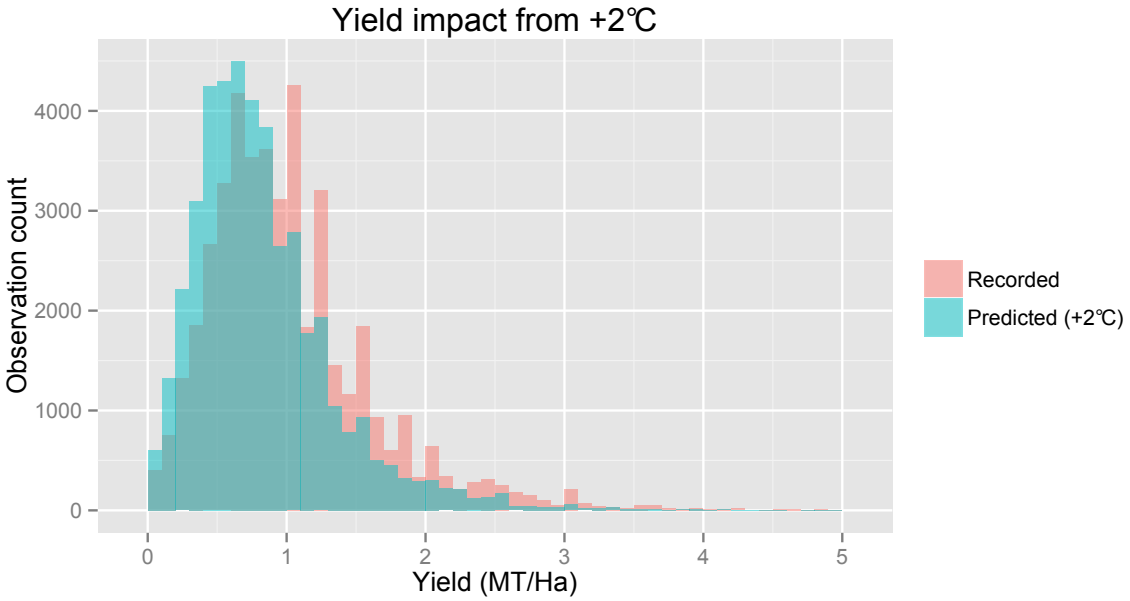


Figure 5.8: Observed yields over the period from 1990 - 2015 are shown in red, and model predictions under weather with temperatures increased by 2°C shown in blue.

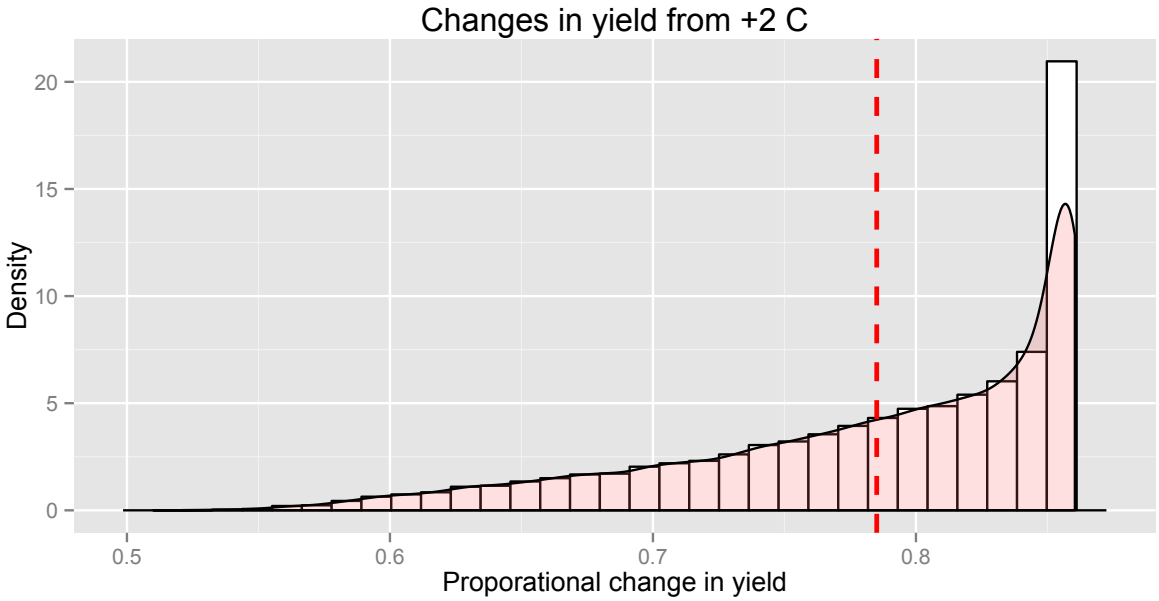


Figure 5.9: Distribution of the proportional change in yields, with a mean yield 79% of historical yields.

## 5.4 Global production

In this section, we estimate the a model like the one for Brazil for all countries. Using the intra-year production estimates in the coffee database, we estimate the relationship between country yields and weather. We use the temperature span of 0°C to 33°C for growing-degree days, as estimated for Brazil.

The first estimate is exactly analogous to the Brazil estimate, in that a single coefficient is estimated across all countries for the global average effect of GDDs, KDDs, frost degrees, and quadratic precipitation. This is reported in table 5.4 and shown schematically in figure 5.10.

| | Log Yield | Production |
|---|---|---|
| GDD / 1000 | 0.238** | 1,710.548 |
| | (0.119) | (5,917.907) |
| KDD / 1000 | −1.935 | −3,955.098 |
| | (1.786) | (43,378.870) |
| Frost Deg. | −0.005 | 284.772 |
| | (0.008) | (1,550.480) |
| Year Precip | −3.454 | 707,932.900 |
| | (12.928) | (483,967.400) |
| Year Precip$^2$ | 14.494 | −10,991,768.000 |
| | (135.355) | (6,955,772.000) |
| FE | *Region, variety* | *RegionVariety* |
| Trends | *Y* | *Y* |
| Errors | *Region* | *Region* |
| Observations | 1,945 | 1,945 |
| $R^2$ | 0.684 | 0.807 |
| Adjusted $R^2$ | 0.676 | 0.802 |
| Residual Std. Error (df = 1896) | 0.441 | 33,325.380 |
| *Note:* | | *p<0.1; **p<0.05; ***p<0.01 |

Table 5.4: Growing degree day model, pooled across all countries.

### 5.4.1 Hierarchical model framework

It is reasonable to expect different countries to have different effects from temperatures. We could estimate each country independently, and this would be an "unpooled" model. However, we also want the model for one country to inform, to an extent supported by the data, the model for another country. To capture this, we will construct a "hierarchical model", where each country's sensitivity to temperature will be drawn from a common distribution, simultaneously estimating each country's parameters and the distribution across all of them.

Furthermore, we allow varieties in different regions to operate differently, as supported by the data. For example, where plentiful data supports a higher optimal growing temperature for Robusta, the model should represent this. If very little data is available, the predicted response should by default conform to an average for that region and variety. Finally, we want to incorporate higher resolution data where it is available. The municipality data in Brazil informs the same common parameters as the Brazil-specific country-level yield data.

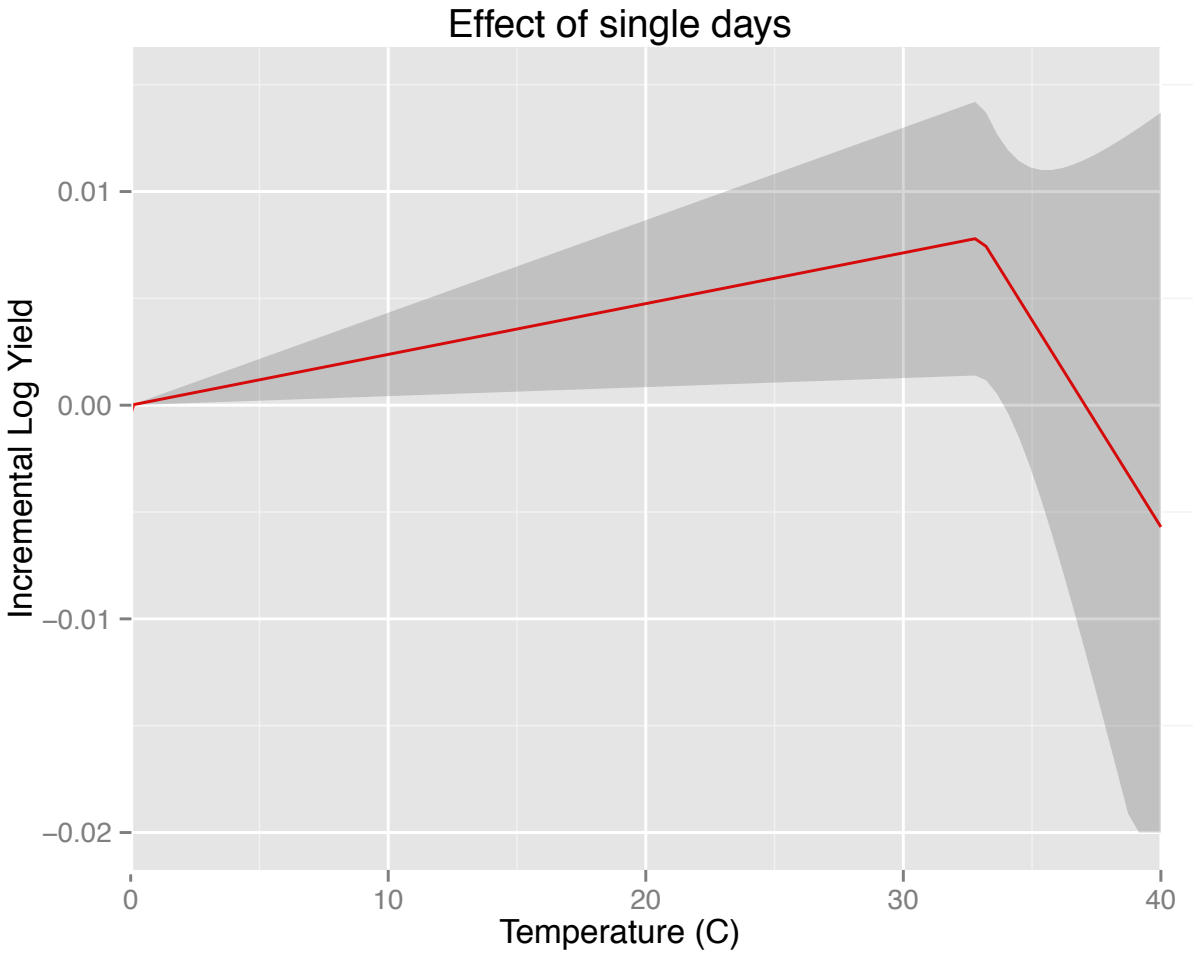


Figure 5.10: Pooled model growing degree-day plot.

We have developed a technique for allowing this kind of data-driven multiple levels of aggregation and degrees of generalization, based on Bayesian Hierarchical Modeling (Gelman et al., 2014) and Inversion Theory (Menke, 2012). Under this technique, each country and sub-country region has its own parameters, but the parameters are further modeled as being related to each other. The hierarchical model is a direct extension of the statistical production model, which can be thought of as many different production models combined together.

**Derivation of the hierarchical modeling system**

Formally, we want to allow each variety in each country to have its own model, consisting of coefficients for growing degree-days, killing degree-days, average minimum temperature, and precipitation. The pooled model is as follows:

$$\log y_{it} = \alpha_i + \beta_v + \gamma g_{it} + \kappa k_{it} + \phi f_{it} + \pi p_{it} + \psi p_{it}^2 + \epsilon_{it}$$

while the partially pooled model starts with the unpooled relationship,

$$\log y_{ivt} = \alpha_i + \beta_v + \gamma_{iv} g_{it} + \kappa_{iv} k_{it} + \phi_{iv} f_{it} + \pi_{iv} p_{it} + \psi_{iv} p_{it}^2 + \epsilon_{ivt}$$

Consider the GDD coefficient for country $i$ and variety $v$, $\gamma_{iv}$. To partial pool across countries for a given variety, this coefficient comes from a distribution of possible coefficient values, characterized by an unknown mean and standard deviation for that variety:

$$\gamma_{iv} \sim \mathcal{N}(\gamma_v, \tau_{\gamma_v})$$

Further, we partially pool these 'hyperparameters' as coming from a distribution across all varieties:

$$\gamma_v \sim \mathcal{N}(\gamma, \tau_\gamma)$$

We apply this for each parameter, $\gamma, \kappa, \phi, \pi, \psi$.

**Estimating a partially-pooled model**

Computationally, estimating this form of model can be very difficult. We construct an innovative framework for doing this using Ordinary Least-Squares matrix algebra.

The Gaussian relationships above, such as $\gamma_{iv} \sim \mathcal{N}(\gamma_v, \tau_{\gamma_v})$, are mathematically equivalent to the OLS-style relationship,

$$\gamma_{iv} = \gamma_v + \tau_{gamma_v}\eta \text{ with } \eta \sim \mathcal{N}(0, 1)$$

Under OLS, error terms are members of a Gaussian distribution, $\epsilon_i \sim \mathcal{N}(0, \sigma_e^2)$. We represent the hyper-model for the $\gamma$ coefficient with the OLS-style relationships

$$\gamma_{iv} = \gamma_v + \epsilon_{iv}$$
$$\gamma_a = \gamma_c + \epsilon_a$$
$$\gamma_r = \gamma_c + \epsilon_r$$

and similarly for the other coefficients. It is then possible to rewrite these and the original unpooled relationship to take the same form, with the same complete set of coefficients:

$$
\begin{array}{rlll}
\log y_{ivt} & = \alpha_i & +\gamma_{iv} g_{it} & +\cdots \\
\log y_{ivt} & = \sum_j \alpha_j \mathbf{1}_{j=i} & +\sum_{ju} \gamma_{ju} g_{it} \mathbf{1}_{ju=iv} \quad +\gamma_a 0 + \gamma_r 0 + \gamma_c 0 & +\cdots \\
0 & = \sum_j \alpha_j 0 & +\sum_{ju} \gamma_{ju} \mathbf{1}_{ju=1a} \quad -\gamma_a 1 - \gamma_r 0 - \gamma_c 0 & +\cdots \\
0 & = \sum_j \alpha_j 0 & +\sum_{ju} \gamma_{ju} \mathbf{1}_{ju=2a} \quad -\gamma_a 1 - \gamma_r 0 - \gamma_c 0 & +\cdots \\
 & & \vdots & \\
0 & = \sum_j \alpha_j 0 & +\sum_{ju} \gamma_{ju} \mathbf{1}_{ju=1r} \quad -\gamma_a 0 - \gamma_r 1 - \gamma_c 0 & +\cdots \\
 & & \vdots & \\
0 & = \sum_j \alpha_j 0 & +\sum_j u \gamma_{ju} \mathbf{1}_{ju=1c} \quad -\gamma_a 0 - \gamma_r 0 - \gamma_c 1 & +\cdots \\
 & & \vdots & \\
0 & = \sum_j \alpha_j 0 & +\sum_j u \gamma_{ju} 0 \quad +\gamma_a 1 + \gamma_r 0 - \gamma_c 1 & +\cdots \\
0 & = \sum_j \alpha_j 0 & +\sum_j u \gamma_{ju} 0 \quad +\gamma_a 0 + \gamma_r 1 - \gamma_c 1 & +\cdots
\end{array}
$$

The first line is the start of the original model to be estimated. The second line re-writes this with more systematically, and in such a way that "constant" terms can be set to zero for fictional observations. The remaining lines are fictional observations added to estimate the entire model.

We have built this approach into a tool for the R statistical package which is available at `https://github.com/eicoffee/hierlm`.

Figure 5.11 shows the effects of partial pooling at different levels. As the level of pooling increases, the range of country-specific values is brought closer together.

The results are shown in table 5.5. Only the hyperparameter means are shown. Each statistically significant country coefficient is listed in Appendix A.3.4, and the remainder are in an online table at `http://eicoffee.net/`. The first column uses only observations at the country level. The second column places a prior on the Brazil coefficients, conforming to the Brazil municipality estimates above. These more-precise estimates then inform the global distribution for each coefficient, which in turn informs all of the countries, including Brazil.

We now extend the analysis to the global context. To do so, we develop a new technique, which allows each country to have its own model, but for all of these models to be informed by each other. Within each country, Arabica and Robusta are assumed to have distinct model parameters, where the data permits.

The growing degree-day effect is greater for the Robusta variety, while the estimated effect of killing degree-days is greatest in regions that grow both Arabica and Robusta. A useful metric is the "break-even" temperature, the crossing point for which lower temperatures improve yields, on average, and higher temperatures depress yields. This is similar for Arabica and combined countries, at about 37°C. The corresponding temperature for Robusta is 40.5°C.

Figure 5.12 shows the variation across countries of the effect of killing degree-days and the break-even temperature. South America and Southern Africa show the least sensitivity to temperature, while Indonesia and the lands near it show the most.

Another way to view these results is to compare the break-even temperature to the average maximum daily temperature. This is shown in figure 5.13. Countries in the lower-left corner have both low maximum temperatures and low break-even temperatures. Since their estimated break-even temperature is over 10°C above their average maximums, these countries are at lower risk of losing their harvests. Countries in the lower-left corner are the most at risk: they have higher temperatures, but remain sensitive to high temperatures. Three countries occupy the upper-right corner: Liberia, Nigeria, and

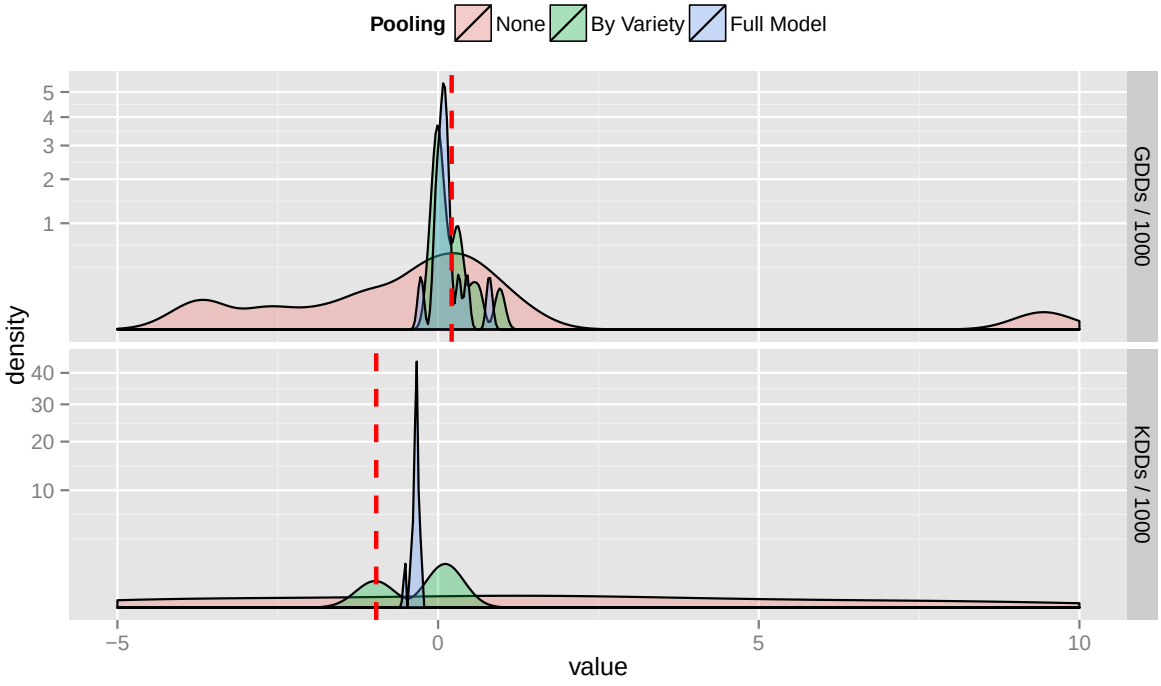


Figure 5.11: Distribution across countries of values for the GDD and KDD coefficients for different levels of pooling.

| | *Dependent variable:* | |
|---|---|---|
| | Countries only | |
| | (1) | (2) |
| GDDs / 1000 (Combined) | 0.079 | 0.217** |
| | (0.123) | (0.095) |
| GDDs / 1000 (Arabica) | 0.131 | 0.229** |
| | (0.112) | (0.103) |
| GDDs / 1000 (Robusta) | 0.161 | 0.401*** |
| | (0.152) | (0.133) |
| KDDs / 1000 (Combined) | −0.110 | −1.801*** |
| | (0.543) | (0.323) |
| KDDs / 1000 (Arabica) | −0.082 | −1.731*** |
| | (0.556) | (0.356) |
| KDDs / 1000 (Robusta) | −0.157 | −1.766*** |
| | (0.543) | (0.348) |
| Avg. Min. (Combined) | −0.077 | −0.108 |
| | (6.344) | (6.248) |
| Avg. Min. (Arabica) | −0.134 | −0.152 |
| | (7.147) | (7.164) |
| Avg. Min. (Robusta) | −0.114 | −0.163 |
| | (8.964) | (8.985) |
| Precip. (Combined) | −4.285 | −2.124 |
| | (5.792) | (2.390) |
| Precip. (Arabica) | −1.689 | −0.156 |
| | (6.058) | (3.254) |
| Precip. (Robusta) | −1.565 | −0.279 |
| | (5.971) | (3.403) |
| Precip.$^2$(Combined) | 5.340 | −5.530 |
| | (82.317) | (28.605) |
| Precip.$^2$(Arabica) | 21.749 | 11.218 |
| | (79.174) | (37.825) |
| Precip.$^2$(Robusta) | 12.794 | 0.264 |
| | (88.198) | (42.271) |
| Observations | 3,011 | 3,016 |
| $R^2$ | 0.902 | 0.903 |
| Adjusted $R^2$ | 0.885 | 0.886 |
| Residual Std. Error | 0.335 (df = 2561) | 0.336 (df = 2566) |
| F Statistic | 52.575*** (df = 450; 2561) | 52.962*** (df = 450; 2566) |
| *Note:* | | *p<0.1; **p<0.05; ***p<0.01 |

Table 5.5: Hierarchical model results, for the mean of the global distribution of coefficients for each parameter and each variety.

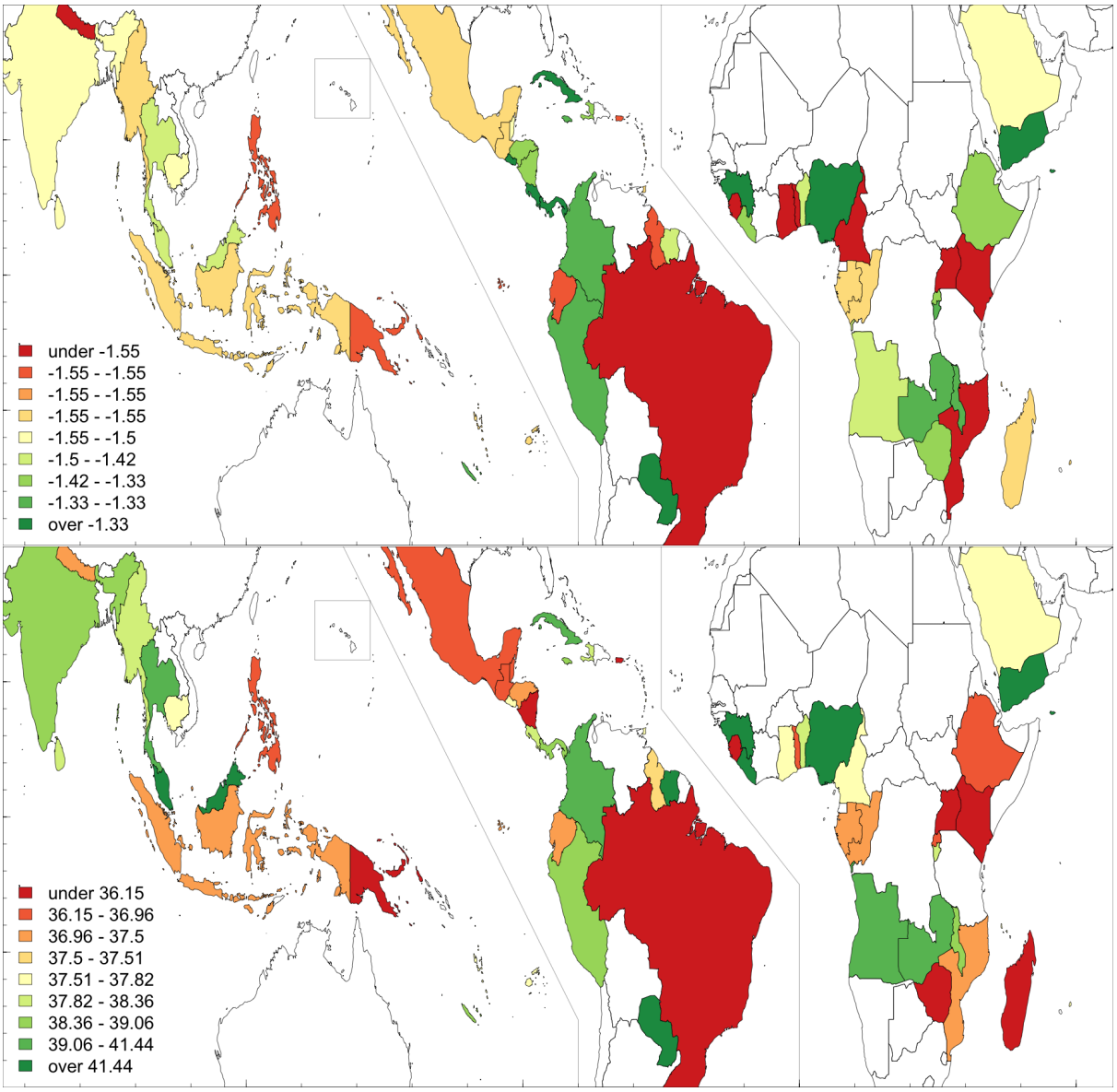


Figure 5.12: Coefficients of killing degree-days and the temperature at which yields decrease, across countries for the partially pooled model.

Guinea. These countries are estimated to have the highest temperature thresholds for yield losses. They are also amongst the countries with the highest maximum temperatures, averaged over their coffee growing regions, suggesting that these countries have achieved some level of adaptation to their high temperatures.

Other countries with similarly high temperatures have much lower break-even temperatures. That is, adaptation to high temperatures does not come inevitably from the experience of them. One explanation for their low temperature sensitivity is that Liberia, Nigeria, and Guinea all produce largely Robusta crops, which has lower sensitivity than Arabica. However, Benin, Togo, and Sri Lanka, with among the highest temperatures, also mainly produce Robusta, and they remain very sensitive to temperature.

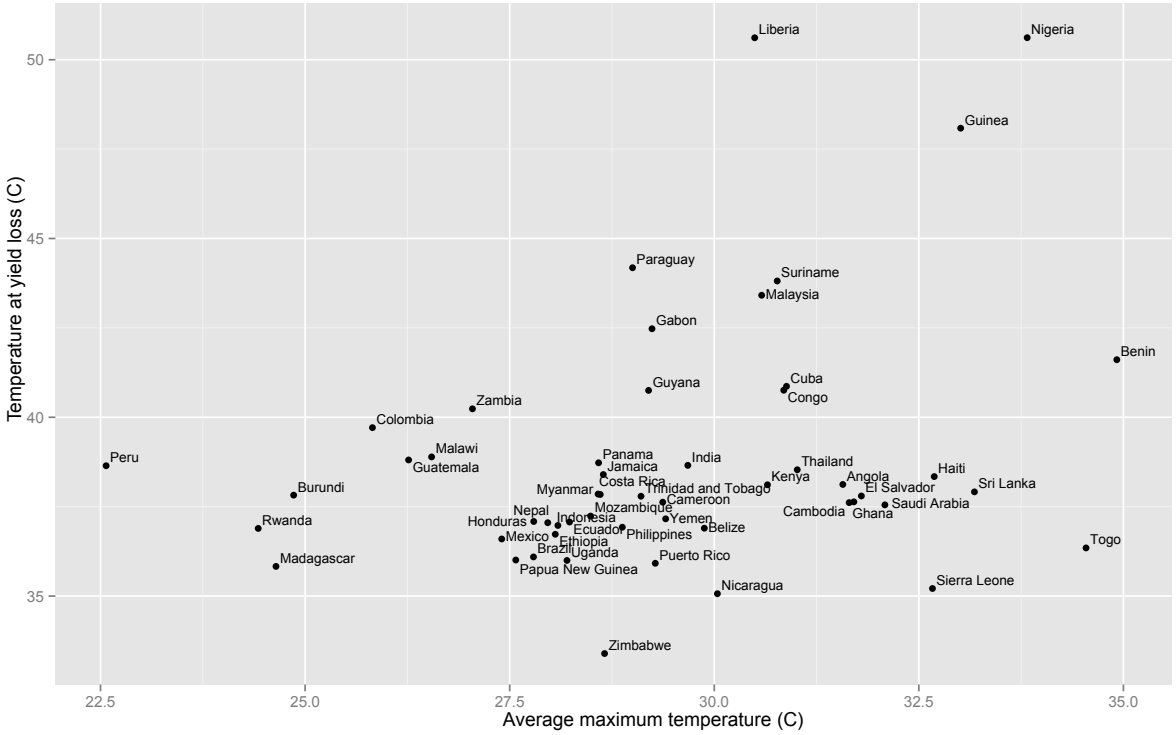


Figure 5.13: Observed average maximum daily temperature, 2004 - 2009, compared to the temperature at which yield losses are predicted.

### 5.4.2 Future productivity

We can use the global hierarchical model to predict yields under the future climate as described by global climate models. We shift temperatures according to the change in the average temperature and apply the average proportional change in precipitation to all daily weather observations from the CFSR dataset.[3]

[3]In section 5.3.6, we perform a similar analysis for the model of Brazilian yields. There, we leave precipitation unchanged, because of the lack of evidence of trends in precipitation in Brazil. However, agreement across climate models on predicted precipitation varies across countries. Here we include the effect of predicted precipitation changes to most accurately represent the predicted climate of 2050. The effects of climate change on precipitation remain very uncertain, despite occasional agreement across models, and the predicted patterns shown in section 1.2.1 should not be construed as confident forecasts.

Then we calculate GDDs, KDDs, average minimum temperatures, and total precipitations, and apply them to the model. Figure 5.14 shows the result.

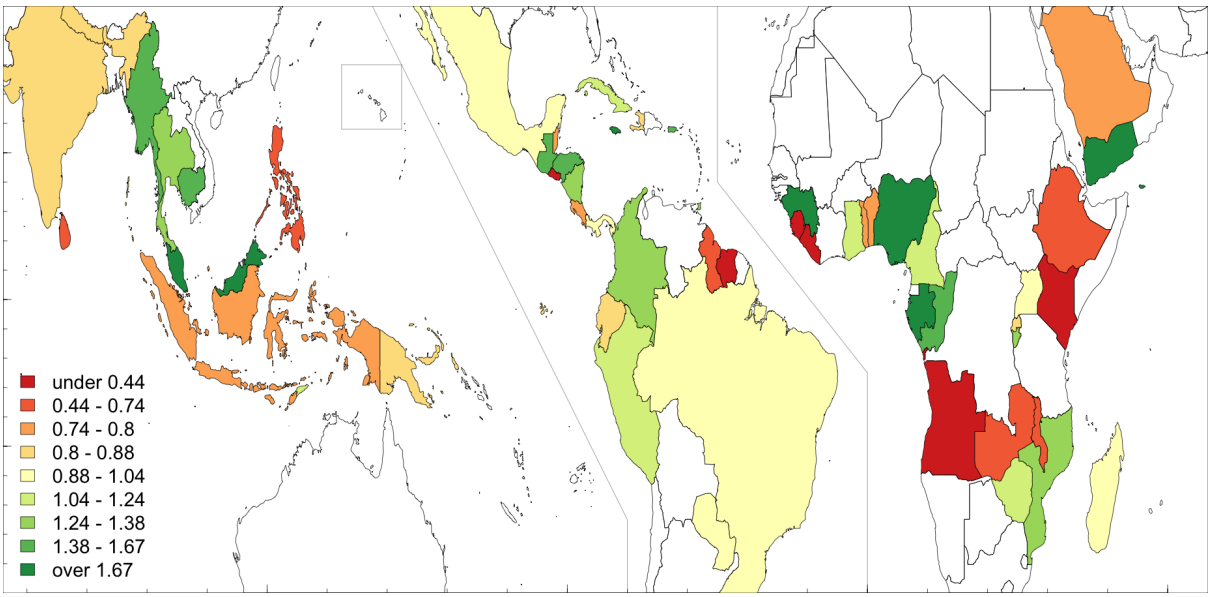


Figure 5.14: Changes in yield by country, for weather averaged over growing regions for each country.

As shown in the map, the impacts vary widely across countries, with some countries losing as much as 70% of their productivity, while others see increases of over 60%. Most areas in South America will experience improvements, while many countries in Central America, Southern and Eastern Africa, and Eastern Oceania will experience losses.

This result shows some general features about the variation across countries, but the actual country predictions have low confidence. In many cases, these country predictions are based on few data points, and the global distribution used to inform all of them is broad because of the uncertainty of predicting country aggregated yields. See appendix 5.4 for more information.

### 5.4.3 Humidity

Humidity can have varying effects on coffee. The plant needs reasonably high levels of humidity during the flowering season to avoid floral atrophy, but humidity is also crucial to the development of coffee rust. For these reasons, the timing of high humidity levels appears to be particularly important. Here we see how Arabica coffee yields respond to a one-standard deviation increase in humidity during each particular month in the year leading up to harvest. Robusta appears to be less sensitive to humidity effects than Arabica.

Humidity data is from the NCEP CFSR. The reanalysis data is available at 1/12° resolution globally, which is then aggregated to the country-month level using weights from the coffee database. The values are reported as specific humidity at 6 hour intervals, which here is averaged over each month for the year prior to harvest.

Monthly effects of humidity are shown in figure 5.15, and the table of coefficients is in Appendix A.3.2.

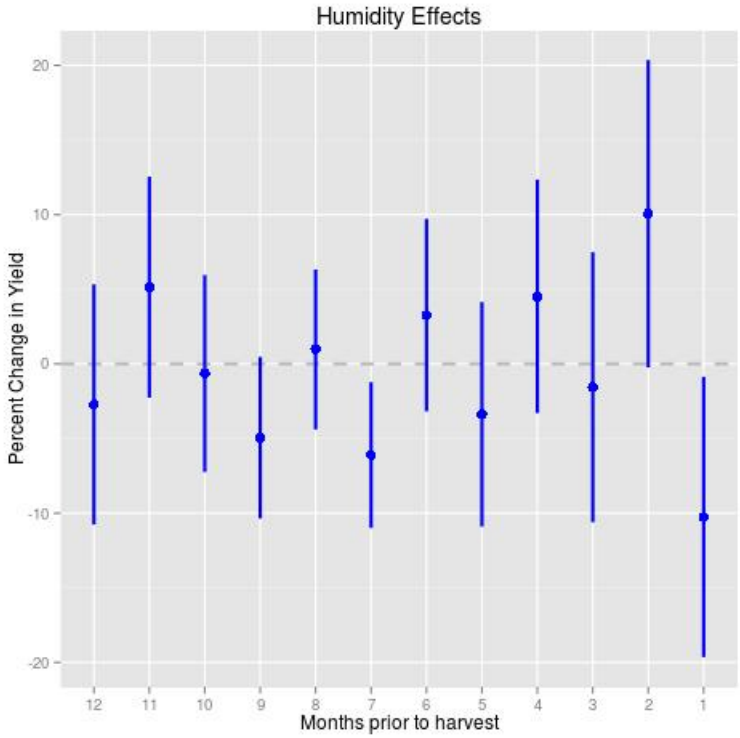


Figure 5.15: Arabica humidity effects. Only the humidity one and seven months before harvest are significant at 95% confidence.

The coefficients result from the following model:

$$log(y) = f(T) + \sum_{m=1}^{12} \beta_m q_m + h_c(t) + \alpha_c + \gamma_t + \epsilon_{ct}$$

where $f(T)$ is a non-linear function of temperature, estimated using the number of days spent in 1-degree C temperature bins, $h_c(t)$ is a country-specific linear time trend, $\alpha_c$ and $\gamma_t$ are country and year fixed-effects. Each $\beta_m$ is the effect of specific humidity $m$ months prior to the beginning of harvest on log yield.

### 5.4.4 Interpreting empirical model results

Climate change impacts coffee production through many different channels. Foremost, climate change reflects changes in temperature and patterns of precipitation– that is, changes in climate mean changes in weather. The models above estimate the relationship between changes in weather and changes in yields, and then extrapolate those changes to their responses under climate change.

There are important differences between unexpected weather shocks and prolonged climate changes. Coffee farming will find ways to adapt to repeated shocks of higher temperatures, and we hope our estimates provide an upper bound on the production impacts of climate change. However, the evidence for such adaptation is limited. Burke and Emerick (2012) study maize in the United States, and while there is a clear potential for adaptation to warmer temperatures, they find almost no evidence of it. The reasons for this empirical result are unclear.

The effects that we measure of temperature on yields cannot be unambiguously interpreted as the biological response to temperatures. Temperatures could be simultaneously affecting other species that then affect coffee. For example, the harmful affects of average minimum temperature could reflect a greater capacity for coffee rust or the coffee berry borer to proliferate in these warmer years. It could also reflect decreased activity on the part of farmers on hot days.

Our results should be taken as representing a holistic effect as it has occurred in the past. The extent to which it will occur in the future may be up to us.

# Chapter 6

# Price interconnections

Coffee forms a complex global network of international relations, not only between producer and consumer countries, but also amongst consumer and producer countries, as shown in figure 6.1. Both consumer and producer countries, for example, import coffee from Italy, a "consumer" country. Producer and consumer countries interact with each other through the global market, and have long-standing trade relations that form the backbone of this market.

Coffee consumption has increased steadily for the past 20 years (see figure 6.2). The greatest drivers behind this recent growth have been producer countries, calling into question many traditional assumptions about the coffee market.

Despite the relatively smooth increase in coffee production, prices have historically swung wildly over the past 50 years, as shown in figure 6.3. There have been many reasons for these swings. These include political and economic changes, speculation, and the effects of disease and the environment.

In this section, we study the determinants of prices in the coffee market, from the perspective of both producer and consumer countries.

Coffee is an important contribution to the economy of many countries. The prices paid to farmers account for over 3% of the GDP of four countries (Burundi, Honduras, Nicaragua, and Ethiopia; see Appendix A.4.5. The total value of coffee to seven countries exceeds 10% of their GDP (those above and Rwanda, Uganda, and Guatemala) (International Coffee Organization, ming). Understanding what drives prices for consumer and producer countries is important to these regions as well as the world's 25 million coffee farmers.

### 6.0.1 Market data

The coffee market model incorporates coffee production divided out by producer countries, coffee consumption divided out by consuming countries, and the national and international drivers of the prices paid to growers and by consumers. The following inputs are used to construct an empirically-grounded market model. All are available at least at a yearly resolution, and are here implicitly indexed by year.

Below, we use a consumer price index[1] to translate prices to year 2000 US dollars, as shown for Arabica

[1] We use a single CPI across all countries, calculated by International Financial Statistics for their "All Items" goods in advanced economies.

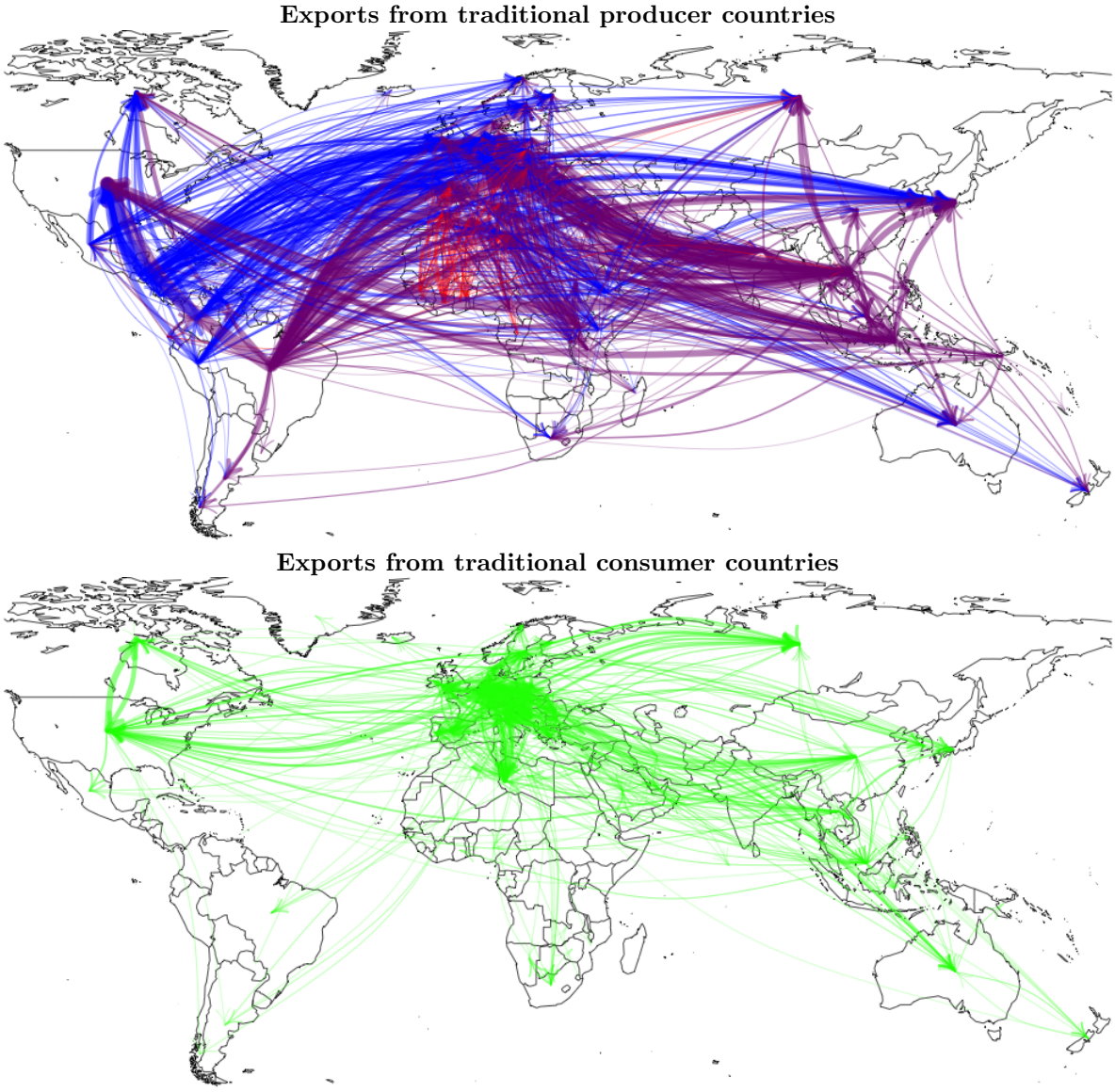


Figure 6.1: Exports from traditional producer (top) and consumer (bottom) countries. Above, blue arrows show Arabica exports, red arrows show Robusta exports, and purple arrows show exports that include both. The width of the lines increases with the yearly exports. Trade data from Comtrade (2015), producer classifications from International Coffee Organization (2015).

| | | |
|---|---|---|
| $q_i$ | Production in country $i$ | USDA and FAO |
| $p_i$ | Price to growers in country $i$ | ICO |
| $d_j$ | Consumption in country $j$ | UN Comtrade |
| $c_j$ | Retail price in country $j$ | ICO |
| $e_{ij}$ | Export from country $i$ to $j$ | UN Comtrade |
| $u$ | International coffee price | World Bank |

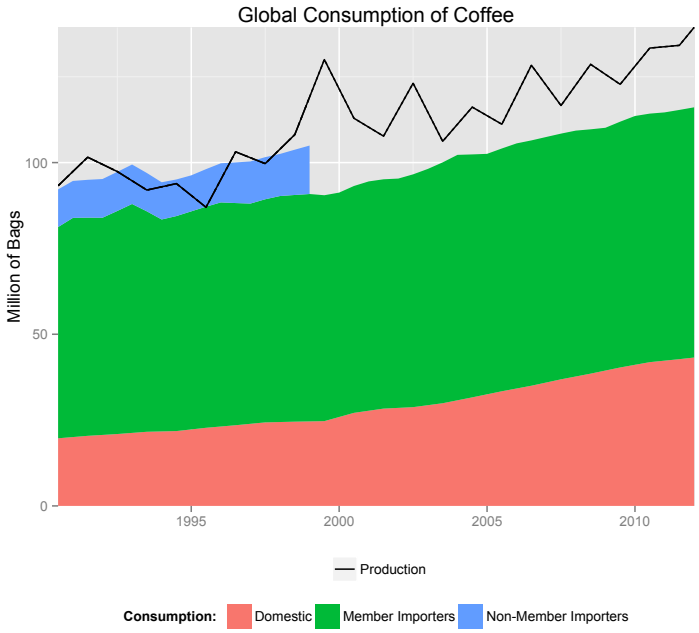


Figure 6.2: Global production (line) and consumption (colored areas) of coffee from ICO data. Non-member country consumption is unavailable after 1999. Most of the recent growth in consumption is driven by consumption within producing countries (domestic consumption), now equaling more than 50% of importing country consumption.

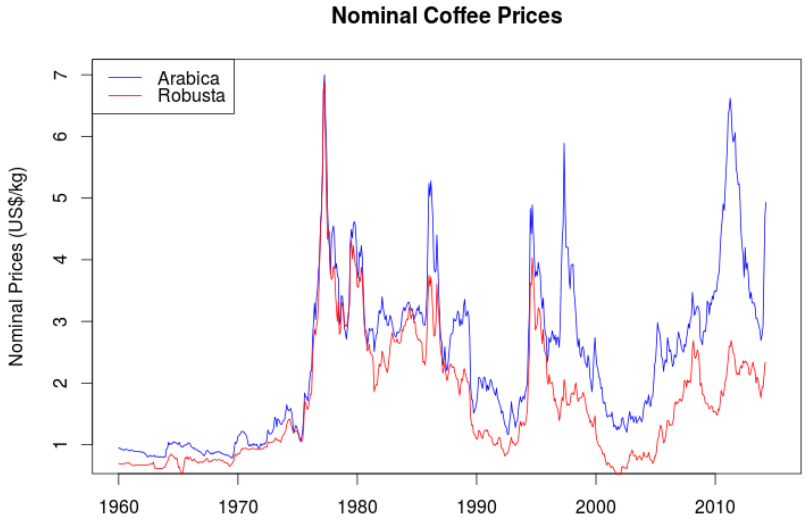


Figure 6.3: Nominal world prices of Arabica and Robusta coffee (in $/kg), from the World Bank Pink Sheet. The general shape is very erratic, with nominal prices not yet returning to their peak in 1977. Robusta prices have also diverged from Arabica prices, as Robusta production has spread, although the two remain closely correlated.

and Robusta international prices in figure 6.4. Coffee consumers have enjoyed a significant reduction in prices, in real terms, since the 1970s and 1980s.

The following sections estimate empirical price relationships. While these are greatly simplified, they provide approximation to the drivers of the international coffee market.

### 6.0.2 International prices and production

International prices a partially driven by global production, but with considerable autocorrelation. The simplest form of this relationship is:

$$u = \alpha_0 + \alpha_1 \sum_i q_i + \alpha_2 u_{t-1}$$

This expression represents the fundamental driver of international coffee prices: scarcity increases prices and a glut of coffee reduces them. $\alpha_1$ is negative to capture this relationship. $\alpha_2$ represents the extent to which prices adjust slowly and are driven by other shocks. If $\alpha_2$ is near 1, coffee prices have a long memory; while if it is near 0, they respond immediately to production changes. The result is estimated in table 6.1.

This estimate places the entire weight of the predictive capacity on the autoregressive term. In other words, the only significant information about the future international price is the current international price.

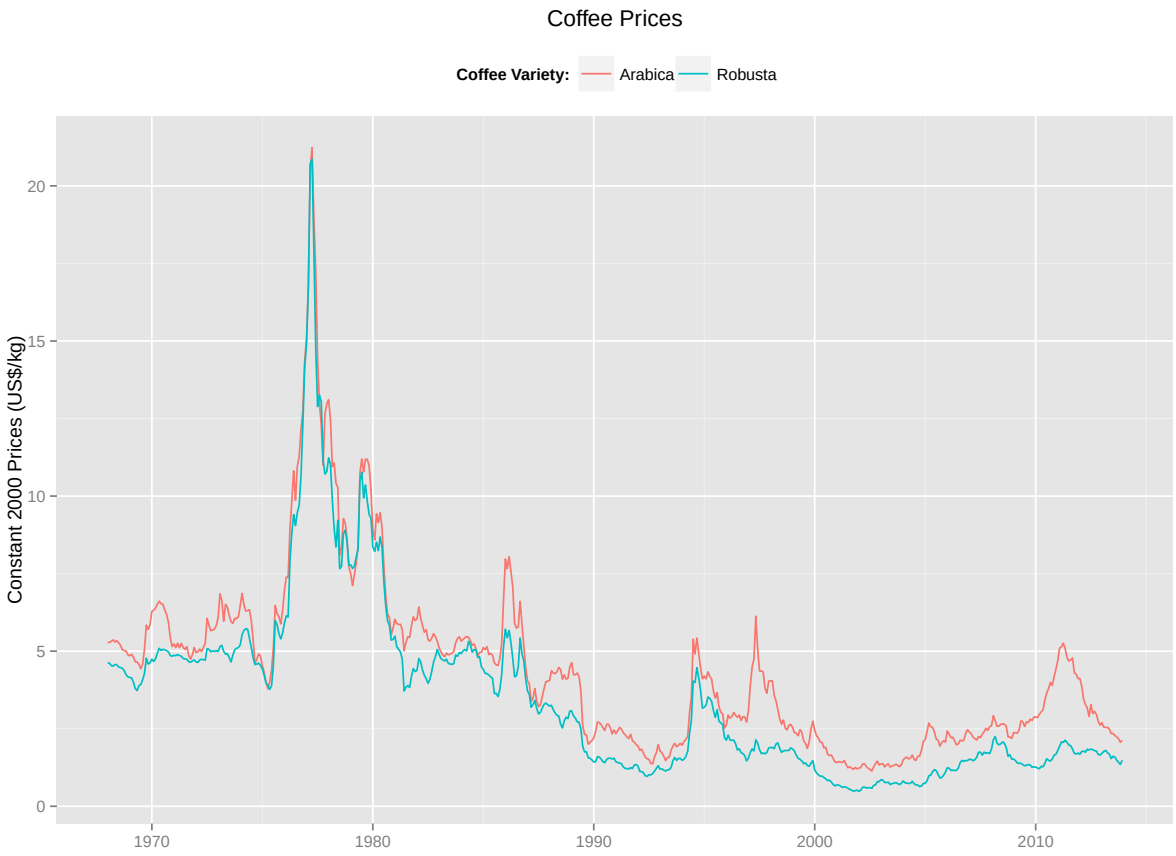


Figure 6.4: Arabica and Robusta green bean coffee prices, in terms of constant year 2000 US$ per kilogram.

| | *Dependent variable:* | |
|---|---|---|
| | Arabica | Robusta |
| | (1) | (2) |
| $\alpha_0$ | 0.059 | 0.074 |
| | (0.075) | (0.060) |
| $\alpha_1$ | −0.00000 | −0.00001 |
| | (0.00001) | (0.00002) |
| $\alpha_2$ | 0.988*** | 0.987*** |
| | (0.007) | (0.007) |
| Observations | 551 | 551 |
| $R^2$ | 0.975 | 0.980 |
| Adjusted $R^2$ | 0.975 | 0.980 |
| Residual Std. Error (df = 548) | 0.458 | 0.410 |
| F Statistic (df = 2; 548) | 10,669.730*** | 13,612.970*** |
| *Note:* | *p<0.1; **p<0.05; ***p<0.01 | |

Table 6.1: Estimate of the effect of production on international prices.

To improve this analysis, we model the dynamics of Arabica and Robusta stocks as a closer proxy for the driving quantities on the market, in Appendix A.4.1. We find that international prices continue to be best explained by their own internal dynamics.

### 6.0.3 Prices to growers

Prices paid to farmers vary across countries by an order of magnitude, as shown in figure 6.5. While this figure represents average prices, the amount paid to farmers also varies year-to-year. We look at two determinants of these fluctuations: the international price paid for coffee and the country production level in that year.

Prices to growers are affected by both international prices and local production:

$$p_i = \beta_0 + \beta_1 q_i + \beta_2 u$$

Farmers are paid more when coffee fetches a higher price on the international market ($\beta_2 > 0$) , but less if there is a relative excess of coffee produced in their country in a given year ($\beta_1 < 0$). We further allow for country-specific unexplained variation. The results of this estimate are shown in figure 6.6 and in the table in Appendix A.4.2. The data is from International Coffee Organization (2015).

Figure 6.6 shows the amount of variance explained (out of 1) by these two parameters. The effect of international prices on prices paid to farmers is very clear, across all countries and globally. Furthermore, this explains 46% of the variation in year-to-year farmer prices.

The effect of production, however, is much less clear. Although it has a significant effect for about 30% of countries, the direction of the effect varies, with almost half of countries showing prices that increase with the level of production. This is at odds with at least a simple view of the relevant economics: we

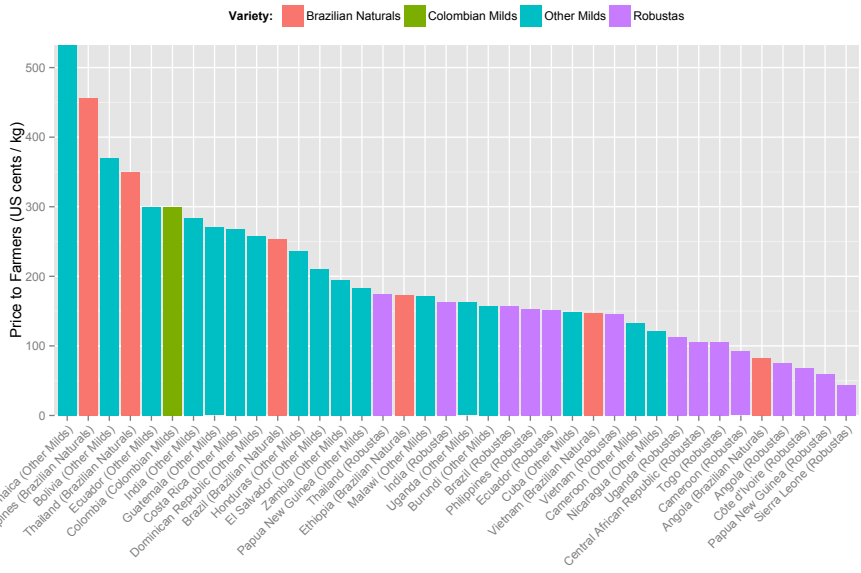


Figure 6.5: Price paid to farmers in U.S. cents per kg, averaged over 2009 - 2013, from the ICO.

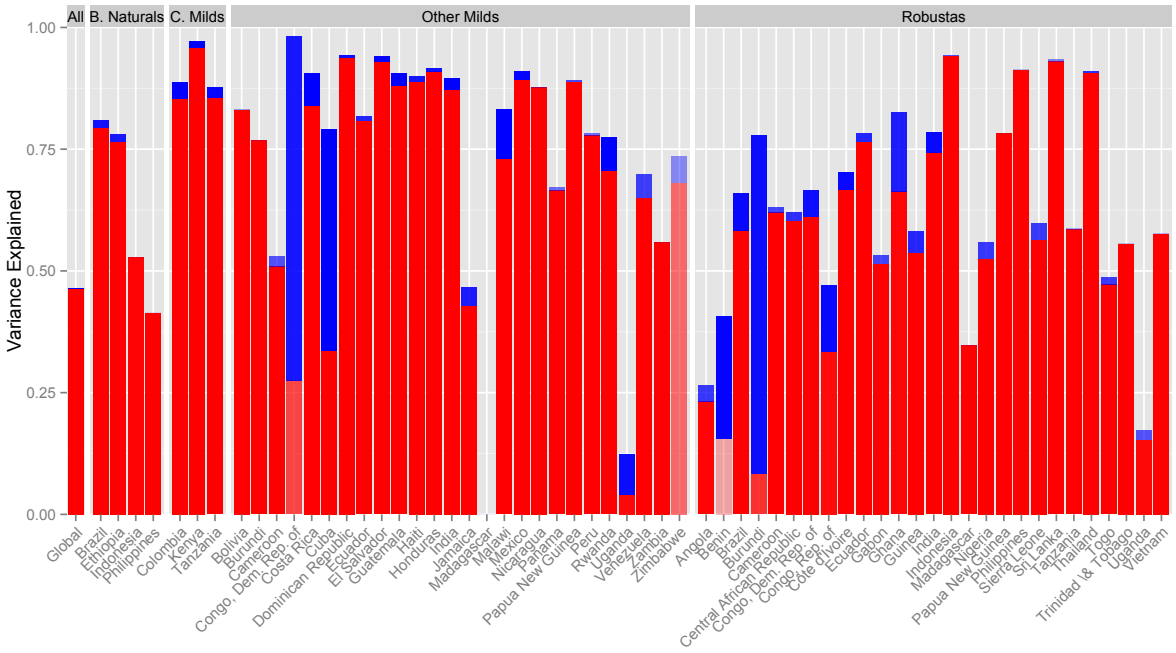


Figure 6.6: Variance of local prices explained by international prices (red) and local production (blue). Bars are faded according to their p-values.

would expect a glut on the market to drive down prices. Even so, the effect of production on farmer prices explain typically less than 1% of the variation in these prices.

Unweighted, Robustas have a mean variance explained by international prices of 57% to 69% for the other Arabica varieties. Weighted by production, the difference is 63% to 82%. This lower explained variance is only slightly reflected in the level of variance explained by country production. This suggests that price changes are also significantly affected by other factors, such as national price interventions.

### 6.0.4 Consumer response to prices

In 2009, consuming countries spent $27.1 billion for coffee (United Nations International Merchandise Trade Statistics, 2009). This value came after a decade of the lowest coffee prices, in real terms, ever seen, below $2.50 per kg. Consumers responded to these low prices by growing the total financial size of the coffee market. In recent years, retail prices for roasted beans in consumer countries have ranged from $6.65 per kg to $14.60 per kg (see 6.7).

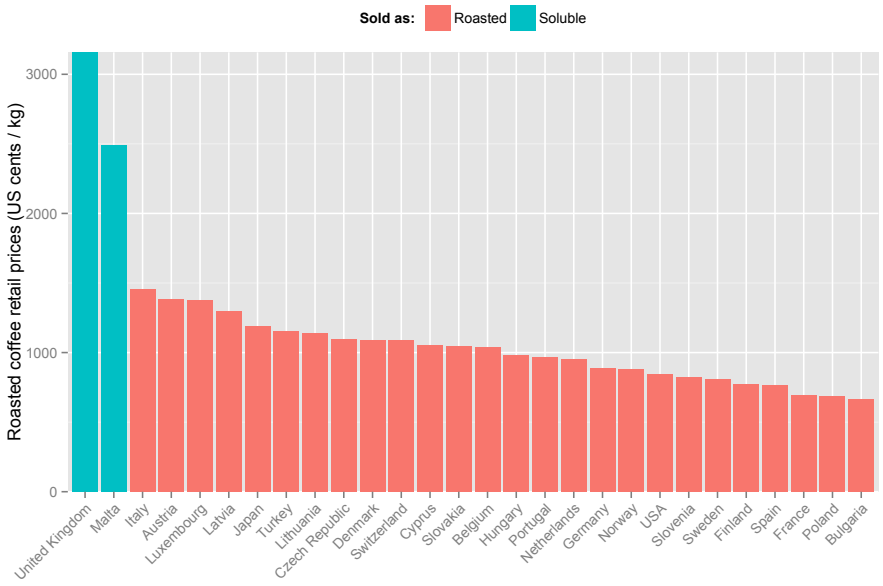


Figure 6.7: Retail price for roasted beans in U.S. cents per kg, between 2009 - 2013, from ICO.

We expect consumption to decrease with retail prices:

$$d_j = \gamma_0 + \gamma_1 c_j + \gamma_2 d_{j,t-1}$$

Demand does not re-calibrate immediately to changes in retail prices ($\gamma_2 > 0$), but we assume that high prices produce a downward force while low prices produce an upward force ($\gamma_1 < 0$). However, we allow for this "economic" force to be dominated by internal consumption dynamics, represented here as external demand shocks that persist through the autoregression term $\gamma_2$. These results are shown in figure 6.8 and in table A.9 in the Appendix. The data is from International Coffee Organization (2015).

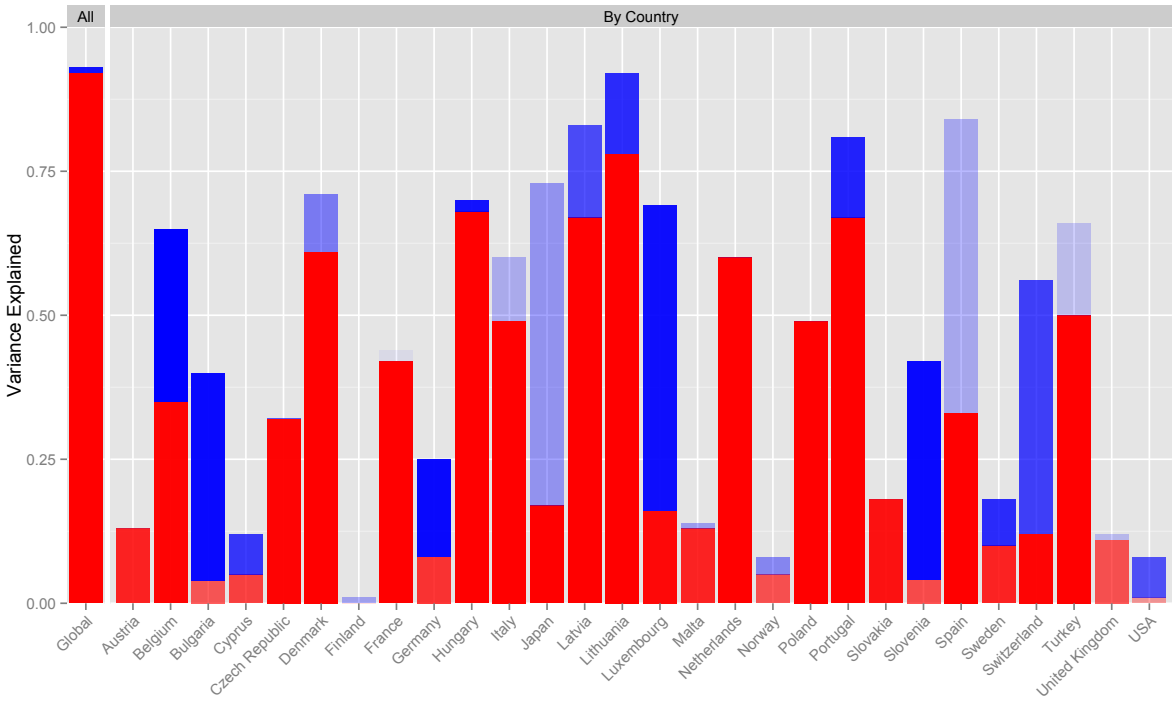


Figure 6.8: Variance of demand as explained by previous-year demand (red) and retail prices (blue). Bars are faded according to their p-values.

Retail prices appear to have an uncertain effect on consumption, with consumption often climbing as retail prices climb. The direction of causality could be a problem in this case, where prices could be being driven higher by higher consumption. Only 1% of the variance in consumption is explained globally by retail prices (see figure 6.8). Mostly, retail prices appear to be determined by their level in the previous year. In other words, they may follow a kind of random walk, determined more endogenously than by external factors.

### 6.0.5 Retail prices follow costs

Finally, we relate retail costs in consuming countries to prices paid to farmers in producing countries. Thurston et al. (2013) shows that for coffee sold in the U.S. and under modest assumptions, retail profit is only 6% of the entire price of the product, and similarly modest shares are taken by actors upstream. We can therefore expect that retail prices are largely driven by economic necessities.

Using a statistical model, we can identify the share of costs going to each country and to some processes within countries.

Retail costs are a composite of the costs for imports from each country, plus a markup:

$$c_j = \phi_j + \sum_i \frac{e_{ij}}{d_j} (p_i + \theta_i + l_{ij})$$

Retailers respond to the costs of their inputs, which combine country-specific production prices ($p_i$), added prices for processing and tariffs ($\theta_i$), a cost related to the transportation between them ($l_{ij}$), and added costs specific to the retailing country ($\phi_j$). The extent to which each of the producing country variables ($p_i$, $\theta_i$, $l_{ij}$) impact the final retail price is determined by the faction imported from each country ($e_{ij}/d_j$). Our results are divided into producer country results and consumer country results. This is because each producing country sells to multiple consuming countries, and visa versa. The producer country results reflect the average of the effects they produce across all consuming countries, while the consuming country results reflect the effects produced by their mix of producing country imports. The trade relation data is from Comtrade (2015).

#### Producer countries

Producer country prices are divided into the share to farmers, in US cents per kg, and an additional mark up inferred from retail prices. See figure 6.9 and the table in Appendix A.4.4.

The "To Farmers" column is reported in ICO data, and included in the table as the mean farmer price across all available years, in constant year 2000 cents. The remaining inferred producing cost for each country is the producer-side markup. While this may not be captured by producing-countries, it is associated with them: where this value is high, a large markup exists between retail prices that import from this country and farmer prices. Most markups are between 450 and 550 cents per kg, with Brazil and Vietnam as notable outliers. The greatest inferred markup comes from Indonesia.

#### Consumer countries

The consumer country values include prices to farmers ("To Farmers") as averaged across all imports; distribution costs (averaged over country-to-country specific inferred transportation costs), the final retail prices (from ICO, averaged over available years in constant year 2000 cents), and the additional markup associated with the consuming country.

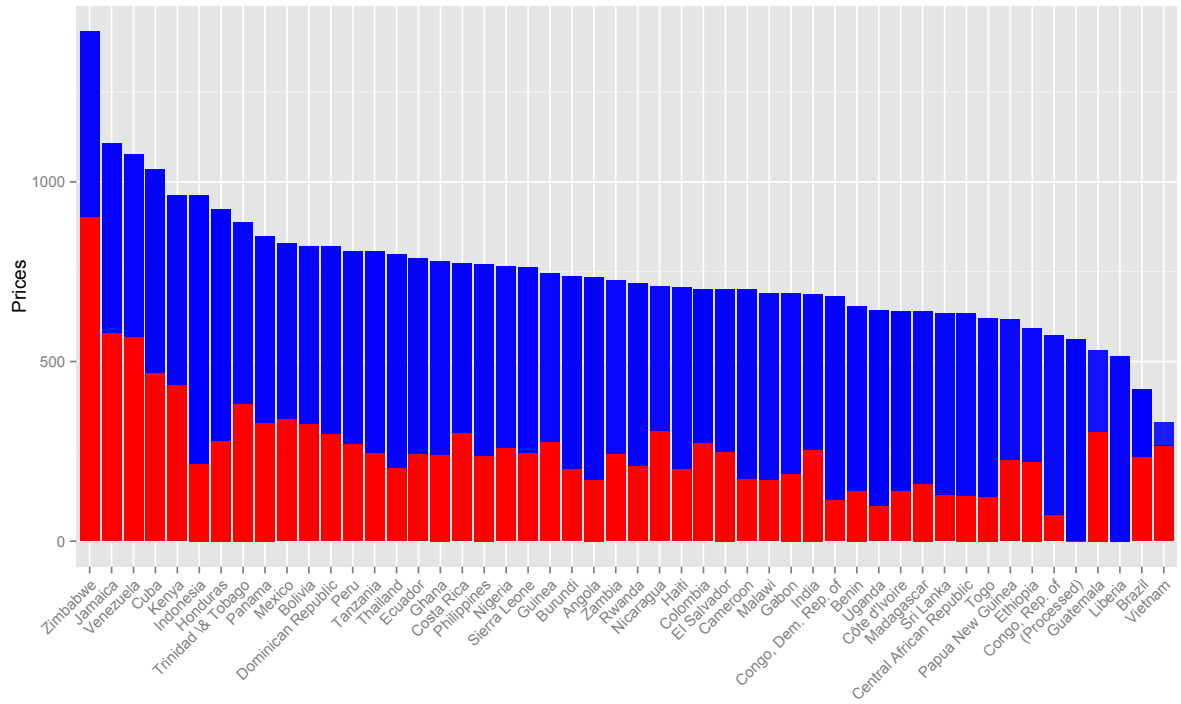


Figure 6.9: Producer country prices to farmers (red) and producer-associated markups (blue). Producer markups are faded by p-value.

The farmer price is taken as the weighted average of farmer prices that make up imports in a given year, and adjusted for 16% loss of weight. See figure 6.10 and table A.11 in the Appendix.

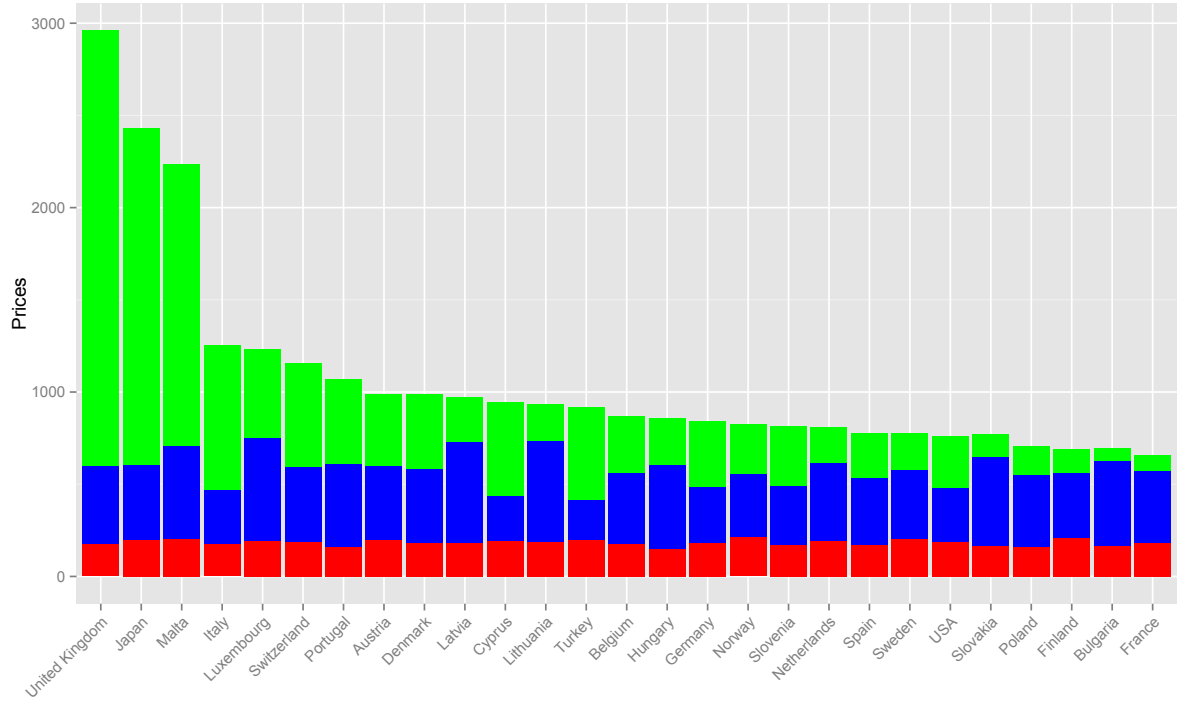


Figure 6.10: Consumer country prices to farmers (red), the distribution network (blue) and consumer-associated markups (green). Distribution prices are faded by p-value.

The largest markups are associated with soluble coffee prices (the United Kingdom and Malta). Japan also has very high markups. Low markups exist in Bulgaria, France, and Slovenia.

# Chapter 7

# Looking ahead

## 7.1 Mitigation and adaptation

The two central responses to climate risk for any sector are mitigation and adaptation. Mitigation refers to the policies, practices, and international agreements that lead to lower greenhouse gas (GHG) emissions. Adaptation, the planning and practices engaged in to manage the risk of a changing climate, is an independent concern from mitigation. It is clear now that all sectors will need proactive adaptation, irrespective of the actions taken toward mitigation.

For the coffee sector, mitigation is synonymous with sustainable environmental practices, and many coffee farms are already performing well. GHGs can be released in the course of coffee production through the application of fertilizers and pesticides, direct fuel and electricity use, depulping and fermentation resulting in methane, and release of nutrients from the soil. Account for all of these, traditional and commercial coffee polycultures have a low carbon footprint, while monocultures produce 50% more GHGs (van Rikxoort et al., 2014).

One of the largest sources of $CO_2$ is deforestation, where there is evidence of both positive and negative interactions with coffee. Coffee plantations reinforces the ties between forests and the economy, resulting in lower deforestation rates in some regions like Ethiopia (Hylander et al., 2013). Elsewhere, such as in Indonesia, periods of high coffee prices have induced increases in deforestation (O'Brien and Kinnaird, 2003). We show that coffee suitability will shift rapidly as a result of climate change. Even where shade trees are maintained, the carbon impact of the loss of forest is far greater (Baker, 2013). For this reason, it is important for the shifts of coffee cultivation to take place solely within present agricultural regions, or in conjunction with reforestation programs, to maintain the balance of carbon.

The coffee industry also receives direct benefits from forests. Coffee farms near forests and their wild pollinators are 20% more productive and produce 27% fewer peaberries (Ricketts et al., 2004). By maintaining forest cover, coffee farms can benefit themselves both directly and through the climate.

While mitigation has long-term consequences, coffee farmers can achieve immediate benefits and lessen the impacts of climate change through adaptation. For example, shade trees in coffee plantations can decrease the temperatures to which plants are exposed by up to 4°C (Jaramillo, 2005). One reason why climate change is such a great risk to coffee producing countries is because many coffee farmers are poor and have a lower capacity to adapt to climate change.

coffee&climate (2015) provides an extensive overview not only of approaches to adaptation, but of the equally important process of evaluating climate vulnerability. Baca et al. (2014) identify nine axes of

vulnerability through focus groups, and associate each with a parameter to measure and track:

| | |
|---|---|
| **Road type** | Time from the farm to the collection center, time from the farm to the nearest market, type of road from the farm to the collection center or nearest market |
| **Transport of products** | Type of transportation from the farm to the market, time from the farm to the bus stop |
| **Quality of housing** | Housing material, basic services |
| **Access to and availability of water** | Source of water for drinking or post-harvest processing, availability of water during the year, distance to the water source, water quality |
| **Conservation** | Area of forest around the water source, area of forest to keep in the farm |
| **Soil and fertility** | Soil type, soil slope, mulch of leaves, soil depth |
| **Food and health** | Number of symptoms of human disease, number of times that person is attended by a doctor, dependency of external products |
| **Migration** | Type and time |
| **Variability of yield** | Average farm yield in four years compared to the local average |

They also identify modes of adaptation for addressing each of these vulnerabilities, and the parameter that provide opportunities for new practices.

| | |
|---|---|
| **Variability of post-harvest infrastructure** | Types or forms to dry coffee |
| **Pollution** | Waste management, release of fermentation residues into water, management of agrochemical containers, coffee waste management, area burning annually |
| **Management of shade trees and reforestation** | Number of trees cut, number of trees planted |
| **Access to education** | Level of education, quality of technical assistance, crops for which receive technical assistance, types of media accessed |
| **Level of knowledge of farming system** | Registration practices and activities, coffee intercropping, pests and diseases |
| **Organization** | Participation, time, benefits |
| **Knowledge of laws and policies** | Policies about coffee sector, environmental laws, land polices |
| **Access to credit** | Term of credit, interest rate of credit, opportunity of credits |
| **Diversification of income** | Number of sources of income |
| **Access to specialty markets** | Destined for sale, special market access |
| **Access to technologies** | Varieties, drip irrigation, water harvesting |

This kind of broad thinking is essential to addressing the adaptation problem in coffee. Small-scale farmers will have a more difficult time adapting to climate change than large-scale ones. As a result, climate change will result not only in changes in coffee cultivation, but will also produce winners and losers amongst the groups planting them.

## 7.2 Future opportunities for research

The coffee production database offers many new opportunities for studying the connection between coffee and its environment across the globe. Over the course of our research, we also uncovered a range of topics worth further research.

One of the most important open questions is how to combine suitability, variability, and production analyses. These three dynamics take place on different spatial and temporal scales, whereby suitability is based on static properties, our variability uses global patterns, and the production model represents the effect of weather on crops from year to year. These three are interrelated, and any region that has large production shocks more frequently than every three years, at the extreme, will be unsuitable for coffee, since coffee plants could never get to a sufficient level of maturity.

Another under-studied area is coffee disease. While all of our empirical estimates implicitly capture the effect of coffee disease, these may end up being the most difficult impacts to adapt to. The coffee berry borer's range has rapidly expanded in recent years, and some of these shifts are related to climate (Magina et al., 2011). Jaramillo et al. (2009) find that a 1-2°C increase in temperature would result in large losses from the coffee berry borer, particularly in regions with high-quality Arabica. Data on coffee diseases is not as plentiful as yield data, but can be collected from many sources.

Our study of the coffee market only scratches the surface of many interesting connections between climate and variability, producers and consumer, and prices and trade. The coffee market is global, complex, chaotic, and sophisticated, with many different kinds of stakeholders. Future work would extrapolate the effects of climate on coffee production amounts and locations to determine the consequences for price and demand.

Both of these are related to an all-important topic we struggled with: coffee quality. While coffee quality has physical determinants, its subjective nature make it very difficult to study. However, the structure of futures contracts provides an entry-point, where quality is quantified and varies over both space and time. This data would allow future research to understand the impact of climate on coffee quality, at least at the country-wide level.

Below are some additional analyses that would be informative.

**Production** Incorporating the role of wind speeds, known to be an important factor in many regions (e.g., Haiti), into the production model.

**Production** Incorporating the changes in climate-driven harvest area to correct reported yields to reflect damage that reduces yields to the extent that the plant is not harvested at all.

**Production** Studying the effect of fertilizer on production, captured in the "fixed effects" of each region in our production model.

**Production** Use the India district data to construct and India model, and incorporate that into the hierarchical global model (see figure A.13 in the Appendix).

**Prices** Disaggregating the country-wide markup values to identify how they differ by coffee type.

# Appendix A

# Supplemental material

## A.1 Extra suitability analysis

### A.1.1 Changes in suitability by country for GAEZ

| Country | Baseline (1000 Ha) | A2 2050 (1000 Ha) | Change (1000 Ha) | % |
|---|---|---|---|---|
| Angola | 63738 | 40508 | -23230 | (-36%) |
| Argentina | 9047 | 12173 | +3126 | (+35%) |
| Australia | 13870 | 7593 | -6277 | (-45%) |
| Bahamas | 3487 | 1821 | -1666 | (-48%) |
| Bangladesh | 11677 | 298 | -11379 | (-97%) |
| Belize | 2652 | 1642 | -1010 | (-38%) |
| Benin | 4129 | 0 | -4129 | (-100%) |
| Bhutan | 0 | 1216 | +1216 | (new) |
| Bolivia | 76211 | 7791 | -68420 | (-90%) |
| Brazil | 785103 | 235221 | -549882 | (-70%) |
| Cambodia | 15559 | 1084 | -14475 | (-93%) |
| Cameroon | 39370 | 34157 | -5213 | (-13%) |
| Central African Republic | 56584 | 33494 | -23090 | (-41%) |
| Chad | 861 | 17 | -844 | (-98%) |
| China | 21597 | 30291 | +8694 | (+40%) |
| Colombia | 100541 | 27018 | -73523 | (-73%) |
| Congo, Dem. Rep. | 230509 | 199389 | -31120 | (-14%) |
| Congo, Rep. | 34477 | 33530 | -947 | (-3%) |
| Costa Rica | 5659 | 2653 | -3006 | (-53%) |
| Cote d'Ivoire | 30012 | 5965 | -24047 | (-80%) |
| Cuba | 14109 | 5786 | -8323 | (-59%) |
| Dominican Republic | 5481 | 3381 | -2100 | (-38%) |
| Ecuador | 20067 | 16909 | -3158 | (-16%) |
| El Salvador | 2331 | 1369 | -962 | (-41%) |
| Equatorial Guinea | 2933 | 2675 | -258 | (-9%) |
| Ethiopia | 39590 | 41674 | +2084 | (+5%) |
| French Guiana | 8592 | 4058 | -4534 | (-53%) |
| Gabon | 27151 | 26178 | -973 | (-4%) |

| Country | Baseline (1000 Ha) | A2 2050 (1000 Ha) | Change (1000 Ha) | % |
|---|---|---|---|---|
| Ghana | 13116 | 770 | -12346 | (-94%) |
| Guatemala | 10667 | 6718 | -3949 | (-37%) |
| Guinea | 18599 | 8595 | -10004 | (-54%) |
| Guinea-Bissau | 1348 | 0 | -1348 | (-100%) |
| Guyana | 21534 | 2672 | -18862 | (-88%) |
| Haiti | 3382 | 754 | -2628 | (-78%) |
| Honduras | 11616 | 7657 | -3959 | (-34%) |
| India | 34293 | 18979 | -15314 | (-45%) |
| Indonesia | 213246 | 104505 | -108741 | (-51%) |
| Jamaica | 1176 | 0 | -1176 | (-100%) |
| Japan | 164 | 39 | -125 | (-76%) |
| Kenya | 20565 | 17816 | -2749 | (-13%) |
| Lao PDR | 22976 | 12597 | -10379 | (-45%) |
| Lesotho | 0 | 268 | +268 | (new) |
| Liberia | 9908 | 9293 | -615 | (-6%) |
| Madagascar | 53116 | 48359 | -4757 | (-9%) |
| Malawi | 8475 | 4583 | -3892 | (-46%) |
| Malaysia | 35720 | 14051 | -21669 | (-61%) |
| Mexico | 54345 | 34878 | -19467 | (-36%) |
| Mozambique | 62931 | 35267 | -27664 | (-44%) |
| Myanmar | 47616 | 31854 | -15762 | (-33%) |
| Nepal | 0 | 3312 | +3312 | (new) |
| Nicaragua | 12968 | 7975 | -4993 | (-39%) |
| Nigeria | 28792 | 1717 | -27075 | (-94%) |
| Panama | 8959 | 4500 | -4459 | (-50%) |
| Papua New Guinea | 51723 | 25520 | -26203 | (-51%) |
| Paraguay | 29591 | 10163 | -19428 | (-66%) |
| Peru | 74724 | 24262 | -50462 | (-68%) |
| Philippines | 38768 | 15724 | -23044 | (-59%) |
| Rwanda | 2296 | 2486 | +190 | (+8%) |
| Senegal | 411 | 0 | -411 | (-100%) |
| Sierra Leone | 7631 | 2006 | -5625 | (-74%) |
| Solomon Islands | 5322 | 2921 | -2401 | (-45%) |
| South Africa | 6796 | 14140 | +7344 | (+108%) |
| South Sudan | 24980 | 3986 | -20994 | (-84%) |
| Sri Lanka | 6507 | 1144 | -5363 | (-82%) |
| Sudan | 272 | 0 | -272 | (-100%) |
| Suriname | 14810 | 447 | -14363 | (-97%) |
| Swaziland | 1516 | 708 | -808 | (-53%) |
| Tanzania UR | 82305 | 61876 | -20429 | (-25%) |
| Thailand | 34606 | 5546 | -29060 | (-84%) |
| Timor-Leste | 1803 | 1242 | -561 | (-31%) |
| Togo | 4082 | 409 | -3673 | (-90%) |
| Uganda | 21578 | 21028 | -550 | (-3%) |
| United States of America | 3960 | 7218 | +3258 | (+82%) |
| Venezuela | 83978 | 12959 | -71019 | (-85%) |
| Viet Nam | 27213 | 11551 | -15662 | (-58%) |
| Zambia | 56972 | 39304 | -17668 | (-31%) |
| Zimbabwe | 3194 | 992 | -2202 | (-69%) |

### A.1.2 Suitability condition distributions

#### Soils and nutrients

Coffee is very sensitive to soil conditions. The Harmonized World Soil Database (FAO/IIASA/ISRIC/ISSCAS/JRC, 2012) contains six soil components for both the topsoil and subsoil, to study this. The comparison between the distribution across the entire tropics, and across coffee regions for Arabica farms is shown in figures A.1 and A.2.

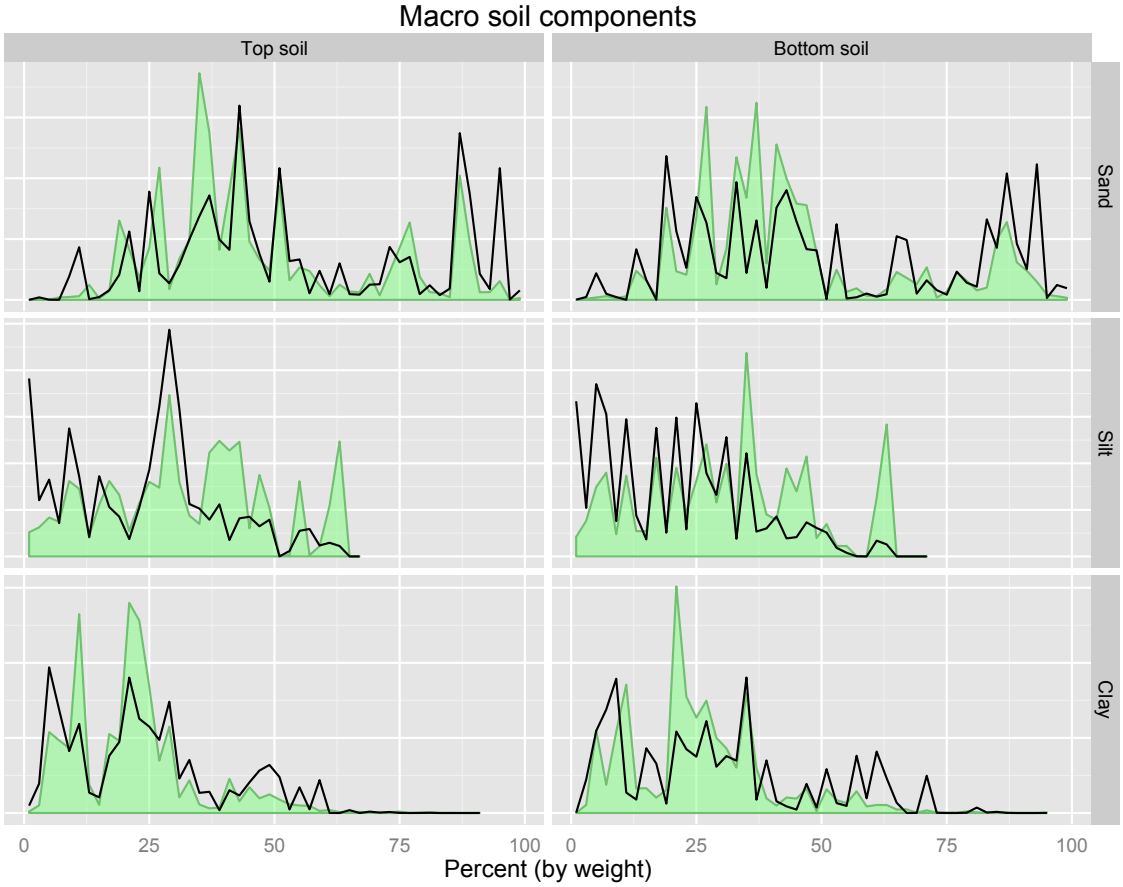


Figure A.1: Comparison of distributions of texture soil components. The faded area shows the distribution of soils generally between 30°N and 30°S. The line shows the distribution of soils, weighted by coffee planting densities.

From the first figure, coffee is more common in soils that have a larger share of sand and smaller share of silt than the norm. Clay also shows effects where coffee is less frequently grown in regions with intermediate quantities of clay. From the second figure, it appears that coffee is suitable in regions with intermediate quantities of calcium carbonate and low levels of gypsum.

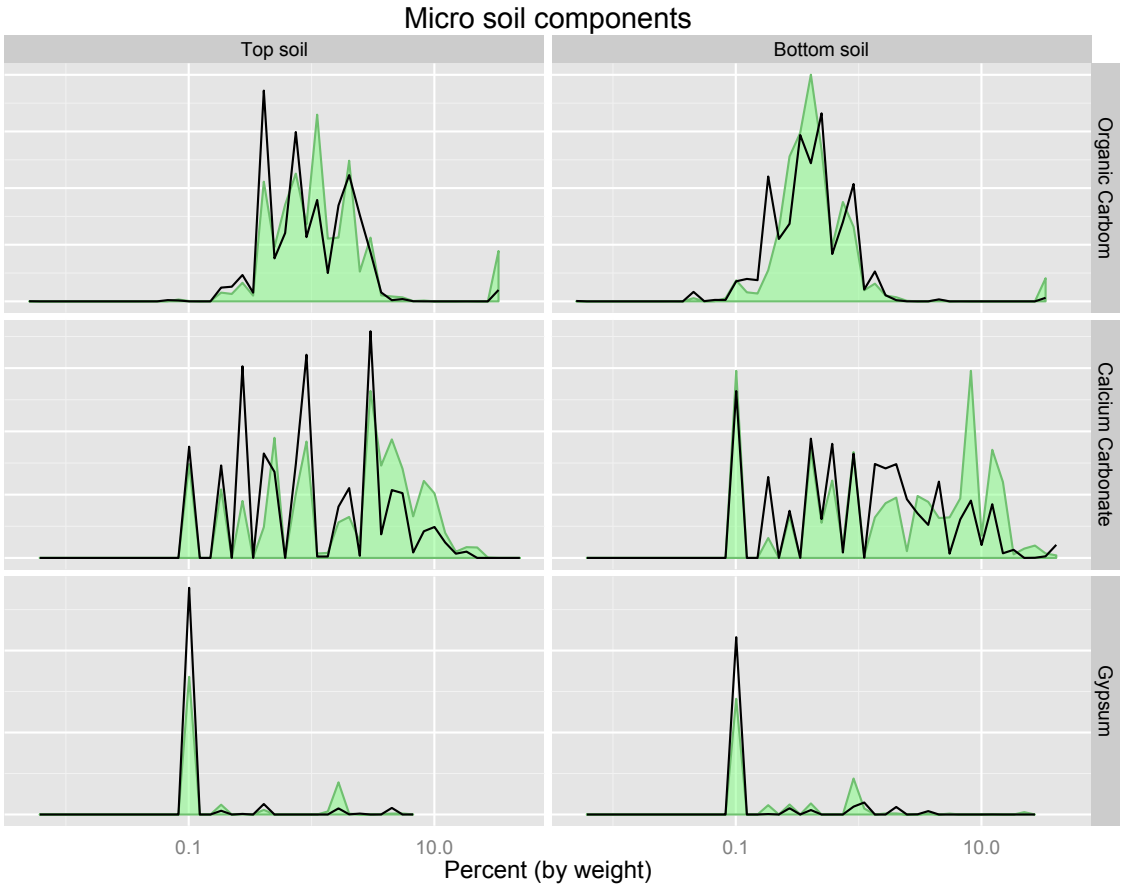


Figure A.2: Comparison of distributions of trace soil components. The faded area shows the distribution of soils generally between 30°N and 30°S. The line shows the distribution of soils, weighted by coffee planting densities.

**Elevation**

The distributional analysis shows a very wide range of elevations, possibly reflecting inaccuracies in the maps of Arabica and Robusta cultivation. See figure A.3.

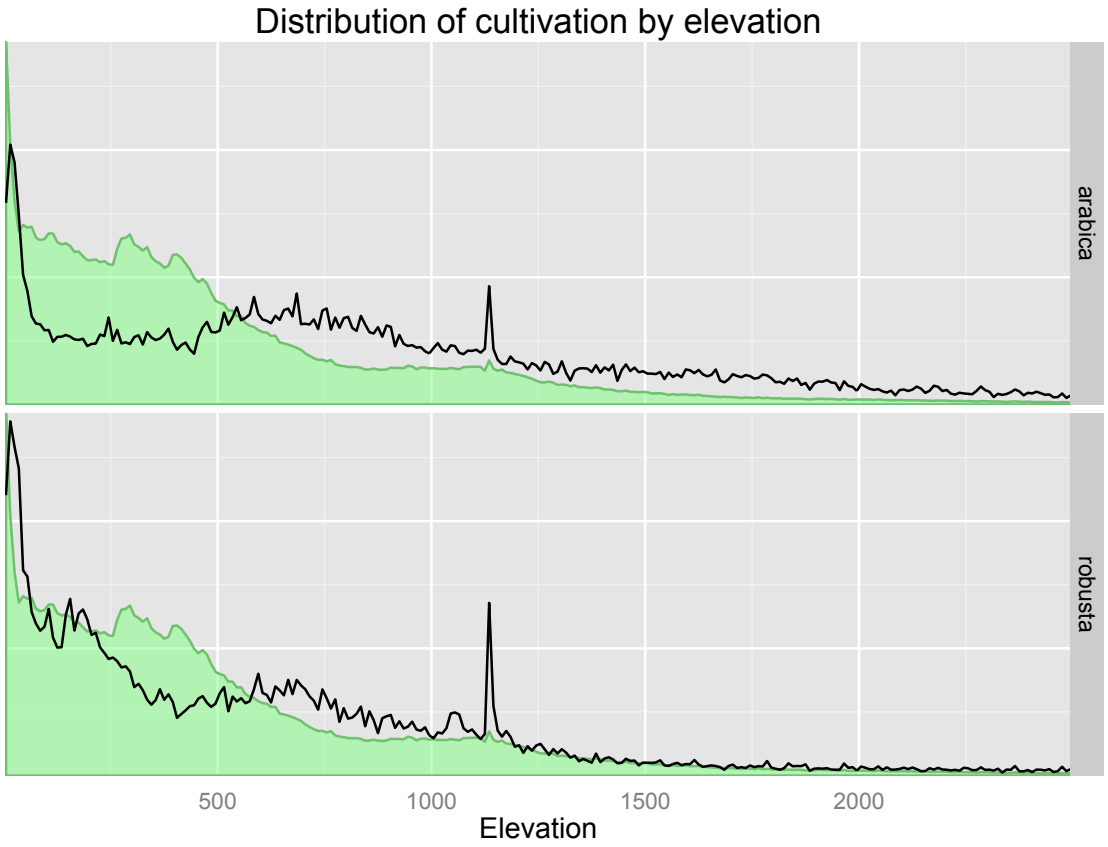


Figure A.3: Distributions of elevation for Arabica and Robusta (lines) and for the tropics in general (green).

Arabica shows clear diminished presence at low elevations (below 550 m) and increased presence at all higher elevations. However, there is still probability mass below 550 m. Similarly, Robusta has extra presence of elevations below 50 m, but still has some elevated presence between 550 m and 1200 m.

The most important result of elevation for coffee cultivation is the temperatures it produces. Hawaii, for example, has excellent coffee-growing temperatures from sea level to 610m, and Arabica coffee is grown across this entire range (Thurston et al., 2013). However, the distributions shown in figure A.3 are probably much more broad than is accurate. This data problem does not undermine the method, except that it increases the amount of uncertainty in the results.

**Bioclimatic variables**

Figure A.4 shows the distributions for all bioclimatic variables. These distributions are more erratic, because of the uneven spread of the observations within them: several bins in these histograms have no locations within their range, because of the discrete valuation of the Bioclim variables.

**Latitude**

We also incorporate latitude itself (see figure A.6). Even if there are increases in temperature, different latitudes will provide different levels of suitability, because of the tilt of the Earth and other processes. We cannot be certain whether coffee will grow effectively outside of these latitudes, even if they appear climatically similar in the future to lower latitudes now. Including the distribution of latitude imposes a slight conservativism on our estimate which is supported by the data.

### A.1.3 Changes in suitability by country for our model

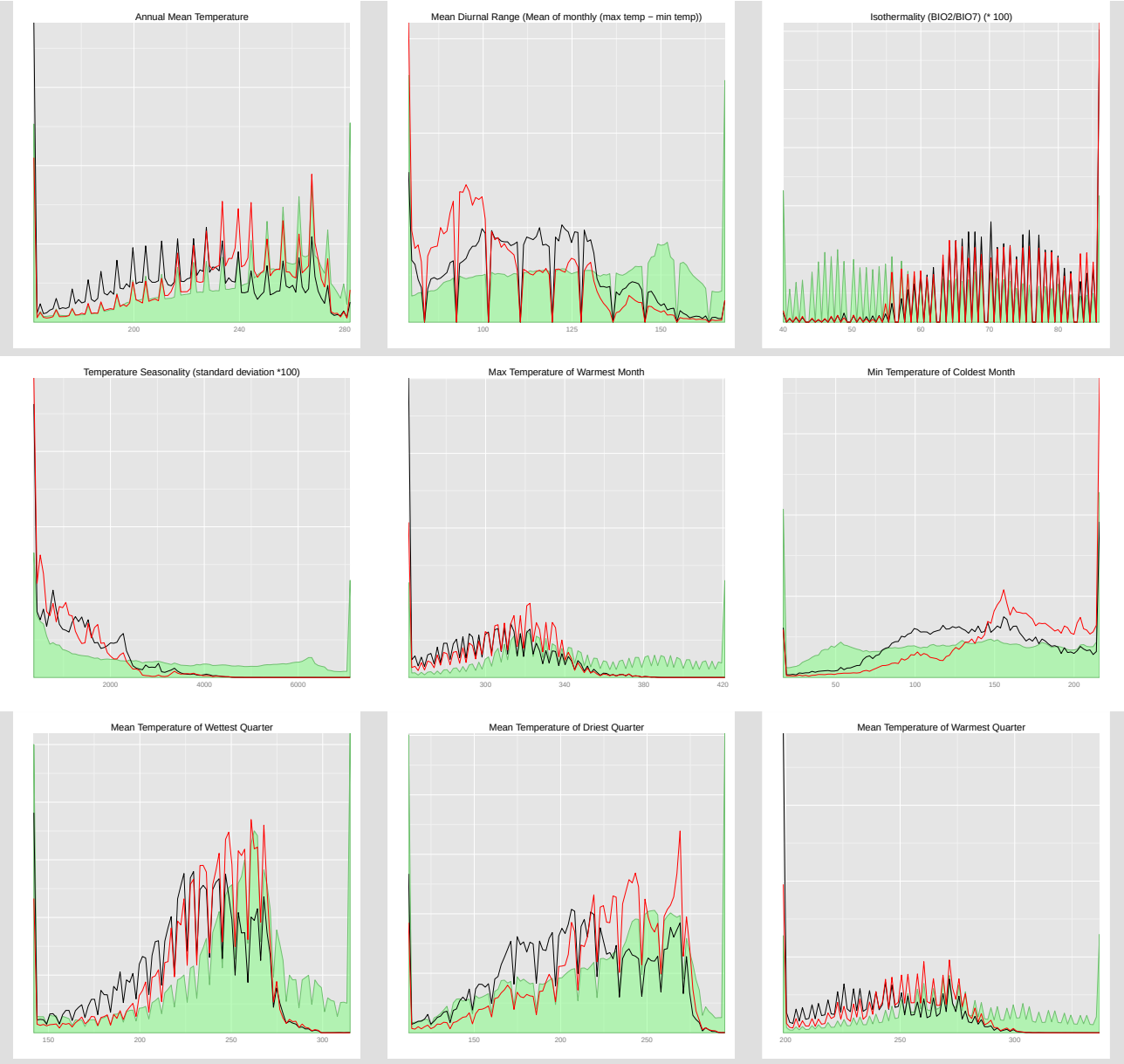


Figure A.4: First set of nine of the 19 variables in the Bioclim dataset, with coffee region distributions shown in black (Arabica) and red (Robusta). We dropped one, the Annual Temperature Range, since the technique implicitly infers it from the minimum and maximum temperatures.

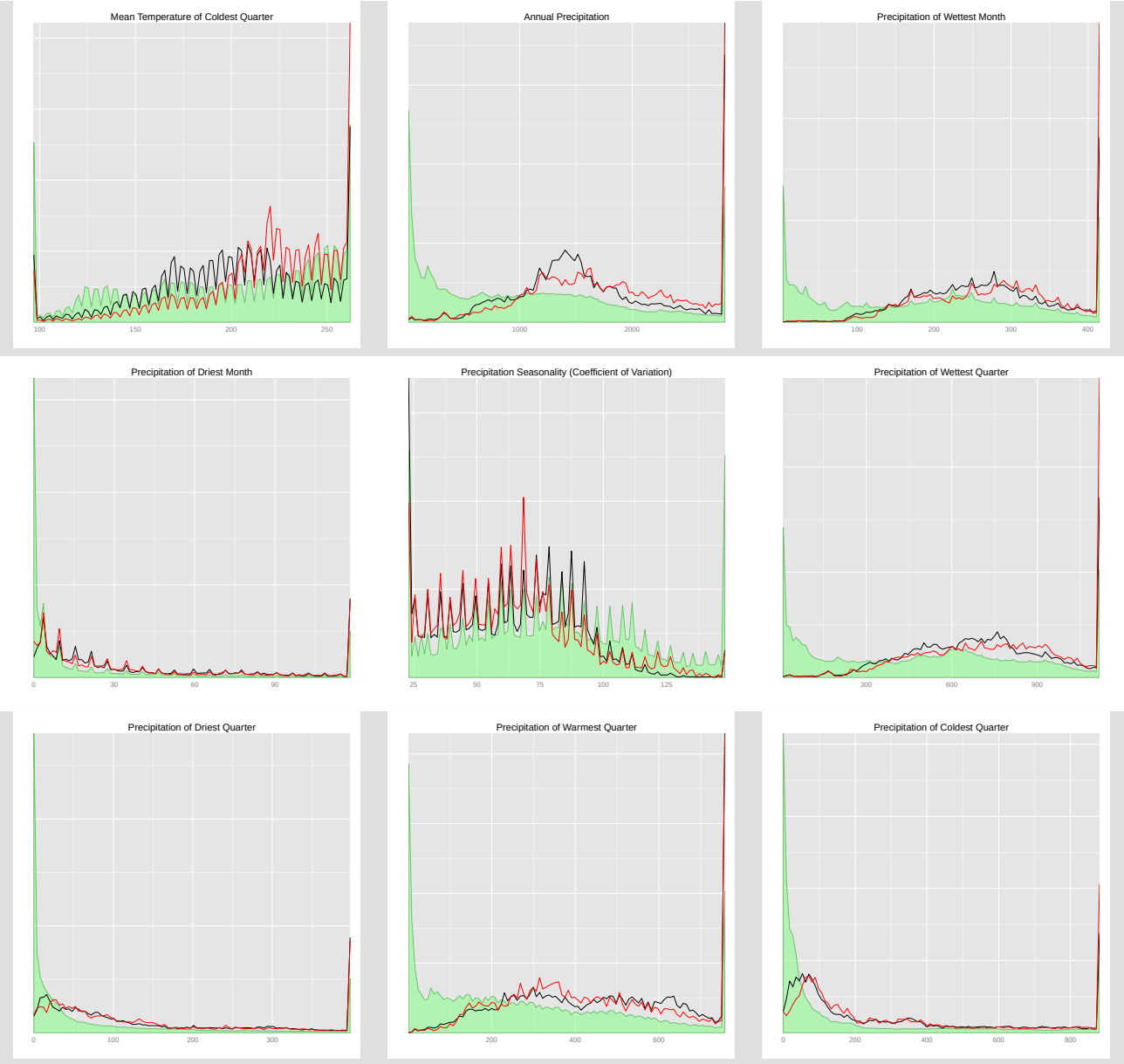


Figure A.5: Second set of nine of the 19 variables in the Bioclim dataset, with coffee region distributions shown in black (Arabica) and red (Robusta). We dropped one, the Annual Temperature Range, since the technique implicitly infers it from the minimum and maximum temperatures.

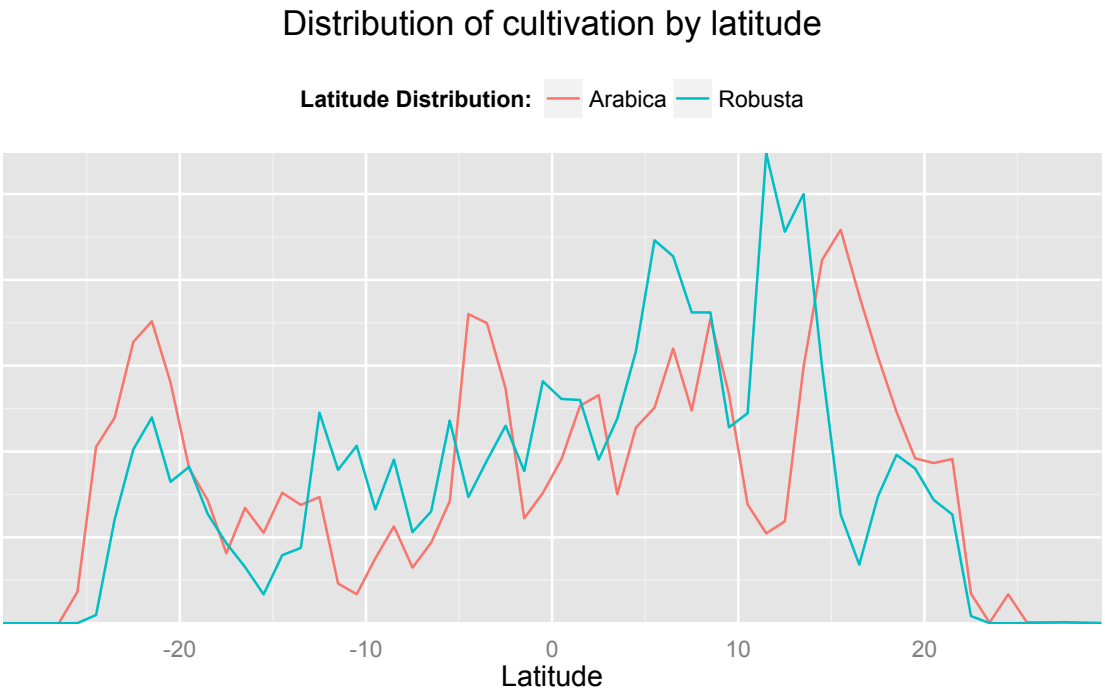


Figure A.6: The distribution of coffee production for Arabica (red) and Robusta (blue) across latitude.

**Arabica Changes, Baseline - 2050, RCP 8.5**

| | Suitable Areas | | | | | | Harvested Areas | |
|---|---|---|---|---|---|---|---|---|
| Country | Baseline (Ha) | Increase (Ha) | Decrease (Ha) | Conf. (%) | Loss (%) | Chng. (%) | Harvest (Ha) | H. Loss (%) |
| Angola | 7832331 | 3163478 | -7540076 | 96.66 | -96.30 | -55.90 | 31000.00 | -43.90 |
| Argentina | 703607 | 500422 | -362311 | 91.07 | -51.50 | 19.60 | | 0.00 |
| Australia | 324109 | 0 | -320158 | 97.77 | -98.80 | -98.80 | | 0.00 |
| Burundi | 642525 | 46216 | -463559 | 87.50 | -72.10 | -65.00 | 27000.00 | -25.70 |
| Belize | 28658 | 0 | -28658 | 100.00 | -100.00 | -100.00 | 47.00 | -100.00 |
| Bolivia | 2975159 | 361779 | -849786 | 100.00 | -28.60 | -16.40 | 30000.00 | -5.40 |
| Brazil | 30031272 | 4064511 | -25719629 | 97.67 | -85.60 | -72.10 | 2120080.00 | -34.70 |
| Bhutan | 0 | 93542 | 0 | 70.01 | | | | 0.00 |
| Botswana | 2559 | 0 | -2559 | 100.00 | -100.00 | -100.00 | | -100.00 |
| Central African Republic | 17019 | 0 | -17019 | 100.00 | -100.00 | -100.00 | 14000.00 | -100.00 |
| Chile | 327 | 242076 | -327 | 99.11 | -99.80 | | | 0.00 |
| China | 267924 | 31940 | -250819 | 91.15 | -93.60 | -81.70 | 62000.00 | -37.90 |
| CÙte d'Ivoire | 34259 | 0 | -34259 | 100.00 | -100.00 | -100.00 | 160000.00 | -100.00 |
| Cameroon | 901606 | 15973 | -637133 | 100.00 | -70.70 | -68.90 | 210000.00 | -25.50 |
| Democratic Republic of the Congo | 9054217 | 328050 | -7382600 | 95.55 | -81.50 | -77.90 | 86000.00 | -29.40 |
| Republic of Congo | 274260 | 0 | -274260 | 100.00 | -100.00 | -100.00 | 10500.00 | -100.00 |
| Colombia | 6333379 | 1130339 | -3333722 | 94.51 | -52.60 | -34.80 | 778084.00 | -19.30 |
| Comoros | 51817 | 603 | -39930 | 96.12 | -77.10 | -75.90 | 885.00 | 0.00 |
| Cape Verde | 552 | 8183 | -552 | 99.44 | -100.00 | | 0.00 | -100.00 |
| Costa Rica | 680983 | 125192 | -388387 | 97.31 | -57.00 | -38.60 | 93774.00 | -14.70 |
| Cuba | 155472 | 0 | -155387 | 98.11 | -99.90 | -99.90 | 28000.00 | -7.40 |
| Dominican Republic | 212045 | 47801 | -64205 | 93.88 | -30.30 | -7.70 | 133342.00 | -2.10 |
| Ecuador | 2169018 | 291030 | -820424 | 90.98 | -37.80 | -24.40 | 78709.71 | -17.50 |
| Eritrea | 616234 | 11180 | -443696 | 100.00 | -72.00 | -70.20 | | 0.00 |
| Spain | 0 | 145055 | 0 | 97.54 | | | | 0.00 |
| Ethiopia | 10236225 | 2117081 | -6834556 | 92.96 | -66.80 | -46.10 | 528571.00 | -28.00 |
| Fiji | 28317 | 0 | -28317 | 100.00 | -100.00 | -100.00 | 30.00 | -100.00 |
| France | 138260 | 32780 | -45329 | 92.31 | -32.80 | -9.10 | 120.00 | 0.00 |
| Gabon | 9451 | 0 | -9451 | 100.00 | -100.00 | -100.00 | 310.00 | -100.00 |
| Guinea | 101123 | 0 | -101123 | 100.00 | -100.00 | -100.00 | 66000.00 | -100.00 |
| Equatorial Guinea | 141982 | 0 | -141982 | 100.00 | -100.00 | -100.00 | 12500.00 | -100.00 |
| Guatemala | 2019079 | 287541 | -934956 | 90.05 | -46.30 | -32.10 | 250000.00 | -25.70 |
| Guyana | 694669 | 1504 | -664846 | 99.68 | -95.70 | -95.50 | 360.00 | -5.20 |
| Honduras | 2549303 | 62862 | -1593540 | 99.31 | -62.50 | -60.00 | 266000.00 | -22.90 |
| Haiti | 336450 | 17876 | -208607 | 98.68 | -62.00 | -56.70 | 92000.00 | -27.00 |
| Indonesia | 7617814 | 705740 | -4902428 | 96.51 | -64.40 | -55.10 | 1233900.00 | -10.90 |
| India | 523680 | 133453 | -329003 | 96.62 | -62.80 | -37.30 | 368687.00 | -1.00 |
| Jamaica | 49008 | 0 | -42530 | 100.00 | -86.80 | -86.80 | 7500.00 | -19.80 |
| Kenya | 5106633 | 888046 | -3200314 | 91.90 | -62.70 | -45.30 | 160000.00 | -27.10 |
| Cambodia | 2239 | 0 | -2239 | 100.00 | -100.00 | -100.00 | 430.00 | -100.00 |
| Lao PDR | 216682 | 0 | -211843 | 100.00 | -97.80 | -97.80 | 56875.00 | -19.00 |
| Sri Lanka | 48813 | 1895 | -26470 | 97.22 | -54.20 | -50.30 | 8460.00 | -0.70 |
| Lesotho | 0 | 1623 | 0 | 76.47 | | | | 0.00 |
| Morocco | 0 | 0 | 0 | 0.35 | | | | 0.00 |

**Arabica Changes, Baseline - 2050, RCP 8.5**

| | Suitable Areas | | | | | | Harvested Areas | |
|---|---|---|---|---|---|---|---|---|
| Country | Baseline (Ha) | Increase (Ha) | Decrease (Ha) | Conf. (%) | Loss (%) | Chng. (%) | Harvest (Ha) | H. Loss (%) |
| Madagascar | 15676837 | 1359696 | -7488575 | 96.47 | -47.80 | -39.10 | 138000.00 | -18.90 |
| Mexico | 23046243 | 3759088 | -12251072 | 96.23 | -53.20 | -36.80 | 695350.00 | -21.10 |
| Myanmar | 82547 | 4844 | -79233 | 93.42 | -96.00 | -90.10 | 12000.00 | -17.60 |
| Mozambique | 3368146 | 143380 | -2974523 | 96.50 | -88.30 | -84.10 | 980.00 | -18.40 |
| Mauritius | 63460 | 0 | -48142 | 100.00 | -75.90 | -75.90 | 0.00 | 0.00 |
| Malawi | 1545688 | 256879 | -1272351 | 90.01 | -82.30 | -65.70 | 2580.00 | -1.10 |
| Malaysia | 561747 | 19748 | -492026 | 96.17 | -87.60 | -84.10 | 19300.00 | -0.50 |
| Namibia | 1209730 | 134161 | -1171642 | 96.62 | -96.90 | -85.80 | | 0.00 |
| New Caledonia | 116243 | 4 | -100629 | 99.37 | -86.60 | -86.60 | 95.00 | 0.00 |
| Nigeria | 3391 | 109 | -3372 | 92.22 | -99.40 | -96.20 | 2200.00 | -2.20 |
| Nicaragua | 657690 | 9958 | -545072 | 100.00 | -82.90 | -81.40 | 123000.00 | -13.70 |
| Nepal | 0 | 0 | 0 | 63.34 | | | 1780.00 | 0.00 |
| Oman | 0 | 0 | 0 | 100.00 | -100.00 | -100.00 | | -100.00 |
| Panama | 379618 | 40024 | -221501 | 94.76 | -58.30 | -47.80 | 30000.00 | -20.30 |
| Peru | 3254385 | 2747945 | -1723632 | 92.61 | -53.00 | 31.50 | 312251.00 | -13.80 |
| Philippines | 1451866 | 102893 | -996757 | 97.58 | -68.70 | -61.60 | 119999.00 | -5.40 |
| Papua New Guinea | 4652101 | 274890 | -2134348 | 96.37 | -45.90 | -40.00 | 73000.00 | -10.60 |
| Puerto Rico | 148890 | 0 | -123066 | 100.00 | -82.70 | -82.70 | 42000.00 | -36.70 |
| Paraguay | 0 | 0 | - | 100.00 | -100.00 | -100.00 | 300.00 | -100.00 |
| Rwanda | 858792 | 108725 | -573378 | 89.08 | -66.80 | -54.10 | 41762.00 | -9.20 |
| Saudi Arabia | 802649 | 1111 | -768697 | 99.03 | -95.80 | -95.60 | 0.00 | 0.00 |
| South Sudan | 140253 | 5615 | -110543 | 93.32 | -78.80 | -74.80 | | 0.00 |
| Solomon Islands | 44906 | 5927 | -44870 | 100.00 | -99.90 | -86.70 | | 0.00 |
| Sierra Leone | 0 | 0 | - | 100.00 | -100.00 | -100.00 | 14000.00 | -100.00 |
| El Salvador | 88234 | 11743 | -59752 | 90.19 | -67.70 | -54.40 | 139958.00 | -33.90 |
| Somaliland | 535507 | 10985 | -533484 | 99.92 | -99.60 | -97.60 | | 0.00 |
| Somalia | 94467 | 4137 | -94467 | 95.80 | -100.00 | -95.60 | | -100.00 |
| S„o TomÈ and Principe | 22915 | 0 | -16475 | 100.00 | -71.90 | -71.90 | 250.00 | 0.00 |
| Swaziland | 94563 | 8035 | -79389 | 78.66 | -84.00 | -75.50 | | 0.00 |
| Thailand | 236767 | 0 | -236761 | 100.00 | -100.00 | -100.00 | 52000.00 | -100.00 |
| Timor-Leste | 201630 | 15264 | -161490 | 99.85 | -80.10 | -72.50 | 55000.00 | -12.10 |
| Taiwan | 17859 | 45193 | -17859 | 85.53 | -100.00 | 153.00 | 0.00 | -100.00 |
| Tanzania | 10120904 | 1745435 | -8474385 | 96.69 | -83.70 | -66.50 | 127335.00 | -21.80 |
| Uganda | 5007871 | 67539 | -4767946 | 99.69 | -95.20 | -93.90 | 310000.00 | -60.20 |
| United States | 457497 | 20861 | -400461 | 98.97 | -87.50 | -83.00 | 2550.00 | -85.70 |
| Venezuela | 5232487 | 259415 | -3729513 | 96.81 | -71.30 | -66.30 | 182000.00 | -3.70 |
| Vietnam | 1469106 | 73643 | -1256133 | 98.44 | -85.50 | -80.50 | 574314.36 | -1.90 |
| Vanuatu | 14532 | 0 | -14417 | 90.77 | -99.20 | -99.20 | 65.00 | 0.00 |
| Yemen | 2949889 | 16273 | -2137856 | 98.63 | -72.50 | -71.90 | 34987.00 | -27.40 |
| South Africa | 2635760 | 760688 | -2252927 | 98.86 | -85.50 | -56.60 | | 0.00 |
| Zambia | 4406514 | 13720 | -4193830 | 95.68 | -95.20 | -94.90 | 7000.00 | -34.40 |
| Zimbabwe | 398934 | 6065 | -390551 | 99.82 | -97.90 | -96.40 | 5397.00 | -31.40 |

**Robusta Changes, Baseline - 2050, RCP 8.5**

| | Suitable Areas | | | | | | Harvested Areas | |
|---|---|---|---|---|---|---|---|---|
| Country | Baseline (Ha) | Increase (Ha) | Decrease (Ha) | Conf. (%) | Loss (%) | Chng. (%) | Harvest (Ha) | H. Loss (%) |
| Angola | 5150021 | 5959656 | -2805429 | 85.92 | -54.50 | 61.20 | 31000.00 | -17.80 |
| Argentina | 1286056 | 2105318 | -1114987 | 91.68 | -86.70 | 77.00 | | 0.00 |
| American Samoa | 0 | 0 | 0 | 100.00 | | | | 0.00 |
| Antigua and Barbuda | 0 | 0 | 0 | 100.00 | | | | 0.00 |
| Australia | 170410 | 3414649 | -114523 | 93.17 | -67.20 | | | 0.00 |
| Burundi | 494565 | 145247 | -284285 | 92.28 | -57.50 | -28.10 | 27000.00 | -14.20 |
| Bangladesh | 0 | 561488 | 0 | 15.07 | | | | 0.00 |
| Bahamas | 0 | 0 | 0 | 50.00 | | | | 0.00 |
| Belize | 0 | 885404 | 0 | 82.07 | 0.00 | | 47.00 | 0.00 |
| Bolivia | 2038575 | 8924087 | -962916 | 65.29 | -47.20 | 390.50 | 30000.00 | -0.10 |
| Brazil | 8450738 | 35586649 | -2304340 | 72.03 | -27.30 | 393.80 | 2120080.00 | -14.00 |
| Barbados | 0 | 12 | 0 | 100.00 | | | | 0.00 |
| Brunei Darussalam | 0 | 13 | 0 | 100.00 | | | | 0.00 |
| Bhutan | 0 | 104353 | 0 | 99.09 | | | | 0.00 |
| Botswana | 405172 | 2386421 | -405166 | 62.82 | -100.00 | 489.00 | | -100.00 |
| Central African Republic | 198116 | 3599572 | -33401 | 84.84 | -16.90 | | 14000.00 | -0.00 |
| Chile | 12937 | 6 | -12937 | 99.95 | -100.00 | -100.00 | | -100.00 |
| China | 3768742 | 550157 | -3466649 | 98.36 | -92.00 | -77.40 | 62000.00 | -7.20 |
| CÙte d'Ivoire | 7815 | 1220362 | -296 | 94.34 | -3.80 | | 160000.00 | -0.10 |
| Cameroon | 1324883 | 5991635 | -175708 | 96.84 | -13.30 | 439.00 | 210000.00 | -1.60 |
| Democratic Republic of the Congo | 9668515 | 16006969 | -6745133 | 82.72 | -69.80 | 95.80 | 86000.00 | -0.70 |
| Republic of Congo | 570588 | 2522891 | -354354 | 92.87 | -62.10 | 380.10 | 10500.00 | -6.70 |
| Colombia | 4831268 | 6170063 | -2722280 | 78.40 | -56.30 | 71.40 | 778084.00 | -8.40 |
| Comoros | 1083 | 41001 | 0 | 78.33 | 0.00 | | 885.00 | 0.00 |
| Cape Verde | 47599 | 10128 | -17921 | 84.26 | -37.70 | -16.40 | 0.00 | 0.00 |
| Costa Rica | 563486 | 158883 | -271265 | 80.43 | -48.10 | -19.90 | 93774.00 | -7.90 |
| Cuba | 188896 | 1498809 | -375 | 83.71 | -0.20 | 793.30 | 28000.00 | -0.00 |
| Cayman Islands | 0 | 15092 | 0 | 100.00 | | | | 0.00 |
| Djibouti | 0 | 0 | 0 | 88.23 | | | | 0.00 |
| Dominica | 0 | 18146 | 0 | 100.00 | | | 610.00 | 0.00 |
| Dominican Republic | 249043 | 1195690 | -73639 | 92.28 | -29.60 | 450.50 | 133342.00 | -0.70 |
| Ecuador | 2266507 | 1056561 | -1267955 | 90.67 | -55.90 | -9.30 | 78709.71 | -1.70 |
| Eritrea | 606180 | 92476 | -303872 | 96.16 | -50.10 | -34.90 | | 0.00 |
| Spain | 0 | 54557 | 0 | 79.99 | | | | 0.00 |
| Ethiopia | 9630697 | 2589937 | -5991843 | 90.52 | -62.20 | -35.30 | 528571.00 | -27.30 |
| Fiji | 31202 | 215943 | -1686 | 91.50 | -5.40 | 686.70 | 30.00 | 0.00 |
| France | 87221 | 96079 | -14879 | 99.72 | -17.10 | 93.10 | 120.00 | 0.00 |
| Gabon | 31063 | 5413957 | -9317 | 99.52 | -30.00 | | 310.00 | -0.00 |
| Ghana | 0 | 196263 | 0 | 98.17 | | | 4000.00 | 0.00 |
| Guinea | 433521 | 831493 | -243442 | 87.70 | -56.20 | 135.60 | 66000.00 | -6.90 |
| Equatorial Guinea | 1050 | 318762 | -11 | 99.57 | -1.10 | | 12500.00 | -0.10 |
| Grenada | 0 | 23207 | 0 | 97.94 | | | | 0.00 |
| Guatemala | 1428221 | 2652766 | -876418 | 82.59 | -61.40 | 124.40 | 250000.00 | -31.40 |
| Guyana | 510369 | 419814 | -48270 | 78.66 | -9.50 | 72.80 | 360.00 | -0.40 |

**Robusta Changes, Baseline - 2050, RCP 8.5**

| | Suitable Areas | | | | | | Harvested Areas | |
|---|---|---|---|---|---|---|---|---|
| Country | Baseline (Ha) | Increase (Ha) | Decrease (Ha) | Conf. (%) | Loss (%) | Chng. (%) | Harvest (Ha) | H. Loss (%) |
| Hong Kong | 0 | 14612 | 0 | 74.94 | | | | 0.00 |
| Honduras | 2594743 | 2282517 | -702365 | 91.15 | -27.10 | 60.90 | 266000.00 | -10.60 |
| Haiti | 434375 | 779343 | -28904 | 92.06 | -6.70 | 172.80 | 92000.00 | -0.50 |
| Indonesia | 5364764 | 19407103 | -1702290 | 93.03 | -31.70 | 330.00 | 1233900.00 | -4.60 |
| India | 191152 | 2193510 | -84498 | 92.31 | -44.20 | | 368687.00 | -1.80 |
| Jamaica | 6010 | 61053 | 0 | 92.30 | 0.00 | | 7500.00 | 0.00 |
| Kenya | 4190724 | 1238752 | -2507363 | 91.06 | -59.80 | -30.30 | 160000.00 | -6.90 |
| Cambodia | 175055 | 427216 | -24262 | 57.23 | -13.90 | 230.20 | 430.00 | -0.00 |
| Saint Kitts and Nevis | 0 | 0 | 0 | 100.00 | | | | 0.00 |
| Lao PDR | 666770 | 1268847 | -273633 | 66.60 | -41.00 | 149.30 | 56875.00 | -2.60 |
| Liberia | 0 | 1323785 | 0 | 99.43 | | | 2800.00 | 0.00 |
| Saint Lucia | 0 | 104 | 0 | 100.00 | | | 0.00 | 0.00 |
| Sri Lanka | 53824 | 44149 | -36806 | 87.67 | -68.40 | 13.60 | 8460.00 | -0.10 |
| Morocco | 0 | 1953628 | 0 | 87.06 | | | | 0.00 |
| Madagascar | 579295 | 5905617 | -430242 | 93.92 | -74.30 | 945.20 | 138000.00 | -21.80 |
| Mexico | 20342425 | 9564738 | -16492118 | 94.79 | -81.10 | -34.10 | 695350.00 | -24.90 |
| Myanmar | 782366 | 972653 | -693545 | 93.04 | -88.60 | 35.70 | 12000.00 | -0.00 |
| Mozambique | 1196437 | 8105709 | -466356 | 86.79 | -39.00 | 638.50 | 980.00 | -8.60 |
| Mauritania | 0 | 9144 | 0 | 99.83 | | | | 0.00 |
| Montserrat | 0 | 0 | 0 | 88.23 | | | | 0.00 |
| Mauritius | 34422 | 107428 | 0 | 89.97 | -0.00 | 312.10 | 0.00 | 0.00 |
| Malawi | 652634 | 1158706 | -259512 | 82.41 | -39.80 | 137.80 | 2580.00 | -14.10 |
| Malaysia | 552660 | 2165838 | -28576 | 95.38 | -5.20 | 386.70 | 19300.00 | -0.10 |
| Namibia | 1325792 | 192435 | -1300052 | 98.90 | -98.10 | -83.50 | | 0.00 |
| New Caledonia | 39667 | 596897 | -1088 | 99.88 | -2.70 | | 95.00 | 0.00 |
| Nigeria | 22291 | 127003 | -2176 | 89.15 | -9.80 | 560.00 | 2200.00 | -0.20 |
| Nicaragua | 680281 | 1773570 | -53620 | 96.00 | -7.90 | 252.80 | 123000.00 | -0.00 |
| Nepal | 0 | 0 | 0 | 100.00 | | | 1780.00 | 0.00 |
| Oman | 0 | 82194 | 0 | 90.57 | 0.00 | | | 0.00 |
| Panama | 385527 | 538364 | -163103 | 83.74 | -42.30 | 97.30 | 30000.00 | -9.50 |
| Peru | 6609345 | 6578036 | -4375019 | 80.81 | -66.20 | 33.30 | 312251.00 | -10.40 |
| Philippines | 1200467 | 2966352 | -368050 | 88.92 | -30.70 | 216.40 | 119999.00 | -5.60 |
| Papua New Guinea | 2390681 | 4469796 | -1276059 | 91.17 | -53.40 | 133.60 | 73000.00 | -11.90 |
| Puerto Rico | 105939 | 352303 | 0 | 98.38 | 0.00 | 332.60 | 42000.00 | 0.00 |
| Paraguay | 0 | 2483538 | 0 | 84.98 | -100.00 | | 300.00 | -100.00 |
| Rwanda | 667299 | 8125 | -512784 | 92.74 | -76.80 | -75.60 | 41762.00 | -36.00 |
| Western Sahara | 0 | 31668 | 0 | 99.03 | | | | 0.00 |
| Saudi Arabia | 828878 | 46020 | -300087 | 100.00 | -36.20 | -30.70 | 0.00 | 0.00 |
| Sudan | 0 | 19421 | 0 | 97.53 | | | | 0.00 |
| South Sudan | 81932 | 306289 | -31559 | 60.11 | -38.50 | 335.30 | | 0.00 |
| Senegal | 0 | 0 | 0 | 100.00 | | | | 0.00 |
| Solomon Islands | 39621 | 378509 | -61 | 98.42 | -0.20 | 955.10 | | 0.00 |
| Sierra Leone | 2290 | 483628 | -2288 | 88.83 | -99.90 | | 14000.00 | -0.00 |
| El Salvador | 178283 | 112387 | -59934 | 62.25 | -33.60 | 29.40 | 139958.00 | -4.10 |

**Robusta Changes, Baseline - 2050, RCP 8.5**

| | Suitable Areas | | | | | | Harvested Areas | |
|---|---|---|---|---|---|---|---|---|
| Country | Baseline (Ha) | Increase (Ha) | Decrease (Ha) | Conf. (%) | Loss (%) | Chng. (%) | Harvest (Ha) | H. Loss (%) |
| Somaliland | 510372 | 402411 | -161477 | 83.59 | -31.60 | 47.20 | | 0.00 |
| Somalia | 0 | 57573 | 0 | 45.79 | -100.00 | | | -100.00 |
| S„o TomÈ and Principe | 7584 | 11738 | -174 | 98.88 | -2.30 | 152.50 | 250.00 | 0.00 |
| Suriname | 0 | 6728 | 0 | 31.93 | | | 488.00 | 0.00 |
| Swaziland | 16051 | 15316 | -16051 | 100.00 | -100.00 | -4.60 | | -100.00 |
| Togo | 0 | 100627 | 0 | 100.00 | | | 27000.00 | 0.00 |
| Thailand | 221535 | 640290 | -70468 | 80.08 | -31.80 | 257.20 | 52000.00 | -0.00 |
| Timor-Leste | 24148 | 145298 | -8755 | 93.06 | -36.30 | 565.40 | 55000.00 | -2.20 |
| Tonga | 0 | 7290 | 0 | 96.30 | | | 10.00 | 0.00 |
| Trinidad and Tobago | 0 | 32 | 0 | 50.01 | | | 350.00 | 0.00 |
| Taiwan | 6208 | 256909 | 0 | 90.01 | -0.00 | | 0.00 | 0.00 |
| Tanzania | 14434260 | 5551037 | -8871902 | 85.55 | -61.50 | -23.00 | 127335.00 | -13.80 |
| Uganda | 6944190 | 1159159 | -5756638 | 80.92 | -82.90 | -66.20 | 310000.00 | -60.40 |
| United States | 129750 | 359497 | -29880 | 88.00 | -23.00 | 254.00 | 2550.00 | -26.80 |
| Saint Vincent and the Grenadines | 0 | 72 | 0 | 100.00 | | | | 0.00 |
| Venezuela | 3515842 | 2313894 | -2227300 | 78.01 | -63.40 | 2.50 | 182000.00 | -2.50 |
| United States Virgin Islands | 0 | 0 | 0 | 100.00 | | | | 0.00 |
| Vietnam | 1883848 | 4343466 | -92368 | 88.85 | -4.90 | 225.70 | 574314.36 | -0.40 |
| Vanuatu | 63133 | 327533 | -1013 | 96.96 | -1.60 | 517.20 | 65.00 | 0.00 |
| Samoa | 0 | 11403 | 0 | 58.88 | | | 35.00 | 0.00 |
| Yemen | 2748339 | 2130013 | -985741 | 91.92 | -35.90 | 41.60 | 34987.00 | -18.50 |
| South Africa | 4799951 | 713212 | -4627116 | 100.00 | -96.40 | -81.50 | | 0.00 |
| Zambia | 1625781 | 704492 | -1063716 | 86.34 | -65.40 | -22.10 | 7000.00 | -51.40 |
| Zimbabwe | 962921 | 347792 | -955963 | 95.36 | -99.30 | -63.20 | 5397.00 | -20.90 |

## A.2 Extra variability analysis

### A.2.1 Computing ENSO impacts

We estimate the impacts of El Niño and La Niña by estimating an "impulse response", which accounts for the multiple overlapping effects of different ENSO years and the monthly climatology of the NINO 3.4 signal.

$$y_t = \alpha + \sum_{Y=Year(t)-N/12+1}^{Year(t)} \sum_{M=1}^{N} \beta_{12(Year(t)-Y)+M}^{Class(Y)} + \gamma \sum_{s=1}^{24} \frac{y_{t-s}}{24} + \mu_{Month(t)}$$

$Year(t)$ is the year for time $t$ and $Month(t)$ is the month for time $t$; $Class(Y)$ is the class of ENSO event that happened in year $Y$ (El Niño and La Niña). $N$ is the number of months to include in the impulse responses.

Here, the $\beta_m^k$ variables describe impulse responses of length $N$ for each class of ENSO event.

### A.2.2 Additional PCA details

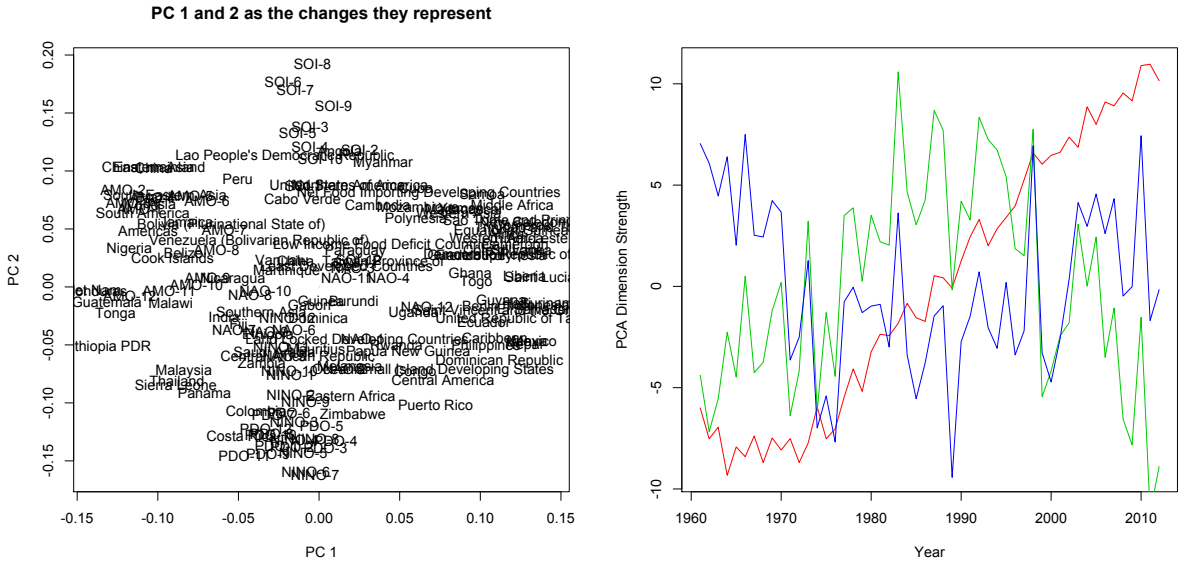


Figure A.7: **Left:** The first and second principal component, in terms of the marginal effects of countries and climate signals. These are displayed more clearly in the main report. **Right:** The values of the first three principal components (PC 1 = red, PC 2 = green, PC 3 = blue) across years. As years progress, PC 1 generally increases, and PC 2 first decreases and then increases.

### A.2.3 Monthly production

Production records are generally maintained on a yearly basis, but different price information is available monthly. Different countries harvest and ship beans during different months, and this information can be used to infer the monthly production added to the global market.


Figure A.8: Inferred monthly production for Arabica and Robusta coffee, based on the harvesting calendars of their producing countries.

We use the coffee harvested calendar from the Sweet Maria's Coffee Production Timetable, which is admittedly uncertain and subject to yearly change. However, they provide a general cycle around which actual yearly production is assumed to vary. We distribute the production for each country amongst its harvesting months, and evenly distribute throughout the year production for countries not represented in the calendar (most notably, Vietnam). We also distinguish between countries that produce Arabica and Robusta coffees, or those that produce a combination of both every year. The result in the figure above shows wide variations from month to month.

It is also interesting that the range of variation has increased significantly. The peak of production each year has increased much faster than the yearly minimum: In the 1960s, the best years produced monthly peaks over 10 million bags, while the slowest months produced only 3 million bags. In the last decade, the greatest monthly production has been over 15 million bags, but the worst months have only produced 5 million bags. The situation is even starker for Arabica coffee, where the worst months in the last decade are comparable to those in the 1960s, although the best months have increased over 20%.

We can use this monthly production data to inform the coffee market model, described below.

### A.2.4 Additional pest control results

#### 4°C global warming temperature data without pest control

With 4°C of warming, the distribution becomes almost completely normal, continuing to move right, though with a smaller right tail. Even with a huge amount of warming, there were no instances above 600 or 66% of the crop. This suggests that with the average monthly infection around 20%, the plants are not healthy enough to sustain a super event like the size of one previously seen. This absolute limit does little to help the predictability on short time scales however.

**Histogram of outbreak sizes and Log-log plot of outbreak sizes**

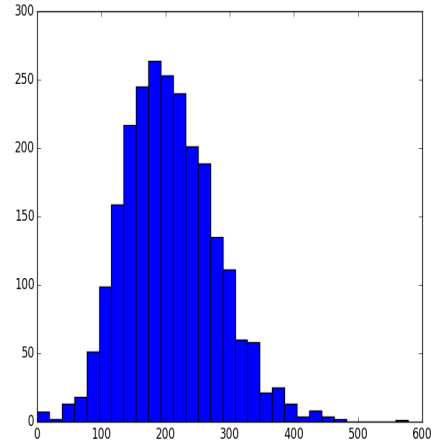


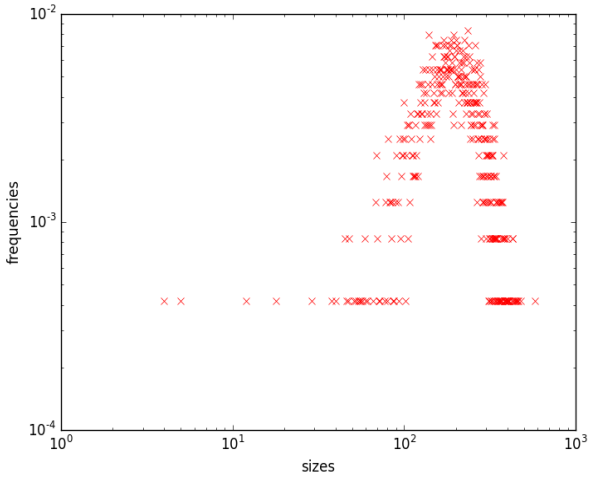


**Time series of outbreak sizes**

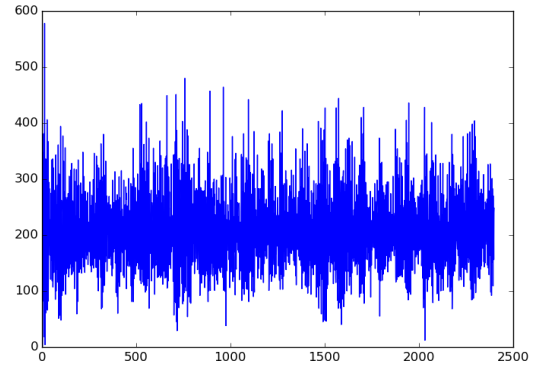


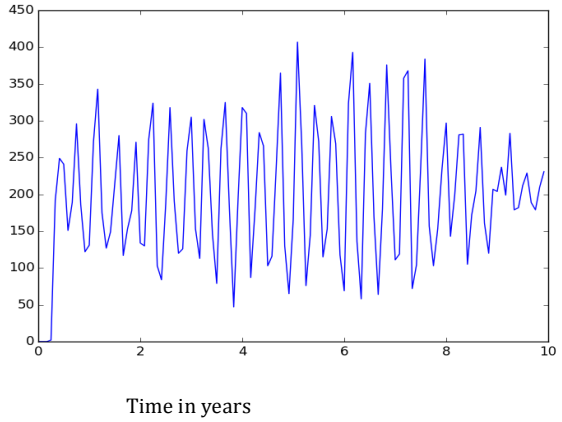


Figure A.9: Results for 4°C warming without pest control.

#### 4°C global warming temperature data with pest control

4°C of warming begins to offset the ability of fungicides to control the fungus population, the highest values in the histogram moves away from zero, shown by the concavity of the Log-log plot, as the curve continues to be thicker in areas than it was with less warming. The time series, as well as the other plots

itself begin to more resemble the model runs in uncontrolled but cooler environments, with the highest values still not going higher than 70%.

**Histogram of outbreak sizes and Log-log plot of outbreak sizes**

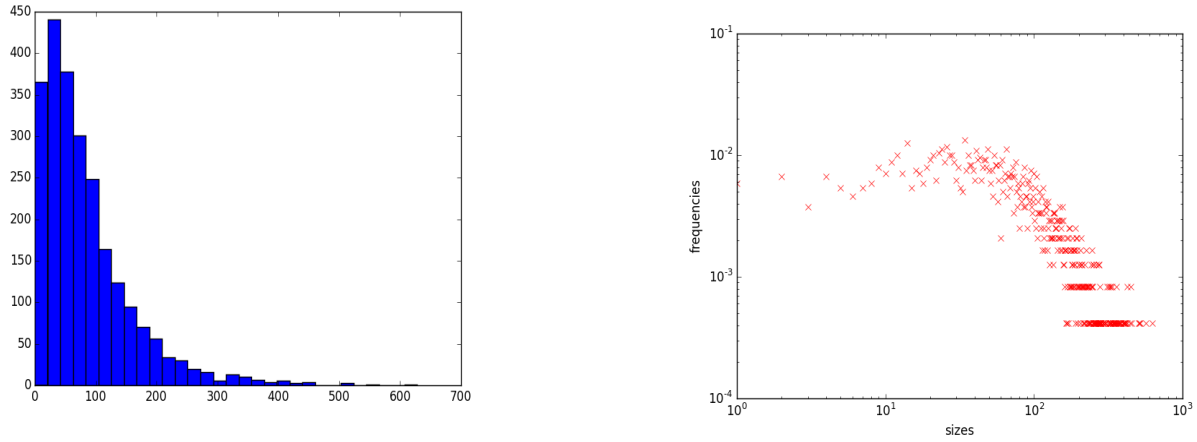


**Time series of outbreak sizes**

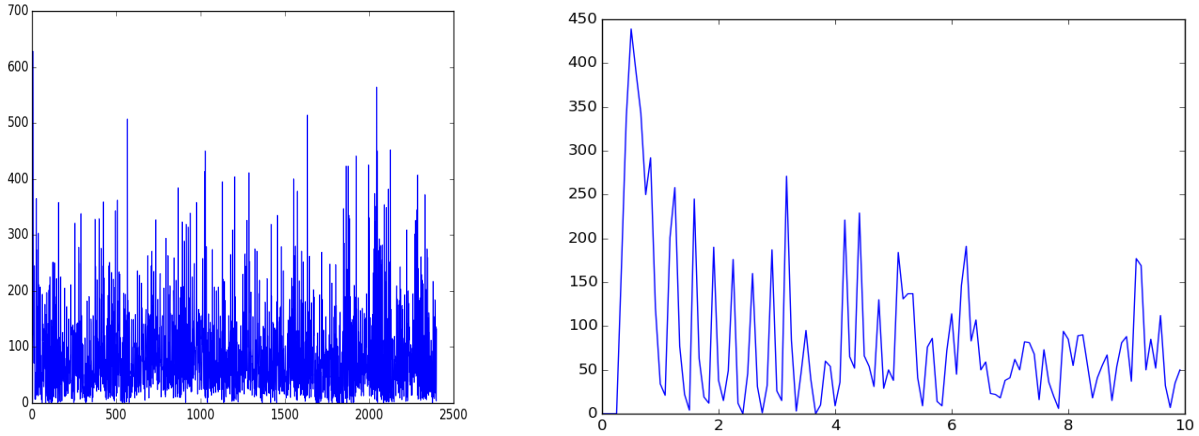

Figure A.10: Results for 4°C warming with pest control.

## A.3 Extra production analsysis

### A.3.1 Selecting temperature limits

### A.3.2 Humidity

### A.3.3 Harvest month effects

Figure A.11 shows the estimated "effect" of harvesting in a given month on yields, from 1962 to 2011, after accounting for country-specific and monthly effects. The gradual increase reflects improvements in coffee production technology, but this increase is not without large shocks. An increase in yields between 1985 and 1990 was followed by a decrease and then another period of increased yields. Countries that

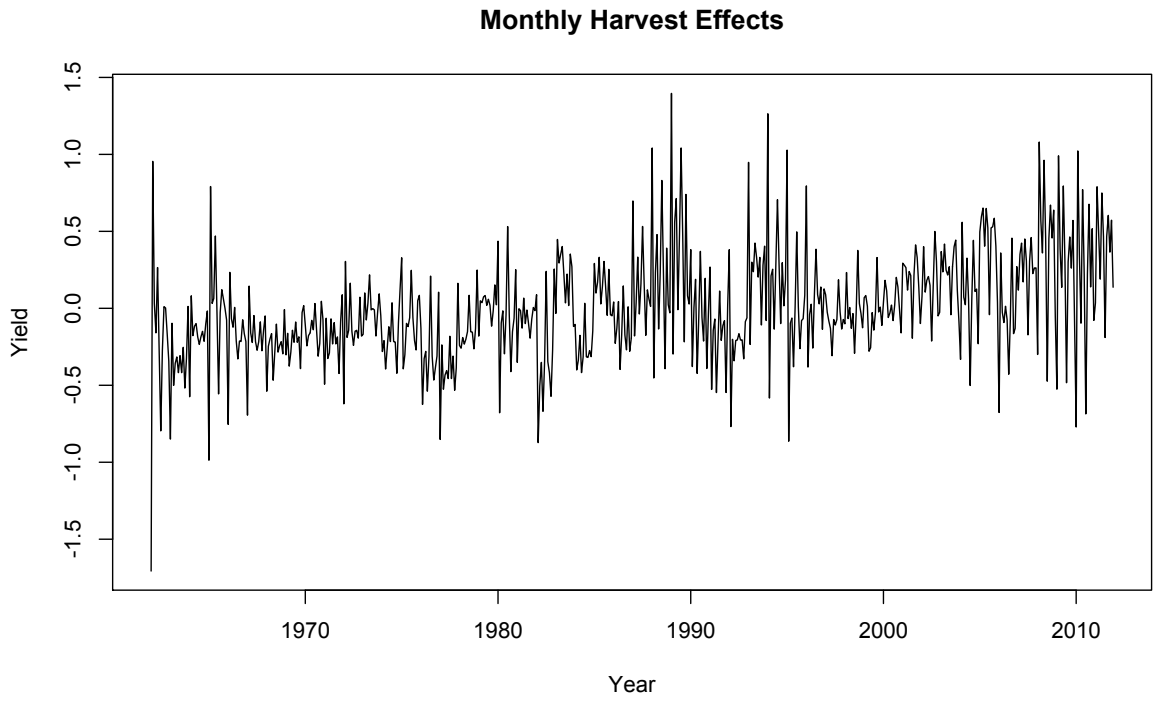


Figure A.11: Monthly harvesting effects. Each point on this curve represents the difference in yields predicted by harvesting in a given month, according to coffee harvest calendars, after accounting for country-specific and month effects. Uses calendars from `https://www.sweetmarias.com/coffee.prod.timetable.php`

| Low \High | 28 | 29 | 30 | 31 | 32 | 33 | 34 |
|---|---|---|---|---|---|---|---|
| -4 | | | | | 87.4211 | 87.4289 | 87.3933 |
| -3 | | | | | | | |
| -2 | | | | | | 87.4290 | |
| -1 | | | | | | | |
| 0 | | | | 87.2986 | 87.4213 | 87.4290 | 87.3934 |
| 1 | | | | | | 87.4290 | |
| 2 | | | | | 87.4212 | 87.4289 | 87.3933 |
| 3 | | | | | | 87.4288 | |
| 4 | | | | 87.2983 | 87.4210 | 87.4286 | |
| 5 | | | 87.0758 | 87.2979 | 87.4206 | | |
| 6 | | | | 87.2978 | 87.4205 | 87.4281 | |
| 7 | | | 87.0755 | 87.2978 | 87.4204 | | |
| 8 | | | | 87.2981 | | | |
| 9 | | | 87.0749 | 87.2979 | 87.4199 | | |
| 10 | 86.7490 | | 87.0737 | 87.2975 | | | |
| 11 | | | 87.0729 | 87.2975 | 87.4182 | | |
| 12 | 86.7398 | | 87.0700 | 87.2954 | | | |
| 13 | | | | | | | |
| 14 | | | | | | | |
| 15 | 86.6988 | | 87.0369 | 87.2645 | | | |

Table A.4: F-statistics for a growing degree-day and killing degree-day model of coffee production, across all countries. The highest F-stats use a maximum temperature of 30°C and a minimum temperature between -3°C and 1 °C.

harvest in different months also show different fortunes, with the greatest yields to countries that harvest in January and the lowest to those that harvest in February. Since the only country that harvests in January but not February is Colombia, this probably reflects the difference between Colombia yields and yields in other February-harvesting countries.

### A.3.4 Hierarchical model coefficients

Only statistically-significant coefficients are listed below. The remaining are available online at `http://eicoffee.net/`.

| | *Dependent variable:* | |
|---|---|---|
| | Countries only | |
| | (1) | (2) |
| GDDs / 1000, Liberia (Robusta) | 0.515** | 0.743*** |
| | (0.213) | (0.202) |
| GDDs / 1000, Gabon (Robusta) | 0.223 | 0.448** |
| | (0.215) | (0.204) |
| GDDs / 1000, Yemen (Arabica) | 0.274 | 0.368** |
| | (0.189) | (0.183) |
| GDDs / 1000, Benin (Robusta) | 0.146 | 0.409** |
| | (0.221) | (0.207) |
| GDDs / 1000, Cuba (Arabica) | 0.222 | 0.322* |
| | (0.194) | (0.189) |

| | *Dependent variable:* | |
|---|---|---|
| | Countries only | |
| | (1) | (2) |
| GDDs / 1000, Angola (Robusta) | 0.121 | 0.354* |
| | (0.217) | (0.205) |
| GDDs / 1000, Malaysia (Robusta) | 0.266 | 0.495** |
| | (0.220) | (0.209) |
| GDDs / 1000, Brazil (Combined) | 0.079 | 0.158*** |
| | (0.208) | (0.052) |
| GDDs / 1000, Guinea (Robusta) | 0.356* | 0.603*** |
| | (0.199) | (0.185) |
| GDDs / 1000, Nigeria (Robusta) | 0.377* | 0.659*** |
| | (0.212) | (0.197) |
| GDDs / 1000, Suriname (Combined) | 0.346* | 0.484** |
| | (0.204) | (0.189) |
| GDDs / 1000, Zambia (Arabica) | 0.217 | 0.300* |
| | (0.178) | (0.173) |
| GDDs / 1000, Paraguay (Arabica) | 0.248 | 0.405*** |
| | (0.165) | (0.156) |
| GDDs / 1000, Guyana (Robusta) | 0.140 | 0.374* |
| | (0.223) | (0.211) |
| GDDs / 1000, Congo (Robusta) | 0.145 | 0.382* |
| | (0.215) | (0.203) |
| KDDs / 1000, Cambodia (Combined) | −0.112 | −1.798*** |
| | (0.567) | (0.363) |
| KDDs / 1000, Ethiopia (Arabica) | −0.082 | −1.731*** |
| | (0.581) | (0.394) |
| KDDs / 1000, Cameroon (Combined) | −0.111 | −1.801*** |
| | (0.568) | (0.364) |
| KDDs / 1000, Ghana (Robusta) | −0.180 | −1.787*** |
| | (0.568) | (0.386) |
| KDDs / 1000, Saudi.Arabia (Combined) | −0.110 | −1.801*** |
| | (0.568) | (0.364) |
| KDDs / 1000, Guatemala (Arabica) | −0.082 | −1.731*** |
| | (0.581) | (0.394) |
| KDDs / 1000, Guatemala (Combined) | −0.110 | −1.801*** |
| | (0.568) | (0.364) |
| KDDs / 1000, Dominica (Combined) | −0.110 | −1.801*** |
| | (0.568) | (0.364) |
| KDDs / 1000, Liberia (Robusta) | −0.123 | −1.732*** |
| | (0.568) | (0.386) |
| KDDs / 1000, Gabon (Robusta) | −0.155 | −1.764*** |
| | (0.568) | (0.386) |
| KDDs / 1000, Gabon (Combined) | −0.110 | −1.800*** |
| | (0.568) | (0.364) |
| KDDs / 1000, Yemen (Combined) | −0.110 | −1.801*** |
| | (0.568) | (0.364) |
| KDDs / 1000, Yemen (Arabica) | −0.078 | −1.728*** |
| | (0.581) | (0.394) |

| | *Dependent variable:* | |
|---|---|---|
| | Countries only | |
| | (1) | (2) |
| KDDs / 1000, Jamaica (Arabica) | −0.082 | −1.731*** |
| | (0.581) | (0.394) |
| KDDs / 1000, Samoa (Combined) | −0.110 | −1.801*** |
| | (0.568) | (0.364) |
| KDDs / 1000, Kenya (Arabica) | −0.082 | −1.731*** |
| | (0.581) | (0.394) |
| KDDs / 1000, Kenya (Combined) | −0.114 | −1.804*** |
| | (0.568) | (0.364) |
| KDDs / 1000, India (Combined) | −0.110 | −1.801*** |
| | (0.568) | (0.364) |
| KDDs / 1000, Saint.Lucia (Combined) | −0.110 | −1.801*** |
| | (0.568) | (0.364) |
| KDDs / 1000, Rwanda (Arabica) | −0.082 | −1.731*** |
| | (0.581) | (0.394) |
| KDDs / 1000, Peru (Arabica) | −0.082 | −1.731*** |
| | (0.581) | (0.394) |
| KDDs / 1000, Vanuatu (Combined) | −0.110 | −1.801*** |
| | (0.568) | (0.364) |
| KDDs / 1000, Malawi (Arabica) | −0.082 | −1.731*** |
| | (0.581) | (0.394) |
| KDDs / 1000, Benin (Robusta) | −0.156 | −1.754*** |
| | (0.565) | (0.384) |
| KDDs / 1000, Benin (Combined) | −0.114 | −1.773*** |
| | (0.559) | (0.358) |
| KDDs / 1000, Cuba (Arabica) | −0.076 | −1.725*** |
| | (0.581) | (0.394) |
| KDDs / 1000, Togo (Robusta) | −0.244 | −1.827*** |
| | (0.560) | (0.380) |
| KDDs / 1000, Tonga (Combined) | −0.110 | −1.801*** |
| | (0.568) | (0.364) |
| KDDs / 1000, Indonesia (Combined) | −0.110 | −1.801*** |
| | (0.568) | (0.364) |
| KDDs / 1000, Mauritius (Combined) | −0.110 | −1.801*** |
| | (0.568) | (0.364) |
| KDDs / 1000, Angola (Combined) | −0.109 | −1.799*** |
| | (0.568) | (0.364) |
| KDDs / 1000, Angola (Robusta) | −0.159 | −1.768*** |
| | (0.568) | (0.386) |
| KDDs / 1000, Trinidad.and.Tobago (Combined) | −0.110 | −1.801*** |
| | (0.568) | (0.364) |
| KDDs / 1000, Nicaragua (Arabica) | −0.084 | −1.733*** |
| | (0.581) | (0.394) |
| KDDs / 1000, Malaysia (Robusta) | −0.159 | −1.768*** |
| | (0.568) | (0.386) |
| KDDs / 1000, Mozambique (Combined) | −0.111 | −1.801*** |
| | (0.568) | (0.364) |

| | *Dependent variable:* | |
|---|---|---|
| | Countries only | |
| | (1) | (2) |
| KDDs / 1000, Uganda (Combined) | −0.111 | −1.801*** |
| | (0.568) | (0.364) |
| KDDs / 1000, Brazil (Combined) | −0.110 | −1.971*** |
| | (0.568) | (0.309) |
| KDDs / 1000, Guinea (Robusta) | −0.101 | −1.703*** |
| | (0.566) | (0.384) |
| KDDs / 1000, Panama (Arabica) | −0.082 | −1.731*** |
| | (0.581) | (0.394) |
| KDDs / 1000, Costa.Rica (Arabica) | −0.081 | −1.731*** |
| | (0.581) | (0.394) |
| KDDs / 1000, Nigeria (Robusta) | −0.085 | −1.674*** |
| | (0.562) | (0.382) |
| KDDs / 1000, Ecuador (Combined) | −0.110 | −1.801*** |
| | (0.568) | (0.364) |
| KDDs / 1000, El.Salvador (Arabica) | −0.081 | −1.729*** |
| | (0.581) | (0.393) |
| KDDs / 1000, Puerto.Rico (Combined) | −0.110 | −1.801*** |
| | (0.568) | (0.364) |
| KDDs / 1000, Thailand (Combined) | −0.109 | −1.796*** |
| | (0.567) | (0.363) |
| KDDs / 1000, Thailand (Robusta) | −0.165 | −1.773*** |
| | (0.568) | (0.386) |
| KDDs / 1000, Haiti (Arabica) | −0.087 | −1.731*** |
| | (0.580) | (0.393) |
| KDDs / 1000, Belize (Combined) | −0.110 | −1.799*** |
| | (0.568) | (0.364) |
| KDDs / 1000, Sierra.Leone (Robusta) | −0.239 | −1.835*** |
| | (0.563) | (0.383) |
| KDDs / 1000, Philippines (Combined) | −0.110 | −1.801*** |
| | (0.568) | (0.364) |
| KDDs / 1000, Timor.Leste (Combined) | −0.109 | −1.799*** |
| | (0.568) | (0.364) |
| KDDs / 1000, Colombia (Arabica) | −0.082 | −1.731*** |
| | (0.581) | (0.394) |
| KDDs / 1000, Burundi (Combined) | −0.110 | −1.801*** |
| | (0.568) | (0.364) |
| KDDs / 1000, Burundi (Arabica) | −0.082 | −1.731*** |
| | (0.581) | (0.394) |
| KDDs / 1000, Fiji (Combined) | −0.110 | −1.801*** |
| | (0.568) | (0.364) |
| KDDs / 1000, Madagascar (Combined) | −0.110 | −1.801*** |
| | (0.568) | (0.364) |
| KDDs / 1000, Nepal (Combined) | −0.110 | −1.801*** |
| | (0.568) | (0.364) |
| KDDs / 1000, Suriname (Combined) | −0.089 | −1.779*** |
| | (0.568) | (0.364) |

| | *Dependent variable:* | |
|---|---|---|
| | Countries only | |
| | (1) | (2) |
| KDDs / 1000, Zambia (Arabica) | −0.082 | −1.731*** |
| | (0.581) | (0.394) |
| KDDs / 1000, Papua.New.Guinea (Combined) | −0.110 | −1.801*** |
| | (0.568) | (0.364) |
| KDDs / 1000, Zimbabwe (Arabica) | −0.094 | −1.742*** |
| | (0.581) | (0.393) |
| KDDs / 1000, New.Caledonia (Combined) | −0.110 | −1.801*** |
| | (0.568) | (0.364) |
| KDDs / 1000, New.Caledonia (Arabica) | −0.082 | −1.731*** |
| | (0.581) | (0.394) |
| KDDs / 1000, Paraguay (Arabica) | −0.043 | −1.660*** |
| | (0.571) | (0.387) |
| KDDs / 1000, Guyana (Robusta) | −0.157 | −1.766*** |
| | (0.568) | (0.386) |
| KDDs / 1000, Guyana (Arabica) | −0.081 | −1.730*** |
| | (0.581) | (0.394) |
| KDDs / 1000, Guyana (Combined) | −0.111 | −1.801*** |
| | (0.568) | (0.364) |
| KDDs / 1000, Honduras (Arabica) | −0.084 | −1.733*** |
| | (0.581) | (0.394) |
| KDDs / 1000, Myanmar (Combined) | −0.110 | −1.800*** |
| | (0.568) | (0.364) |
| KDDs / 1000, Mexico (Combined) | −0.110 | −1.801*** |
| | (0.568) | (0.364) |
| KDDs / 1000, Congo (Robusta) | −0.165 | −1.773*** |
| | (0.568) | (0.386) |
| KDDs / 1000, Congo (Combined) | −0.111 | −1.800*** |
| | (0.568) | (0.364) |
| KDDs / 1000, Sri.Lanka (Combined) | −0.108 | −1.793*** |
| | (0.567) | (0.363) |
| KDDs / 1000, Comoros (Combined) | −0.110 | −1.801*** |
| | (0.568) | (0.364) |
| Avg. Min., Liberia (Robusta) | −0.817*** | −0.873*** |
| | (0.141) | (0.140) |
| Avg. Min., Gabon (Robusta) | −0.642*** | −0.714*** |
| | (0.181) | (0.180) |
| Avg. Min., Yemen (Combined) | 0.402* | 0.369* |
| | (0.208) | (0.207) |
| Avg. Min., Jamaica (Arabica) | 0.297** | 0.269** |
| | (0.117) | (0.116) |
| Avg. Min., Kenya (Arabica) | −1.325*** | −1.369*** |
| | (0.288) | (0.288) |
| Avg. Min., Kenya (Combined) | −0.755*** | −0.794*** |
| | (0.156) | (0.154) |
| Avg. Min., Malawi (Arabica) | −0.255* | −0.288** |
| | (0.141) | (0.140) |

| | *Dependent variable:* | |
|---|---|---|
| | Countries only | |
| | (1) | (2) |
| Avg. Min., Angola (Combined) | −0.367* | −0.400** |
| | (0.199) | (0.198) |
| Avg. Min., Angola (Robusta) | 0.218** | 0.178* |
| | (0.110) | (0.108) |
| Avg. Min., Malaysia (Robusta) | 2.766*** | 2.680*** |
| | (0.164) | (0.162) |
| Avg. Min., Brazil (Combined) | −0.077 | −0.091*** |
| | (34.091) | (0.020) |
| Avg. Min., Guinea (Robusta) | 0.329*** | 0.300** |
| | (0.125) | (0.124) |
| Avg. Min., El.Salvador (Arabica) | −0.525*** | −0.526*** |
| | (0.145) | (0.145) |
| Avg. Min., Sierra.Leone (Robusta) | −1.196*** | −1.197*** |
| | (0.147) | (0.147) |
| Avg. Min., Suriname (Combined) | −1.532*** | −1.559*** |
| | (0.174) | (0.172) |
| Avg. Min., Zambia (Arabica) | −0.204 | −0.237* |
| | (0.125) | (0.123) |
| Avg. Min., Congo (Robusta) | −1.389*** | −1.441*** |
| | (0.155) | (0.154) |
| Avg. Min., Sri.Lanka (Combined) | −0.426*** | −0.402*** |
| | (0.140) | (0.139) |
| Precip., Brazil (Combined) | −4.285 | 0.347*** |
| | (6.691) | (0.030) |
| Precip., Suriname (Combined) | −12.378* | −10.271** |
| | (6.552) | (4.007) |
| Precip.$^2$, Brazil (Combined) | 5.340 | 0.366*** |
| | (88.871) | (0.039) |
| Observations | 3,011 | 3,016 |
| $R^2$ | 0.902 | 0.903 |
| Adjusted $R^2$ | 0.885 | 0.886 |
| Residual Std. Error | 0.335 (df = 2561) | 0.336 (df = 2566) |
| F Statistic | 52.575*** (df = 450; 2561) | 52.962*** (df = 450; 2566) |
| *Note:* | | *p<0.1; **p<0.05; ***p<0.01 |

Table A.5: Humidity Effects

| | *Dependent variable:* |
|---|---|
| Month prior to harvest | log(yield) |
| 1 | −8.562 |
| | (12.703) |
| 2 | 17.386 |
| | (12.509) |
| 3 | −2.607 |
| | (13.406) |
| 4 | −23.317* |
| | (12.756) |
| 5 | 4.781 |
| | (13.223) |
| 6 | −30.035** |
| | (12.008) |
| 7 | 15.021 |
| | (14.797) |
| 8 | −14.813 |
| | (16.496) |
| 9 | 19.024 |
| | (16.429) |
| 10 | −6.111 |
| | (17.747) |
| 11 | 35.636* |
| | (18.228) |
| 12 | −33.730** |
| | (15.444) |
| Observations | 738 |
| $R^2$ | 0.895 |
| Adjusted $R^2$ | 0.881 |
| Residual Std. Error | 0.191 (df = 653) |
| F Statistic | 66.164*** (df = 84; 653) |
| *Note:* | *p<0.1; **p<0.05; ***p<0.01 |

## A.4 Extra market analsysis

### A.4.1 Stock analysis

As an improvement, we note that prices are determined more directly by the stocks of coffee beans available to coffee markets. Therefore, we explore adding stocks of Arabica and Robusta to the model. These are not recorded separately by variety, although the USDA Foreign Agricultural Service reports total coffee stocks. We use a Bayesian model to infer the stocks, informed simultaneously by monthly production and the ability of these stocks to inform prices. The inferred stocks are shown in figure A.12.

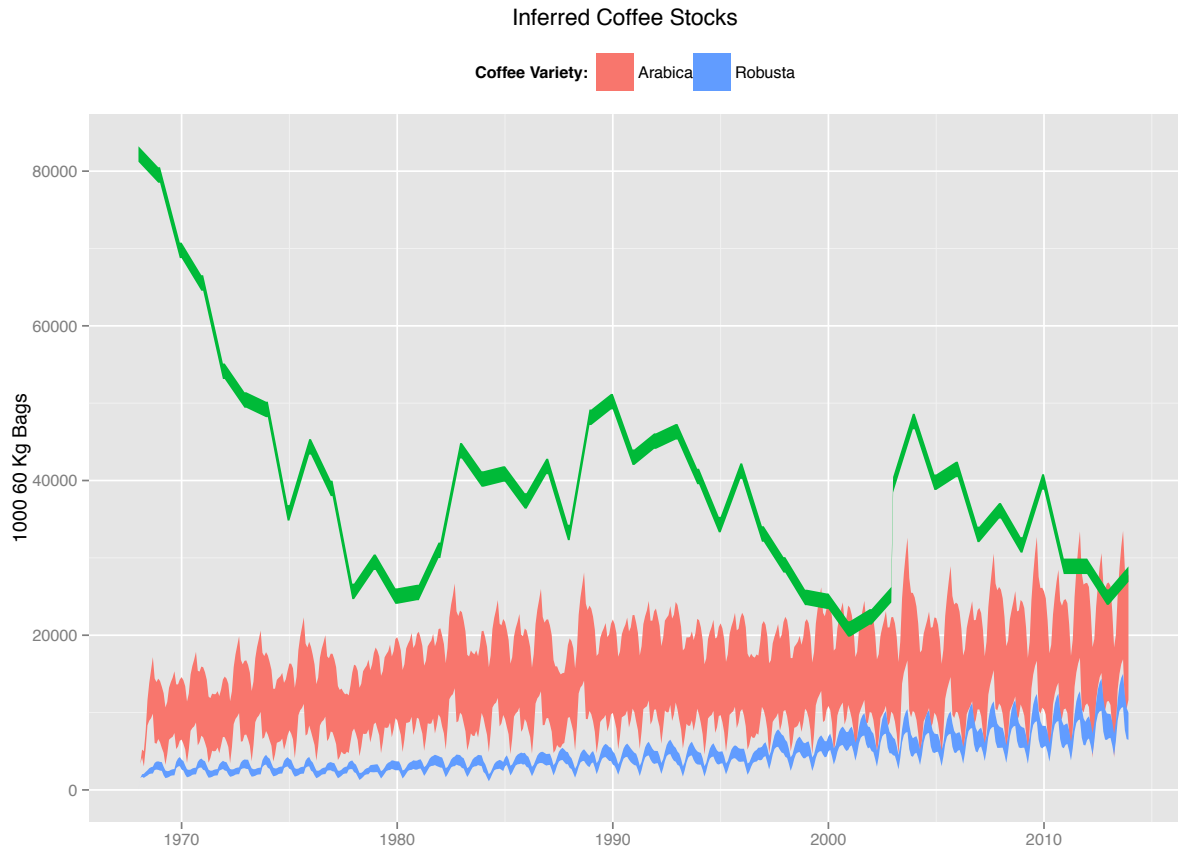


Figure A.12: Inferred stocks of Arabica (red) and Robusta (blue) coffee, compared with reported stocks (green) summed over all countries. Arabica and Robusta curves are shown with 50% confidence intervals, while the recorded curve is shown with a constant width.

Reported stocks were much higher than those inferred by the model. This is because the model attempts to use low initial stocks to explain the high international coffee prices in the 1970s. Later, bursts in stock correspond closely with increases in recorded stocks– for example, in 1982, 1988, and 2003. However, the model predicts a rapid decrease in the stock after the burst, while recorded stocks remain high after each event. This could reflect the sensitivity of the market to "fresh" green beans, rather than stored

ones.

The stocks are estimated simultaneously with the effect they have on the prices, thereby using the price to inform the level of stock. We further estimate the price in logs, and add an effect of the CPI ($c_t$), to produce our final model:

$$\log u = \alpha_0 + \alpha_1 s_i + \alpha_2 \log u_{t-1} \alpha_3 \log c_t$$

The estimates and their standard deviations are shown in table A.7. The effect of stock levels is still negative as expected, but not statistically significant. The autocorrelation in $\alpha_2$ is decreased because of the other informative elements. The coefficients also suggest that as CPI increases, international prices decrease, although this might just reflect the general downward trend in prices.

| | Arabica | | Robusta | |
|---|---|---|---|---|
| | Mean | Std. Dev. | Mean | Std. Dev. |
| $\alpha_0$ | 0.96 | 1.08 | 0.48 | 0.6 |
| $\alpha_1$ | $-8.47 \times 10^{-7}$ | $4.32 \times 10^{-6}$ | $-8.85 \times 10^{-6}$ | $1.17 \times 10^{-5}$ |
| $\alpha_2$ | 0.73 | 0.31 | 0.89 | 0.14 |
| $\alpha_3$ | −0.16 | 0.17 | −0.08 | 0.1 |

Table A.7: Coefficient estimates for the full stock model. Only $\alpha_2$, the coefficient on delayed international price, is significant at a 95% level.

### A.4.2 Explaining prices to farmers

Estimates for the determinants of prices to growers of coffee.

| Country | Type | International | Log Product. | Int. V.E. | Prod. V.E. | Int. P(>\|t\|) | Prod. P(>\|t\|) |
|---|---|---|---|---|---|---|---|
| Colombia | Colombian Milds | 16.190 | -0.004 | 0.855 | 0.033 | 0.000 | 0.001 |
| Kenya | Colombian Milds | 42.872 | -0.037 | 0.958 | 0.013 | 0.000 | 0.001 |
| Tanzania | Colombian Milds | 26.367 | 0.110 | 0.856 | 0.022 | 0.000 | 0.022 |
| Bolivia | Other Milds | 26.126 | 0.126 | 0.831 | 0.002 | 0.000 | 0.635 |
| Burundi | Other Milds | 13.918 | 0.006 | 0.768 | 0.000 | 0.000 | 0.819 |
| Cameroon | Other Milds | 17.297 | -0.043 | 0.509 | 0.021 | 0.000 | 0.351 |
| Congo, Dem. Rep. of | Other Milds | 5.788 | -0.148 | 0.275 | 0.708 | 0.297 | 0.098 |
| Costa Rica | Other Milds | 21.069 | -0.052 | 0.839 | 0.066 | 0.000 | 0.000 |
| Cuba | Other Milds | 14.087 | 0.584 | 0.337 | 0.455 | 0.000 | 0.000 |
| Dominican Republic | Other Milds | 32.377 | -0.040 | 0.937 | 0.006 | 0.000 | 0.046 |
| Ecuador | Other Milds | 23.186 | -0.025 | 0.807 | 0.010 | 0.000 | 0.151 |
| El Salvador | Other Milds | 33.379 | -0.018 | 0.930 | 0.011 | 0.000 | 0.010 |
| Guatemala | Other Milds | 20.445 | -0.019 | 0.881 | 0.025 | 0.000 | 0.002 |
| Haiti | Other Milds | 19.746 | 0.097 | 0.888 | 0.012 | 0.000 | 0.094 |
| Honduras | Other Milds | 35.087 | 0.009 | 0.910 | 0.007 | 0.000 | 0.072 |
| India | Other Milds | 17.230 | -0.039 | 0.873 | 0.023 | 0.000 | 0.006 |
| Jamaica | Other Milds | 18.733 | 1.791 | 0.428 | 0.038 | 0.000 | 0.113 |
| Madagascar | Other Milds | 0.211 | -0.074 | 0.000 | 0.001 | 0.987 | 0.933 |
| Malawi | Other Milds | 28.364 | 0.277 | 0.731 | 0.102 | 0.000 | 0.004 |
| Mexico | Other Milds | 25.079 | -0.023 | 0.892 | 0.018 | 0.000 | 0.016 |
| Nicaragua | Other Milds | 39.074 | -0.010 | 0.877 | 0.001 | 0.000 | 0.641 |
| Panama | Other Milds | 13.132 | -0.131 | 0.665 | 0.008 | 0.000 | 0.451 |
| Papua New Guinea | Other Milds | 21.258 | -0.023 | 0.888 | 0.003 | 0.000 | 0.302 |
| Peru | Other Milds | 47.729 | -0.013 | 0.778 | 0.006 | 0.000 | 0.458 |
| Rwanda | Other Milds | 13.679 | 0.084 | 0.706 | 0.069 | 0.000 | 0.005 |
| Uganda | Other Milds | 2.894 | 0.043 | 0.040 | 0.083 | 0.039 | 0.053 |
| Venezuela | Other Milds | 22.230 | 0.138 | 0.650 | 0.048 | 0.001 | 0.261 |
| Zambia | Other Milds | 13.538 | -0.041 | 0.559 | 0.000 | 0.000 | 0.852 |
| Zimbabwe | Other Milds | 14.874 | 3.177 | 0.681 | 0.055 | 0.455 | 0.585 |
| Brazil | Brazilian Naturals | 22.184 | 0.001 | 0.794 | 0.016 | 0.000 | 0.067 |
| Ethiopia | Brazilian Naturals | 14.567 | -0.006 | 0.765 | 0.015 | 0.000 | 0.097 |
| Indonesia | Brazilian Naturals | 31.851 | 0.005 | 0.528 | 0.001 | 0.011 | 0.919 |
| Philippines | Brazilian Naturals | 28.897 | -0.040 | 0.414 | 0.001 | 0.005 | 0.901 |
| Angola | Robustas | 6.650 | 0.010 | 0.232 | 0.033 | 0.019 | 0.241 |
| Benin | Robustas | 0.449 | -0.637 | 0.155 | 0.252 | 0.711 | 0.016 |
| Brazil | Robustas | 27.762 | 0.002 | 0.583 | 0.077 | 0.000 | 0.028 |
| Burundi | Robustas | 5.382 | 1.301 | 0.082 | 0.696 | 0.210 | 0.055 |
| Cameroon | Robustas | 10.715 | 0.012 | 0.620 | 0.012 | 0.000 | 0.283 |
| Central African Republic | Robustas | 7.394 | 0.039 | 0.602 | 0.018 | 0.000 | 0.196 |

| | | | | | | | |
|---|---|---|---|---|---|---|---|
| Congo, Dem. Rep. of | Robustas | 10.625 | -0.023 | 0.610 | 0.055 | 0.000 | 0.059 |
| Congo, Rep. of | Robustas | 1.318 | 0.227 | 0.333 | 0.137 | 0.047 | 0.030 |
| Côte d'Ivoire | Robustas | 9.459 | 0.006 | 0.667 | 0.036 | 0.000 | 0.030 |
| Ecuador | Robustas | 36.988 | -0.022 | 0.764 | 0.018 | 0.000 | 0.154 |
| Gabon | Robustas | 9.228 | 0.409 | 0.514 | 0.018 | 0.000 | 0.286 |
| Ghana | Robustas | 6.622 | -0.721 | 0.663 | 0.164 | 0.023 | 0.123 |
| Guinea | Robustas | 14.037 | -0.434 | 0.537 | 0.045 | 0.000 | 0.157 |
| India | Robustas | 23.426 | 0.007 | 0.743 | 0.043 | 0.000 | 0.030 |
| Indonesia | Robustas | 25.263 | 0.003 | 0.942 | 0.002 | 0.000 | 0.339 |
| Madagascar | Robustas | 6.512 | 0.004 | 0.347 | 0.001 | 0.001 | 0.813 |
| Nigeria | Robustas | 8.682 | -0.439 | 0.525 | 0.034 | 0.001 | 0.240 |
| Papua New Guinea | Robustas | 28.154 | 0.028 | 0.783 | 0.000 | 0.000 | 0.923 |
| Philippines | Robustas | 23.835 | -0.007 | 0.913 | 0.000 | 0.000 | 0.780 |
| Sierra Leone | Robustas | 11.475 | 0.181 | 0.563 | 0.034 | 0.000 | 0.245 |
| Sri Lanka | Robustas | 31.224 | -0.183 | 0.930 | 0.005 | 0.001 | 0.547 |
| Tanzania | Robustas | 16.526 | -0.018 | 0.585 | 0.003 | 0.000 | 0.689 |
| Thailand | Robustas | 28.468 | -0.022 | 0.906 | 0.004 | 0.000 | 0.193 |
| Togo | Robustas | 5.642 | 0.022 | 0.472 | 0.016 | 0.000 | 0.255 |
| Trinidad & Tobago | Robustas | 24.719 | 0.426 | 0.555 | 0.001 | 0.002 | 0.786 |
| Uganda | Robustas | 2.255 | -0.005 | 0.153 | 0.019 | 0.026 | 0.354 |
| Vietnam | Robustas | 77.812 | -0.001 | 0.576 | 0.002 | 0.000 | 0.745 |
| Global | All | 25.651 | -0.002 | 0.463 | 0.000 | 0.000 | 0.000 |

### A.4.3 Explaining consumer demand

| Country | Retail Pr. | Previous Yr. | Ret. V.E. | Prev. V.E. | Ret. Pr(>\|t\|) | Prev. Pr(>\|t\|) |
|---|---|---|---|---|---|---|
| Austria | 0.01 | 0.35 | 0.00 | 0.13 | 0.88 | 0.14 |
| Belgium | -0.47 | 1.13 | 0.30 | 0.35 | 0.00 | 0.01 |
| Bulgaria | 0.15 | 0.20 | 0.36 | 0.04 | 0.03 | 0.37 |
| Cyprus | -0.02 | 0.23 | 0.07 | 0.05 | 0.24 | 0.28 |
| Czech Republic | -0.01 | 0.69 | 0.00 | 0.32 | 0.37 | 0.01 |
| Denmark | 0.03 | 0.83 | 0.10 | 0.61 | 0.53 | 0.00 |
| Finland | 0.04 | 0.03 | 0.01 | 0.00 | 0.70 | 0.88 |
| France | -0.00 | 0.66 | 0.02 | 0.42 | 0.95 | 0.00 |
| Germany | -0.08 | -0.35 | 0.17 | 0.08 | 0.04 | 0.22 |
| Hungary | -0.06 | 0.86 | 0.02 | 0.68 | 0.07 | 0.00 |
| Italy | 0.02 | 0.79 | 0.11 | 0.49 | 0.74 | 0.00 |
| Latvia | 0.01 | 0.72 | 0.16 | 0.67 | 0.32 | 0.00 |
| Lithuania | 0.01 | 0.83 | 0.14 | 0.78 | 0.18 | 0.00 |
| Luxembourg | -1.42 | 0.52 | 0.53 | 0.16 | 0.06 | 0.03 |
| Malta | 0.00 | 0.43 | 0.01 | 0.13 | 0.68 | 0.15 |
| Netherlands | -0.05 | 0.74 | 0.00 | 0.60 | 0.76 | 0.00 |
| Poland | 0.00 | 0.77 | 0.00 | 0.49 | 0.86 | 0.00 |
| Portugal | -0.02 | 0.79 | 0.14 | 0.67 | 0.14 | 0.00 |
| Slovakia | 0.00 | -0.46 | 0.00 | 0.18 | 0.93 | 0.08 |
| Slovenia | 0.02 | 0.21 | 0.38 | 0.04 | 0.03 | 0.32 |
| Spain | 0.01 | 0.91 | 0.51 | 0.33 | 0.72 | 0.00 |
| Sweden | -0.04 | 0.30 | 0.08 | 0.10 | 0.18 | 0.15 |
| United Kingdom | 0.01 | 0.36 | 0.01 | 0.11 | 0.80 | 0.35 |
| Japan | 0.00 | 0.78 | 0.56 | 0.17 | 0.64 | 0.00 |
| Norway | 0.03 | 0.23 | 0.03 | 0.05 | 0.58 | 0.34 |
| Switzerland | -0.04 | 0.58 | 0.44 | 0.12 | 0.27 | 0.02 |
| Turkey | -0.00 | 1.02 | 0.16 | 0.50 | 0.82 | 0.00 |
| USA | -0.01 | 0.12 | 0.07 | 0.01 | 0.35 | 0.64 |
| Global | -0.01 | 0.70 | 0.01 | 0.92 | 0.08 | 0.00 |

Table A.9: Determinants of consumption of coffee.

### A.4.4 Inferred markups

#### Producer country markups

Mark-ups over the prices paid to farmers, by producer country, in US cents per pound. These are estimated simultaneous with the consumer country mark-ups.

| Country | To Farmers | Mark Up | Std. Dev. |
|---|---|---|---|
| Bolivia | 148.59 | 223.80 | 112.91 |
| Brazil | 107.06 | 84.80 | 31.14 |
| Burundi | 91.43 | 242.62 | 113.93 |
| Cameroon | 79.02 | 239.24 | 105.61 |
| Sri Lanka | 59.24 | 228.88 | 117.07 |
| Colombia | 124.50 | 194.32 | 70.11 |

| Country | To Farmers | Mark Up | Std. Dev. |
|---|---|---|---|
| Congo, Dem. Rep. of | 52.37 | 257.35 | 116.00 |
| Costa Rica | 137.20 | 214.23 | 102.04 |
| Cuba | 212.77 | 256.45 | 122.19 |
| Dominican Republic | 135.59 | 236.17 | 113.14 |
| Ecuador | 110.42 | 246.34 | 115.02 |
| El Salvador | 113.71 | 204.70 | 99.97 |
| Ethiopia | 101.05 | 168.01 | 94.98 |
| Gabon | 84.70 | 228.00 | 113.03 |
| Ghana | 108.59 | 244.26 | 121.38 |
| Guatemala | 137.95 | 102.30 | 70.70 |
| Guinea | 126.11 | 212.57 | 109.47 |
| Haiti | 91.81 | 229.51 | 114.36 |
| Honduras | 126.66 | 292.54 | 113.00 |
| Indonesia | 97.53 | 339.22 | 88.09 |
| Côte d'Ivoire | 63.74 | 226.83 | 96.66 |
| Jamaica | 262.39 | 239.55 | 116.14 |
| Kenya | 198.15 | 239.01 | 109.90 |
| Madagascar | 72.44 | 218.01 | 109.38 |
| Malawi | 77.87 | 235.31 | 117.05 |
| Mexico | 155.06 | 221.07 | 106.49 |
| Nicaragua | 139.47 | 182.82 | 96.48 |
| Panama | 149.15 | 235.36 | 106.61 |
| Papua New Guinea | 102.78 | 177.36 | 100.33 |
| Peru | 123.27 | 243.61 | 106.00 |
| Rwanda | 95.20 | 230.81 | 113.27 |
| India | 114.96 | 196.25 | 92.03 |
| Vietnam | 120.97 | 29.68 | 25.36 |
| Thailand | 93.03 | 268.90 | 122.50 |
| Togo | 55.70 | 225.31 | 108.66 |
| Uganda | 44.89 | 246.98 | 80.22 |
| Tanzania | 111.59 | 254.27 | 120.02 |
| Venezuela | 258.16 | 230.70 | 115.24 |
| Zambia | 110.58 | 219.19 | 112.56 |
| Congo, Rep. of | 33.52 | 226.88 | 120.91 |
| Nigeria | 118.40 | 228.59 | 114.78 |
| Sierra Leone | 111.94 | 234.04 | 110.40 |
| Zimbabwe | 408.97 | 234.58 | 118.08 |
| Central African Republic | 58.13 | 229.93 | 116.94 |
| Trinidad & Tobago | 173.12 | 228.67 | 114.16 |
| Philippines | 107.48 | 241.64 | 119.16 |
| Angola | 77.44 | 255.29 | 117.56 |
| Benin | 63.19 | 233.40 | 112.44 |
| Liberia | NA | 234.01 | 115.80 |
| (Processed) | NA | 254.26 | 34.22 |

**Consumer country markups**

| Country | To Farmers | Distribution | Retail | Mark Up | Std. Dev. |
|---|---|---|---|---|---|
| Austria | 89.40 | 184.31 | 448.67 | 175.07 | 34.15 |
| Belgium | 79.54 | 173.86 | 392.38 | 139.93 | 38.09 |
| Bulgaria | 74.88 | 208.52 | 283.88 | 31.51 | 25.96 |
| Cyprus | 86.47 | 112.54 | 429.70 | 230.73 | 35.58 |
| Denmark | 84.43 | 179.78 | 447.29 | 184.20 | 33.37 |
| Finland | 93.54 | 162.29 | 309.97 | 58.43 | 31.33 |
| France | 82.91 | 176.00 | 283.45 | 37.98 | 26.30 |
| Germany | 83.16 | 136.86 | 380.83 | 162.09 | 35.53 |
| Hungary | 68.32 | 205.45 | 387.22 | 114.71 | 39.63 |
| Italy | 81.08 | 132.38 | 571.66 | 356.53 | 37.01 |
| Latvia | 82.82 | 249.52 | 441.37 | 109.76 | 42.82 |
| Lithuania | 86.29 | 248.47 | 422.60 | 89.78 | 43.23 |
| Luxembourg | 87.45 | 254.18 | 559.21 | 217.24 | 48.44 |
| Malta* | 92.70 | 228.81 | 1019.96 | 692.57 | 41.21 |
| Netherlands | 88.05 | 192.84 | 366.49 | 86.88 | 34.92 |
| Poland | 71.99 | 178.79 | 317.54 | 70.10 | 32.04 |
| Portugal | 74.36 | 202.26 | 484.34 | 206.79 | 34.62 |
| Slovakia | 76.42 | 219.32 | 342.90 | 54.81 | 31.93 |
| Slovenia | 77.50 | 144.39 | 367.10 | 146.78 | 38.11 |
| Spain | 77.46 | 165.04 | 350.89 | 109.90 | 31.78 |
| Sweden | 93.92 | 168.28 | 350.25 | 89.53 | 34.55 |
| United Kingdom* | 81.04 | 190.61 | 1354.07 | 1070.48 | 37.39 |
| Japan | 91.23 | 182.71 | 1107.51 | 828.59 | 35.21 |
| Norway | 98.18 | 152.83 | 372.36 | 122.48 | 36.67 |
| Switzerland | 84.83 | 184.49 | 524.88 | 254.33 | 35.19 |
| Turkey | 91.25 | 99.09 | 416.92 | 226.54 | 39.70 |
| USA | 85.46 | 133.48 | 345.80 | 127.57 | 37.40 |

Table A.11: Mark-ups over the prices paid to farmers, by consumer country, in US cents per pound. These are estimated simultaneous with the producer country mark-ups.

### A.4.5 Economic importance of coffee

| Country | Variety | Farm ($/kg) | Itnl. ($/kg) | Production (kg) | Local Value ($) | Intl Value ($) | GDP ($) | (%) |
|---|---|---|---|---|---|---|---|---|
| Angola | arabica | 0.82 | 2.74 | 0 | 0 | 0 | 4408065910 | 0.00 |
| Angola | robusta | 0.59 | 1.46 | 1698000 | 1004067 | 2483891 | 4408065910 | 0.01 |
| Bolivia | arabica | 3.70 | 2.74 | 8442000 | 31232762 | 23162986 | 11362240323 | 0.20 |
| Brazil | arabica | 2.12 | 2.74 | 2026500000 | 4294893862 | 5560268994 | 1019917358692 | 0.55 |
| Brazil | robusta | 1.39 | 1.46 | 711900000 | 991280609 | 1041391089 | 1019917358692 | 0.10 |
| Burundi | arabica | 1.28 | 2.74 | 16026000 | 20465292 | 43971809 | 1320071226 | 3.33 |
| Burundi | robusta | | 1.46 | 0 | | 0 | 1320071226 | 0.00 |
| Cameroon | arabica | 1.41 | 2.74 | 5532000 | 7807333 | 15178588 | 18629569264 | 0.08 |
| Cameroon | robusta | 0.97 | 1.46 | 39630000 | 38314825 | 57972087 | 18629569264 | 0.31 |
| Central African Republic | robusta | 0.91 | 1.46 | 1518000 | 1378446 | 2220581 | 1631792478 | 0.14 |
| Colombia | arabica | 2.38 | 2.74 | 597966000 | 1422490591 | 1640686804 | 175186920716 | 0.94 |
| Congo, Dem. Rep. of | arabica | | 2.74 | 5262000 | | 14437767 | 14788569483 | 0.10 |
| Congo, Dem. Rep. of | robusta | | 1.46 | 11724000 | | 17150259 | 14788569483 | 0.12 |
| Congo, Rep. of | robusta | | 1.46 | 0 | | 0 | 7163015187 | 0.00 |
| Costa Rica | arabica | 2.15 | 2.74 | 104058000 | 223638738 | 285512199 | 23899924562 | 1.19 |
| Côte d'Ivoire | robusta | 0.61 | 1.46 | 121800000 | 73750900 | 178173107 | 18513289732 | 0.96 |
| Cuba | arabica | 1.39 | 2.74 | 7740000 | 10766855 | 21236853 | 49991611345 | 0.04 |
| Dominican Republic | arabica | 2.14 | 2.74 | 27162000 | 58194207 | 74526537 | 42066031892 | 0.18 |
| Ecuador | arabica | 2.45 | 2.74 | 25110000 | 61503896 | 68896301 | 47883528950 | 0.14 |
| Ecuador | robusta | 1.30 | 1.46 | 17400000 | 22547442 | 25453301 | 47883528950 | 0.05 |
| El Salvador | arabica | 1.70 | 2.74 | 87264000 | 148428732 | 239433167 | 18219072282 | 1.31 |
| Ethiopia | arabica | 1.47 | 2.74 | 315408000 | 465181914 | 865409979 | 18472707950 | 4.68 |
| Ghana | robusta | | 1.46 | 2214000 | | 3238713 | 14161252979 | 0.02 |
| Guatemala | arabica | 2.24 | 2.74 | 232476000 | 521865895 | 637862864 | 31344823589 | 2.03 |
| Guinea | robusta | | 1.46 | 23412000 | | 34247855 | 3208509564 | 1.07 |
| Haiti | arabica | | 2.74 | 19368000 | | 53141520 | 4429227578 | 1.20 |
| Honduras | arabica | 1.92 | 2.74 | 227994000 | 438103331 | 625565245 | 11134160781 | 5.62 |
| India | arabica | 2.35 | 2.74 | 98028000 | 230277245 | 268967209 | 1109531099998 | 0.02 |
| India | robusta | 1.43 | 1.46 | 187410000 | 268898827 | 274149605 | 1109531099998 | 0.02 |
| Indonesia | arabica | 2.09 | 2.74 | 69150000 | 144393359 | 189732347 | 353469522531 | 0.05 |
| Indonesia | robusta | 0.82 | 1.46 | 461700000 | 377800422 | 675390175 | 353469522531 | 0.19 |
| Jamaica | arabica | 5.55 | 2.74 | 1686000 | 9360707 | 4626012 | 1107577481 | 0.04 |
| Kenya | arabica | 1.45 | 2.74 | 47946000 | 69690082 | 131553248 | 22500842427 | 0.58 |
| Liberia | robusta | | 1.46 | 1836000 | | 2685762 | 839609172 | 0.32 |
| Madagascar | arabica | 0.99 | 2.74 | 1632000 | 1611367 | 4477848 | 5652013484 | 0.08 |
| Madagascar | robusta | 0.79 | 1.46 | 30264000 | 23879354 | 44271190 | 5652013484 | 0.78 |
| Malawi | arabica | 1.54 | 2.74 | 1560000 | 2402418 | 4280296 | 3465670842 | 0.12 |
| Mexico | arabica | 2.00 | 2.74 | 251100000 | 502945556 | 688963012 | 94313175944 | 0.07 |
| Nicaragua | arabica | 1.17 | 2.74 | 99240000 | 115978241 | 272292670 | 7096139115 | 3.84 |
| Nigeria | robusta | | 1.46 | 2226000 | | 3256267 | 144037995041 | 0.00 |

| Country | Variety | Farm ($/kg) | Itnl. ($/kg) | Production (kg) | Local Value ($) | Intl Value ($) | GDP ($) | (%) |
|---|---|---|---|---|---|---|---|---|
| Panama | arabica | | 2.74 | 7044000 | | 19327182 | 2125364815 | 0.09 |
| Papua New Guinea | arabica | 1.59 | 2.74 | 59610000 | 94843298 | 163556691 | 6141247952 | 2.66 |
| Papua New Guinea | robusta | 0.56 | 1.46 | 2748000 | 1542012 | 4019866 | 6141247952 | 0.07 |
| Peru | arabica | 1.13 | 2.74 | 224640000 | 253661686 | 616362609 | 96436263271 | 0.64 |
| Philippines | arabica | 2.01 | 2.74 | 1950000 | 3915230 | 5350370 | 123566704265 | 0.00 |
| Philippines | robusta | 1.33 | 1.46 | 27990000 | 37124998 | 40944707 | 123566704265 | 0.03 |
| Rwanda | arabica | 0.76 | 2.74 | 17640000 | 13479953 | 48400269 | 3504265695 | 1.38 |
| Sierra Leone | robusta | 0.44 | 1.46 | 3414000 | 1517699 | 4994113 | 1998841063 | 0.25 |
| Sri Lanka | arabica | | 2.74 | 594000 | | 1629805 | 31081582880 | 0.01 |
| Sri Lanka | robusta | | 1.46 | 1446000 | | 2115257 | 31081582880 | 0.01 |
| Tanzania | arabica | 0.91 | 2.74 | 31134000 | 28441963 | 85424828 | 18155123928 | 0.47 |
| Tanzania | robusta | 0.38 | 1.46 | 19248000 | 7401039 | 28156617 | 18155123928 | 0.16 |
| Thailand | arabica | 3.50 | 2.74 | 0 | 0 | 0 | 199643270642 | 0.00 |
| Thailand | robusta | 1.30 | 1.46 | 53166000 | 69270076 | 77773000 | 199643270642 | 0.04 |
| Togo | robusta | 0.96 | 1.46 | 20520000 | 19786230 | 30017341 | 2406177565 | 1.25 |
| Trinidad & Tobago | robusta | | 1.46 | 336000 | | 491512 | 18345375584 | 0.00 |
| Uganda | arabica | 1.37 | 2.74 | 37038000 | 50823541 | 101624102 | 12065197411 | 0.84 |
| Uganda | robusta | 1.03 | 1.46 | 143748000 | 148064470 | 210279374 | 12065197411 | 1.74 |
| Venezuela | arabica | | 2.74 | 50298000 | | 138006617 | 171452404755 | 0.08 |
| Vietnam | arabica | 1.47 | 2.74 | 30684000 | 45130389 | 84190128 | 72353243154 | 0.12 |
| Vietnam | robusta | 1.26 | 1.46 | 1108206000 | 1395836280 | 1621120737 | 72353243154 | 2.24 |
| Zambia | arabica | 1.91 | 2.74 | 3132000 | 5972119 | 8593517 | 11256721495 | 0.08 |
| Zimbabwe | arabica | | 2.74 | 2538000 | | 6963712 | 5603223515 | 0.12 |

## A.5 India Production

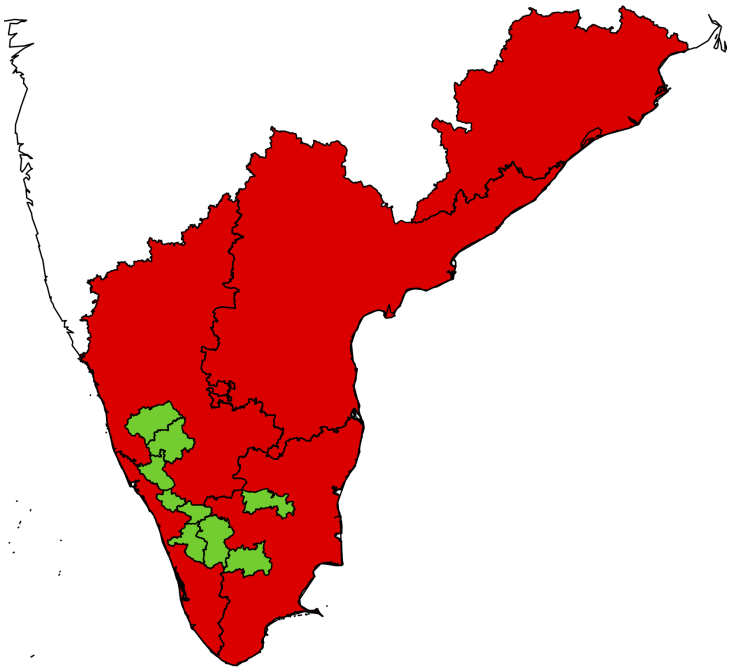

Figure A.13: State and district regions with coffee production records.

# Appendix B

# Coffee production database

The coffee database consists of paired production and growing region files. The database consists of both the final files and the code for generating standardized versions of input source files. The standardized versions have the same format as the merged database.

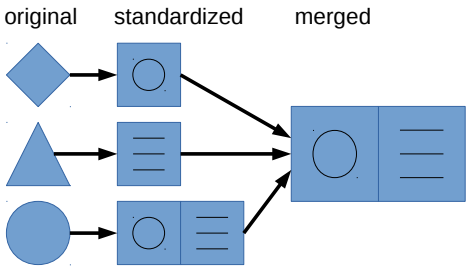


The coffee database is available in a sharable form, at `https://bitbucket.org/jrising/coffeedb/`. Request for access.

## B.1 Standardized format

### B.1.1 Growing Region Files

Growing regions are stored as raster (gridded) files describe "masks" of which regions are under harvest in a given month. They are at a resolution of 12 pixels per degree (a grid width of 5 minutes), and cover the entire area from 180°W to 180°E longitude, and 30°S to 30°N latitude.

The grids are stored as NetCDF files. Each NetCDF file contains a "harvest" variable and a "confidence" variable. The harvest variable specifies areas under harvest in a given month, and has dimensions Longitude x Latitude x 12, with a separate mask for each month. Values may range between 0 and 1, based on how much evidence there is of harvest there. The confidence mask describes the level of confidence in the information, also from 0 to 1.

Note that neither the "harvest" nor "confidence" variables describe the portion of a given grid cell under harvest. Instead, both relate to the evidence that the grid cell contains areas under harvest. The

difference between the harvest value and confidence value is expanded upon in the Merging Growing Region Files section.

### B.1.2 Production Files

Production data consists of a `.csv` file that specifies the production, planted area, harvested area, and yields (as data is available for each) in a given year and a given region. Where the data describes sub-country regions, an additional region definition file (`*-regions.csv`) and a shapefile database (collections of a `.shp`, `.shx`, and `.dbf` file) describe an association between the production records and growing regions. Each polygon in the shapefile database identifies a region for which production data is available in one or more years, and region definition files specify which region is described in each record.

The production file has the following column header:

`year,region,variety,produced,prod-se,harvested,harv-se,planted,plant-se,yield,yield-se`

`year` is the year being described. Not all years need to be represented for a region. `variety` is Arabica, Robusta, or combined. `region` is the region identifier in the associated region definitions file. This may change across years. `produced` is the calendar year production, measured in metric tonnes. `prod-se` is the standard error of the production estimate. It may be `NA` if the error estimate is available, but this will cause any other estimate to be chosen over it if one is available. `harvested` is the harvested area in hectares, and `harv-se` is its standard error. This may be `NA`. `planted` is the planted area in hectares, and `plan-se` is its standard error. This may be `NA`. `yield` is the yield in terms of MT per hectare, and `yield-se` is its standard error. The yield is computed as production divided by planted area. This may be `NA`.

The region definitions file has the following column header:

`region,PID,weight`

`region` is a region identifier, unique across the entire database. If there are multiple rows with the same region identifier, all of these PIDs will be combined in the region. `PID` is a polygon IDs in the associated growing region file. The same `PID` may occur in multiple regions, since different regions may be used to describe different years. `weight` is a measure of the accuracy of the production region definitions. In general, `weight` is calculated as *(mean planted area) / (total polygon area)*, and is between 0 (no confidence) and 1 (full confidence).

## B.2 Generating merged database files

### B.2.1 Merging growing region files

Region definition files are merged according to the weight of evidence of harvest in each month. At every point, the new weight in the combined region definitions is,

$$w(x,y) = \sum_i \frac{w_i(x,y)c_i(x,y)}{c_i(x,y)}$$
$$c(x,y) = \sum_i c_i(x,y)$$

This formulation allows confidence to increase where multiple data sources are available, and causes contradictory maps (for example, one that says that coffee is grown in a region and one that says it is not) to result in averaged values.

| | Arabica 1 | Arabica 0 | Combined 1 | Combined 0 |
|---|---|---|---|---|
| Arabica 1, Robusta 0 | 1, 0 | 0.5, 0 | 1, 0 | 0.5, 0 |
| Arabica 0, Robusta 0 | 0.5, 0 | 0, 0 | 0.5, 0.5 | 0, 0 |

Additional logic is used where maps that describe Arabica and Robusta growth separately are combined with those that lump them together.

### B.2.2 Merging production files

Production files are merged using a Bayesian approach, with a uniform prior. Each estimate (a given year-region value for production, harvested area, or planted area) is translated into a distribution, $p(y_i)$. Then the merged estimate of production is,

$$p(y) = \prod_i p(y_i)$$

This allows the database to account for uncertainty in the estimates, as well as allowing corroborating records to decrease the amount of uncertainty. Additional logic used where time series that split out Arabica and Robusta growth (such as the USDA Foreign Agricultural Service) are combined with ones that lump them together (such as FAO).

**Combining estimates**

1. Associate uncertainty with each observation ($k\sqrt{v_{it}}$).
2. Case 1: Same or Combined + (Arabica or Robusta):

$$\mu* = \frac{\frac{\mu_1}{\sigma_1^2} + \frac{\mu_2}{\sigma_2^2}}{\frac{1}{\sigma_1^2} + \frac{1}{\sigma_2^2}}$$
$$\sigma*^2 = \frac{\sigma_1^2\sigma_2^2}{\sigma_1^2 + \sigma_2^2}$$

3. Case 2: Combined + Arabica + Robusta:

$$\max_{a,r} \mathcal{N}(a|\mu_a, \sigma_a)\mathcal{N}(r|\mu_r, \sigma_r)\mathcal{N}(a + r|\mu_c, \sigma_c)$$

$\sigma_a*$ and $\sigma_r*$ from Inverse Hessian.

## B.3 Production maps

We performed a geospatial matching between diagrams in the gray literature and countries maps.

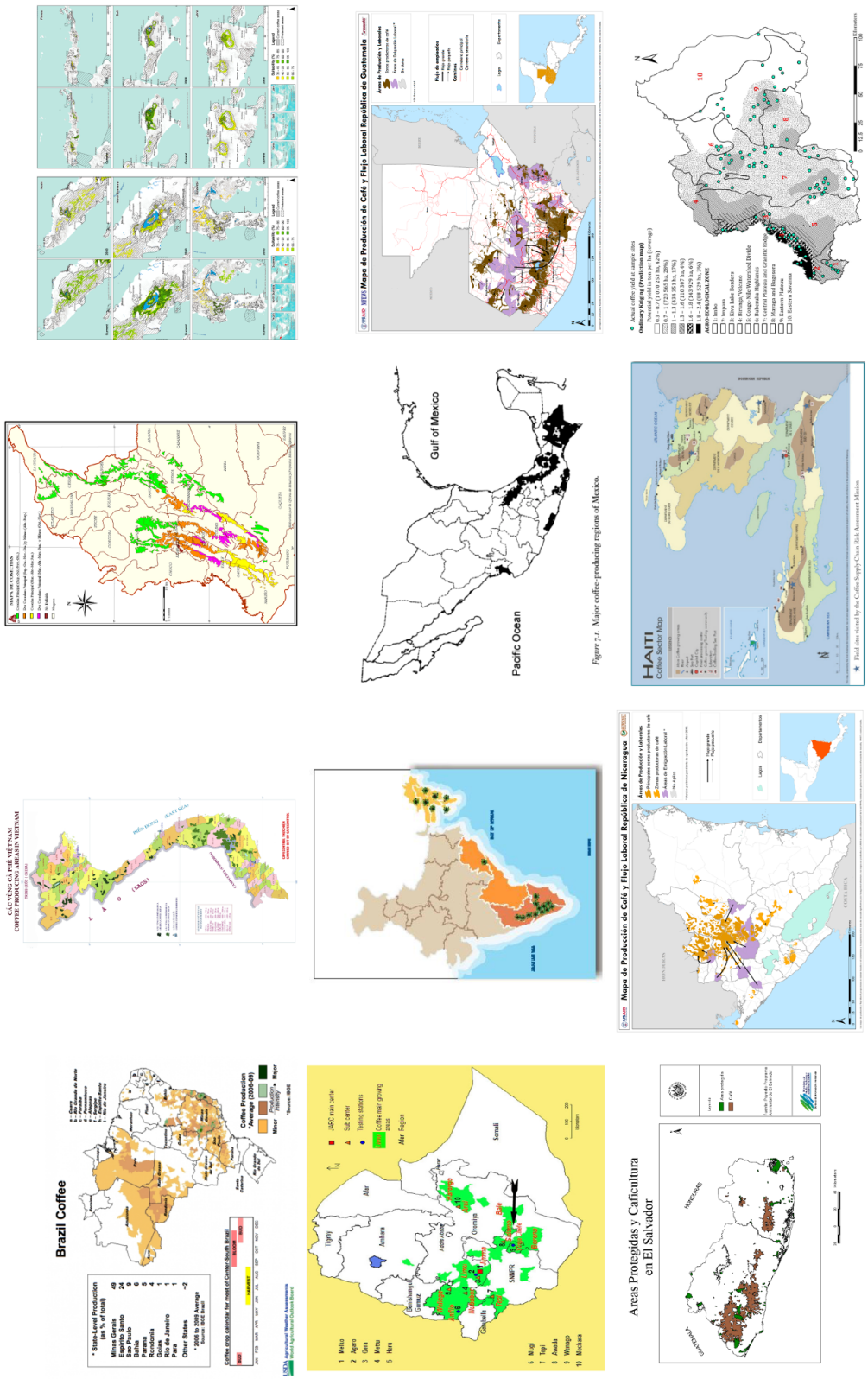


Figure B.1: Coffee growing region maps for Brazil, Vietnam, Colombia, Indonesia, Ethiopia, India, Mexico, Guatemala, El Salvador, Nicaragua, Haiti, and Rwanda, collected from various sources (see main text for the table).

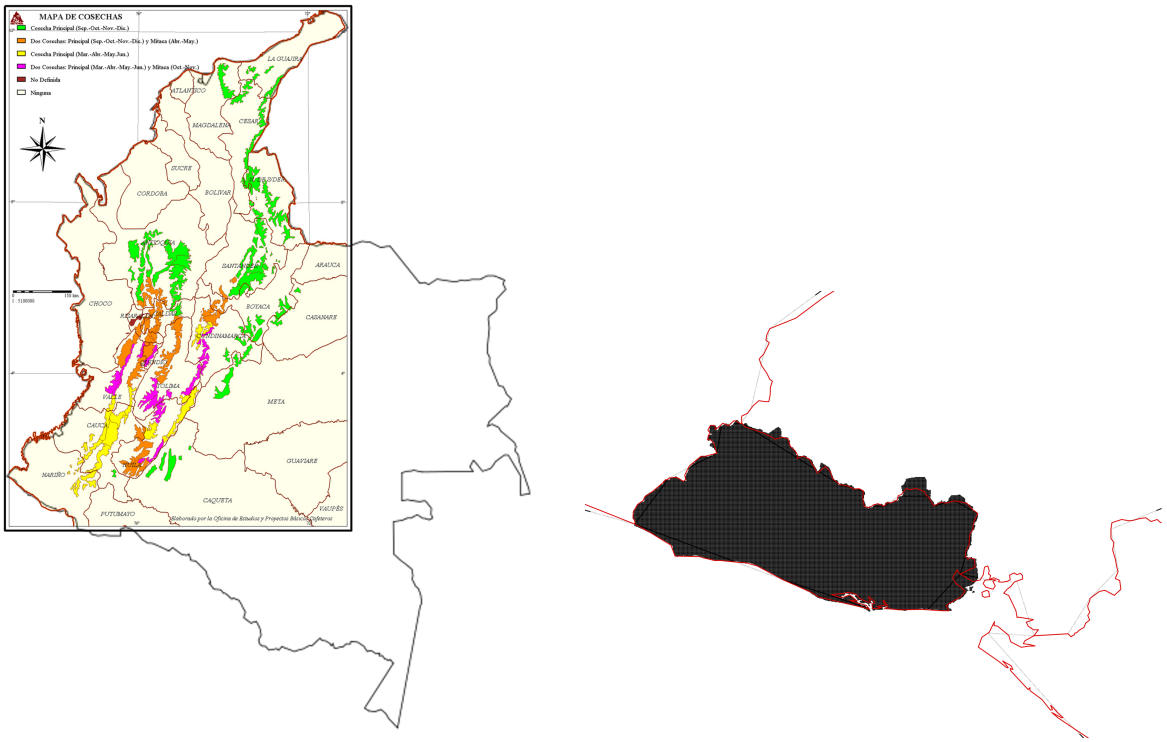


Figure B.2: Two examples of the geospatial matching process, using hand correspondences for Colombia (left) and country-wide shape matching for El Salvador (right).

# Appendix C

# Tool documentation

## C.1 Top-level structure

The tools directory contains the data and scripts for performing a range of functions produced in the course of this research. Both `python` and `R` are used as scripting languages, and results are produced as `.csv` comma-delimited tables, `.nc4` NetCDF4 files, `shapefiles`, and images.

The top-level directory contains the following:

**data** Pre-processed data files, and original source data in the `data/sources` subdirectory.

**extdata** Larger, "external" data files which are not stored in the source control repository.

**lib** Common function definitions.

**climate** A tool to study the changes in GCM projections.

**suitability** A tool for generating suitability results.

**variability** A tool to estimating variability from climate signals.

**production** A tool to estimating yields from weather.

The `extdata` directory is not stored in the normal repository. It is available at `http://eicoffee.net/files/extdata/`.

## C.2 Suitability tool

### C.2.1 Conditions and Intake Methods

The "intake" methods estimate the distribution of observed harvests across environmental variables, including soil, elevation, temperature, and precipitation climatologies. They write the `[variable]dist.csv` and `[var1][var2]corr.csv` files in the `data` directory. These are written in R, and the individual files corresponding to input variables need to be refreshed if their underlying data changes (for example, if a new collection of climate estimates is produced).

Each quality used to determine suitability is described in a condition object, stored in the `conditions` subdirectory.

### C.2.2 Calculating present suitabilities

The `suitability.py` tool calculates suitability under present conditions. The configuration and process for doing this is at the end of the `suitability.py` file after the if __name__ == '__main__': line, including which variety suitability is calculated for.

## C.3 Variability tool

Two tools are available to study the role of global variability of coffee production. Both use the range of five climate signals

`linproj.py` produces a naïve estimate of coffee under a future constellation of climate signals, using a linear model. This combines the effects of El Niño/La Niña with those of AMO, SOI, PDO, and NAO, without interactions.

`estimate.py` uses the principal component analysis results to project a constellation of climate signals into the most likely part of the interactive space of the combined climate-yield system, and then reports the associated yields.

## C.4 Production tool

The production tool sets up a framework for asking production questions, using data from the hierarchical model.

`model.py` creates a general class for storing and applying estimates for a given country and variety.

`global.py` loads all models estimated in the hierarchical model, to be applied to changes in GDDs, KDDs, and the other predictors.

# Bibliography

Alves, M. d. C., de Carvalho, L., Pozza, E., Sanches, L., and Maia, J. d. S. (2011). Ecological zoning of soybean rust, coffee rust and banana black sigatoka based on brazilian climate changes. *Procedia Environmental Sciences*, 6:35–49.

Arbenz, P. (2013). Bayesian copulae distributions, with application to operational risk management—some comments. *Methodology and Computing in Applied Probability*, 15(1):105–108.

Baca, M., Läderach, P., Haggar, J., Schroth, G., Ovalle, O., et al. (2014). An integrated framework for assessing vulnerability to climate change and developing adaptation strategies for coffee growing families in mesoamerica. *PloS one*, 9(2):e88463.

Baker, P. S. (2013). Coffee as a global system. In *Coffee: A Comprehensive Guide to the Bean, the Beverage, and the Industry*.

Bell, G. D., Halpert, M. S., Kousky, V. E., Gelman, M. E., Ropelewski, C. F., Douglas, A. V., and Schnell, R. C. (1999). Climate assessment for 1998. *Bulletin of the American Meteorological Society*, 80(5):1040–1040.

Bernardes, T., Moreira, M. A., Adami, M., Giarolla, A., and Rudorff, B. F. T. (2012). Monitoring biennial bearing effect on coffee yield using modis remote sensing imagery. *Remote Sensing*, 4(9):2492–2509.

Bunn, C., Läderach, P., Rivera, O. O., and Kirschke, D. (2015). A bitter cup: climate change profile of global production of arabica and robusta coffee. *Climatic Change*, 129(1-2):89–101.

Burke, M. and Emerick, K. (2012). Adaptation to climate change: Evidence from us agriculture. *Available at SSRN 2144928*.

CIAT (2010). Climate adaptation and mitigation in the kenyan coffee sector. Technical report, International Center for Tropical Agirculture, Cali, Colombia.

coffee&climate (2015). Climate change adaptation in coffee production. Technical report.

Comtrade, U. (2015). United nations commodity trade statistics database. Available at `http://comtrade.un.org`.

Dauzat, J., Griffon, S., Roupsard, O., Vaast, P., and Rodrigues, G. (2014). Building the foundations of a coffea arabica fspm. In *Embrapa Informática Agropecuária-Resumo em anais de congresso (ALICE)*. In: INTERNATIONAL CONFERENCE ON FUNCTIONAL-STRUCTURAL PLANT MODELS, 7., 2013, Saariselkä. Proceedings... Vantaa: Finnish Society of Forest Science, 2013.

Davis, A. P., Gole, T. W., Baena, S., and Moat, J. (2012). The impact of climate change on indigenous arabica coffee (coffea arabica): predicting future trends and identifying priorities. *PloS one*, 7(11):e47981.

Eitzinger, A., Läderach, P., Carmona, S., Navarro, C., and Collet, L. (2013). Prediction of the impact of climate change on coffee and mango growing areas in haiti. Technical report, Full Technical Report. Centro Internacional de Agricultura Tropical (CIAT), Cali, Colombia. http://dapa. ciat. cgiar. org/wp-content/uploads/2014/03/CC_impact_coffeemango_Haiti_CRS-CIAT_final. pdf.

Enfield, D. B., Mestas-Nunez, A. M., Trimble, P. J., et al. (2001). The atlantic multidecadal oscillation and its relation to rainfall and river flows in the continental u. s. *Geophysical Research Letters*, 28(10):2077–2080.

Epstein, P. R. (1999). Climate and health. *Science(Washington)*, 285(5426):347–348.

FAO/IIASA/ISRIC/ISSCAS/JRC (2012). Harmonized world soil database (hwsd). *FAO, Rome, Italy and IIASA, Laxenburg, Austria*.

Ferreira, S. and Boley, R. (1991). Hemileia vastatrix. *Crop Knowledge Master. Available at: www. extento. hawaii. edu/kbase/crop/type/h_ vasta. htm. Acessed on*, 7(27):2012.

Gay, C., Estrada, F., Conde, C., Eakin, H., and Villers, L. (2006). Potential impacts of climate change on agriculture: A case of study of coffee production in veracruz, mexico. *Climatic Change*, 79(3-4):259–288.

Gelman, A., Carlin, J. B., Stern, H. S., and Rubin, D. B. (2014). *Bayesian data analysis*, volume 2. Taylor & Francis.

Georgiou, S., Jacques, A., and Imbach Bartol, P. A. (2014). An analysis of the weather and climate conditions related to the 2012 epidemic of coffee rust in guatemala. technical report.

GISTEMP Team (2015). GISS Surface Temperature Analysis (GISTEMP). Dataset accessed 2015-06-05 at http://data.giss.nasa.gov/gistemp/.

Goddard, L. and Dilley, M. (2005). El niño: catastrophe or opportunity. *Journal of Climate*, 18(5):651–665.

Gonzalez, R. J. (2010). *Zapotec science: Farming and food in the Northern Sierra of Oaxaca*. University of Texas Press.

Guilford, G. (2014). How climate change and a deadly fungus are threatening the world's coffee supply. Retrieved from `http://www.citylab.com/weather/2014/06/how-climate-change-and-a-deadly-fungus-are-threatening-the-worlds-coffee-supply/371994/`.

Guzmán Martínez, O., Jaramillo Robledo, A., and Baldión Rincón, J. V. (1999). Anuario meteorologico cafetero, 1998.

Hansen, J., Ruedy, R., Sato, M., and Lo, K. (2010). Global surface temperature change. *Reviews of Geophysics*, 48(4).

Hijmans, R. J., Cameron, S. E., Parra, J. L., Jones, P. G., Jarvis, A., et al. (2005). Very high resolution interpolated climate surfaces for global land areas. *International journal of climatology*, 25(15):1965–1978.

Hsiang, S. M. and Meng, K. C. (2015). Tropical economics. *American Economic Review*, 105(5):257–61.

Hylander, K., Nemomissa, S., Delrue, J., and Enkosa, W. (2013). Effects of coffee management on deforestation rates and forest integrity. *Conservation biology*, 27(5):1031–1040.

International Coffee Council (1998). The "el niño southern oscillation event (enso)" and its impact on coffee production. Technical report. Available at `http://www.ico.org/documents/eb3657r1e.pdf`.

International Coffee Organization (2015a). Climate change and coffee: Enhancing the coffee sector's response to climate change. Technical report.

International Coffee Organization (2015b). ICO Historical Data. Supplied by ICO, May 7, 2015.

International Research Institute for Climate and Society (2015). IRI/CPC ENSO Predictions Plume. Available at `http://iri.columbia.edu/our-expertise/climate/forecasts/enso/current/`, accessed on Sep. 23, 2015.

International Research Institute for Climate and Society (2016). What changes in rainfall are typical during el niño? `http://iridl.ldeo.columbia.edu/maproom/IFRC/FIC/elninorain.html`. Accessed: 2016-01-25.

IPCC (2014). Climate change 2014: Impacts, adaptation, and vulnerability. part a: Global and sectoral aspects. contribution of working group ii to the fifth assessment report of the intergovernmental panel on climate change. Technical report.

Jaramillo, A. (2005). Solar radiation and rainfall distribution within coffee plantations (coffea arabica l.). *Rev Acad Col Ci Ex Fıs Ntles (Colombia)*, 29:371–382.

Jaramillo, J. (2013). Coffee under threat. In *Coffee: A Comprehensive Guide to the Bean, the Beverage, and the Industry*.

Jaramillo, J., Chabi-Olaye, A., Kamonjo, C., Jaramillo, A., Vega, F. E., Poehling, H.-M., Borgemeister, C., et al. (2009). Thermal tolerance of the coffee berry borer hypothenemus hampei: predictions of climate change impact on a tropical insect pest. *PLoS One*, 4(8):e6487.

Jaramillo, J., Muchugu, E., Vega, F. E., Davis, A., Borgemeister, C., and Chabi-Olaye, A. (2011). Some like it hot: the influence and implications of climate change on coffee berry borer (hypothenemus hampei) and coffee production in east africa. *PLoS One*, 6(9):e24528.

Jarvis, A., Reuter, H. I., Nelson, A., and Guevara, E. (2008). Hole-filled srtm for the globe version 4. *available from the CGIAR-CSI SRTM 90m Database (http://srtm. csi. cgiar. org)*.

Jassogne, L., Lderach, P., and van Asten, P. (2013). The impact of climate change on coffee in uganda: Lessons from a case study in the rwenzori mountains. *Oxfam Policy and Practice: Climate Change and Resilience*, 9(1):51–66.

Jones, J. W., Hoogenboom, G., Porter, C. H., Boote, K. J., Batchelor, W. D., Hunt, L., Wilkens, P. W., Singh, U., Gijsman, A. J., and Ritchie, J. T. (2003). The dssat cropping system model. *European journal of agronomy*, 18(3):235–265.

Keating, B. A., Carberry, P. S., Hammer, G. L., Probert, M. E., Robertson, M. J., Holzworth, D., Huth, N. I., Hargreaves, J. N., Meinke, H., Hochman, Z., et al. (2003). An overview of apsim, a model designed for farming systems simulation. *European Journal of Agronomy*, 18(3):267–288.

Körner, C., Morgan, J., and Norby, R. (2007). Co2 fertilization: When, where, how much? In *Terrestrial ecosystems in a changing world*, pages 9–21. Springer.

Kutywayo, D., Chemura, A., Kusena, W., Chidoko, P., and Mahoya, C. (2013). The impact of climate change on the potential distribution of agricultural pests: the case of the coffee white stem borer (monochamus leuconotus p.) in zimbabwe. *PloS one*, 8(8):e73432.

Laderach, P., Lundy, M., Jarvis, A., Ramirez, J., Portilla, E. P., Schepp, K., and Eitzinger, A. (2009). *Predicted impact of climate change on coffee supply chains*. na.

Lockwood, D. R. and Lockwood, J. A. (2008). Grasshopper population ecology: catastrophe, criticality, and critique. *Ecology and Society*, 13(1):34.

Magina, F., Makundi, R., Maerere, A., Maro, G., and Teri, J. (2011). Temporal variations in the abundance of three important insect pests of coffee in kilimanjaro region, tanzania. In *Proceedings, 23rd International Scientific Colloquium on Coffee. Association Scientifique Internationale du Café (ASIC), Bali, Indonesia*, pages 1114–1118.

Magrath, J. (2014). Coffee rust fungus threatens employment collapse in central america.

Malkin, E. (2014). A coffee crop withers. Retrieved from `http://www.nytimes.com/2014/05/06/business/international/fungus-cripples-coffee-production-across-central-america.html`.

Maro, G., Mrema, J., Msanya, B., Janssen, B., and Teri, J. (2014). Developing a coffee yield prediction and integrated soil fertility management recommendation model for northern tanzania. *International Journal of Plant & Soil Science*, 3(4):380–396.

Mason, S. J. and Goddard, L. (2001). Probabilistic precipitation anomalies associated with enso. *Bulletin of the American Meteorological Society*, 82(4):619–638.

Maxey, M. (2015). Arabica coffee from yemen: Hope in a time of turmoil. Available at `https://www.linkedin.com/pulse/arabica-coffee-from-yemen-hope-time-turmoil-michael-maxey`.

McGrath, J. M. and Lobell, D. B. (2013). Regional disparities in the co2 fertilization effect and implications for crop yields. *Environmental Research Letters*, 8(1):014054.

Menke, W. (2012). *Geophysical data analysis: discrete inverse theory*. Academic press.

Modern Farmer (2014). Battling the coffee rust: Photos of farmers fighting an epidemic. Retrieved May 16, 2015, from `http://modernfarmer.com/2014/08/battlingcoffee-growers-struggleepidemic/`.

Monfreda, C., Ramankutty, N., and Foley, J. A. (2008). Farming the planet: 2. geographic distribution of crop areas, yields, physiological types, and net primary production in the year 2000. *Global biogeochemical cycles*, 22(1).

NCAR (2015). Ncep/ncar reanalysis monthly jeans and other derived variables. Retrieved 17 Apr. 2015 from `http://www.esrl.noaa.gov/psd/data/gridded/data.ncep.reanalysis.derived.html`.

Nelsen, R. B. (2013). *An introduction to copulas*, volume 139. Springer Science & Business Media.

NOAA Climate Prediction Center (CPC) (2015). Climate indices: Monthly atmospheric and ocean time series. Available at `http://www.esrl.noaa.gov/psd/data/climateindices/list/`.

Nzeyimana, I., Hartemink, A. E., and Geissen, V. (2014). Gis-based multi-criteria analysis for arabica coffee expansion in rwanda. *PloS one*, 9(10):e107449.

O'Brien, T. G. and Kinnaird, M. F. (2003). Caffeine and conservation. *Science(Washington)*, 300(5619):587.

Ovalle-Rivera, O., Läderach, P., Bunn, C., Obersteiner, M., and Schroth, G. (2015). Projected shifts in coffea arabica suitability among major global producing regions due to climate change.

Pachauri, R. K., Allen, M., Barros, V., Broome, J., Cramer, W., Christ, R., Church, J., Clarke, L., Dahe, Q., Dasgupta, P., et al. (2014). Climate change 2014: Synthesis report. contribution of working groups i, ii and iii to the fifth assessment report of the intergovernmental panel on climate change.

Page, S. E., Siegert, F., Rieley, J. O., Boehm, H.-D. V., Jaya, A., and Limin, S. (2002). The amount of carbon released from peat and forest fires in indonesia during 1997. *Nature*, 420(6911):61–65.

Ricketts, T. H., Daily, G. C., Ehrlich, P. R., and Michener, C. D. (2004). Economic value of tropical forest to coffee production. *Proceedings of the National Academy of Sciences of the United States of America*, 101(34):12579–12582.

Rodríguez, D., Cure, J. R., Cotes, J. M., Gutierrez, A. P., and Cantor, F. (2011). A coffee agroecosystem model: I. growth and development of the coffee plant. *Ecological modelling*, 222(19):3626–3639.

Ropelewski, C. F. and Halpert, M. (1989). Precipitation patterns associated with the high index phase of the southern oscillation. *Journal of climate*, 2(3):268–284.

Saha, S., Moorthi, S., Pan, H.-L., Wu, X., Wang, J., Nadiga, S., Tripp, P., Kistler, R., Woollen, J., Behringer, D., et al. (2010). The ncep climate forecast system reanalysis. *Bulletin of the American Meteorological Society*, 91(8):1015–1057.

Schlenker, W. and Roberts, M. J. (2009). Nonlinear temperature effects indicate severe damages to us crop yields under climate change. *Proceedings of the National Academy of sciences*, 106(37):15594–15598.

Schneider, A., Friedl, M., Woodcock, C. E., et al. (2003). Mapping urban areas by fusing multiple sources of coarse resolution remotely sensed data. In *Geoscience and Remote Sensing Symposium, 2003. IGARSS'03. Proceedings. 2003 IEEE International*, volume 4, pages 2623–2625. IEEE.

Schroth, G., Läderach, P., Cuero, D. S. B., Neilson, J., and Bunn, C. (2014). Winner or loser of climate change? a modeling study of current and future climatic suitability of arabica coffee in indonesia. *Regional Environmental Change*, pages 1–10.

Sharf, S. (2014). Mondelez to take bigger sip of $81b global coffee industry with de master joint venture. Retrieved from `http://www.forbes.com/sites/samanthasharf/2014/05/07/mondelez-to-take-bigger-sip-of-81b-global-coffee-industry-with-de-master-joint-venture/`.

Stocker, T., Qin, D., Plattner, G.-K., Tignor, M., Allen, S. K., Boschung, J., Nauels, A., Xia, Y., Bex, V., and Midgley, P. M. (2014). *Climate change 2013: The physical science basis*. Cambridge University Press Cambridge, UK, and New York.

Sweet Maria (2015). World coffee production timetable. Available at `http://sweetmarias.com/coffee.prod.timetable.php`.

Thurston, R. W., Morris, J., and Steiman, S. (2013). *Coffee: A Comprehensive Guide to the Bean, the Beverage, and the Industry*. Rowman & Littlefield Publishers.

Ubilava, D. (2012). El niño, la niña, and world coffee price dynamics. *Agricultural Economics*, 43(1):17–26.

United Nations International Merchandise Trade Statistics (2009). Commodity pages, 071, coffee and coffee substitutes. In *Yearbook 2009*. `http://comtrade.un.org/pb/CommodityPagesNew.aspx?y=2009`, accessed June 11, 2011.

van Rikxoort, H., Schroth, G., Läderach, P., and Rodríguez-Sánchez, B. (2014). Carbon footprints and carbon stocks reveal climate-friendly coffee production. *Agronomy for Sustainable Development*, 34(4):887–897.

Varangis, P. N. et al. (2003). *Dealing with the coffee crisis in Central America: Impacts and strategies*, volume 2993. World Bank Publications.

Villegas, N., Barrientos, J. C., and Málikov, I. (2012). Relationship between ocean-atmospheric parameters and green coffee production in colombia. *Revista Colombiana de Ciencias Hortícolas*, 6(1):88–95.

WDPA Consortium (2004). World database on protected areas. *World Conservation Union and UNEP-World Conservation Monitoring Centre, New York, New York, USA*.

# Acknowledgments

We would like to thank **Walter Baethgen** at the International Research Institute for Climate and Society for his thoughtful reviews of the work here and all of his comments and suggestions.

Many thanks also to:

**Andrea Illy**, illycaffè S.p.A., Chairman/CEO

**Mario Cerutti**, Lavazza S.p.A., Corporate Relations

**Belay Begashaw**, Columbia Global Centers, Director

**Mauricio Galindo**, International Coffee Organization, Head of Operations

**Alexandra Tunistra**, Root Capital, Advisory Services

**Amir Jina**, University of Chicago, Economics

**Joann de Zegher**, Stanford University, Environment and Resources

**Marion Dumas**, Columbia University, School of International and Public Affairs